NON-HEME IRON PROTEINS FROM ANAEROBIC BACTERIA INVOLVED IN NITROSATIVE STRESS PROTECTION

by

RADU SILAGHI-DUMITRESCU

(under the direction of Donald M. Kurtz, Jr.)

ABSTRACT

Acetogenic bacteria grow anaerobically and use CO_2 and an electron donor such as H_2 to produce acetate. Some acetogens, such as *Moorella thermoacetica*, can alternatively use nitrate instead of CO_2 as terminal electron acceptor. In its natural habitat, *M. thermoacetica* is likely to encounter the toxic gas, nitric oxide (NO), generated either endogenously from nitrate reduction or exogenously, as a response to colonization or infection. Reported here is the characterization of a non-heme iron flavoprotein, FprA, from *M. thermoacetica*, which acts as a non-respiratory nitric oxide reductase, catalyzing reduction of NO to N_2O by NADH *in vivo* and *in vitro*. Also characterized is a flavo-iron reductase from *M. thermoacetica*, Hrb, which functions as an efficient NADH:FprA oxidoreductase. FprA's mechanism of NO reduction and its role in counteracting nitrosative stress are addressed with the use of structural, kinetic, spectral, biochemical and molecular biological methods. Evidence that FprAs from sulfate-reducing bacteria function as non-respiratory nitric oxide reductases is also presented.

INDEX WORDS: FprA, nitric oxide reductase, oxidase, nitrosative stress, oxidative stress, non-heme iron, nitrosyl, crystal structure, flavoprotein, diiron, mechanism

NON-HEME IRON PROTEINS FROM ANAEROBIC BACTERIA INVOLVED IN NITROSATIVE STRESS PROTECTION

By

RADU SILAGHI-DUMITRESCU

B. S., "Babes-Bolyai" University, Romania, 1997

M.S., "Babes-Bolyai" University, Romania, 1998

A Dissertation Submitted to the Graduate Faculty of The University of Georgia in Partial Fulfillment of the Requirements for the Degree

DOCTOR OF PHILOSOPHY

ATHENS, GEORGIA

2004

NON-HEME IRON PROTEINS FROM ANAEROBIC BACTERIA INVOLVED IN NITROSATIVE STRESS PROTECTION

by

RADU SILAGHI-DUMITRESCU

Major Professor:	Donald M. Kurtz, Jr.
Committee:	William N. Lanzilotta
	Robert S. Phillips

Electronic Version Approved:
Maureen Grasso
Dean of the Graduate School
The University of Georgia
December 2004

To Laura, Catalin, and Mihnea

……

To him I owe my eyes that I can see the dawn,
To him I owe my heart wherein is pity born;
Whene'er I hear the tempest, I hear him pass along
Midst multitude of voices raised in a holy song;
And yet of his great mercy I beg still one behest:
That I at last be taken to his eternal rest.

Be curses on the fellow who would my praise acclaim,
But blessings upon him who does my soul defame;
Believe no matter whom who slanders my renown,
Give power to the arm that lifts to strike me down;
Let him upon the earth above all others loom
Who steals away the stone that lies upon my tomb.

Hunted by humanity, let me my whole life fly
Until I feel from weeping my very eyes are dry;
Let everyone detest me no matter where I go,
Until from persecution myself I do not know;
Let misery and horror my heart transform to stone,
That I may hate my mother, in whose love I have grown;
Till hating and deceiving for me with love will vie,
And I forget my suffering, and learn at last to die.

Dishonoured let me perish, an outcast among men;
My body less than worthy to block the gutter then,
And may, o God of mercy, a crown of diamonds wear
The one who gives my heart the hungry dogs to tear,
While for the one who in my face does callous fling a clod
In your eternal kingdom reserve a place, o God.

Thus only, gracious Father, can I requitance give
That you from your great bounty vouched me the joy to live;
To gain eternal blessings my head I do not bow,
But rather ask that you in hating compassion show.
Till comes at last the evening, your breath will mine efface,
And into endless nothing I go, and leave no trace

[From "A Dacian's Prayer", by Mihai Eminescu (1850-1889)]

ACKNOWLEDGEMENTS

Dr. Donald M. Kurtz, Jr., is thanked for his generous mentorship. Dr. Eric D. Coulter (Kurtz group) is thanked for his essential contribution in initiating this project, for practical training and for helpful discussions. Drs. Amaresh Das and Lars Ljungdahl are thanked for their contribution on the microbiology and molecular biology side of the project, for helpful discussions and practical training on anaerobic cell culture. Drs. Kim Yong Ng and Rathinam Vishwanathan (Kurtz group) and thanked for their contribution to the *D. vulgaris* FprA project. Drs. Boi Hanh Huynh, Ricardo Garcia and Guy Jameson are thanked for the Mössbauer and rapid freeze-quench experiments. Dr. William N. Lanzilotta is thanked for training and involvement in the FprA crystallography project. Drs. Shi Jin (Kurtz group), Zhi-Jie Liu and Ashit Shah (Wang group) are thanked for helpful discussions and for their contributions in preliminary screening in the FprA crystallography project. Dr. Ramesh Iyer and Angela Sas (Kurtz group) are thanked for their contribution over the past few months of the FprA project. Dr. Richard Conover (Johnson group) is thanked for technical assistance with the EPR spectrometer. Dr. Michael Dean Clay and Jennifer Kathleen Schwartz (Solomon group, Stanford) are thanked for FprA MCD experiments (not shown in the present work). Dr. Pierre Moenne-Loccoz (OHSU) is thanked for FprA FTIR experiments (not shown in the present work). Dr. Robert S. Phillips is thanked for access to a stopped-flow instrument used for preliminary experiments. Drs. Michael K Johnson, Robert S. Phillips, Robert A. Scott and Michael W. Adams are thanked for their generous input into the project as members

of the Advisory Committee. Past and present members of the Kurtz group are thanked for quality, enthusiastic work environment, from which the present project has benefited greatly. Dr. Florin-Dan Irimie (Head of the Biochemistry division) and Luminita Silaghi-Dumitrescu (Dean of Chemistry) form the “Babes-Bolyai” University in Romania are thanked for tolerating my absence from work for the past four years.

TABLE OF CONTENTS

Page

CHAPTER 1

NITRIC OXIDE BIOCHEMISTRY. NITROSATIVE STRESS AND NITRIC OXIDE REDUCTASES

Nitric oxide has long been known as a poisonous gas. The surprising discovery that NO is in fact one of the most important signaling agents in living organisms has led to strong interest in NO chemical biology within the past two decades. Biological nitric oxide chemistry is almost invariably linked to transition metals and metalloproteins.[1-12] This chapter provides an overview of the bioinorganic chemistry of nitric oxide, particularly in bacteria, its connections to oxidative stress, to the bacterial nitrogen cycle, and to the central players in nitric oxide biochemistry, the nitric oxide-reducing enzymes. The chapter ends with an introduction to the focus of the research reported in this Dissertation: a novel class of bacterial nitric oxide reductases.

Figure 1.1 illustrates the rich family of nitrogen oxide congeners; the formation of many of these species is thermodynamically allowed under physiological conditions and, as described in the following sections, has implications for metabolism and toxicity in living organisms.

Nitric oxide is a well-known ligand to transition metal ions. The four classical coordination modes of NO to transition metal ions (M): terminal linear, terminal bent, μ_2-bridging, and μ_3-bridging, are illustrated in Figure 1.3.[14] Additionally, bidentate[15] and isonitrosyl coordination have recently been described.[14]

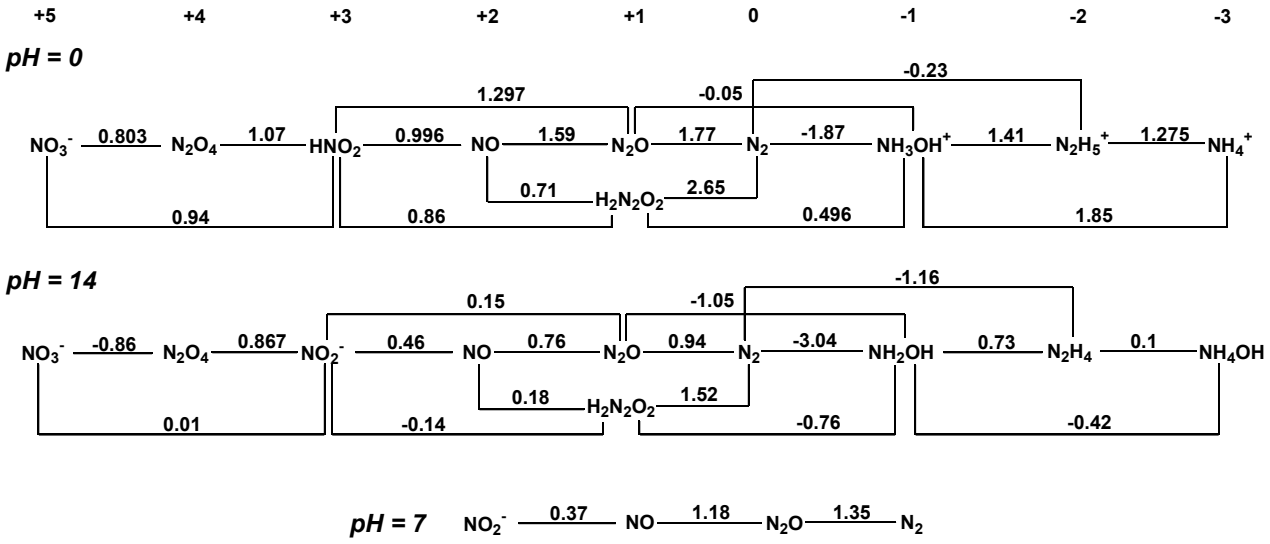

Figure 1.1. Reduction potential diagrams for nitrogen oxides and oxyanions (in volts vs. NHE). pH 0 and 14 data are from ref. 13; pH 7 data are from ref. 5.

1.1. Chemistry of nitric oxide relevant to biology.

As illustrated by the molecular orbital diagram in Figure 1.2, nitric oxide is a free radical, with a formal N-O bond order of 2.5.[14]

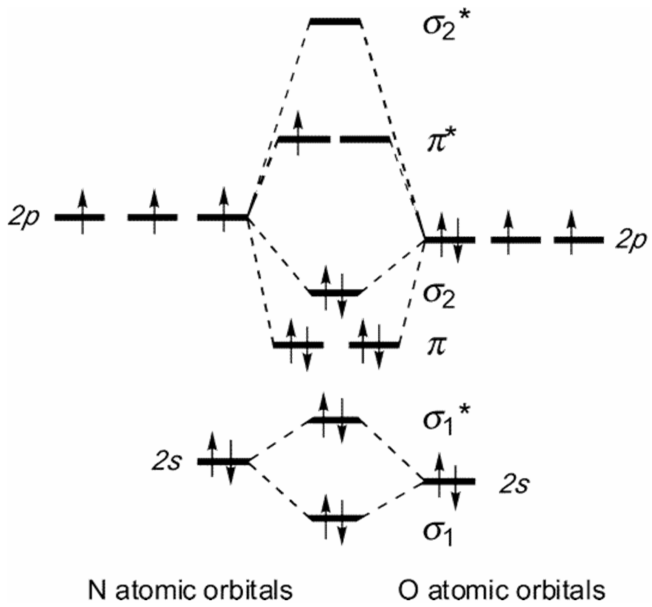

Figure 1.2. Molecular orbital diagram for nitric oxide.

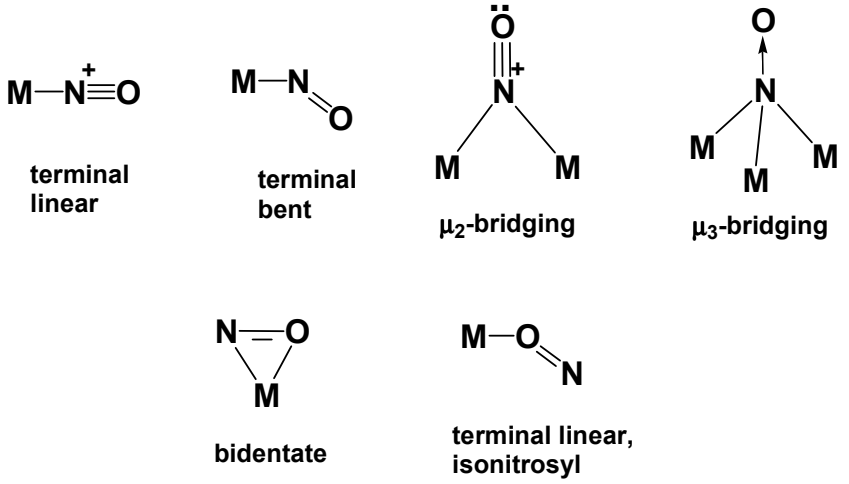

Figure 1.3. Modes of nitrosyl coordination to transition metal ions.

The valence electronic configurations for terminal nitric oxide binding to transition metal complexes can be described using the Enemark and Feltham $\{MNO\}^n$ formalism,[16] where "n" is the sum of metal *d* electrons plus the electrons in the NO antibonding orbitals. This formalism reflects the general difficulty in assigning the valence electrons to predominantly iron or NO-based orbitals. $\{MNO\}^n$ moieties with $n \leq 6$ feature linear M-N-O geometry in octahedral complexes and bent geometry in five-coordinate complexes. When $n \geq 7$, the M-N-O moiety is bent in octahedral complexes but may be linear in five-coordinate and four-coordinate complexes. Linear M-N-O complexes may be formally regarded as containing an NO^+ ligand, whereas bent complexes may be formally regarded as containing an NO^- ligand.[16]

The overwhelming majority of biological NO coordination complexes involve protein-bound iron. The most common of these are $S = 1/2$ $\{FeNO\}^7$ and $S = 0$ $\{FeNO\}^6$ heme complexes, which have bent and linear Fe-N-O geometries, respectively.[12] Metal-porphyrin or non-porphyrin NO complexes of manganese, cobalt, copper, and ruthenium relevant to biology are also known.[14] Nitric oxide binds to biological non-heme Fe(II) centers, generating $S = 3/2$ $\{FeNO\}^7$

adducts.[1,6,8-11,17-33] EXAFS, Mössbauer, UV-Vis, MCD, FTIR, resonance Raman, as well as computational results have been used to support a description of synthetic non-heme $\{FeNO\}^7$ units as $S = 5/2$ Fe(III) antiferromagnetically coupled to an $S = 1$ NO^-.[17,24,27] However, alternative computational studies interpreted the same experimental results as indicating a strongly covalent (as opposed to antiferromagnetically coupled) iron-NO interaction in $S = 3/2$ $\{FeNO\}^7$ complexes, so that assignment of formal oxidation states to Fe and NO (i.e., Fe(II) or Fe(III), $NO^\bullet$ or NO^-) would be inappropriate.[34,35] In contrast to $S = 3/2$ $\{FeNO\}^7$, a consensus appears to have emerged on the electronic structure of synthetic non-heme $S = 1/2$ $\{FeNO\}^7$ complexes, namely, $S = 1/2$ NO• bound to an $S = 0$ Fe(II) center.[27,35] The $S = 1/2$ spin state for $\{FeNO\}^7$ is unknown in non-heme iron proteins, but is the usual spin state in heme proteins. $\{FeNO\}^6$ heme protein complexes, usually described as Fe^{2+}-NO^+, are relatively labile in most heme complexes, whereas non-heme $\{FeNO\}^6$ complexes are normally not encountered in bio-inorganic chemistry. A major exception is nitroprusside, $[Fe(CN)_5NO]^{2-}$, which is widely used as a nitrosyl (formally NO^+) donor for *in vivo* experiments and therapeutically in humans.[36,37]

Under anaerobic conditions the non-heme diferrous site of the O_2-binding protein, hemerythrin, forms a stable mono-nitrosyl adduct, for which EPR, Mössbauer,[38] and computational[34] results show is best described as an $S = 3/2$ $\{FeNO\}^7$ unit antiferromagnetically-coupled to an $S = 2$ Fe(II) center. This $S = 1/2$ [Fe(II),$\{FeNO\}^7$] diiron site can undergo one-electron oxidation to an EPR-silent state, described as containing an $S = 5/2$ Fe(III) unit coupled to an $S = 3/2$ $\{FeNO\}^7$ unit.[38,39] Under anaerobic conditions *in vitro*, non-heme diiron sites of dioxygen-activating proteins such as bacterioferritin, methane monooxygenase and ribonucleotide reductase form relatively stable di-$\{Fe\text{-}NO\}^7$ adducts, which decay to yield sub-stoichiometric amounts of N_2O.[20,22,26,40] These di-$\{Fe\text{-}NO\}^7$ adducts show EPR, Mössbauer and

UV-vis absorption spectral features that are consistent with two S = 3/2 $\{FeNO\}^7$ units antiferromagnetically-coupled to each other giving an S = 0 ground state. As discussed above, since S = 3/2 $\{FeNO\}^7$ units are almost unanimously described as arising from antiferromagnetic coupling between S = 5/2 Fe(III) and S = 1 NO^-, binding of the two NO molecules, one to each iron of a high-spin di-ferrous site results in formal reduction of the nitrogen atoms to the oxidation state found in N_2O. As such, subsequent release of N_2O and H_2O as products would be a formally non-redox process, but one which requires protons. Given this requirement, it is perhaps not surprising that nitric oxide reduction is not a known physiological function for these non-heme diiron proteins: their active sites are relatively hydrophobic and buried in the protein interior, a feature consistent with their physiological function of binding and activating molecular oxygen.[40-42] Related to these di-$\{Fe\text{-}NO\}^7$ enzyme complexes is the synthetic non-heme di-$\{Fe\text{-}NO\}^7$ compound shown in Figure 1.4. This compound is stable in non-aqueous solvents and has not been reported to produce N_2O to any significant extent.[21] In both the proteins and the synthetic complex the $\{FeNO\}^7$ units are antiferromagnetically coupled through a bridging oxygen, from solvent in the proteins or alkoxy in the synthetic complex, yielding an S = 0 ground state. No other examples of synthetic di-$\{Fe\text{-}NO\}^7$ complexes have been reported.

Two synthetic S = 0 non-heme $\{FeNO\}^8$ complexes arising from electrochemical reduction of S = 1/2 $\{FeNO\}^7$ complexes have been reported.[43-45] Based on structural, spectroscopic and computational data, these complexes are described as Fe(III)-NO^-.[43,45] Somewhat similarly, reduction of the S = 1/2 $\{FeNO\}^7$ complex of myoglobin or reaction of deoxymyoglobin with the HNO donor, Angeli's salt, results in formation of a heme S = 0 $\{Fe\text{-}N(H)\text{-}O\}^8$ adduct.[46] No examples of intermediate- or high-spin $\{FeNO\}^8$ have been reported so far.

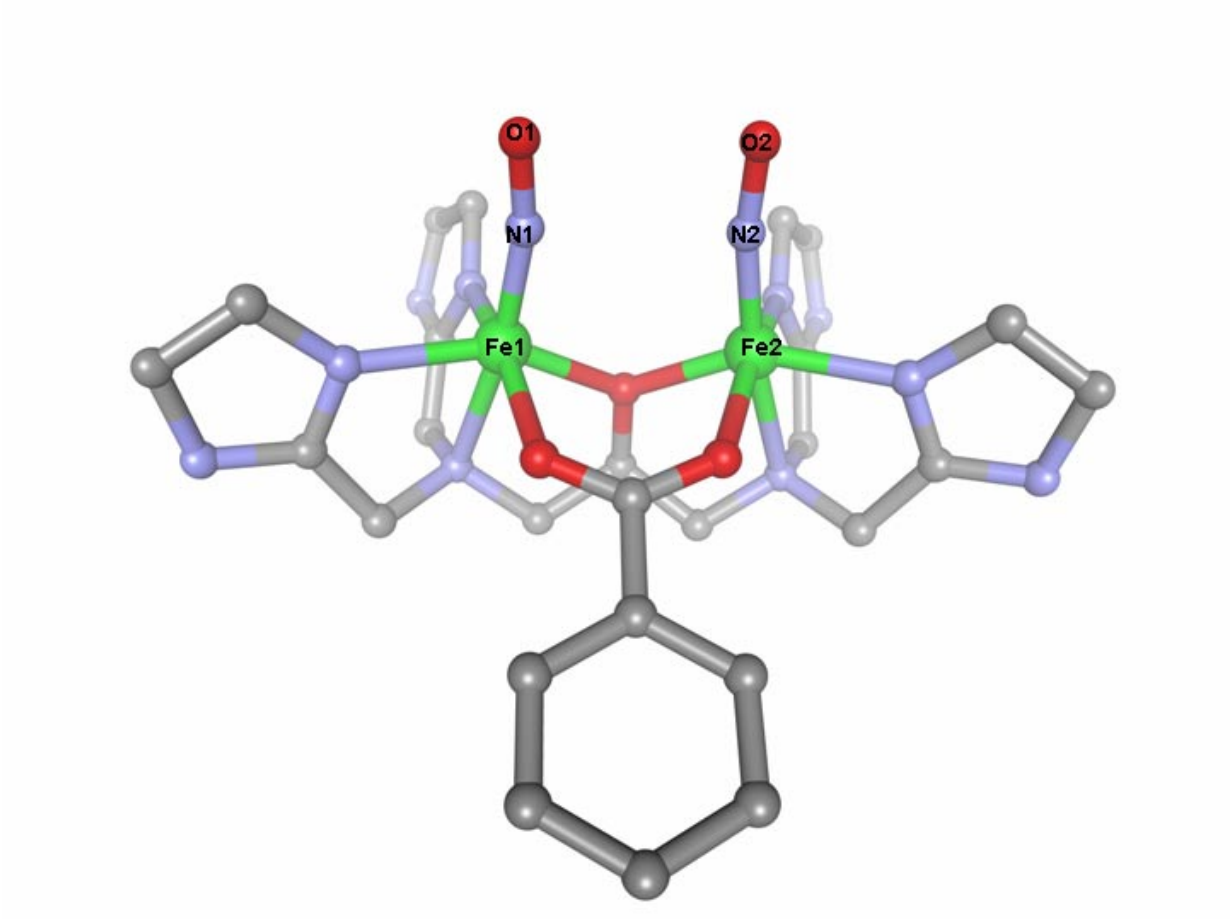

Figure 1.4. Crystal structure of $[Fe_2(Et\text{-}HPTB)(O_2CPh)](BF_4)_2$, (iron shown in green, nitrogen in blue, oxygen in red, carbon in gray).

Mononuclear di-nitrosyl complexes, described as $S = 0$ $\{Fe(NO)_2\}^8$ and $S = 1/2$ $\{Fe(NO)_2\}^9$, have been reported to form upon anaerobically exposing the *E. coli* ferric uptake regulatory protein, Fur, to NO.[47,48] This finding may be of physiological relevance, since Fur is known to be involved, more or less directly, in the bacterial response to nitrosative stress (discussed in the next section).[47-49] Di-nitrosyl complexes are also assumed to form upon exposure of iron-sulfur proteins to NO – a reaction responsible at least partially for the toxicity of NO to bacteria.[14,50]

1.2. Oxidative and nitrosative stress

Biological oxidative stress is traditionally associated with the presence of reactive oxygen species (ROS), either as a byproduct of aerobic respiration or as a response to infection. ROS (superoxide, hydrogen peroxide, hydroxyl radical, singlet oxygen, ozone) contain oxygen atoms in oxidation or spin sates different from and usually more reactive than those of the relatively stable triplet O_2. ROS have the potential of damaging a wide range of biomolecules, including DNA, proteins, cofactors, lipids, and sugars. Aerobic organisms, defined as those using O_2 as terminal respiratory electron acceptor, have, therefore, developed well-defined "oxidative stress protection" (OSP) systems, which include the enzymes superoxide dismutase (SOD), catalase, and peroxidase, which catalyze reactions 1.1-1.3, respectively.[51,52]

$$2O_2^- + 2H^+ \rightarrow O_2 + H_2O_2 \qquad \text{(SOD)} \qquad 1.1$$

$$2H_2O_2 \rightarrow O_2 + 2H_2O \qquad \text{(catalase)} \qquad 1.2$$

$$2e^- + H_2O_2 + 2H^+ \rightarrow 2H_2O \qquad \text{(peroxidase)} \qquad 1.3$$

Two out of these three reactions represent disproportionations, while the third is a reduction.

Anaerobic bacteria and archaea use electron acceptors other than O_2 for respiration and normally cannot survive exposure to air for extended periods. Upon exposure to air, some anaerobic bacteria and archaea are thought to deal with oxidative stress in an entirely reductive, rather than disproportionative, manner, using the enzymes superoxide reductase (SOR) and rubrerythrin (Rbr).[51,53,54] Rbr is a peroxidase, while SOR catalyzes reduction of superoxide to hydrogen peroxide, reaction 1.4.

$$O_2^- + 2H^+ + e^- \rightarrow H_2O_2 \qquad \text{(SOR)} \qquad 1.4$$

The electrons required by Rbr and SOR may be delivered by the small $[Fe(SCys)_4]$-containing protein, rubredoxin (Rd), but most likely originate from the cellular NAD(P)H pool. Another

component of the OSP in anaerobic microbes has been proposed to be a class of flavo-diiron proteins known as FprA (type A flavoprotein), or "rubredoxin oxygen oxidoreductase" (ROO).[55-57] FprA/ROO was shown to catalyze *in vitro* the four-electron reduction of dioxygen to water (dioxygen reductase, or oxidase), reaction 1.5.

$$O_2 + 4e^- + 4H^+ \rightarrow 2\ H_2O \qquad \text{(oxidase)} \qquad 1.5$$

More recent *in vivo* and *in vitro* evidence however suggests a different physiological function for these flavo-diiron proteins, which is discussed in Section 1.5, and which is the focus of the research described in this Dissertation.[50,58] A proposed advantage of the reductive OSP pathway in anaerobes (compared to the aerobic dismutative pathway) is that it avoids re-generation of O_2 (a toxic species for anaerobes). A second advantage of the reductive OSP pathway has been proposed to be modulation of the redox potential inside the cell, such that under oxidizing conditions ROS-sensitive enzymes would be confined to more oxidized but less ROS-reactive states.[51,54] The fact that SOR, Rbr, Rd and FprA/ROO are all non-heme iron proteins[51] perhaps remains to be fully appreciated.

In addition to oxidative stress, bacteria must cope with "nitrosative" stress due to transient exposure to nitrogen oxides and oxyanions, namely nitrite, NO_2-; nitric oxide, NO; nitrogen dioxide, NO_2; nitrogen trioxide, N_2O_3; peroxynitrite, $ONOO^-$.[1,59-62] The central player in nitrosative stress is nitric oxide.[2-4,6,25,63] In anaerobes, NO is generated not only endogenously as a consequence of nitrate/nitrite reduction, but also exogenously, either by other bacteria or as a host response to infection or colonization.[2-4,6,25,61-63] When not generated via nitrite reduction (cf. Section 1.3), NO is synthesized from arginine by nitric oxide synthases, and, as such, serves as an important signaling molecule in a variety of organisms, ranging from bacteria and yeasts to humans.[3,64-66] The main targets of nitric oxide in bacteria have been shown to be

metalloenzymes, especially those containing iron-sulfur clusters, hemes, and thiols.[2-4,6,25,63] Binding of NO to the heme iron of terminal oxidases has been proposed to be responsible for inhibition of respiration, which leads to accumulation of excess reducing equivalents and, thus, renders cellular redox-active centers more susceptible to oxidative damage.[67] Reaction of NO with protein-bound iron-sulfur clusters was found to inhibit enzymes involved in crucial metabolic pathways.[50,68]

Nitrosyl adducts of organic thiols, RS-NO (formally $[(RS^-)(NO^+)]$), are readily formed from nitrite and free thiols, especially under acidic conditions, where nitrous acid, HNO_2, may be formally regarded as $(NO^+)(OH^-)$. The mechanisms of RS-NO formation *in vivo* (i.e., whether it involves direct reaction of thiols or disulfides with nitrite, NO, NO^+ or other species) are unknown.[7] As expected from the known reactivity of NO^+ in organic chemistry, RS-NO species are efficient nitrosating agents *in vivo*.[69] Under anaerobic conditions, RS-NO may be metabolized by a glutathione-dependent formaldehyde dehydrogenase[70].

In addition to directly interacting with biological targets, NO has also been proposed to convert to more reactive (and presumably more toxic) species by undergoing redox reactions.[7,71,72] Direct (outer-sphere) NO reduction to nitroxyl, $^3NO^-$, is essentially thermodynamically prohibited *in vivo* due to an NO/NO^- reduction potential more negative than -500 mV vs NHE at pH 7.2.[73] Under physiological conditions, nitroxyl is thought to exist almost exclusively as singlet HNO with an estimated pK_a of 11.6, and the reduction potential of HNO is estimated to be more positive than -0.33 V.[73] Nitroxyl donors such as Angeli's salt, $Na_2(ONNO_2)$, have been shown to affect living organisms in manners different from (and often opposite to) nitric oxide donors, suggesting different biological mechanisms for NO and NO^- toxicity. While NO has the potential to act as antioxidant (see below) in addition to generating

nitrosative (oxidative-type) stress, NO^- is both more reactive than NO, and generates more toxic species under aerobic conditions. For instance, NO^- induces DNA damage, depletes cellular thiols, and directly inhibits DNA-repair proteins under conditions where NO has a cytoprotective effect due to its intrinsic antioxidant properties (see below) and to the more limited toxicity of reactive nitrogen species resulting from NO (auto)oxidation.[71,74]

Peroxynitrite, $ONOO^-$, has been proposed to form *in vivo* via reaction of NO with superoxide or via reaction of NO^- with dioxygen. The latter reaction was more recently shown to be highly unlikely, due to the fact that nitroxyl is present *in vitro* not as $^3NO^-$ (which reacts rapidly with dioxygen) but rather as ^1HNO, whose reaction with triplet dioxygen is spin-forbidden, and, therefore extremely slow.[75] Peroxynitrite may react with enzyme active sites, getting reduced by alkylhydroperoxide reductase to NO_2,[49] isomerized by hemoproteins to nitrate, or activated by hemoproteins, generating high-valent oxo species. Peroxynitrite is also a nitrating agent for aromatic amino acid residues, mainly tyrosine.[76] Methionine may be oxidized to methionine sulfoxide by peroxynitrite; this sulfoxide formation is potentially toxic to the cell and is reversed by the enzyme peptide methionine sulfoxide reductase.[49] Peroxynitrite also reacts rapidly ($k = 10^4$ s^{-1}) with CO_2, generating the anhydride $ONOOCO_2^-$, 1-carboxylato-2-nitrosodioxidane, which is a potent nitrating agent.[76,77]

Much of the data on NO toxicity (described above) has been gathered from *in vitro* or *in vivo* experiments using exogenously added NO or NO donors at micromolar-to-millimolar concentrations. On the other hand, at lower concentrations, 25-125 nM, NO was shown to act as a potent *antioxidant* by efficiently blocking the oxidative action of a Fe(II)-H_2O_2 mixture ("Fenton reagent") *in vitro*. This antioxidant activity was proposed to arise mainly via reaction of NO with a transient Fe(IV)-oxo or Fe(IV)-hydroxo intermediate formed upon Fe(II)-catalyzed

H_2O_2 heterolysis.[78] This observation reveals the "good" side of NO – the side that allows it to serve as *non-toxic* messenger at least in organisms ranging form yeasts to humans.[64,65,74] Intriguingly, such antioxidant activity of NO was proposed to have been instrumental for the appearance of life on Earth.[79]

Under anaerobic conditions, most of the NO encountered within a bacterial cell is reduced by nitric oxide reductases (see Sections 1.3-1.6). Under aerobic conditions, bacterial globins, such as flavohemoglobin and truncated hemoglobins, have been proposed to act as NO dioxygenases (reaction 1.6), a reaction that has also been demonstrated for human hemoglobin and myoglobin.[68,80,81]

$$e^- + NO + O_2 \rightarrow NO_3^- \qquad \text{(flavohemoglobin)} \qquad 1.6$$

However, the exact physiological functions of flavohemoglobin and truncated hemoglobins are still under dispute.[82,83] The bacterial regulatory proteins OxyR, SoxR,[84] norR,[36] FNR,[85] Fur[48] have all been shown to be involved in regulating nitric oxide reductase or S-nitrosothiol reductase activities. Of these regulatory proteins, a key role was demonstrated in *E. coli* for norR in controlling the expression of the main nitrosative stress protection (NSP) enzymes – flavohemoglobin and flavorubredoxin (proposed to act as nitric oxide dioxygenase and nitric oxide reductase, respectively).[49] Indeed, upon exposure of *E. coli* to 0.1 or 1 mM NO-releasing agents (RSNO or sodium nitrite), transcription of the genes encoding flavohemoglobin and flavorubredoxin (together with that encoding a reductase for flavorubredoxin) was elevated by one order of magnitude more than transcription of any other oxidative stress protection protein, and this induction was norR-dependent, i.e., norR-deficient strains did not show this induction by NO. Sensing of NO in these regulatory proteins is achieved via either S-nitrosylation of cysteine residues or binding to non-heme iron centers.[49]

1.3. The bacterial nitrogen oxide cycle

Under anaerobic conditions, many microorganisms can sustain growth by using nitrate as respiratory terminal electron acceptor.[2,3,86] Much like dioxygen, partially reduced products of nitrate may be toxic to living cells. While respiratory dioxygen reduction delivers all four electrons in one single step (essentially as in reaction 1.5), respiratory nitrate reduction in bacteria and archaea is more complex, proceeding *stepwise* on more than one possible pathway. Bacteria in fact exhibit a wide range of metabolic reactions with various oxides of nitrogen, sometimes referred to as the bacterial nitrogen cycle, which is diagrammed in Figure 1.5.[2-4]

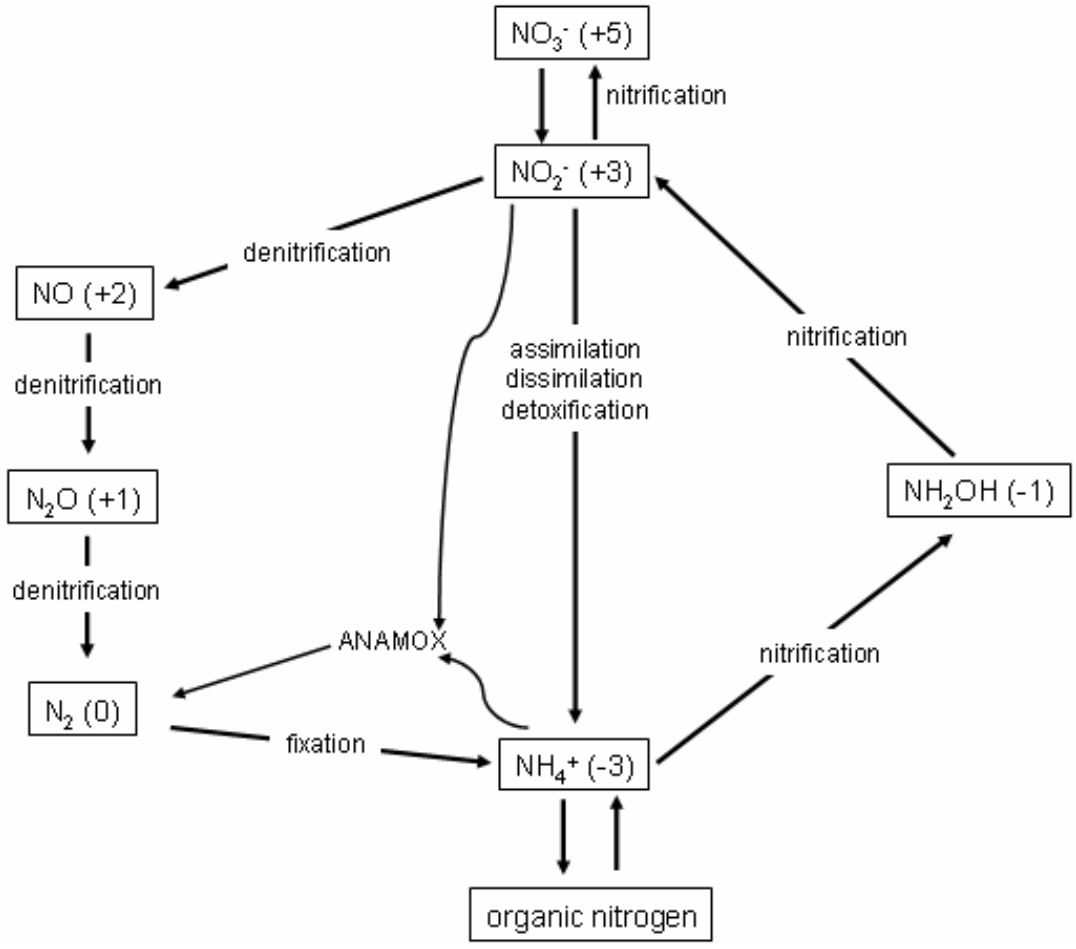

Figure 1.5. Schematic diagram of the bacterial nitrogen cycle, adapted from refs. 2-5. The oxidation states of nitrogen are shown in parentheses for each species.

A few terms commonly used in discussing the bacterial nitrogen cycle are defined as follows.[5] Reduction of nitrogen oxyanions (nitrate, nitrite) via gaseous nitrogen oxides to dinitrogen is termed *denitrification* (a wider definition assumes that *any* process leading to nitrate reduction is denitrifying). The reverse process is called *nitrification*. Nitrate and nitrite may be reduced to ammonia for the purpose of nitrogen *assimilation* (incorporation into organic matter, non-energy conserving) or *dissimilation* (using nitrate as respiratory electron acceptor, i.e., energy-conserving, but without incorporating the final reduced product into organic matter*)*. Reduction of dinitrogen to ammonia is termed nitrogen *fixation*. Finally, ANAMOX is a process proposed to generate molecular nitrogen from nitrate and ammonia. All the known enzymes catalyzing the reactions of the nitrogen cycle are metalloenzymes. [2-5]

Nitrate reduction to nitrite is catalyzed by nitrate reductases, which are molybdopterin enzymes.[2-5] The subsequent reduction of nitrite is catalyzed by two types of nitrite reductases: those reducing nitrite to ammonia (cytochrome *c* nitrite reductase, siroheme-containing nitrite reductase) and those reducing nitrite to nitric oxide (copper-containing nitrite reductase, cytochrome cd_1 nitrite reductase). For those nitrite reductases catalyzing nitrite reduction to ammonia, NO and hydroxylamine are proposed to constitute reaction intermediates, which are never released from the active site.[2-5] In cytochrome *c* nitrite reductase,[2,3,87-89] NO is reduced to NH_4^+ via reaction 1.7, in a mechanism proposed by Einsle and co-workers to involve an $\{FeNO\}^6 \rightarrow \{FeNO\}^7 \rightarrow \{FeNO\}^8$ at the lysine-ligated heme active site.[87] Consistent with this proposal of NO intermediacy, *E. coli* cytochrome *c* nitrite reductase was also shown to effectively protect *E. coli* from NO, implying an NO reductase function for this enzyme under nitrosative stress conditions. On the other hand, cytochrome cd_1 nitrite reductase, which reduces nitrite to NO *in vivo*,[90] can also reduce NO to N_2O (reaction 1.8), but only *in vitro*.[91]

$$6e^- + NO_2^- + 8H^+ \rightarrow NH_4^+ + 2H_2O \quad \text{(cytochrome } c \text{ nitrite reductase)} \quad 1.7$$

$$2e^- + NO + 2H^+ \rightarrow N_2O + H_2O \quad \text{(nitric oxide reductase, NOR)} \quad 1.8$$

The nitrite reductases thus reduce NO either as part of cellular metabolism (cytochrome *c* nitrite reductase), or in physiologically-irrelevant reactions (cytochrome cd_1 nitrite reductase).

When produced by an NO-forming nitrite reductase, nitric oxide is further reduced to N_2O by nitric oxide reductases, which, as discussed below, contain either cytochrome *bd*-or P450-type active sites.[2-5] Nitrous oxide (a relatively inert gas) may either be released as end-product or further reduced to molecular nitrogen by nitrous oxide reductases (which are multinuclear copper proteins).[2-5] Molecular nitrogen is reduced to ammonia by nitrogenases.[2-5] Thus, biological nitrate reduction leads to one of three end-products: ammonia (which may be readily incorporated into organic matter), nitrous oxide, or dinitrogen. Additionally, ANAMOX, a little understood biological process is proposed to generate molecular nitrogen from nitrate and ammonia via hydroxylamine and hydrazine.[2-5]

Nitrification is an oxidative pathway starting from ammonia and also generates partially reduced nitrogen oxides. Thus, oxidation of ammonia to hydroxylamine is catalyzed by ammonia monooxygenase (a little understood enzyme, apparently related to the particulate methane monooxygenase), and is followed by oxidation of hydroxylamine to nitrite by hydroxylamine oxidase (a multiheme enzyme). These oxidations provide electrons necessary for respiratory electron transfer chains that facilitate lithotrophic ("rock-eating", i.e. extracting energy from inorganic compounds) growth.[2-4]

1.4. Canonical (respiratory) nitric oxide reductases

Under anaerobic conditions, the bulk of nitric oxide produced by respiratory denitrification is reductively consumed by nitric oxide reductases (NORs) via reaction 1.7, producing N_2O.[1-4] This reaction is part of the bacterial nitrogen cycle (cf. Figure 1.5), and is catalyzed by two types of respiratory NORs, classified as "bacterial" and "fungal".[1] Perhaps due to the large kinetic stability of the product, N_2O,[92] fungi release nitrous oxide as the final product.[93-97] On the other hand, N_2O produced by bacterial respiratory NOR is further reduced by nitrous oxide reductases to N_2.[1]

The NOR reaction is thermodynamically very favorable at pH 7 (cf. Figure 1.1). The fact that enzymes are required to catalyze this reaction *in vivo* is consistent with a large kinetic barrier. As discussed in Section 1.2, the one-electron reduction of NO to NO^-, which is known to readily dimerize and generate N_2O in a proton-dependent dehydration reaction, is thermodynamically prohibited (unless NO^- is protonated to generate ^1HNO, as discussed in Section 1.2). The NO dimer, $(NO)_2$, is much easier to oxidize than isolated NO but $(NO)_2$ does not normally form under physiological conditions.[73] As shown below, one strategy for NO reduction by NOR employs active sites designed to attract two NO molecules close to each other, perhaps effectively creating an NO dimer – at which point reduction by physiological electron donors becomes more kinetically feasible.

Fungal NORs are the better understood of the two canonical classes of NOR, and knowledge of the fungal NOR mechanism may serve as a guide in understanding the bacterial NOR mechanism. Fungal NORs are soluble proteins that belong to the superfamily of cytochromes P450 and are commonly referred to as P450nor.[1,93-99] The P450nor active site consists of a solvent-exposed, cysteinate-ligated heme. Two possible mechanisms of P450nor–

catalyzed NO reduction are shown in Figure 1.6.[88,100] Binding of NO *trans* to the cysteine ligand at the five-coordinate ferric form of the active site heme iron is followed by reduction of this $\{FeNO\}^6$ complex by NAD(P)H to formally $\{FeNO\}^8$. Subsequent attack of a second molecule of NO leads to formation of a nitrogen-nitrogen bond and liberation of N_2O. Consistent with the mechanism shown in Figure 1.6, a significantly lower K_m has been measured for binding of the first NO molecule (heme-bound) compared to the second NO (for which no binding site has been identified). Besides the starting $\{FeNO\}^6$ species, only one intermediate, absorbing at 444 nm, has been experimentally observed.[99,100]

The details of the P450nor mechanism, and in particular the identity of the 444-nm intermediate, were for a while controversial. The initially proposed mechanism[99,101] (top half of Figure 1.6) involved two sequential one-electron transfers from NAD(P)H to the starting $\{FeNO\}^6$ complex. The resulting $\{FeNO\}^8$ species would constitute the 444-nm intermediate, and would react with NO, eventually liberating the unstable hyponitrite anion, $ONNO^{2-}$ (most probably in its protonated form, $H_2N_2O_2$). Hyponitrite is known to be extremely unstable at neutral pH, decomposing to N_2O and water (but is stable at strongly basic or acidic pHs).[92] The two protons required for hyponitrite protonation are readily accessible at the P450nor active site, which is solvent-exposed and also features proton-donating amino acid side-chains.[94,95] A variation on the $\{FeNO\}^8$ mechanism invoked double protonation of the oxygen atom of the NO ligand, yielding water and an iron-bound nitride ("FeN" in the top half of Figure 1.6).[101]

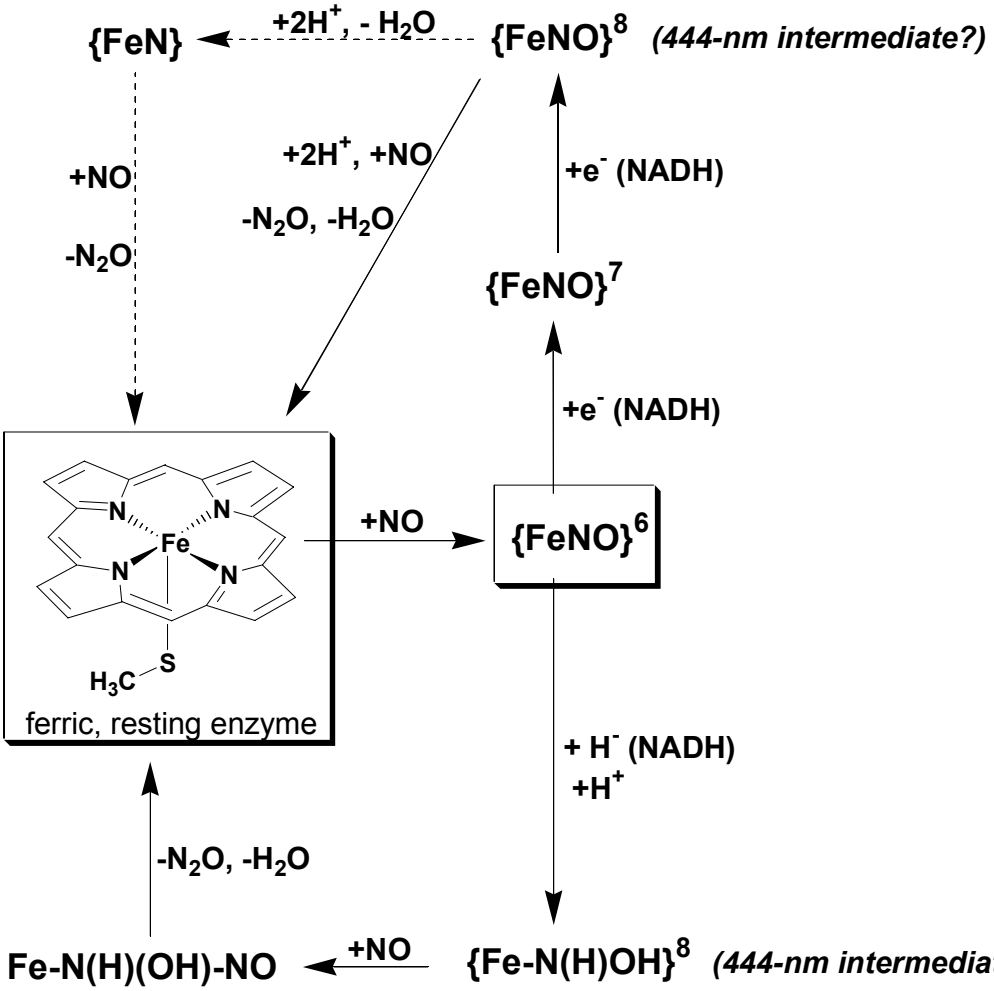

Figure 1.6. Proposed mechanisms for P450nor-catalyzed reduction of NO to N_2O.[88] The formulae of the species unambiguously known to be involved in the catalytic cycle are boxed.

More recent data however support an alternative mechanism (bottom half of Figure 1.6),[88,89,100] in which the first committed step is direct hydride transfer from NAD(P)H to the nitrogen atom of $\{FeNO\}^6$, forming an iron-bound HNO unit, $\{Fe\text{-}(H)NO\}^8$. The latter would undergo protonation to form $\{Fe\text{-}(H)NOH\}^8$, which is favored but not conclusively proven to be the "444-nm intermediate" over the monoprotonated versions, $\{Fe\text{-}(H)NO\}^8$ or $\{FeNOH\}^8$.[88] Subsequent NO addition would yield the unstable HO-N(H)-N=O, which would dissociate from the heme and decompose to H_2O and N_2O. Kinetic isotope effects, using deuterium-substituted NADH, indicated that hydride transfer from NADH to $\{FeNO\}^6$ was involved in the rate-

determining step upon formation of the 444-nm intermediate. Support for this mechanism was the observation that the 444-nm intermediate could be generated by chemical reduction of $\{FeNO\}^6$ with the hydride donor sodium borohydride, or by addition of pulse radiolysis-generated $NHOH^{\cdot}$ radicals to the ferric (resting) form of the active site heme.[100] DFT calculations have subsequently shown that the two-electron (hydride) mechanism is preferred over the initially-proposed one-electron mechanism. A key role was identified for the axial thiolate ligand at the P450nor active site in controlling the mechanism within the framework of a proposed "thiolate obstruction" paradigm ,[88,102] which states that anionic ligands (such as thiolate) inhibit one-electron reduction of heme-NO (or heme-dioxygen) adducts. This inhibition of one-electron reduction avoids entrapment of the P450nor active site as the thermodynamically stable $\{FeNO\}^7$, which is not catalytically competent and which is known to be an inhibited state of P450nor. Thus, to avoid $\{FeNO\}^7$, P450nor reduces $\{FeNO\}^6$ in a two-electron process with NADH.[88]

Bacterial respiratory NORs (BR-NORs) are membrane-bound and closely related to cytochrome oxidases. These NORs are structurally and mechanistically less well-characterized than fungal NOR.[1,3,4] BR-NORs are divided into two sub-classes depending on their proximal electron donor: quinol or cytochrome *c*. The active sites of BR-NORs consist of a heme/non-heme diiron complex. In the di-ferric resting state, the histidine-ligated *b*-type heme iron is proposed to be connected to the non-heme iron via a solvent bridge, which is lost upon reduction. The ligands to the non-heme iron are thought to be mainly nitrogen and oxygen, but their actual number and identity have not been established. The reduced, diferrous, state of the active site reacts with NO to generate N_2O. NO does not bind to the diferric active site except at very high concentrations where NO acts as inhibitor (presumably by binding to the ferric heme). The

electrons required for turnover are supplied either by electron transfer proteins (cytochrome *c*, cupredoxin, or azurin) or by quinones.[1,3,4]

Two different mechanisms have been proposed for catalytic NO reduction by BR-NORs: sequential and dinitrosyl. These mechanisms are illustrated in Figure 1.7. The sequential mechanism would involve attack of free NO on a metal-bound NO, which is either bridging or terminal (cf. Figure 1.7, **A)**. The dinitrosyl mechanism would involve coordination of *both* NO molecules to the active site metal(s) prior to N-N bond formation (cf. Figure 1.7, **B** or **C)**. The two NO molecules could conceivably distribute equally between the heme and non-heme iron, forming a di-$\{Fe\text{-}NO\}^7$ intermediate **B**, or both NOs could coordinate to the non-heme iron (yielding a $\{Fe(NO)_2\}^8$, intermediate **C**. A mechanism involving two NO's binding to the same side of the heme has not been proposed, since cis-$(NO)_2$ heme complexes are not known to exist. The sequential and dinitrosyl mechanisms are both consistent with the reaction shown in Scheme 1.1, involving successive binding of two NO molecules to the active site and nitrogen-nitrogen bond formation in the rate-determining step.[103] Nitric oxide adducts of the heme (S = 1/2 $\{FeNO\}^7$) as well as non-heme (S = 3/2 $\{FeNO\}^7$) ferrous iron at the active site of bacterial NORs have been detected, but it is unclear to what extent these species are formed on the catalytic pathway from NO to N_2O.[103-105]

It is difficult to distinguish between the two alternative mechanisms for BR-NORs, particularly since *both* types are known to be operational in non-enzymatic systems such as Pd, Hg, and activated carbon catalysts.[92] Both mechanisms would, however, require the addition of protons, since H_2O is also a product. The identity of the proton donors in BR-NORs is unknown, mostly because a crystal structure is not available for any protein in this class.

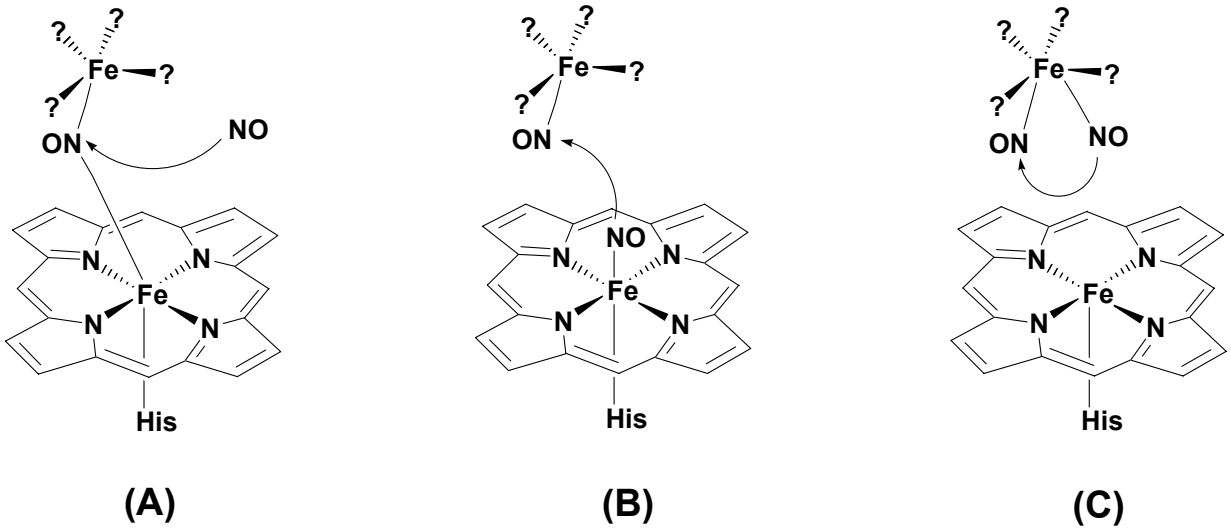

Figure 1.7. Alternative catalytic intermediates proposed for bacterial NORs. The histidine ligand at the heme may or may not be displaced upon NO binding.[104,105]

$$E_{red} + NO \overset{K_1}{\rightleftharpoons} E_{red}\text{-}NO$$

$$E_{red}\text{-}NO + NO \overset{K_2}{\rightleftharpoons} E_{red}\text{-}(NO)_2$$

$$E_{red}\text{-}(NO)_2 \xrightarrow{k_{cat}} E_{ox} + N_2O$$

Scheme 1.1

1.5. Towards a novel class of nitric oxide reductases

The "type A flavoproteins" (FprA) appear to be widespread among bacteria and archaea, with homologs apparently also found in the blood-sucking insect, *Anopheles gambiae* and in some pathogenic protists.[106-108] FprAs contain a flavin-binding site harbored by a C-terminal flavodoxin-like domain, and a set of potential ligands to a diiron site harbored within an N-

terminal metallo-β-lactamase-like domain.[106,109] An alignment of the ~100 FprA amino acid sequences known as of early 2004 is shown in Appendix A.

A summary of the properties of the six FprAs that had been isolated prior to the research described in this thesis is given in Table 1.1, and their amino acid sequence alignment is shown in Figure 1.8. FMN (flavin monoucleotide) was demonstrated to be a cofactor in all cases, but reported metal contents have been variable. Some FprAs contain an extra electron-transfer domain fused to the C-terminus. Thus, the *Synechocystis* FprA[106] contains an extra FAD (flavin adenine dinucleotide) cofactor, and the *E. coli* FprA was named flavorubredoxin (FlRd) because of its C-terminal rubredoxin-like domain.[106] Appendix A in fact shows that ~50% of the known FprA amino acid sequences contain extra C-terminal polypeptide stretches suggestive of an additional cofactor (either flavin or rubredoxin).

D. gigas ROO, an FprA that had initially been found to exhibit rubredoxin:oxygen oxidoreductase activity *in vitro*,[51,55,56] was reported to contain heme cofactors in solution but not in crystalline state.[110] The crystal structure of *D. gigas* ROO showed no obvious heme binding sites. Until the crystal structure of *D. gigas* ROO[110] became available, no non-heme iron had been reported in any FprA other than in *E. coli* FlRd.[106] The *D. gigas* ROO crystal structure, however, revealed the presence of a non-heme diiron site in the metallo-β-lactamase domain, the ligands for which are indicated in Figures 1.8 and 1.9.[110] Following this report, the *Synechocystis* and *E. coli* FprA were revisited, and found to contain an excess of ~2 Fe/monomer, thus implicating a diiron site in those proteins as well.[111,112] Conceivably, the *M. thermoautotrophicum* and *R. capsulatus* FprAs listed in Table 1.1 may also contain a diiron cofactor.

Table 1.1 Main characteristics of previously characterized FprAs.[a]

Organism	Name proposed	Cofactors	*In vitro* reactivity	*In vivo* properties	Crystal structure
Desulfovibrio gigas	Rubredoxin oxygen oxidoreductase (ROO)[55,56]	FMN 2 Fe 2 hemes[55,56,110]	O_2 reductase[55,56]	Not reported	yes[110]
Moorella thermoacetica	FprA[113]	FMN Fe	Not reported	Not reported	no
Methanobacterium thermoautotrophicum	Flavoprotein A[106,114]	FMN	e^- transfer?	Induced by iron limitation	no
Rhodobacter capsulatus	FprA[106,115]	FMN	e^- transfer	*Not* involved in iron limitation or oxidative stress?	no
Escherichia coli	flavorubredoxin[106,112]	FMN 2 Fe Fe(SCys)$_4$	O_2 reductase, NO reductase	NO reductase	no
Synechocystis sp. PCC 6803	ATF[106,111]	FMN FAD 2 Fe	O_2 reductase	Not reported	no

[a]All six FprAs listed in Table 1.1 were reported to be homodimers in solution with the exception of *E. coli* FlRd (homotetramer).

```
Moorella          -----------------MSQPVAITDGIYWVGAVDWNIRYFHGPAFSTHRGTTYNAYLIV
D. gigas          -----------------MQATKIIDGFHLVGAIDWNSRDFHGYTLSP-MGTTYNAYLVE
E. coli           -------------------MSIVVKNNIHWVGQRDWEVRDFHGTEYKTLRGSSYNSYLIR
Methanobacterium  ----------------MKARAEKIADGLYWTGVLDWDIRNYHGYTLQG---TTYNAYLVF
Rhodococcus       MSVPPFTIRPAAPRLDGPTGPVAVAPGVHWVGALDPGLRNFDVILKTAN-GTTYNAYAVR
Synechocystis     -----MFTTPLPPQKRLSTQTEAIAKNITAIRSLDWD-RDRFDIEFGLQNGTTYNSYLIQ
                                       .  :  ..      *   *            ::**:* :

Moorella          -DDKTALVDTVYEPFKEELIAKLKQIKDPV----KLDYLVVNHTESDHAGAFPAIMELCP
D. gigas          -DEKTTLFDTVKAEYKGELLCGIASVIDPK----KIDYLVIQHLELDHAGALPALIEACQ
E. coli           -EEKNVLIDTVDHKFSREFVQNLRNEIDLA----DIDYIVINHAEEDHAGALTELMAQIP
Methanobacterium  GDEGVALIDNSYPGTFQELMARMEDAFNREGREMRVDFIVQNHVERDHSGVLVELHRRFP
Rhodococcus       GSEGVAVIDTVKAEFAGDFFARLEAVARYD----EIRLIVLNHLEPDHTGAVPELLRRAP
Synechocystis     -ADKVALVDSSHEKFRQLYLDLLQGLIDPQ----RIDYLIVSHTEPDHSGLVKDILQLNP
                   :  .:.*.          .  :             :  :: .* * **:* .  :
```

```
Moorella          DAHVLCTQRAFDSLKAHYSHID--FNYTIVKTGTSVSLGK-RSLTFIEAPMLHWPDSMFT
D. gigas          PEKIFTSSLGQKAMESHFHYKD--WPVQVVKHGETLSLGK-RTVTFYETRMLHWPDSMVS
E. coli           DTPIYCTANAIDSINGHHHHPE--WNFNVVKTGDTLDIGNGKQLIFVETPMLHWPDSMMT
Methanobacterium  EAEIHCTEVAVEGLLKHYPALEG-TEFRTVKTGDSIDLGG-RTLTFLEAPLLHWPDSMFT
Rhodococcus       QAQVRLSPRGLPMLRALLKDDFERYDIKGVTTGQSVSLGD-RDLQFFTTPFVHWPDTQCT
Synechocystis     RITVVATKVALQFLDNFVHQPF---ERIQVKSGDRLDLGQGHDLEFVSAPNLHWPDTMLT
                    :  :  .   :               *. *  :.:*  : : *  :  :****:  :

Moorella          YVPEEALLLPNDAFGQHIATSVRFDDQVDAGLIMDEAAKYYANILMPFSNLITKKLDEIQ
D. gigas          WFADEKVLISNDIFGQNIAASERFSDQIPVHTLERAMREYYANIVNPYAPQTLKAIETLV
E. coli           YLTGDAVLFSNDAFGQHYCDEHLFNDEVDQTELFEQCQRYYANILTPFSRLVTPKITEIL
Methanobacterium  FL-DTGILFSNDAFGQHLCYPQRLDTEIPEYILMDAAKKFYANLITPLSKLVLRKFDEVK
Rhodococcus       WLAAERVLFTCDLFGSHYCDGRLFNDLVGDFRFS--FEYYFDRIMRPFRSFVAQALDLIE
Synechocystis     YDPATEILFTCDVFGMHYCSDAVFD--IDLGKIAPDYQFYYDCLMGPNARSVLAAMKRMD
                 :     :*:. * ** : .    :.  :    :      ::  :: *        :  :

Moorella          KINLA--IKTIAPSHGIIWR--K----DPGRIIEAYARWAEG--QGKAKAVIAYDTMWLS
D. gigas          GAGVA--PEFICPDHGVIFRGAD----QCTFAVQKYVEYAEQ--KPTNKVVIFYDSMWHS
E. coli           GFNLP--VDMIATSHGVVWR--D----NPTQIVELYLKWAAD--YQEDRITIFYDTMSNN
Methanobacterium  ELGLLDKIGMIAPSHGQIWT-------EPMKIIEAYTAWATG--KVKKKVTVIYDTMHHS
Rhodococcus       PLDFG----IIAPAHGPILRSHPRDYLTHTRRLISSRLAAET--GSEKTLLIFYVSAYGA
Synechocystis     NLGTIS---TVANGHGPLLR------HNVGELLHRYRHWSESQSKAEKTVVVFYVADYGY
                   .       :.  ** :              :      :           : * :

Moorella          TEKMAHALMDGLVAGG--CEVKLFKLSVSDRNDVIKEILDARAVLVGSPTINNDILPVVS
D. gigas          TEKMARVLAESFRDEG--CTVKLMWCKACHHSQIMSEISDAGAVIVGSPTHNNGILPYVA
E. coli           TRMMADAIAQGIAETDPRVAVKIFNVARSDKNEILTNVFRSKGVLVGTSTMNNVMMPKIA
Methanobacterium  TAMMAHAIAEGAMSEG--ADVRVYYLHEDDRSEIVKDILDSHAIALGAPAIYDEPYPSVG
Rhodococcus       TAQLAQAIHDGAAESP-DVRVSLFDLEGGEITPFLDLIEEADGIALGTPTINGDAVRTIW
Synechocystis     GDRLSQAIAKGITKTG--VGVDMVDLSSADPQEIQELVGHASGVVLGMPPLQANADLSTN
                    :: .: ..         * :      .   .   :  : .: :* ..

Moorella          PLLDDLVGLRPK---NKVGLAFGAYGWGGGAQKILEERLKAAKIELIAEPGPTVQWVPRG
D. gigas          GTLQYIKGLRPQ---NKIGGAFGSFGWSGESTKVLAEWLTGMGFDMPATP-VKVKNVPTH
E. coli           GLVEEMTGLRFR---NKRASAFGSHGWSGGAVDRLSTRLQDAGFEMSLSL--KAKWRPDQ
Methanobacterium  DLLMYLRGLKFNRTGQRRAMVFGSMGGRGGATGTMQKLLADAGFDVMEAD--EIYYVPNN
Rhodococcus       EMLAALVDIETR---GKLGAAFGSYGWSGEAVRLVETRLQGLKMRLPEPG-LRVKLHPSA
Synechocystis     -FGAVLAAMQPK----QVFGLYESYGGDDEPIDPLRTKFLDLGLREAFKV-IKVKDTPSE
                      :  :. .    :    : : *  . .   :   :    :             *

Moorella          EDLQRCYELGRKIA-----ARIAD-----------------------------------
D. gigas          ADYEQLKTMAQTIARAL-KAKLAA-----------------------------------
E. coli           DALKLCREHGREIARQWALAPLPQSTVNTVVKEETSA--------TTTADLGPRMQCSVC
Methanobacterium  EELDACFEAGRRLAG-----DLNE-----------------------------------
Rhodococcus       AELKEGRAFGRRLADHLTGRAAPREVDFAEIAAR-------------------------
Synechocystis     STYQLCDESGTDLGQNLIQAAKIKQLKSLDSDLEKAIGRISGGLYIITAQKGEVKGAMLA
                    .     .  :.

Moorella          ------------------------------------------------------------
D. gigas          ------------------------------------------------------------
E. coli           QWIYDPAKGEPMQDVAPGTPWSEVPDNFLCPECSLGKDVFEELASEAK------------
Methanobacterium  ------------------------------------------------------------
Rhodococcus       ------------------------------------------------------------
Synechocystis     SWVSQASFNPPGFTVAVAKDRAIESLMQVGDRFVLNILEEGNYQILMKHFLKRFPPGADR
```

```
Moorella         ------------------------------------------------------------
D. gigas         ------------------------------------------------------------
E. coli          ------------------------------------------------------------
Methanobacterium ------------------------------------------------------------
Rhodococcus      ------------------------------------------------------------
Synechocystis    FAGVKTQTASNGSPILTDALAYLECEVASRMECSDHWIVYSQVTNGRVAKAEGLTAVHHR

Moorella             ------
D. gigas             ------
E. coli              ------
Methanobacterium     ------
Rhodococcus          ------
Synechocystis        KVGNYY
```

Figure 1.8. CLUSTAL-W[116] amino sequence alignment of the FprAs listed in Table 1. Proposed diiron ligand residues are shown in red, flavin binding[110] residues are shown in orange. '*' indicates positions which have a single, fully conserved residue; ':' indicates that one of the following 'strong' groups is fully conserved: STA, NEQK, NHQK, NDEQ, QHRK, MILV, MILF, HY, FYW; '.' indicates that one of the following 'weaker' groups is fully conserved: CSA, ATV, SAG, STNK, STPA, SGND, SNDEQK, NDEQHK, NEQHRK, FVLIM, HFY. The C-termini (~last four rows of the alignment) of *E. coli* flavorubredoxin and *Synechocystis* FprA exhibit no sequence homology to each other, since one encodes a rubredoxin and the other encodes a flavodoxin domain.

The crystal structure of the *D. gigas* ROO[110] is shown in Figure 1.9. The protein crystallized as a head-to-tail dimer, with the metallo-β-lactamase-like domain of one monomer next to the flavodoxin-like domain of the other monomer with FMN-diiron pairs at the subunit interfaces. Neither the FMN cofactors nor the diiron sites are directly solvent accessible. The closest ligand of the diiron site is ~4 Å away from the nearest FMN atom. The histidine and carboxylate ligands to the irons are characteristic of non-heme diiron sites in other enzymes, but the stoichiometry, namely, three histidines and three carboxylates per diiron site, is unique. For comparison, the diiron sites in O_2-activating enzymes (methane monooxygenase, ribonucleotide reductase) contain two histidine and four carboxylate ligands.[40] Rubrerythrin (a peroxidase) redox cycles between a 2-His/4-carboxylate and a 1-His/5-carboxylate diiron site.[117] Hemerythrin, which reversibly binds dioxygen, features a 5-His/2-carboxylate coordination.[118]

The unique ligand-diiron stoichiometry is perhaps reflected in the lack of any detectable amino acid sequence homology between FprAs and the other diiron proteins. One of the two iron atoms at the *D. gigas* ROO diiron site has an unusual square-planar coordination, with a water and a putative dioxygen molecule present at the axial positions, the latter with its oxygens at 2.4 Å and 2.6 Å away from the two irons. The presence of a dioxygen molecule near the iron is mostly speculative due to the low resolution (2.5 Å) of the crystal structure. The oxidation states of the irons in this crystal structure were assumed (but not known) to be Fe(III). Fe(III)-dioxygen adducts are not known in biology, but the putative presence of such an adduct in *D. gigas* ROO was taken as an important mechanistic clue for the proposed oxidase function of this enzyme.[110]

Following an initial report on the dioxygen reductase activity of *D. gigas* ROO[55,56] and the proposal that FprA/ROO's act as energy-conserving dioxygen reductases, oxidase activity (reaction 1.5) was detected *in vitro* for other FprAs, but not for those where the protein contained no iron (cf. Table 1). Involvement of at least the oxidase-active FprAs in oxidative stress defense was a tempting hypothesis, especially since the organisms containing them were either obligate or facultative anaerobes.[51] Transcription of a gene encoding an FprA in the obligate anaerobe, *C. perfringens,* has recently been shown to be induced by exposure to air;[119] on the other hand, transcription of the flavorubredoxin gene from the facultative anaerobe, *E. coli,* was reported to be repressed under aerobic growth conditions.[120] *M. thermoautotrophicum* FprA was found to be induced by iron limitation, conditions under which an electron-transfer protein, polyferredoxin, was repressed. Based on this observation, together with the ability of this FprA to accept electrons derived from molecular hydrogen in the presence of native hydrogenase components, it was suggested that this FprA could be an electron transport protein.[106,114] In *R. capsulatus* (a facultative anaerobe) the FprA gene is found in a *nif*-regulated operon, linking FprA to nitrogen

fixation metabolism.[115] A *R. capsulatus* ΔFprA mutant showed essentially no significant sensitivity to iron limitation or to microaerobic growth conditions. A slight decrease in nitrogenase activity was detected in the mutant compared to the wild-type strain, but the magnitude of the difference was considered too small to be physiologically relevant.

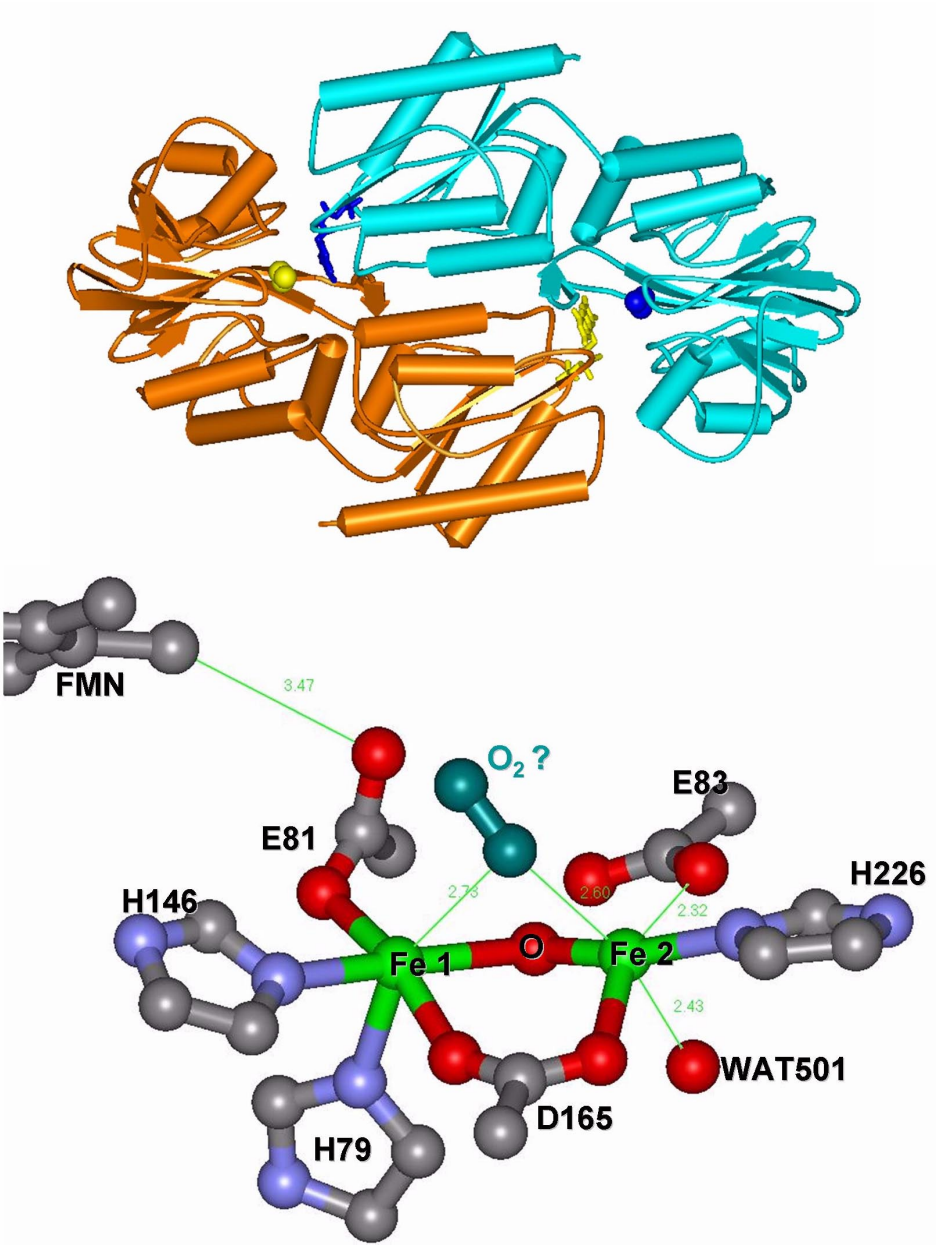

Figure 1.9. Crystal structure of *D. gigas* ROO (pdb code 1E5D).[110] Top: the homodimer viewed along the two-fold rotation axis. The two monomers are shown in blue and orange and cofactors are shown in purple or yellow. Bottom: diiron site and portion of the FMN. Drawings were rendered in Viewerlite.

A clue to the function of at least some FprAs was the observation that transcription of the *E. coli* flavorubredoxin gene, *flRd*, could be induced by exogenous nitric oxide, sodium nitroprusside, or nitrite, and that the *flRd* transcription level was elevated under anaerobic vs. aerobic growth conditions even in the absence of exogenous NO.[36,50,120] An *E. coli* mutant strain (ΔFlRd) containing a disrupted FlRd gene showed impaired growth upon anaerobic exposure to nitric oxide and exhibited lower whole-cell NOR activity than the wild-type. This ΔFlRd strain was protected against NO-induced killing by a plasmid containing the FlRd gene.[50] The accumulated genetic evidence thus established *E. coli* flavorubredoxin as the first representative of a new class of nitric oxide reductases. Purified *E. coli* flavorubredoxin was subsequently shown to have NOR activity with a low reported K_m for NO (> 1 μM), by the same group that had previously reported it to be a dioxygen reductase.[58] A similarly low K_m was inferred from NO uptake measurements with intact *E. coli* cells.[50] The diiron site was proposed to be the site of NO reduction,[50,58] but there was no direct evidence for involvement of the diiron site in the NOR activity. At the start of this research, NOR activity had not been reported for any other FprA, including the *D. gigas* ROO, and the mechanism of NO reduction by FprAs was unknown. Also, while the stoichiometry of 1 NADH oxidized to 2 NO reduced suggested that N_2O was the product of NO reduction by flavorubredoxin, this N_2O was in fact never experimentally observed.[58]

1.6. The OSP cluster of *Moorella thermoacetica*

Moorella thermoacetica (formerly, *Clostridium thermoaceticum*[121]), originally isolated from horse manure, is the most thoroughly studied member of the acetogens, a group of gram-positive, obligately anaerobic bacteria found in virtually any anoxic environment.[122-124] *M.*

thermoacetica is also thermophilic, growing optimally at 58 °C. For many years it was believed that *M. thermoacetica* could use only carbon dioxide as terminal electron acceptor and that the conversion of carbon dioxide into acetate via the Wood-Ljungdahl pathway was obligatory for growth and survival of this bacterium.[123,124] In the Wood-Ljungdahl (a.k.a., acetyl-CoA) pathway, one-carbon molecules such as CO_2 or its partially-reduced congeners can be converted to methyl groups and attached to a (CO_2-derived) CO moiety to generate acetyl-CoA and eventually acetate (hence the name "acetogen"). This respiratory process assimilates inorganic carbon, and the flow of electrons from a reducing substrate (e.g., H_2) to the Wood-Ljungdahl pathway generates a chemiosmotic gradient which allows ATPase-dependent energy generation.[124]

Recent studies indicate that, when given a choice, *M. thermoacetica* will use nitrate preferentially over carbon dioxide as respiratory electron acceptor via an apparently dissimilatory pathway with a variety of small carbon compounds as electron donors.[86,125,126] Thus, *M. thermoacetica* must be able to cope with lower nitrogen oxides (i.e., nitrosative stress), generated either endogenously via the reductive enzymatic or non-enzymatic side-reactions of nitrite or exogenously. The latter may well be unavoidable when growing in a nitrate-rich ecosystem, especially in view of the redox potentials listed in Figure 1.1 for species involved in the biological nitrogen cycle. The enzymes responsible for nitrate and nitrite reduction in *M. thermoacetica* have not been identified. A search of the *M. thermoacetica* genome sequence (www.ncbi.nlm.nih.gov) reveals the presence of a canonical nitrate reductase subunit homolog (a *b*-type cytochrome, involved in electron transfer, accession number GI:49237230), but no putative proteins are annotated as the other subunits of the nitrate reductase, or as reductases for nitrite, nitric oxide, or nitrous oxide. However, the gene encoding a putative protein annotated as

sulfite reductase (siroheme-containing, accession number GI:49237228) is located next to that for the nitrate reductase *b*-type cytochrome and could conceivably function as the dissimilatory nitrite reductase, since *M. thermoacetica* is not known to utilize sulfate as electron acceptor.[127]

In 2001 the Kurtz and Ljungdahl groups at the University of Georgia reported a five-gene "oxidative stress protection" (OSP) cluster in *M. thermoacetica* (cf. Figure 1.10).[113] This OSP cluster contains two operons: one with genes encoding a superoxide reductase (*rbo*) and rubredoxin (*rub*), and a second with genes encoding rubrerythrin (*rbr*), an FprA (*fprA*) and a high-molecular weight rubredoxin (*hrb*). Consistent with the organization shown in Figure 1.10, Northern blot analysis showed *rbr-fpra-hrb, fprA-hrb*, and *rbo-rub* transcripts. Purified recombinant *M. thermoacetica* Rbr and Rd had properties that were very similar to those of previously characterized homologues. Together with the presence of the SOR homolog, *rbo*, these results suggested involvement of the entire OSP cluster in oxidative stress protection (cf. Section 1.2).[113]

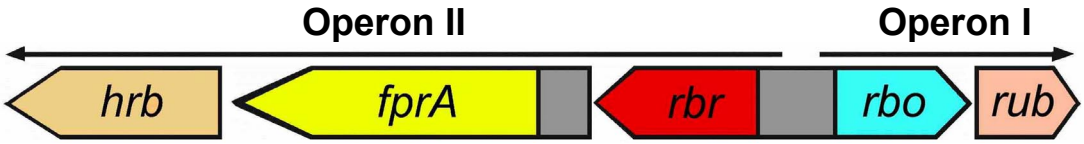

Figure 1.10. The OSP gene cluster of *M. thermoacetica*. Arrow-heads indicate direction of transcription. Gray areas indicate intergenic regions containing possible transcriptional promoter sites.[113]

In this initial study by the Kurtz and Ljungdahl groups the recombinant *M. thermoacetica* FprA was isolated as a homodimer, as expected from the *D. gigas* ROO crystal structure (cf. Figure 1.9), but contained sub-stoichiometric amounts of FMN and iron. The Hrb was not isolated. The structures and reactivities of the *M. thermoacetica* FprA and Hrb thus remained unknown. While clues to FprA structure and reactivity could be drawn from comparisons with

previously characterized homologues (discussed above), Hrb appeared to be the first representative of a novel class of proteins containing a rubredoxin domain and another unidentified domain. Since Hrb and FprA were co-transcribed, the obvious implication was that Hrb functions as redox partner to FprA, analogously to rubredoxin (encoded by *rub*) donating electrons to 2Fe-SOR (encoded by *rbo*).[113] Reported herein are the results of efforts to characterize the two less understood components of the *M. thermoacetica* OSP cluster, FprA and Hrb. Their biochemical characterization, *in vivo* and *in vitro* reactivity, kinetics analyses, as well as structural characterization of the FprA are reported. Also reported are isolation and characterization of an FprA from the sulfate-reducing bacterium, *Desulfovibrio vulgaris*.[128] Characterizations of the *M. thermoacetica* and *D. vulgaris* FprAs may contribute towards an understanding of the structural and functional variability among FprAs, particularly the apparent O_2 reductase/NOR dichotomy.

1.7. References

(1) Hendriks, J.; Oubrie, A.; Castresana, J.; Urbani, A.; Gemeinhardt, S.; Saraste, M. *Biochim. Biophys. Acta* **2000**, *1459*, 266-273.

(2) Berks, B. C.; Ferguson, S. J.; Moir, J. W. B.; Richardson, D. J. *Biochim Biophys Acta* **1995**, *1232*, 97-173.

(3) Watmough, N. J.; Butland, G.; Cheesman, M. R.; Moir, J. W. B.; Richardson, D. J.; Spiro, S. *Biochim. Biophys. Acta* **1999**, *1411*, 456-474.

(4) Richardson, D. J.; Watmough, N. J. *Curr. Opinion Chem.Biol.* **1999**, *3*, 207-219.

(5) Zumft, W. G. *Microbiol. Mol. Biol. Rev.* **1997**, *61*, 533-616.

(6) Cooper, C. E. *Biochim. Biophys. Acta* **1999**, *1411*, 290-309.

(7) Butler, A. R.; Flitney, F. W.; Williams, D. L. *Trends Pharmacol. Sci.* **1995**, *16*, 18-22.

(8) Butler, A. R.; Megson, I. L. *Chem. Rev.* **2002**, *102*, 1155-1166.

(9) Ford, P. C.; Lorkovic, I. M. *Chem.Rev.* **2002**, *102*, 993-1018.

(10) Hayton, T. W.; Legzdins, P.; Sharp, W. B. *Chem. Rev.* **2002**, *102*, 935-992.

(11) Wasser, I. M.; de Vries, S.; Moenne-Loccoz, P.; Schroeder, I.; Karlin, K. D. *Chem. Rev.* **2002**, *102*, 1201-1234.

(12) Wyllie, G. R. A.; Scheidt, W. R. *Chem. Rev.* **2002**, *102*, 1067-1090.

(13) Bard, A. J.; Parsons, R.; Jordan, J. *Standard potentials in aqueous chemistry, Marcel Dekker, New York, 1985*.

(14) McCleverty, J. A. *Chem. Rev.* **2004**, *104*, 403 -418.

(15) Tocheva, E. I.; Rosell, F. I.; Mauk, A. G.; Murphy, M. E. *Science* **2004**, *304*, 867-870.

(16) Enemark, J. H.; Feltham, R. D. *Coord. Chem. Rev.* **1974**, *13*, 339.

(17) Brown, C. A.; Pavlovski, M. A.; Westre, T. E.; Zhang, Y.; Hedman, B.; Hodgson, K. O.; Solomon, E. I. *J. Am. Chem. Soc.* **1995**, *117*, 715-732.

(18) Chiou, Y.-M.; Que, L., Jr. *Inorg. Chem.* **1995**, *34*, 3270-3278.

(19) Clay, M. D.; Cosper, C. A.; Jenney, F. E.; Adams, M. W. W.; Johnson, M. K. *Proc. Natl. Acad. Sci. USA* **2003**, *100*, 3796-3801.

(20) Coufal, D. E.; Tavares, P.; Pereira, A. S.; Huynh, B. H.; Lippard, S. J. *Biochemistry* **1999**, *38*, 4504-4513.

(21) Feig, A. L.; Bautista, M. T.; Lippard, S. J. *Inorg. Chem.* **1996**, *35*, 6892-6898.

(22) Haskin, C. J.; Ravi, N.; Lynch, J. B.; Munck, R.; Que, L., Jr. *Biochemistry* **1995**, *34*, 11090-11098.

(23) Hodges, K. D.; Wollman, R. G.; Kessel, S. L.; Hendrickson, D. N.; Van Derveer, D. G.; Barefield, E. K. *J. Am. Chem. Soc.* **1979**, *101*, 906-917.

(24) Jackson, T. A.; Yikilmaz, E.; Miller, A. F.; Brunold, T. C. *J. Am. Chem. Soc.* **2003**, *125*, 10833-10845.

(25) Kelm, M. *Biochim. Biophys. Acta* **1999**, *1411*, 273-289.

(26) LeBrun, N. E.; Andrews, S. C.; Moore, G. R.; Thomson, A. J. *Biochem. J.* **1997**, *326*, 173-179.

(27) Li, M.; Bonnet, D.; Bill, E.; Neese, F.; Weyhermuller, T.; Blum, N.; Sellman, D.; Wieghardt, K. *Inorg. Chem.* **2002**, *41*, 3444-3456.

(28) Lopes, L. G. F.; Sousa, E. H. S.; Miranda, J. C. V.; Oliveira, C. P.; Carvalho, I. M. M.; Batista, A. A.; Ellena, J. J.; Castellano, E. E.; Nascimento, O. R.; Moreira, I. S. *J. Chem. Soc., Dalton Trans.* **2002**, 1903-1906.

(29) Pohl, K.; Wieghardt, K.; Nuber, B.; Weiss, J. *J. Chem. Soc., Dalton Trans.* **1987**, 187.

(30) Ray, M.; Golombek, A. P.; Hendrich, M. P.; Glenn, P. A. Y.; Liable-Sands, L. M.; Rheingold, A. L.; Borovik, A. S. *Inorg. Chem.* **1999**, *38*, 3110-3115.

(31) Roach, P. L.; Clifton, I. J.; Hensgens, C. M.; Shibata, N.; Schofield, C. J.; Hajdu, J.; Baldwin, J. E. *Nature* **1997**, 827.

(32) Yang, T.-C.; Wolfe, M.; Neibergall, M. B.; Mekmouche, Y.; Lipscomb, J. D.; Hoffman, B. M. *J. Am. Chem. Soc.* **2003**, *125*, 2034-2035.

(33) Zhang, Z.; Ren, J.; Harlos, K.; McKinnon, C. H.; Clifton, I. J.; Schofield, C. J. *FEBS Lett.* **2002**, *517*, 7-12.

(34) Rodriguez, J. H.; Xia, Y. M.; Debrunner, P. G. *J. Am. Chem.Soc.* **1999**, *121*, 7846-7863.

(35) Silaghi-Dumitrescu, R.; Kurtz , D. M., Jr. *Chemtracts Inorg. Chem.* **2003**, *16*, 468-473.

(36) Hutchings, M. I.; Mandhana, N.; Spiro, S. *J. Bacteriol.* **2002**, *184*, 4640-4643.

(37) Wang, P. G.; Xian, M.; Tang, X.; Wu, X.; Wen, Z.; Cai, T.; Janczuk, A. J. *Chem. Rev.* **2002**, *102*, 1091 - 1134.

(38) Nocek, J. M.; Kurtz, D. M., Jr.; Sage, J. T.; Xia, Y. M.; Debrunner, P.; Shiemke, A. K.; Sanders-Loehr, J.; Loehr, T. M. *Biochemistry* **1988**, *27*, 1014-1024.

(39) Nocek, J. M.; Kurtz, D. M., Jr.; Pickering, R. A.; Doyle, M. P. *J Biol Chem.* **1984**, *259*, 12334-12338.

(40) Wallar, B. J.; Lipscomb, J. D. *Chem. Rev.* **1996**, *96*, 2625-2657.

(41) Hogbom, M.; Huque, Y.; Sjoberg, B. M.; Nordlund, P. *Biochemistry* **2002**, *41*, 1381-1389.

(42) Solomon, E. I.; Brunold, T. C.; Davis, M. I.; Kemsley, J. N.; Lee, S.-K.; Lehnert, N.; Neese, F.; Skulan, A. J.; Yang, Y.-S.; Zhou, J. *Chem. Rev.* **2000**, *100*, 235-350.

(43) Garcia-Serres, R. G.; Grapperhaus, C. A.; Bothe, E.; Bill, E.; Weyhermuller, T.; Neese, F.; Wieghardt, K. *J. Am. Chem. Soc.* **2004**, *126*, 5138-5153.

(44) Hauser, C.; Glasser, T.; Bill, E.; Weyhermuller, T.; Wieghardt, K. *J. Am. Chem. Soc.* **2000**, *122*, 4352-4365.

(45) Lebrero, M. C. G.; Scherlis, D. A.; Estiu, G. L.; Olabe, J. A.; Estrin, D. A. *Inorg. Chem.* **2001**, *40*, 4127.

(46) Sulc, F.; Immoos, C. E.; Pervitsky, D.; Farmer, P. J. *J. Am. Chem. Soc.* **2004**, *126*, 1096-1101.

(47) D'Autréaux, B.; Horner, O.; Oddou, J. L.; Jeandey, C.; Gambarelli, S.; Berthomieu, C.; Latour, J. M.; Michaud-Soret, I. *J. Am. Chem. Soc.* **2004**, *126*, 6005-6016.

(48) D'Autreaux, B.; Touati, D.; Bersch, B.; Latour, J.-M.; Michaud-Soret, I. *Proc. Natl. Acad. Sci. USA* **2002**, *99*, 16619-16624.

(49) Mukhopadhyay, P.; Zheng, M.; Bedzyk, L. A.; Larossa, R. A.; Storz, G. *Proc. Natl. Acad. Sci. USA* **2004**, *101*, 745-750.

(50) Gardner, A. M.; Helmick, R. A.; Gardner, P. R. *J. Biol. Chem.* **2002**, *277*, 8172-8177.

(51) Kurtz, D. M., Jr.; Coulter, E. D. *Chemtracts Inorg. Chem.* **2001**, *14*, 407-435.

(52) Valentine, J.; Wertz, D.; Lyons, T.; Liou, L.; Goto, J.; Gralla, E. *Curr. Opinion Chem.Biol.* **1998**, *2*, 253-262.

(53) Lumppio, H.; Shenvi, N.; Summers, A.; Voordouw, G.; Kurtz, D. M., Jr. *J. Bacteriol.* **2001**, *183*, 101-108.

(54) Jenney, F. J.; Verhagen, M.; Cui, X.; Adams, M. *Science* **1999**, *286*, 306-308.

(55) Chen, L.; Liu, M. Y.; LeGall, J.; Fareleira, P.; Santos, H.; Xavier, A. V. *Biochem. Biophys. Res. Commun.* **1993**, *193*, 100-105.

(56) Chen, L.; Liu, M. Y.; Legall, J.; Fareleira, P.; Santos, H.; Xavier, A. V. *Eur. J. Biochem.* **1993**, *216*, 443-448.

(57) Gomes, C. M.; Silva, G.; Oliveira, S.; LeGall, J.; Liu, M. Y.; Xavier, A. V.; Rodrigues-Pousada, C.; Teixeira, M. *J. Biol. Chem.* **1997**, *272*, 22502-22508.

(58) Gomes, C. M.; Giuffre, A.; Forte, E.; Vicente, J. B.; Saraiva, L. M.; Brunori, M.; Teixeira, M. *J. Biol. Chem.* **2002**, *277*, 25273-25276.

(59) Ridnour, L. A.; Thomas, D. D.; Mancardi, D.; Espey, M. G.; Miranda, K. M.; Paolocci, N.; Feelisch, M.; Fukuto, J.; Wink, D. A. *Biol Chem.* **2004**, *385*, 1-10.

(60) Anjum, M. F.; Stevanin, T. M.; Read, R. C.; Moir, J. W. *J. Bacteriol.* **2002**, *184*, 2987-2993.

(61) Poock, S. R.; Leach, E. R.; Moir, J. W.; Cole, J. A.; Richardson, D. J. *J. Biol. Chem.* **2002**, *277*, 23664-23669.

(62) Frey, A. D.; Farres, J.; Bollinger, C. J.; Kallio, P. T. *Appl. Environ. Microbiol.* **2002**, *68*, 4835-4840.

(63) Li, H.; Samouilov, A.; Liu, X.; Zweier, J. L. *Biochemistry* **2003**, *42*, 1150-1159.
(64) Alderton, W. K.; Cooper, C. E.; Knowles, R. G. *Biochem. J.* **2001**, *357*, 593-615.
(65) Domitrovic, T.; Palhano, F. L.; Barja-Fidalgo, C.; DeFreitas, M.; Orlando, M. T. D.; Fernandes, P. M. B. *FEMS Yeast Res.* **2003**, *1560*, 1-6.
(66) Cutruzzola, F. *Biochim. Biophys. Acta* **1999**, *1411*, 231-249.
(67) Woodmansee, A. N.; Imlay, J. A. *Mol. Microbiol.* **2003**, *49*, 11-22.
(68) Gardner, A. M.; Gardner, P. R. *J. Biol. Chem.* **2002**, *277*, 8166-8171.
(69) Mallis, R. J.; Thomas, J. A. *Arch. Biochem. Biophys.* **2000**, *383*, 60-69.
(70) Liu, L.; Hausladen, A.; Zeng, M.; Que, L.; Heitman, J.; Stamler, J. S. *Nature* **2001**, *410*, 490-494.
(71) Miranda, K. M.; Nims, R. W.; Thomas, D. D.; Espey, M. G.; Citrin, D.; Bartberger, M. D.; Paolocci, N.; Fukuto, J. M.; Feelisch, M.; Wink, D. A. *J. Inorg. Biochem.* **2003**, *93*, 52-60.
(72) Hughes, M. N. *Biochim. Biophys. Acta* **1999**, *1411*, 263-272.
(73) Bartberger, M. D.; Liu, W.; Ford, E.; Miranda, K. M.; Switzer, C.; Fukuto, J. M.; Farmer, P. J.; Wink, D. A.; Houk, K. N. *Proc. Natl. Acad. Sci. USA* **2002**, *99*, 10958-10963.
(74) Miranda, J. C. V.; Paolocci, N.; Katori, T.; Thomas, D. D.; Ford, E.; Bartberger, M. D.; Espey, M. G.; Kass, D. A.; Feelisch, M.; Fukuto, J.; Wink, D. A. *Proc. Natl. Acad. Sci. USA* **2003**, *100*, 9196-9201.
(75) Shafirovich, V.; Lymar, S. V. *Proc. Natl. Acad. Sci. USA* **2002**, *99*, 7340-7345.
(76) Herold, S.; Kalinga, S.; Matsui, T.; Watanabe, Y. *J. Am. Chem. Soc.* **2004**, *126*, 6945-6955.
(77) Meli, R.; Nauser, T.; Koppenol, W. H. *Helv. Chim. Acta* **1999**, *82*, 722-725.
(78) Sharpe, M. A.; Robb, S. J.; Clark, J. B. *J. Neurochem.* **2003**, *87*, 386-394.
(79) Feelisch, M.; Martin, J. F. *Trends Ecol. Evol.* **1995**, *10*, 496-499.
(80) Brunori, M. *Trends Biochem. Sci.* **2001**, *26*, 209-210.
(81) Moller, J. K.; Skibsted, L. H. *Chem. Rev.* **2002**, 1167-1178.
(82) Bonamore, A.; Gentili, P.; Ilari, A.; Schinina, M. E.; Boffi, A. *J. Biol. Chem.* **2003**, *278*, 22272-22277.
(83) Silaghi-Dumitrescu, R. *Arch. Biochem. Biophys.* **2004**, *424*, 137-140.
(84) Hausladen, A.; Privalle, C. T.; Keng, T.; DeAngelo, J.; Stamler, J. S. *Cell* **1998**, *86*, 719-729.
(85) daCosta, P.; Teixeira, M.; Saraiva, L. *FEMS Microbiology Lett.* **2003**, *218*, 385-393.

(86) Seifritz, C.; Daniel, S. L.; Gossner, A.; Drake, H. L. *J. Bacteriol.* **1993**, *175*, 8008-8013.

(87) Einsle, O.; Messerschmidt, A.; Huber, R.; Kroneck, P. M. H.; Neese, F. *J. Am. Chem. Soc.* **2002**, *124*, 11737-11745.

(88) Silaghi-Dumitrescu, R. *Eur. J. Inorg. Chem.* **2003**, 1048-1052.

(89) Averill, B. A. *Chem. Rev.* **1996**, *96*, 2951-2964.

(90) Silaghi-Dumitrescu, R. *Inorg. Chem.* **2004**, *43*, 3715-3718.

(91) Silvestrini, M. C.; Falcinelli, S.; Ciabatti, I.; Cutruzzola, F.; Brunori, M. *Biochimie* **1994**, *76*, 641-654.

(92) Trogler, W. C. *Coord. Chem. Rev.* **1999**, *187*, 303-327.

(93) Nakahata, K.; Tanimoto, T.; Hatano, K.; Usuda, K.; Shoun, H. *J. Biol. Chem.* **1993**, *268*, 8350-8355.

(94) Shimizu, H.; Obayashi, E.; Gomi, Y.; Arakawa, H.; Park, S.-Y.; Nakamura, H.; Adachi, S.-i.; Shoun, H.; Shiro, Y. *J. Biol. Chem.* **2000**, *275*, 4816-4826.

(95) Shimizu, H.; Park, S.-Y.; Shiro, Y.; Adachi, S.-i. *Acta Cryst. D* **2002**, *58*, 81-89.

(96) Shiro, Y.; Fujii, M.; Iizuka, T.; Adachi, S.-i.; Tsukamoto, K.; Nakahara, K.; Shoun, H. *J. Biol. Chem.* **1995**, *270*, 1617-1623.

(97) Shoun, H.; Tanimoto, T. *J. Biol. Chem.* **1991**, *266*, 11078-11082.

(98) Obayashi, E. *J. Am. Chem. Soc.* **1997**, *119*, 7807-7816.

(99) Obayashi E, T. S., Shiro Y *J. Am. Chem. Soc.* **1998**, *120*, 12964-12965.

(100) Daiber, A.; Nauser, T.; Takaya, N.; Kudo, T.; Weber, P.; Hultschig, C.; Shoun, H.; Ullrich, V. *J. Inorg. Biochem.* **2002**, *88*, 343-352.

(101) Harris, D. L. *Int. J. Quantum Chem.* **2002**, *88*, 133-200.

(102) Silaghi-Dumitrescu, R.; Silaghi-Dumitrescu, I. *Rev. Roum. Chim.* **2004**, *3-4*, 257-268.

(103) Girsch, P.; de Vries, S. *Biochim. Biophys. Acta* **1997**, *1318*, 202-216.

(104) Pinakoulaki, E.; Stavrakis, S.; Urbani, A.; Varotsis, C. *J. Am. Chem. Soc.* **2002**, *124*, 9378-9379.

(105) Stavrakis, S.; Pinakoulaki, E.; Urbani, A.; Varotsis, C. *J. Phys. Chem. B* **2002**, *106*, 12860-12862.

(106) Wasserfallen, A.; Ragettli, S.; Jouanneau, Y.; Leisinger, T. *Eur. J. Biochem.* **1998**, *254*, 325-332.

(107) Sarti, P.; Fiori, P. L.; Forte, E.; Rappelli, P.; Teixeira, M.; Mastronicola, M.; Sanciu, G.; Giuffre, A.; Brunori, M. *Cell. Mol. Life Sci.* **2004**, *61*, 618-623.

(108) Andersson, J. O.; Sjongren, A. M.; Davis, L. A. M.; Embley, T. M.; Roger, A. J. *Curr. Biol.* **2003**, *13*, 94-104.

(109) Gomes, C. M.; Frazao, C.; Xavier, A. V.; Legall, J.; Teixeira, M. *Protein Sci.* **2002**, *11*, 707-712.

(110) Frazão, C.; Silva, G.; Gomes, C. M.; Matias, P.; Coelho, R.; Sieker, L.; Macedo, S.; Liu, M. Y.; Oliveira, S.; Teixeira, M.; Xavier, A. V.; Rodrigues-Pousada, C.; Carrondo, M. A.; Le Gall, J. *Nat. Struct. Biol.* **2000**, *7*, 1041-1045.

(111) Vicente, J. B.; Gomes, C. M.; Wasserfallen, A.; Teixeira, M. *Biochem. Biophys. Res. Commun.* **2002**, *294*, 82-87.

(112) Gomes, C. M.; Vicente, J. B.; Wasserfallen, A.; Teixeira, M. *Biochemistry* **2000**, *39*, 16230-16237.

(113) Das, A.; Coulter, E. D.; Kurtz, D. M., Jr.; Ljungdahl, L. G. *J. Bacteriol.* **2001**, *183*, 1560-1567.

(114) Nolling, J.; Ishii, M.; Koch, J.; Pihl, T.; Reeve, J. N.; Thauer, R. K.; Hedderich, R. *Eur J Biochem* **1995**, *257*, 628-638.

(115) Jouanneau, Y.; Meyer, C.; Asso, M.; Guigliarelli, B.; Willison, J. C. *Eur. J. Biochem.* **2000**, *267*, 780-787.

(116) Combet, C.; Blanchet, C.; Geourjon, C.; Deléage, G. *Trends Biochem. Sci.* **2000**, *25*, 147-150.

(117) Jin, S.; Kurtz , D. M., Jr.; Liu, Z. J.; Rose, J.; Wang, B. C. *J. Am. Chem. Soc.* **2002**, *124*, 9845-9855.

(118) Kurtz, D. M., Jr. *in Essays in Biochemistry*, Ballou, D. P. Ed., Portland Press, Ltd 1999, pp1985-1100.

(119) Jean, D.; Briolat, V.; Reysset, G. *Microbiology* **2004**, *150*, 1649-1659.

(120) daCosta, P.; Teixeira, M.; Saraiva, L. *FEMS Microbiology Lett.* **2003**, *218*, 385-393.

(121) Collins, M. D.; Lawson, P. A.; Willems, A.; Cordoba, J. J.; Fernandez-Garayzabal, J.; Garcia, P.; Cai, J.; Hippe, H.; Farrow, J. A. *Int. J. Syst. Bacteriol.* **1994**, *44*, 812-826.

(122) Das, A.; Ljungdahl, L. G. In *Encyclopedia of Microbiology*; 2nd ed.; Lederberg, J., Ed.; Academic Press: San Diego, CA, 2000; Vol. 1, pp 18-27.

(123) Drake, H. L. In *Acetogenesis*; Drake, H. L., Ed.; Chapman & Hall: New York, N.Y., 1994, pp 3-49.

(124) Drake, H. L.; Daniel, S. L. *Res. Microbiol.* **2004**, *155*, 422-436.

(125) Frostl, J. M.; Seifritz, C.; Drake, H. L. *J. Bacteriol.* **1996**, *178*, 4597-4603.

(126) Arendsen, A. F.; Soliman, M. Q.; Ragsdale, S. W. *J. Bacteriol.* **1999**, *181*, 1489-1495.

(127) Drake, H. L.; Daniel, S. L. *Res. Microbiol.* **2004**, *155*, 422-436.

(128) Heidelberg, J. F.; Seshadri, R.; Haveman, S. A.; Hemme, C. L.; Paulsen, I. T.; Kolonay, J. F.; Eisen, J. A.; Ward, N.; Methe, B.; Brinkac, L. M.; Daugherty, S. C.; Deboy, R. T.; Dodson, R. J.; Durkin, A. S.; Madupu, R.; Nelson, W. C.; Sullivan, S. A.; Fouts, D.; Haft, D. H.; Selengut, J.; Peterson, J. D.; Davidsen, T. M.; Zafar, N.; Zhou, L.; Radune, D.; Dimitrov, G.; Hance, M.; Tran, K.; Khour, i. H.; Gill, J.; Utterback, T. R.; Feldblyum, T. V.; Wall, J.; Voordouw, G.; Fraser, C. M. *Nat. Biotechnol.* **2004**, *22*, 554-559.

CHAPTER 2

A FLAVO-DIIRON PROTEIN AND HIGH-MOLECULAR WEIGHT RUBREDOXIN FROM *MOORELLA THERMOACETICA* WITH NITRIC OXIDE REDUCTASE ACTIVITY

2.1. Introduction

As discussed in Chapter 1, a five-gene "oxidative stress protection" cluster in *M. thermoacetica* has recently been described (cf. Figure 1.10).[1] Within this cluster are two co-transcribed genes, *fprA* (for A-type flavoprotein) and *hrb* (for high-molecular weight rubredoxin), whose encoded proteins have no known functions and for which only preliminary characterizations were reported. As discussed in Chapter 1, *M. thermoacetica* FprA is expected to be a flavo-diiron protein with dioxygen and/or nitric oxide reductase activities. The gene, *hrb*, encodes a unique 229-residue protein, Hrb, the amino acid sequence of which can be divided into two domains, based on homologies to other proteins. The N-terminal domain sequence is homologous to a flavoprotein with ferric reductase activity from the sulfate-reducing archaeon, *Archaeoglobus fulgidus,*[2,3] and the C-terminal domain sequence is homologous to the non-heme iron, electron transport protein, rubredoxin (cf. Figure 2.1).[1] This chapter presents characterizations of *M. thermoacetica* FprA and Hrb and demonstrates the NO reductase functionality of FprA both in vitro and in vivo.

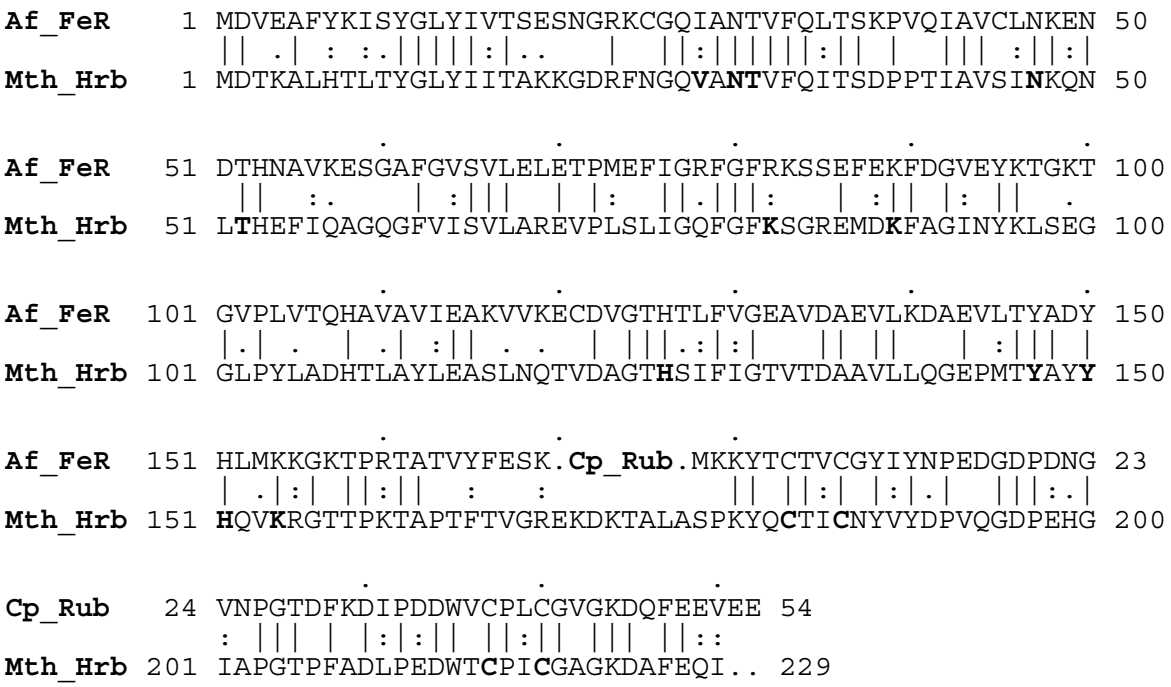

Figure 2.1 Amino acid sequence alignment of *M. thermoacetica* Hrb (Mth_Hrb) vs. *A. fulgidus* ferric reductase (Af_FeR) and *C. pasteurianum* rubredoxin (Cp_Rub). Residues involved in FMN/NAD(P) binding domain of Af_FeR and iron ligand cysteine residues in Cp_Rub are shown in bold letters**.**

2.2. Materials and methods

Reagents and General Procedures. *M. thermoacetica* (ATCC 39073) was grown at 58 ºC in the presence of 100 mM methanol under 100 % CO_2 either in the presence or absence of reducing agents (Na_2S, 0.25 g/L; cysteine-HCl, 0.25 g/L).[4,5] *M. thermoacetica* cell extracts were prepared by breakage of the cells in a French press.[6] All solutions were prepared in deionized water. Glucose oxidase from *Aspergillus niger*, β-D-(+)glucose, catalase from bovine liver, horse heart cytochrome *c*, NADH, and NADPH (Sigma Chemical Co.) and protein molecular weight standards (Bio-Rad, Inc.) were used without further purification. Redox dyes were purchased from Aldrich or Sigma. Molecular biology manipulations followed standard protocols.[7] DNA restriction and ligating enzymes were obtained from New England Biolabs, Inc. Stock solutions (25 mM) of DEA NONOate (diethylammonium (Z)-1-(N,N-diethylamino) diazen-1-ium-1,2-

diolate, Cayman Chemicals, Inc.) were prepared in 0.01 M NaOH. DEA NONOate is stable at high pH but decomposes to release NO gas (1.5 mols NO/1 mol DEA NONOate) when added to assay mixtures at ~ pH 7. Where indicated, solutions were made anaerobic by repetitive vacuum/argon or N_2 gas exchange or extensive purging with argon or N_2 gas. Gaseous nitric oxide (98.5%) was purchased from Aldrich. The NO was purified by bubbling through 100 mL of a 10% KOH solution. The purified NO gas was used to prepare saturated NO solutions (~1.8 mM) by bubbling the gas through anaerobic deionized water for 15 minutes. Protein purity was judged by SDS-PAGE (15% polyacrylamide gels) and Coomassie blue staining.[8] Western blotting followed a standard procedure.[9] Antibodies against purified recombinant *M. thermoacetica* FprA and Hrb were raised in rabbits at the Animal Care and use Facility at the University of Georgia, and purified from serum by a standard procedure.[10]

FprA Expression and Purification. All cultures used for overexpression and isolation of FprA were grown aerobically in M-9 minimal media containing 100 μg ampicilin/mL at 37°C in an incubator/shaker, and all columns were run aerobically at room temperature. Fifty-milliliter cultures of *E. coli* BL21-Gold (DE3) (Stratagene, Inc.) transformed with pFprA (a pET-21(b+) (Novagen, Inc.) derivative containing the *M. thermoacetica fprA*[1]). After overnight growth the 50-mL cultures were used to inoculate 1-L volumes of the same media. The 1-L cultures were grown with shaking at 37 °C to an O.D. 600nm of ~0.6, at which point isopropyl-β-D-thiogalactoside (IPTG, 100 mg/L) was added to induce expression of FprA. The cultures were supplemented at the time of induction with 10 mg of ferrous sulfate per liter or 10 mg of zinc sulfate per liter for zinc-substituted proteins. After a further 4 hrs incubation/shaking at 37 °C, the cells were harvested by centrifugation. Unless otherwise specified, the buffer used throughout protein purification was 50 mM MOPS pH 7.3, hereafter referred to as “buffer”.

After a -80 °C freeze-thaw cycle the cells harvested from 12 L of culture were resuspended in ~120 mL of buffer and 40- to 60-mL portions were lysed by sonication (2 minutes, with 10-sec pulses at 10-sec intervals, on ice).[11] The supernatant after centrifugation at 30,000g for 30 minutes was loaded (typically, 20% of the resuspended, sonicated lysate volume per column run) onto a 1.6 x 2.5 HiTrap anion-exchange column (Amersham Pharmacia BioTek(APBT)) equilibrated with buffer and eluted at a flow rate of 3 mL/min using a gradient of NaCl. FprA eluted as a yellow-orange fraction at ~200 mM NaCl. Fractions exhibiting similar UV-vis absorption spectra were pooled, concentrated to ~0.5 mL/L culture, and loaded onto a HiPrep 16/60 Sephacryl S-100 column (APBT) equilibrated with buffer + 250 mM NaCl and eluted at 0.5 mL/min. Yellow-orange eluting fractions exhibiting similar UV-vis absorption spectra were pooled, and desalted by repeated cycles of concentrations and dilutions with buffer at 4 °C in an Amicon concentrator using a membrane with a nominal molecular mass cut-off of 10 kDa. The desalted protein solution was concentrated to ~5 mL and loaded onto a 1.6 x 2.5 HiTrap anion-exchange column equilibrated with buffer and eluted at a flow rate of 3 mL/min using a gradient of NaCl. The FprA eluted as a single yellow-orange band. Yields of the purified recombinant FprA were typically ~48 mg/12 L of *E. coli* culture. Purified FprA was stored as ~ 1 mM stocks in desalted buffer at -80°C. An analogous protocol was used to express and purify recombinant FprA in similar yields using plasmid, pFprA-pCYB1 transformed into *E. coli* BL21 Codon + RIL (Stratagene, Inc.). The plasmid, pFprA-pCYB1 was constructed by inserting the PCR-amplified *M. thermoacetica fprA*[1] into the *Nde*I/*Eco*RI restriction sites of pCYB1 (New England Biolabs, Inc.).

His-tagged FprA Expression and Purification. In order to obtain a recombinant His-tagged FprA, the stop codon in pFprA was removed using the QuickChange mutagenesis kit

(Stratagene, Inc.) with the primers 5′-CGCATAGCCGATCTGAATTCGAGCTC-3′ (forward) and 5′-GAGCTCGAATTCAGATCGGCTATGCG-3′ (reverse) following procedures described in the product manual. The His-tagged FprA (containing 6 His residues at the C-terminus) was expressed in *E. coli* strain BL21 Gold (DE3) using a procedure identical to that described for the non-His-tagged FprA, except that the cultures were supplemented with 1 mg ^{57}Fe/L (iron powder, 95 atom% ^{57}Fe enriched, Advanced Materials Technologies, Ltd.) dissolved in a two-fold molar excess of concentrated H_2SO_4) when the protein was to be used for Mössbauer spectroscopy. Cells harvested from 5 L of culture were subjected to one freeze-thaw cycle, then re-suspended in 50 mL of 50 mM phosphate pH 7 containing 300 mM NaCl (high-salt buffer), sonicated and centrifuged as described for non-His-tagged FprA, and loaded onto a column containing 10-mL of cobalt-containing Talon Cell-thru resin (Clontech Laboratories, Inc.) equilibrated in the high-salt buffer, at 4°C. His-tagged FprA eluted as pure protein (as judged by SDS-PAGE) upon washing the column with the high-salt buffer containing 150 mM imidazole. The eluted protein was then transferred into 50 mM MOPS pH 7.3, by repeated dilutions and concentrations in an Amicon cell (YM10 membrane). His-tagged FprA yields were typically ~9 mg/L *E. coli* culture.

Hrb expression and purification. The full-length *hrb* was PCR-amplified from *M. thermoacetica* genomic DNA[1] by Amaresh Das using the appropriate forward and reverse oligonucleotide primers with sequences duplicating the 5′ and 3′ ends, respectively, of the gene. The primers also contained unique restriction sites at their 5′ ends, *Nde*I for the forward primer and *Eco*RI for the reverse primer. The purified PCR product (QIAquick PCR purification kit, Qiagen, Inc.) was digested with *Nde*I and *Eco*RI and ligated into the corresponding restriction sites of pCYB1 (New England Biolabs, Inc.) yielding pHrb. Recombinant Hrb was expressed

from *E. coli* BL21 Codon + RIL (Stratagene, Inc.) that had been transformed with pHrb and was purified by procedures identical to those described for FprA with the following exceptions. Low-light conditions and 4-°C buffers were used, because prolonged exposure of Hrb to normal room light and temperature were found to promote protein degradation. Also, the final HiTrap anion-exchange step was not used because, based on SDS-PAGE, the preceding gel filtration step yielded a pure protein. Hrb yields were typically ~10 mg/L *E. coli* culture. Hrb was stored as ~1 mM stocks at -80°C.

Analytical Methods. Protein concentrations were determined using the Bio-Rad protein assay (Bio-Rad, Hercules, CA) with bovine serum albumin as the standard. Metal contents of Hrb and FprA were determined by inductively coupled plasma-atomic emission analysis at the University of Georgia Chemical Analysis Facility. Flavin was identified and quantified as described previously.[1] Molar absorptivities (listed in Table 1) were determined from the protein quantitations, and these values were subsequently used to calculate all protein concentrations from measured absorbances. Native molecular weights of proteins were established by gel filtration, using a Sephacryl S300 column calibrated by Dr. Eric Coulter, using horse spleen ferritin (450 kDa), bovine catalase (240 kDa), aldolase (158 kDa), bovine serum albumin (68 kDa), hen egg albumin (45 kDa), chymotrypsinogen A (25 kDa), and horse heart cytochrome c (12.5 kDa), in 50 mM HEPES, pH 7.3, containing 100 mM NaCl.

Redox potentials. A spectrophotometric, dye-mediated, electrochemical titration method was used similar to that described for *E. coli* FlRd.[12] All measurements were conducted at room temperature (~23 ºC) in 50 mM MOPS pH 7.0. A platinum/glass combination microelectrode (Brinkmann, Inc.) attached to a potential meter was inserted through a tight-fitting rubber septum into a specially designed quartz cuvette containing 4 mL of anaerobic solution under an argon

atmosphere. The solution contained either 30 μM Hrb or 40 μM FprA (monomer basis) in 50 mM MOPS pH 7.0 and 0.5 μM of each of the following redox dyes(reduction potentials, $E^{o'}$, vs SHE): methyl viologen(-446 mV), phenosafranine(-244 mV), anthraquinone-2,6-disulfonate(-184 mV), indigo carmine(-120 mV), indigo trisulfonate(-75 mV), indigo tetrasulfonate(-38 mV), methylene blue(+8 mV), toluidine blue(+34 mV), phenazine methosulfate(+92 mV).[12] Into these solutions were injected small aliquots (1-10 μl) of a concentrated stock solution of sodium dithionite in the same buffer. After each addition, thorough mixing and equilibration (2-10 min after mixing), the potential and UV-visible absorption spectrum were recorded. For Hrb, absorbance data collected at 450 nm were used to fit a Nernst equation corresponding to the sum of two redox processes: one corresponding to a two-electron reduction of the FMN, the other to a one-electron reduction of the $[Fe(SCys)_4]$ site. A midpoint potential similar to the latter was obtained for absorbance data collected at 570 nm and separately fitting as a one-electron process for reduction of the $[Fe(SCys)_4]$ site. For FprA, absorbance data collected at 464 nm were used to fit a Nernst equation corresponding to a sum of two one-electron processes for sequential reduction of the FMN. This analysis assumes that the diiron site makes negligible contribution to the A_{464}.

Enzymatic Assays. NADH-dependant oxidase (O_2-consumption) assays were monitored in air-saturated buffer by the rates of either decreasing absorbance at 340 nm due to O_2-dependent NADH oxidation or O_2 consumption measured polarographically using a Yellow Springs Instruments Model 5300 biological oxygen monitor equipped with a Clark-type oxygen electrode. NADH-dependent NO reductase (NO consumption) activities were assayed anaerobically by monitoring the decrease in absorbance at 340 nm. NO, from either a stock DEA NONOate or an NO-saturated aqueous solution, was introduced into the anaerobic assay mixture

(1-mL total volume) in a 1-cm path cell via a Hamilton gas-tight syringe and the rate of decrease in A_{340} due to NADH consumption was measured. Anaerobicity was ensured by utilizing a glucose (10 mM), glucose oxidase (10 Units) and catalase (150 Units) dioxygen-scrubbing system in the assay mix. Alternatively, the NADH-dependent NO reductase activity was followed under the conditions described above, but measuring the decrease in NO concentration with a Clark-type NO-sensitive electrode (2mm diameter, WPI, Inc.). NO electrode measurements were performed with stirring inside the NO chamber (WPI, Inc.), where anaerobicity of the reaction mixture (typically a 2-mL volume) was maintained by continuously purging the headspace with nitrogen gas through a needle inserted into one of the two narrow ports. The second port was used for adding the reagents via Hamilton gas-tight syringes. Appendix B shows a schematic diagram of this chamber, with details of the operation procedure. All assays were performed at pH 7.0 and room temperature, unless otherwise noted. The NO electrode was calibrated using a nitrite/iodide/H_2SO_4 mixture, as described in the NO electrode manual. Further details of the assay protocols, including component concentrations, are provided in the figure legends.

Spectroscopy. Ultraviolet-visible absorption spectra were obtained in 1-cm pathlength quartz cuvettes on a Shimadzu UV-2401PC scanning spectrophotometer. EPR spectra were recorded on a Bruker ESP-300E spectrometer equipped with an ER-4116 dual-mode cavity and an Oxford Instruments ESR-9 flow cryostat. Mössbauer spectra were recorded in the laboratory of Boi Hanh Huynh at the Department of Physics, Emory University on either a weak-field spectrometer with a Janis 8DT variable temperature cryostat or a strong-field spectrometer furnished with CNDT/SC Super-Varitemp cryostat encasing an 8T superconducting magnet. Both spectrometers operate in a constant acceleration mode in transmission geometry. The zero

velocity of the spectra refers to the centroid of a room temperature spectrum of metallic iron foil. The Mössbauer spectra were analyzed using the WMOSS program (WEB Research Co. Edina, MN) based on a spin Hamiltonian formalism conventionally used for Mössbauer analysis. Mössbauer spectroscopy employed as-isolated His-tagged ^{57}Fe-enriched FprA (0.5 mM homodimer in 50 mM MOPS pH 7.3).

FprA Complementation of E. coli Growth Sensitivity to NO. E. coli strain AG300, containing a disrupted FlRd gene, was kindly provided by Paul R. Gardner.[13] The anaerobic culture medium contained 60 mM K_2HPO_4, 33 mM KH_2PO_4, 7.6 mM $(NH_4)_2SO_4$, 1.7 mM sodium citrate, 1 mM $MgSO_4$, 10 μM $MnCl_2$, 10 μM thiamin hydrochloride, 2% potassium gluconate, 0.25% casamino acids, ampicilin (0.1 g/L) and chloramphenicol (0.1 g/L). For anaerobic growth, a protocol routinely employed by Amaresh Das in growing *M. thermoacetica* under anaerobic conditions was used, where the culture bottles are made anaerobic, sealed, and then used for growth without any need for maintaining an anaerobic environment *around* the bottles (i.e., an anaerobic chamber was *not* used at any point throughout these growth studies). Thus, the medium (in a 1- or 2-liter Erlenmeyer flask, covered with aluminum foil) was preheated 10 minutes in an autoclave at 100 °C, then purged with N_2 for ~20 minutes (during which time the temperature dropped to ~50-60 °C). This medium was then aliquoted in 25- or 100-mL volumes into narrow-neck culture bottles, so that the ratio of culture medium volume to head-space would be ~4:1. The bottles were purged with N_2 gas for 5-15 minutes (with longer times for larger volumes), *before* and also *after* aliquoting the media. The bottles were then sealed by crimping with 1-cm thick rubber septa and autoclaved. At this point the culture medium and headspace in the bottles were assumed to be anaerobic and to remain so throughout the growth study. All subsequent additions to these flasks (e.g., inoculation, induction, NO

addition) were injected through the septa with disposable 1-mL syringes or with Hamilton 50-μL syringes. Ten-milliliter cultures of *E. coli* AG300 transformed with either pCYB1 or pFprA-pCYB1 were grown aerobically overnight with shaking in 15-mL Falcon tubes at 37°C in LB medium containing ampicilin (0.1 g/L) and chloramphenicol (0.1 g/L). One-half-milliliters of these aerobic cultures were inoculated into 25 mL of anaerobic culture medium in the sealed bottles described above. The anaerobic cultures were grown without shaking at 37 °C until O.D. 550 nm ~0.6 (typically 8 hours to overnight), at which point 0.5 mL aliquots of these cultures were used to inoculate fresh 25-mL batches of anaerobic culture medium, which were then incubated without shaking at 37 °C until O.D. 550 nm ~0.6. This cycle was repeated a third time. At O.D. ~0.6, 1-mL aliquots of the third subcultures were used to inoculate 150-mL flasks each containing 100 mL of anaerobic culture medium. Results reported below were obtained with these 100-mL cultures. IPTG (0.05 mg/L) was added to each 100-mL culture at O.D. 550 nm ~0.1. Where required, aliquots of either an NO-saturated aqueous solution or 25 mM DEA NONOate were added to the 100-mL cultures 60 minutes after IPTG addition. Concentrations of added NO are given in the figure legends. Optical densities were measured by removing 1-mL aliquots of medium from the culture bottles, using sterile disposable 1-mL syringes.

2.3. Results and discussion

Expression of FprA and Hrb in M. thermoacetica. The original investigation of *fprA* and *hrb*[1] demonstrated their transcriptions but not their translations in *M. thermoacetica*. Antibodies were, therefore, raised against the purified recombinant FprA and Hrb and used to probe *M. thermoacetica* cell extracts by immunoblotting. The Western blots in Figure 2.2, obtained by Dr. Amaresh Das, show that FprA and Hrb are produced in *M. thermoacetica* grown anaerobically

with methanol/CO_2 as electron donor/acceptor, i.e., via the Wood-Ljungdahl pathway (cf. Section 1.8). A lag phase in growth was noted in the absence of added reducing agents similar to that reported when *M. thermoacetica* cultures were exposed to small amounts of O_2.[5]

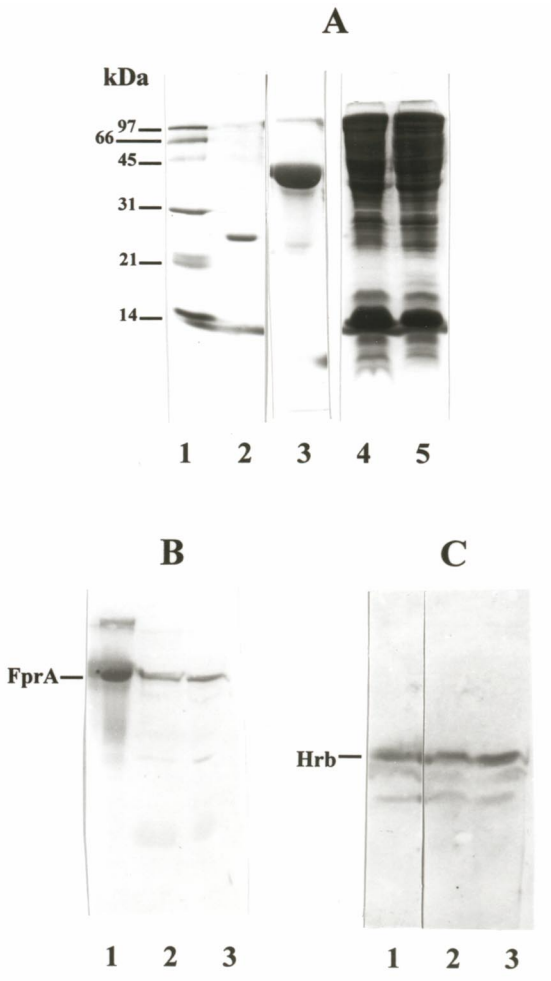

Figure 2.2. SDS-PAGE (A) and Western blots (B and C) of whole cell extracts of *M. thermoacetica* probed with antibodies raised against recombinant *M. thermoacetica* FprA (B) or Hrb (C). Panel A: Lane 1, protein standards; lane 2, purified Hrb (2 μg); lane 3, purified FprA (2 μg); lanes 4 and 5, *M. thermoacetica* cell extracts (30 μg) grown in either the absence (lane 4) or presence (lane 5) of reducing agents (cf. Materials and Methods). (A strong band of molar mass ~14 kDa in lanes 4 and 5 corresponds to lysozyme used to lyse the cells.) Panels B and C: Lanes 1 contain purified recombinant FprA (Panel B) or Hrb (Panel C). Lanes 2 and 3 are the same as lanes 4 and 5, respectively, of Panel A.

Properties of Recombinant M. thermoacetica FprA. The originally reported expression and isolation of recombinant *M. thermoacetica* FprA from *E. coli* cultured in LB media yielded a

protein with substoichiometric amounts of cofactors relative to that expected for full occupancy of its metal- and flavin-binding domains.[1] As can be seen from the analytical data in Table 1, however, when *E. coli* harboring the *fprA* expression plasmid was grown in minimal medium supplemented with ferrous sulfate at the time of induction of FprA expression, the isolated and purified protein reproducibly contained 1.9 irons per FprA monomer. This stoichiometry is close to the 2 expected for full occupancy of the dimetal site. Similarly, the 0.8-0.9 FMN/FprA monomer indicates nearly full occupancy of the single flavin binding site expected in each subunit. The recombinant FprA was isolated as a stable homodimer (cf. Table 2.1). When the recombinant FprA was expressed from *E. coli* cultures grown in minimal medium supplemented with zinc sulfate, the isolated protein had the same FMN content as for FprA isolated from iron-supplemented cultures but contained approximately 2 zinc per monomer and very little iron. The protein prepared in this latter fashion is referred to as Zn-FprA. The optical absorption spectra of the as-isolated, recombinant *M. thermoacetica* FprA and Zn-FprA, shown in Figure 2.3, are dominated by FMN. The difference absorption spectrum, FprA - Zn-FprA, is presumably due to the diferric site and/or the proximal FMN site that is perturbed by the Zn^{2+}-for-Fe^{3+} substitution. This latter possibility precludes firm conclusions about the diiron site structure or oxidation state from the FprA - Zn-FprA difference UV-vis absorption spectrum. Therefore, the iron environment in FprA was probed with ^{57}Fe Mössbauer spectroscopy.

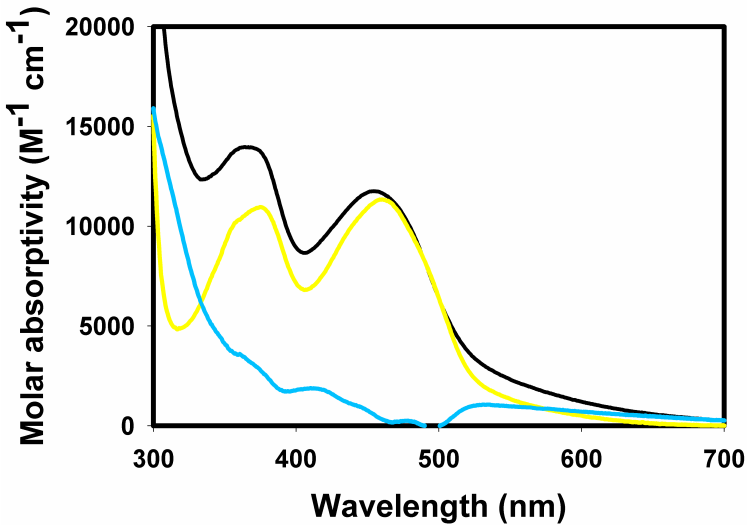

Figure 2.3. UV-vis absorption spectrum of recombinant as-isolated *M. thermoacetica* FprA (black trace), Zn-FprA (yellow trace) and the difference spectrum: FrpA minus Zn-FprA (blue trace). Buffer is 50 mM MOPS pH 7.3. Spectra were obtained under an aerobic atmosphere. The molar absorptivities plotted on the y-axis are expressed on a protein monomer basis.

The optical absorption spectrum, cofactor content and catalytic activity (see below) of the His-tagged FprA were identical to those of the non-His-tagged protein. ^{57}Fe Mössbauer spectra of the as-isolated, His-tagged FprA enriched with ^{57}Fe, shown in Figure 2.4, can be fit to two quadrupole doublets having the same isomer shift but different quadrupole splittings and asymmetric parameters (listed in the figure legend), and assuming diamagnetism. The isomer shift is typical of high-spin ferric iron, and the two quadrupole doublets suggest two different iron environments. The fact that the high-field Mössbauer spectrum (Figure 2.4B) can be well fit with the assumption of diamagnetism proves that the two ferric irons are antiferromagnetically coupled with a diamagnetic ground state. Consistent with this conclusion, the EPR spectrum of the as-isolated FprA obtained at 5 K (not shown) shows only a weak *g*-4.3 resonance, indicative of adventitiously bound ferric iron, plus a narrow symmetrical resonance at *g* 2.005, due to an organic free radical, presumably a small portion of FMN semiquinone.

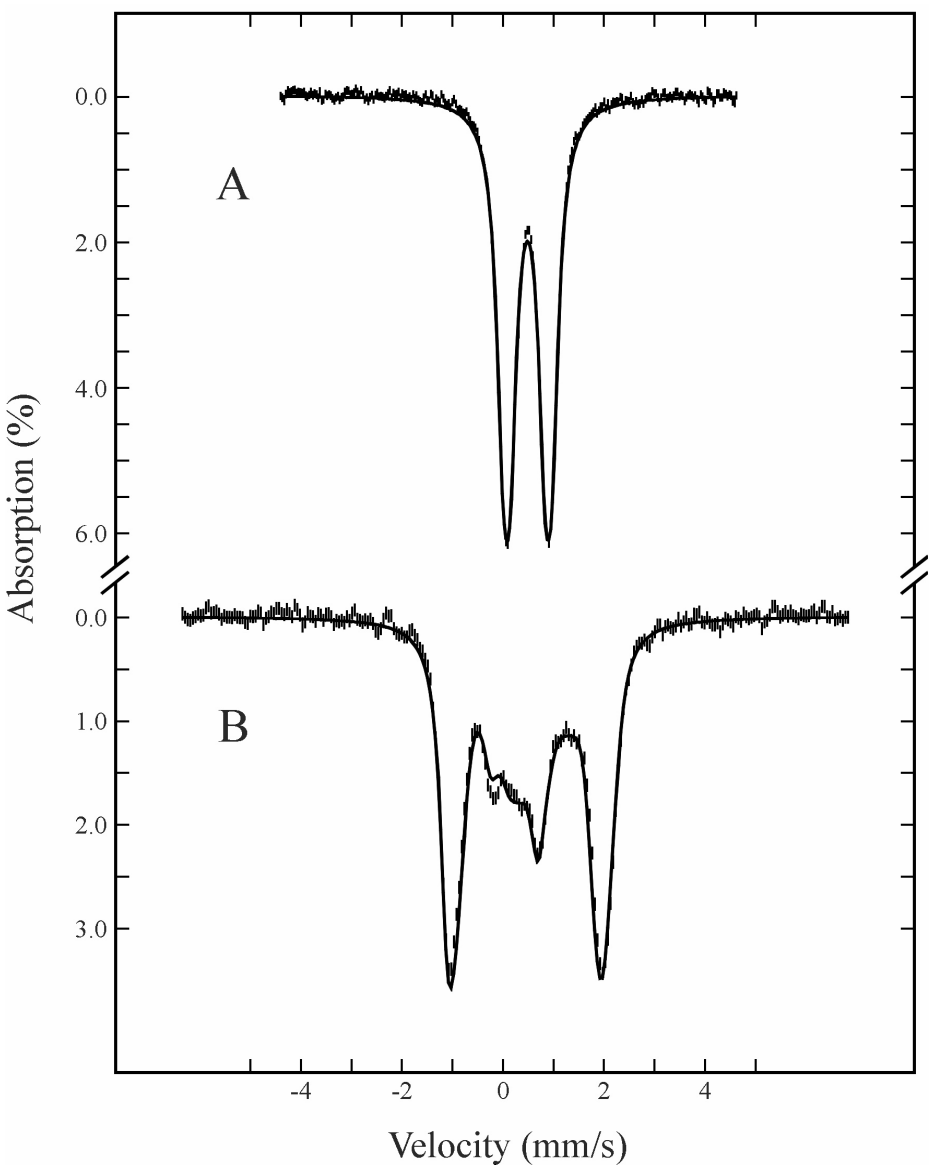

Figure 2.4. Mössbauer spectra of ^{57}Fe-enriched His-tagged as-isolated *M. thermoacetica* FprA (0.5 mM homodimer in 50 mM MOPS pH 7.3) recorded at 4.2 K in magnetic fields of 50 mT (A) and 8 T (B) applied parallel to the γ-ray beam. The solid lines overlaying the experimental spectra (hatched marks) are least-squares fits to the data using two equal-intensity quadrupole doublets with $\delta_1 = \delta_2 = 0.49 \pm 0.02$ mm/sec, $\Delta E_{Q1} = -0.69 \pm 0.03$ mm/sec, $\Delta E_{Q2} = 0.97 \pm 0.03$ mm/sec, $\eta_1 = 0.8$ and $\eta_2 = 0.0$, and assuming diamagnetism. The fitted linewidth for both quadrupole doublets was 0.33 mm/sec.

Table 2.1. Properties of Purified Recombinant FprA and Hrb from *M. thermoacetica*

	FprA	Hrb
Molecular Mass, kDa		
Calc'd from sequence	44.3	24.9
From SDS-PAGE	45	23
From gel filtration	91	45
Cofactor content, mol/mol homodimer		
Iron[a] (Zinc)[b]	3.8 ± 0.5 (4)[b]	2.0 ± 0.1 (2)[b]
FMN	1.7 ± 0.1	1.6 ± 0.3
Optical Absorption Spectra, nm(ε ,mM homodimer^{-1}cm^{-1})[c]	278 350 374,sh 450(24)	278 350 377,sh 450,474(34) 565,sh
Reduction Potentials (mV vs SHE)[d]		
FMN_{ox}/FMN_{sq}	-117	-121
FMN_{sq}/FMN_{red}	-220	-121
$[Fe^{III/II}(SCys)_4]$	-	-30

[a]For proteins grown in M9 minimal medium supplemented with ferrous ammonium sulfate. [b]Parenthetical values are zinc content of proteins expressed from *E. coli* cultured in M9 minimal medium supplemented with $ZnSO_4$ in place of $FeSO_4$. [c]In 50 mM MOPS pH 7.3. [d] In 50 mM MOPS pH 7.0. The estimated error range for each listed potential is ±10 mV.

Comparisons with carboxylato-bridged, non-heme diiron synthetic complexes and diiron proteins show that antiferromagnetic coupling in diferric sites is invariably associated with a single atom bridge.[14] Since there is no evidence for acid-labile sulfide in FprA, the most obvious candidate for a single atom bridge is solvent. In fact, the X-ray crystal structure of *D. gigas* ROO showed an apparent solvent bridge between the two irons, which were separated by 3.4 Å.[15] The two different iron environments of *M. thermoacetica* FprA revealed by the Mössbauer spectra

are consistent with the asymmetric coordination sphere of the ROO diiron site.[15] Redox potentials for the two sequential one-electron redox processes of the FMN cofactor in FprA are listed in Table 2.1 and the corresponding Nernst plot is shown in Figure 2.5. The average of these two potentials is similar to that reported for the FMN in *E. coli* FlRd (-160 mV[12]) but the FMN_{ox}/FMN_{sq} (-117 mV) and FMN_{sq}/FMN_{red} (-220 mV) potentials are somewhat more separated from each other in *M. thermoacetica* FprA.

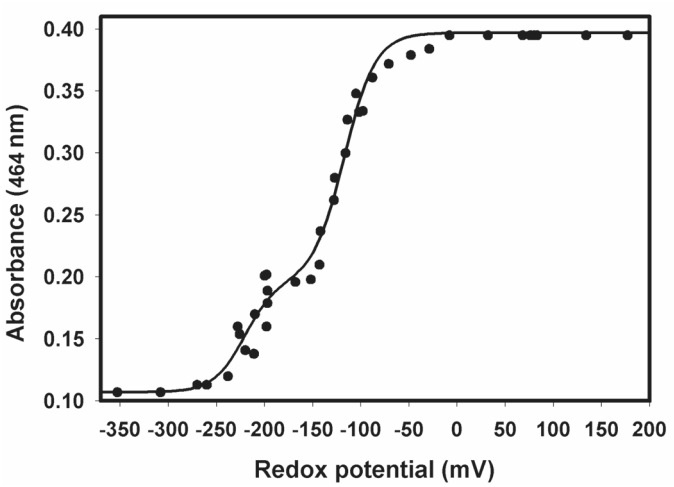

Figure 2.5. Nernst Plot of A_{464} vs reduction potential for the electrochemical titration of *M. thermoacetica* FprA in 50 mM MOPS pH 7 and at room temperature, according to the procedure described in Materials and Methods. The solid curve is a fit of the Nernst equation to the absorbance data assuming two sequential one-electron processes with midpoint potentials of -117 and -220 mV vs SHE.

Properties of Recombinant M. thermoacetica Hrb. When expressed and purified as described in Materials and Methods, a soluble recombinant Hrb was obtained which reproducibly contained 1 iron per subunit (cf. Table 2.1). This stoichiometry is consistent with the single rubredoxin-like domain in the deduced Hrb amino acid sequence.[1] The recombinant Hrb was isolated as a homodimer. The flavin in recombinant Hrb was identified as FMN, which varied between 1.3 and 1.9 FMN per homodimer. A stoichiometry of 2 FMN/homodimer would be expected for full occupancy of the N-terminal ferric reductase-like domain of Hrb. Incomplete

occupancy of the flavin binding sites was also noted in the *A. fulgidus* ferric reductase, which shares homology with the flavin-binding domain of Hrb. Only 1 FMN per homodimer was found in the X-ray crystal structure of the ferric reductase after in vitro reconstitution.[16] Using the same method as for Zn-FprA, a recombinant zinc-substituted Hrb (Zn-Hrb) was isolated, which contained FMN, approximately 1 Zn/monomer and very little iron (cf. Table 1).

The UV-vis absorption spectra of as-isolated recombinant Hrb and the corresponding Zn-Hrb are shown in Figure 2.6, and spectral data are listed in Table 2.1. Also shown in Figure 2.6 is the difference absorption spectrum: Hrb minus Zn-Hrb, which closely resembles that of oxidized rubredoxin. The optical absorption spectrum of as-isolated Hrb is, thus, the sum of FMN and rubredoxin-like [$Fe^{III}(SCys)_4$] absorptions, as predicted from amino acid sequence homologies (cf. Figure 2.1).[1]

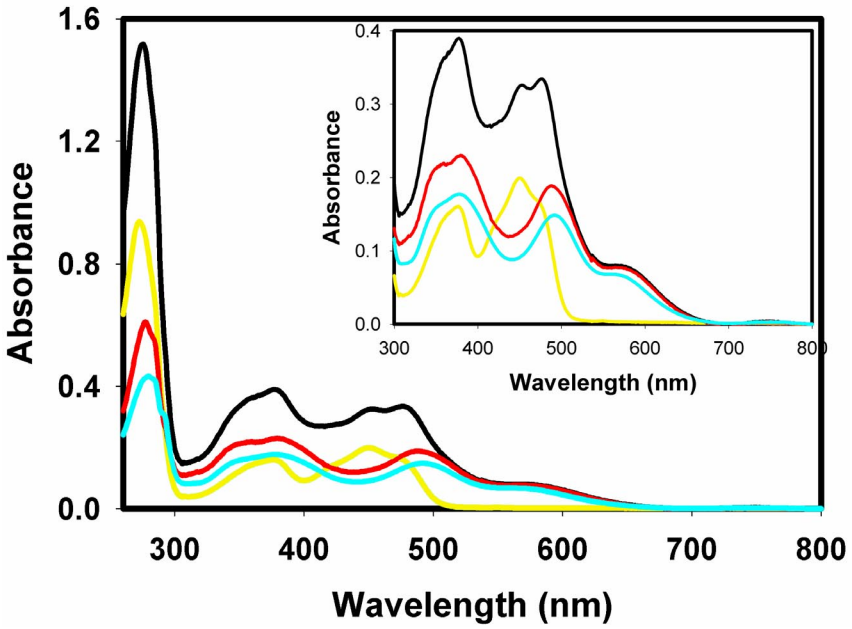

Figure 2.6. UV-vis absorption spectra of as-isolated recombinant *M. thermoacetica* Hrb (20 μM monomer, black trace), as-isolated Zn-Hrb (20 μM, yellow trace). difference spectrum of Hrb minus Zn-Hrb (red trace), and *P. furiosus* rubredoxin (blue trace), in aerobic 25 mM MOPS, pH 7.3. Inset contains the same spectra with the absorbance scale expanded by a factor of 4.

The as-isolated Hrb also shows both an X-band EPR spectrum at 4 K (Figure 2.7) with g values at 4.35 and 9.65 and a reduction potential of the [Fe(SCys)$_4$] site (-30 mV, cf. Table 2.1 and Figure 2.8) that are within the ranges of those reported for rubredoxins.[17,18]

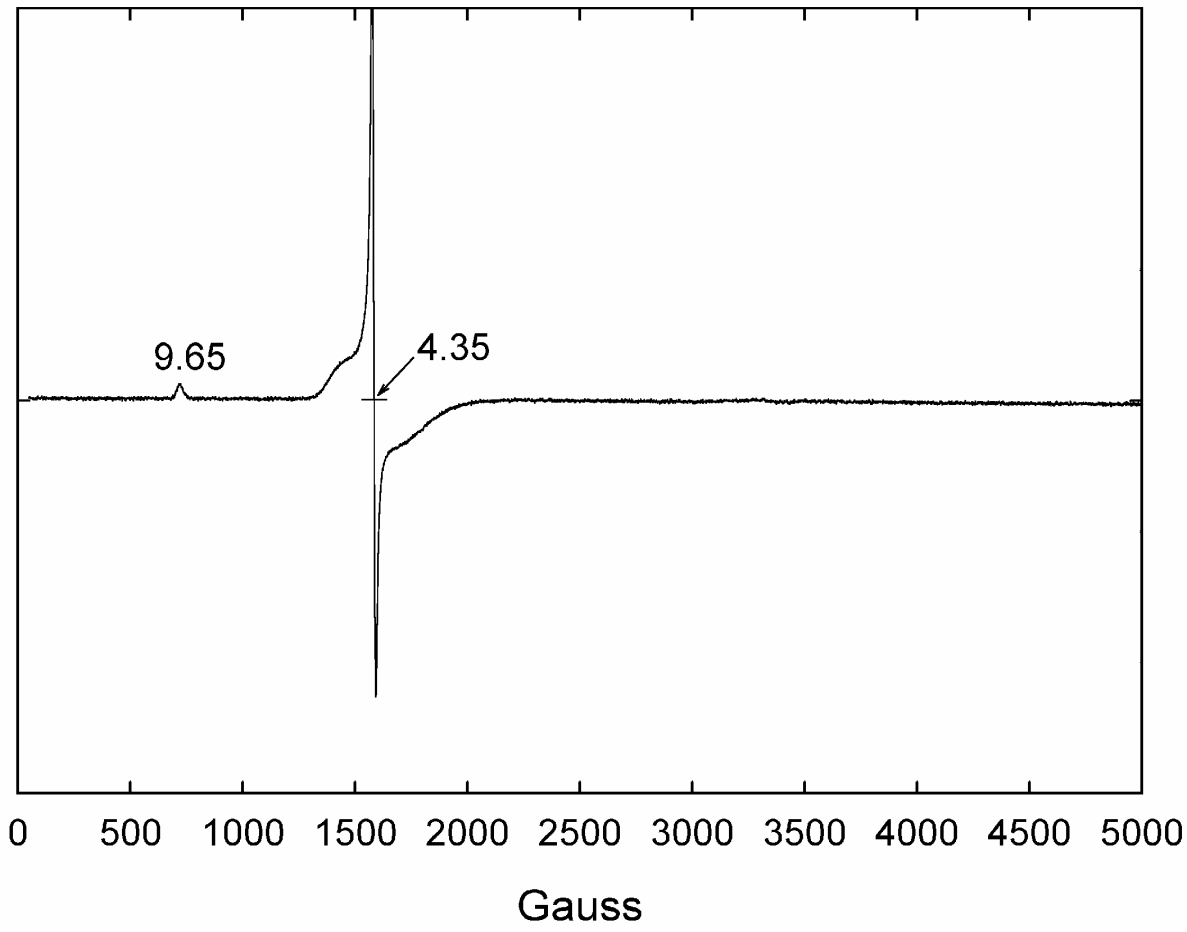

Figure 2.7. First derivative X-band EPR spectrum of recombinant as-isolated *M. thermoacetica* Hrb (100 μM in iron sites) in 50 mM MOPS pH 7.3. EPR conditions: temperature, 4.2 K; microwave frequency, 9.602 GHz; microwave power, 2 mW; modulation amplitude, 6.34 G. g values are listed at the maximum intensity of the lower-field feature (9.65), and at the zero crossing of the higher-field feature (4.35).

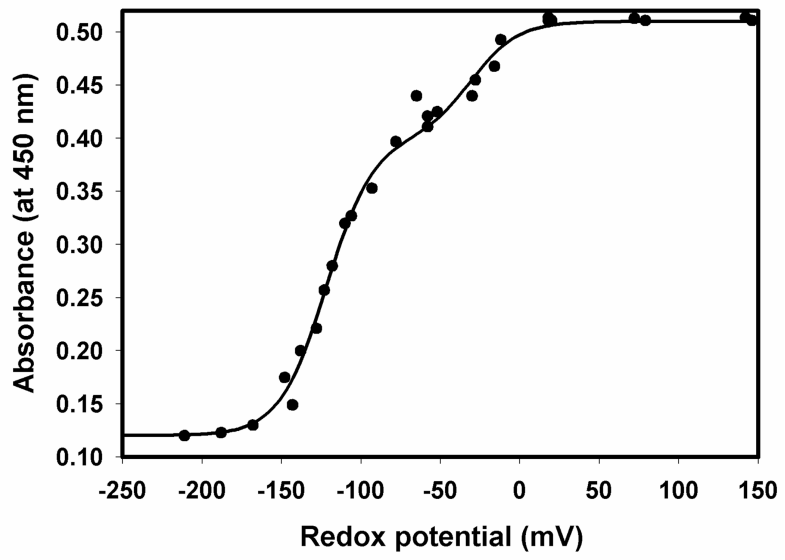

Figure 2.8. Nernst Plot of A_{450} vs. reduction potential for the electrochemical titration of recombinant *M. thermoacetica* Hrb in 50 mM MOPS pH 7 and room temperature, according to the procedure described in Materials and Methods. The solid curve is a fit of the Nernst equation to the data assuming a two-electron process with a midpoint potential of -121 and a one-electron process with a midpoint potential of -30 mV vs. SHE.

UV-vis absorption spectra obtained during an anaerobic titration of Hrb with NADH are shown in Figure 2.9. The spectral changes indicate that NADH reduces both cofactors of Hrb, but the difference spectrum shows that the absorption features of the oxidized (ferric) $[Fe(SCys)_4]$ site disappear essentially completely after the first reducing equivalent of NADH is added. This first reducing equivalent, thus, ends up in the $[Fe(SCys)_4]$ site, as expected from its more positive reduction potential relative to that of the FMN cofactor (cf. Table 2.1). The semiquinone of FMN (i.e., the one-electron reduced form) which is either red (anionic) or blue (neutral) depending on protonation state[19] did not appear to accumulate during either the NADH or electrochemical titrations (cf. Figures 2.8, 2.9). The absorption features appearing at ~310 and 330 nm upon reduction of Hrb are characteristic of the reduced, i.e., ferrous $[Fe(SCys)_4]$ site.[20] Since NADH is not known to directly reduce $[Fe^{III}(SCys)_4]$ sites, these results imply that the electron flow is: NADH → Hrb-FMN → Hrb-$[Fe(SCys)_4]$.

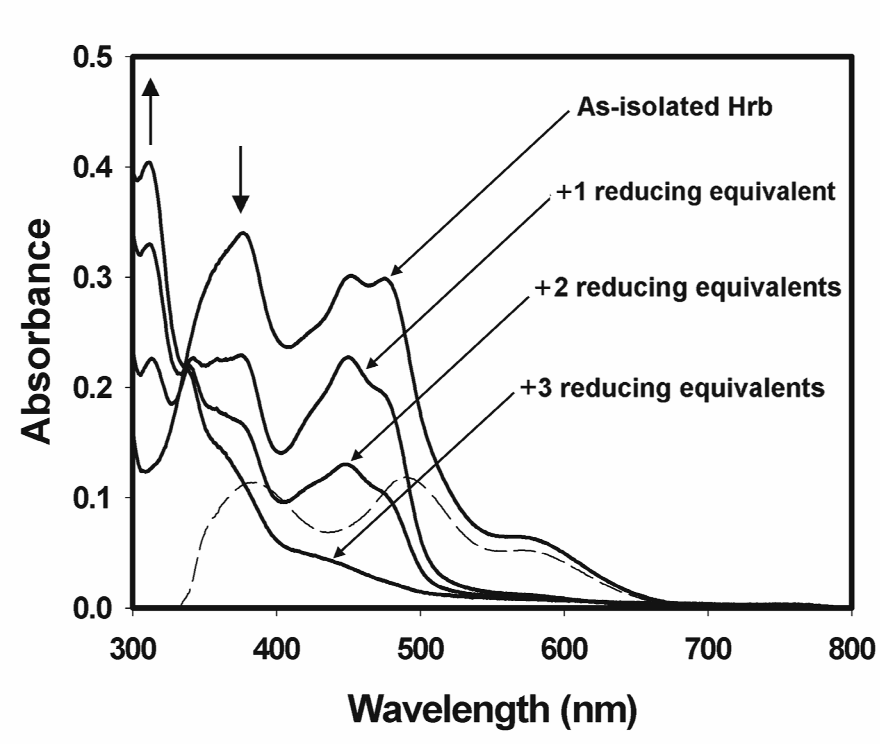

Figure 2.9. UV-vis absorption spectral changes upon anaerobic titration of recombinant *M. thermoacetica* Hrb (16 μM monomer) with NADH in 25 mM MOPS, pH 7.3. Arrows indicate direction of absorbance changes with increasing NADH. The difference spectrum of as-isolated Hrb minus "+1 reducing equivalent", is shown as a dashed trace.

As-isolated Hrb in buffered solutions was prone to apparent autoproteolysis over the course of several hours at room temperature, giving rise to two fragments corresponding in size to the ferric reductase-like and rubredoxin-like domains. This fragmentation of Hrb coincided with progressive loss of its NADH:FprA oxidoreductase activity. Thawed Hrb solutions were, therefore, routinely handled for only short periods and kept either on ice or at 4 ºC.

NADH:FprA Oxidoreductase Activity of Hrb. The absorption spectrum of the recombinant *M. thermoacetica* FprA does not change in the presence of excess NADH or NADPH under either aerobic or anaerobic conditions, indicating that the FMN in FprA is not reduced by these pyridine nucleotides. However, as shown in Figure 2.10, when catalytic

amounts of Hrb are added to anaerobic solutions of as-isolated FprA, addition of ≥3 reducing equivalents of NADH per FprA monomer converts the absorption spectrum of the FMN in FprA to that characteristic of the anionic semiquinone form, which has a prominent absorption feature at 390 nm and shoulder at 480 nm.[19] The first two reducing equivalents of added NADH presumably enter the diferric site. Additions of >3 reducing equivalents of NADH do not cause further reduction of the semiquinone. Excess sodium dithionite converts the FprA absorption spectrum to that characteristic of the two-electron reduced FMN, i.e. the hydroquinone ($FMNH_2$). In contrast to reduction of FprA with catalytic Hrb, the inset to Figure 2.10 shows that the FMN semiquinone does not accumulate upon titration of an equimolar Hrb:FprA mixture with NADH. It appears that, during the initial stages (i.e., the first 2-3 reducing equivalents) of this equimolar mixture titration, the [$Fe(SCys)_4$] site of Hrb is reduced concomitantly with the FMN of FprA. Based on the Western blots (cf. Figure 2.2), this equimolar ratio of Hrb to FprA may be closer to that typically occurring in vivo. Analogous experiments in which NADH was replaced with NADPH showed that Hrb has very little NADPH:FprA oxidoreductase activity.

Zn-Hrb shows no NADH:FprA oxidoreductase activity under the conditions of Figure 2.10, even though the FMN in Zn-Hrb *is* reduced by NADH (spectra not shown). This result, together with those in Figures 2.10 and 2.9, indicate that Hrb's NADH:FprA oxidoreductase activity involves the electron flow pathway: NADH → Hrb-FMN → Hrb-[$Fe(SCys)_4$] → FprA, and that the [$Fe(SCys)_4$] site in Hrb is the proximal electron donor to the FMN and/or diiron site of FprA.

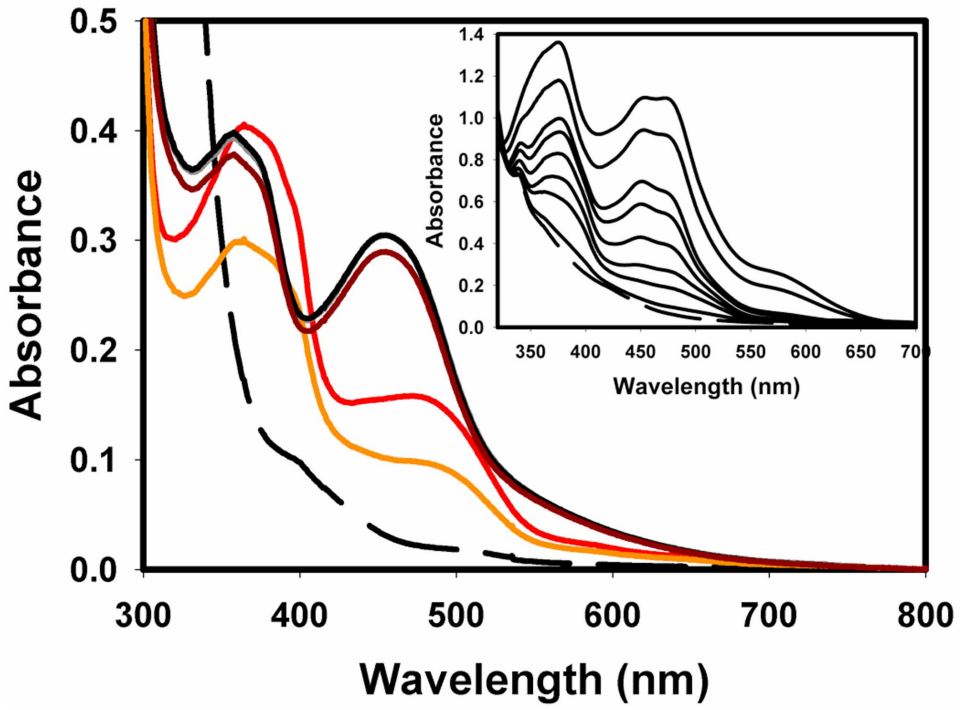

Figure 2.10. UV-vis absorption spectra obtained upon titration of recombinant *M. thermoacetica* FprA (20 μM in monomer) and catalytic Hrb (0.5 μM monomer) with NADH in anaerobic 50 mM MOPS, pH 7.3. Black trace: as-isolated, no NADH. Maroon trace: after addition of two reducing equivalents of NADH per FprA monomer. Red trace: after addition of three reducing equivalents. Orange trace: 20 minutes after addition of four reducing equivalents. Dashed trace: fully-reduced FprA, using a large excess of sodium dithionite. Inset shows monotonically decreasing UV-vis absorption during titration of equimolar FprA:Hrb (39 μM monomer, each) with NADH in anaerobic 50 mM phosphate pH 7. Top trace: no NADH added. The remaining seven traces were recorded immediately after each of seven sequential additions of one reducing equivalent per monomer of NADH. Dashed trace: spectrum taken 5 minutes after addition of the seventh reducing equivalent (no further spectral changes were observed at longer incubation times).

NADH:Dioxygen Oxidoreductase Activity of Hrb/FprA. Dioxygen reductase activity of FprA homologs from other bacteria have been reported.[3,12,21] Figure 2.11 shows that the recombinant *M. thermoacetica* FprA is also an active dioxygen reductase, but only when combined with Hrb. Similarly, Hrb has only a small background NADH oxidase activity in the absence of FprA (cf. legend to Figure 2.11). Analyses of the plots in Figure 2.11 (solid curve in panel A) gave K_m = 2 μM (monomer basis) for Hrb/FprA. Using an oxygen electrode, the mol

ratio of NADH oxidized:O_2 reduced under the conditions of Figure 2.11 was determined to be ~2:1, i.e., Hrb/FprA catalyzes the four-electron reduction of dioxygen to water by NADH, as has been verified for other FprAs. The K_m for O_2 is discussed below when comparing NO reductase activity. The Zn-FprA, when substituted for FprA, showed no dioxygen reductase activity above background under the conditions of Figure 2.11, consistent with participation of the diiron site in this activity. The data in Figure 2.11 were obtained from initial rates. During these assays a gradual and irreversible loss of the dioxygen reductase activity of FprA was noted similar to that observed (but not noted by the authors) in the kinetic traces previously reported for *E. coli* FlRd.[12] This inactivation for *M. thermoacetica* FprA is illustrated by ΔA_{340} vs. time traces shown in Chapter 3 (Figure 3.6).

NADH:NO Oxidoreductase Activity of Hrb/FprA. The fact that *M. thermoacetica* is a strict anaerobe and can use nitrate as electron acceptor, together with the observation that *E. coli* FlRd, an FprA homolog, showed NO consumption activity, prompted an examination of this latter activity for *M. thermoacetica* Hrb/FprA. Figure 2.12A shows that the Hrb/FprA combination does indeed have NADH:NO oxidoreductase activity under anaerobic conditions using DEA NONOate as the source of NO and that no such activity is observed when Zn-FprA is substituted for FprA. The parallel progression curves for NADH consumption and decomposition of the NONOate shows that the rate-determining step under these conditions is release of NO from the NONOate. Figure 2.12A also shows that the total amount of NADH oxidized is proportional to the total amount of NO released by the decomposition of DEA NONOate. A plot of these and additional such data in Figure 2.12B gives a stoichiometry of 1 mol NADH oxidized: 2 mol NO released, consistent with reduction of NO to N_2O. Omission of either FprA or Hrb from the assay mixture resulted in no consumption of NADH above background (similar

to that shown in Figure 2.12 with Zn-FprA). As shown in Figure 2.13, successive additions of aliquots of saturated aqueous NO solutions in place of DEA NONOate to anaerobic assay mixtures similar to those described in Figure 2.12, also yielded ~1:2 mol/mol NADH oxidized:NO added. The NO-dependent NADH consumption activity of FprA/Hrb showed no diminution in either rate or extent, even after as many as twelve successive 5-μM injections of NO over the course of 30 min.

Figure 2.14A plots the NADH:NO reductase activities of FprA/Hrb at saturating Hrb and NADH and fits to the Michaelis-Menten equation (dotted curve with parameters listed below). A significantly improved fit, especially at the lowest and highest NO concentrations, was obtained by adopting a kinetic scheme (Scheme 2.1) originally proposed for bacterial respiratory NORs that contain a binuclear heme:non-heme iron active site (cf. Chapter 1).[22,23] According to this scheme, at saturating levels of NADH and Hrb, reduction of two NO to N_2O occurs at a single reduced FprA active site (E_{red}).

$$E_{red} + NO \overset{K_1}{\rightleftharpoons} E_{red}\text{-}NO$$

$$E_{red}\text{-}NO + NO \overset{K_2}{\rightleftharpoons} E_{red}\text{-}(NO)_2$$

$$E_{red}\text{-}(NO)_2 \xrightarrow{k_{cat}} E_{ox} + N_2O$$

Scheme 2.1

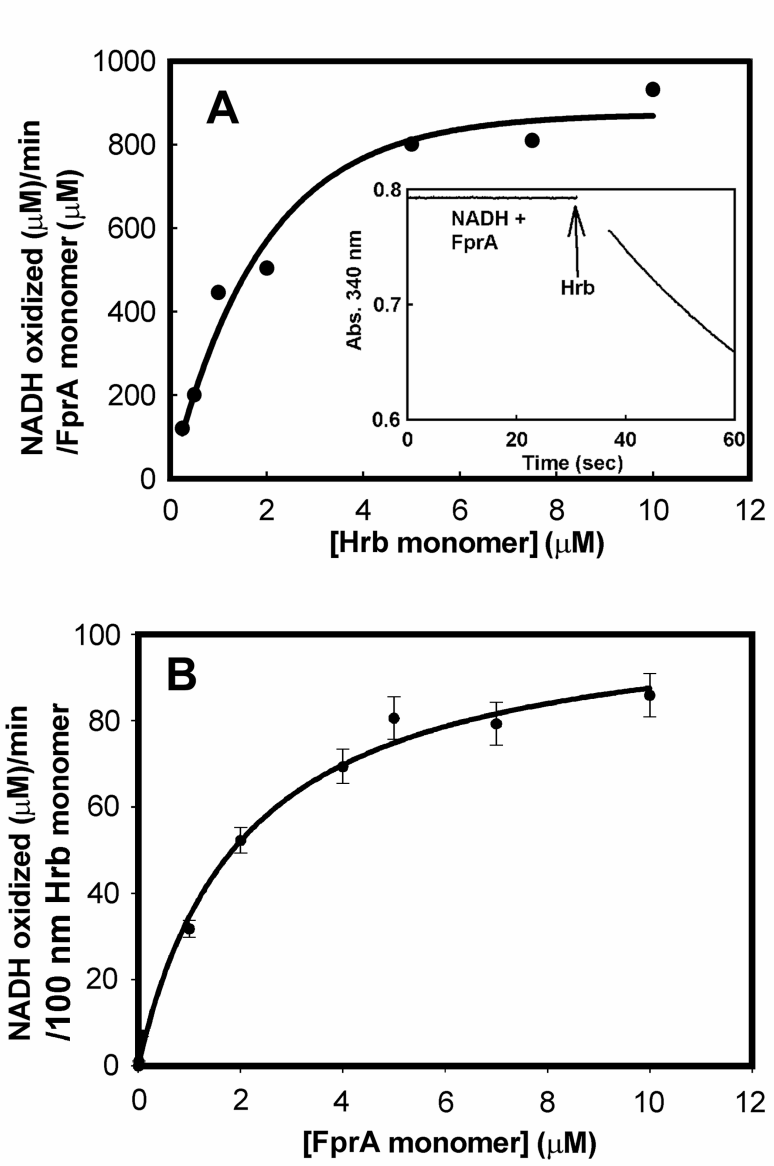

Figure 2.11. Concentration dependences of NADH:O_2 oxidoreductase activity of *M. thermoacetica* FprA/Hrb. Solid curves in panels A and B represent Michaelis-Menten equations fitted to the experimental data. (A) Plot of activity vs. Hrb concentration. Conditions: 50 nM FprA homodimer, 200 μM NADH and the indicated concentrations of Hrb in air-saturated 50 mM MOPS pH 7.0 at 25 ^{o}C. Inset: NADH oxidase activity monitored as $\Delta A_{340\ nm}$ vs. time in a solution containing 120 μM NADH in air-saturated 100 MES at pH 5.6 and 23 ^{o}C with FprA (50 nM homodimer) added at zero time and Hrb (50 nM homodimer) added at the time indicated by the arrow. The slope of the line after the addition of Hrb corresponds to 30 μM NADH oxidized/minute. The background NADH oxidase activity of Hrb in the absence of FprA under these conditions is ~1 μM NADH oxidized/minute. (B) Plot of activity vs FprA concentration. Conditions: 50 nM Hrb homodimer, 200 μM NADH, and the indicated concentrations of FprA in air-saturated 50 mM phosphate pH 7.

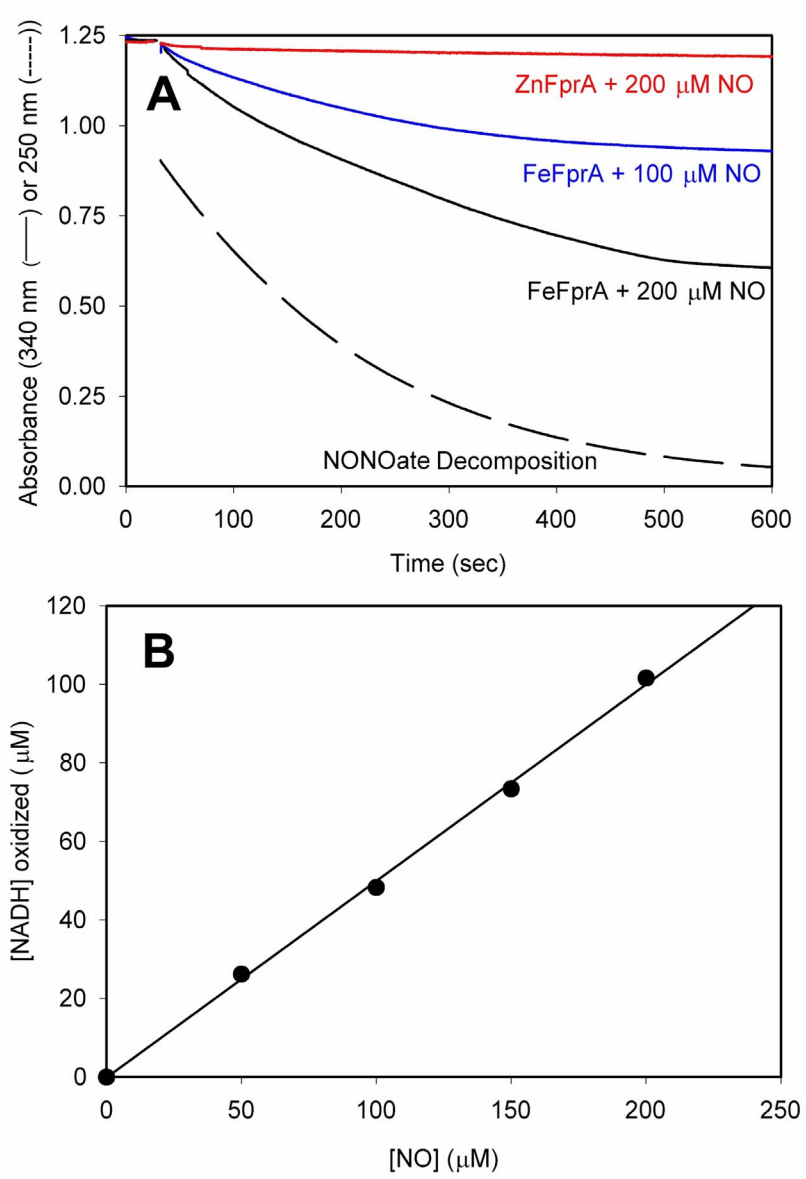

Figure 2.12. NADH:NO oxidoreductase activity of recombinant *M. thermoacetica* Hrb/FprA using DEA NONOATE as the source of NO. Conditions: 0.22 μM FprA (or Zn-FprA) homodimer, 0.25 μM Hrb homodimer, 200 μM NADH in anaerobic 100 mM potassium phosphate pH 7.0 containing 0.3 mM EDTA, 10 mM glucose + 10 U/mL glucose oxidase, and 150 U/mL catalase. (A) Rate of NADH oxidation was monitored at 340 nm and of decomposition of 133 μM DEA NONOATE at 250 nm (each mol of DEA NONOATE releases 1.5 mol NO). (B) Plot of NADH oxidized vs. NO released from DEA NONOATE.

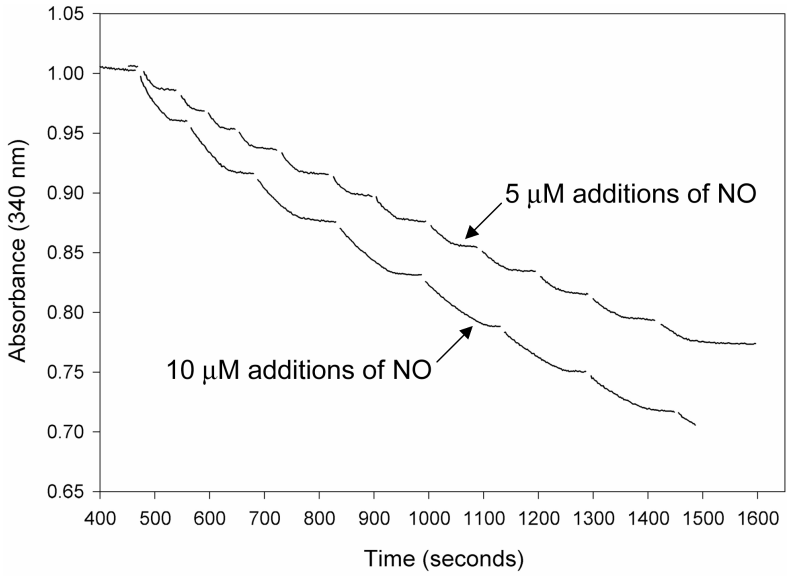

Figure 2.13. NADH consumption (as decrease in $A_{340\ nm}$) during titration of *M. thermoacetica* recombinant FprA and Hrb with successive aliquots of a saturated NO solution to give either 5 or 10 μM NO per addition. The titrations were performed anaerobically on solutions of FprA and Hrb (each 0.2 μM in monomer) and 150 μM (starting) NADH in 50 mM MOPS pH 7.3 containing 10 mM glucose, 10 U glucose oxidase/mL and 150 U catalase/mL in a 1-cm pathlength cuvette.

The rate law applying to Scheme 2.1 is: [22,23]

$$v = (V_{max}[NO]^2)/(K_1+K_2[NO]+[NO]^2) \qquad (1),$$

where ν is the initial velocity. Fits of equation 1 to the data plotted in Figure 2.14A yielded the solid curve with parameters: V_{max} = 27.3 ± 0.4 μM/min, corresponding to k_{cat} = 46 s^{-1} on a FprA monomer, i.e., active site basis, K_1 = 5.1 ± 1.0 μM, K_2 = 2.1 ± 0.3 μM. Unlike the respiratory NORs, no evidence for inhibition of FprA's NO reductase activity by NO was apparent at the highest concentrations of NO used in this work. Mechanisms consistent with Scheme 2.1 have been proposed for *E. coli* FlRd,[13] although the kinetics were not analyzed in this fashion.[24] The similar values of K_1 and K_2 suggest that, if Scheme 1.1 is operative in FprA, then the bindings of the two NO's, presumably one to each iron of the diiron site, are largely independent of each other.

Plots of the NADH:NO and NADH:O_2 reductase activities as a function of NO and O_2 concentrations, respectively, are shown in Figure 2.14B. Fits of these data to the Michaelis-Menten equation yielded the kinetic parameters, K_m: 4 μM for NO, 26 μM for O_2; k_{cat}: 50 s^{-1} for O_2, 48 s^{-1} for NO (on an FprA monomer basis); k_{cat}/K_m: 2 $s^{-1}\mu M^{-1}$ for O_2, 12 $s^{-1}\mu M^{-1}$ for NO. As can be clearly seen from these values and the plots in Figure 2.14B, *M. thermoacetica* recombinant FprA/Hrb is a more efficient NO than O_2 reductase by virtue of its lower K_m for NO.

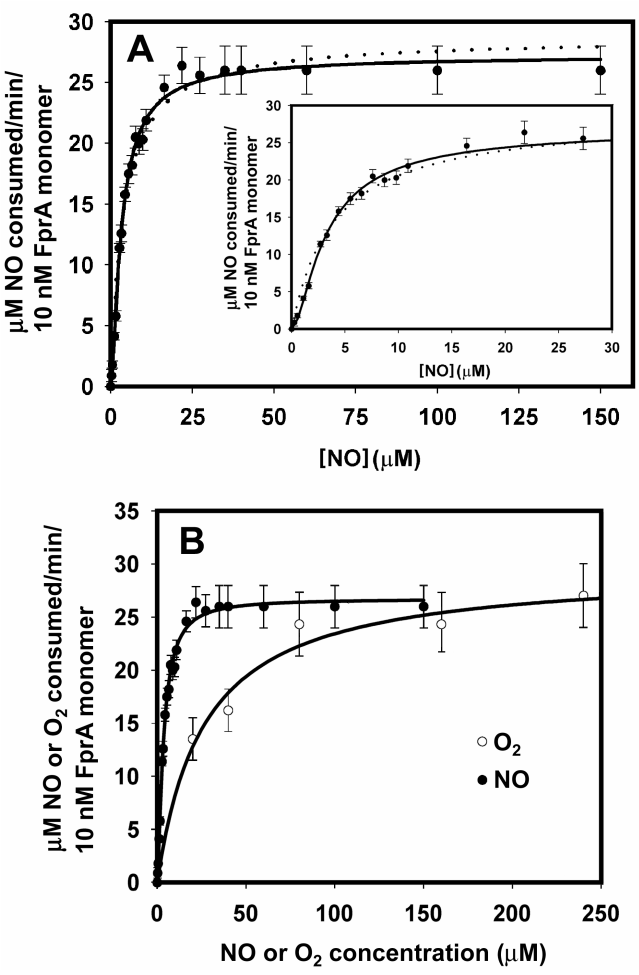

Figure 2.14. NO concentration dependence of NADH:NO reductase activity of Hrb/FprA (Panel A) and comparisons of NO and O_2 concentration dependences of the respective NADH:NO reductase and NADH:O_2 reductase activities of Hrb/FprA (Panel B) at saturating Hrb and NADH. Both O_2 and NO reductase assay solutions contained 5 μM Hrb homodimer, 5 nM FprA homodimer and 200 μM NADH in 50 mM phosphate pH 7. All rates were measured at room

temperature (~23 ºC). (A) NO reductase assay solutions were anaerobic and contained 5 mM glucose, 8 U /mL glucose oxidase, 150 U/mL catalase and the indicated initial concentrations of NO (added from a saturated aqueous solution). The NO reductase reactions were initiated by addition of FprA, and rates were measured by monitoring NO consumption using an NO electrode. Figure 2.15 illustrates representative individual traces monitoring NO consumption rates with the NO electrode. The dotted curve represents a fit of the data to the Michaelis-Menten equation with the parameters listed in the text. The solid curve represents a least-squares fit of the data to equation 1 listed in the text. (B) NO reductase data (filled circles) is same as plotted in Panel A. O_2 reductase assay solutions were made up anaerobically, and reactions were initiated by addition of O_2-saturated buffer to give the indicated initial concentrations of O_2. Rates were measured by monitoring NADH consumption at 340 nm and O_2 consumption rates (open circles) are plotted as one-half the NADH consumption rates. Solid curves are fits to the Michaelis-Menten equation using parameters listed in the text.

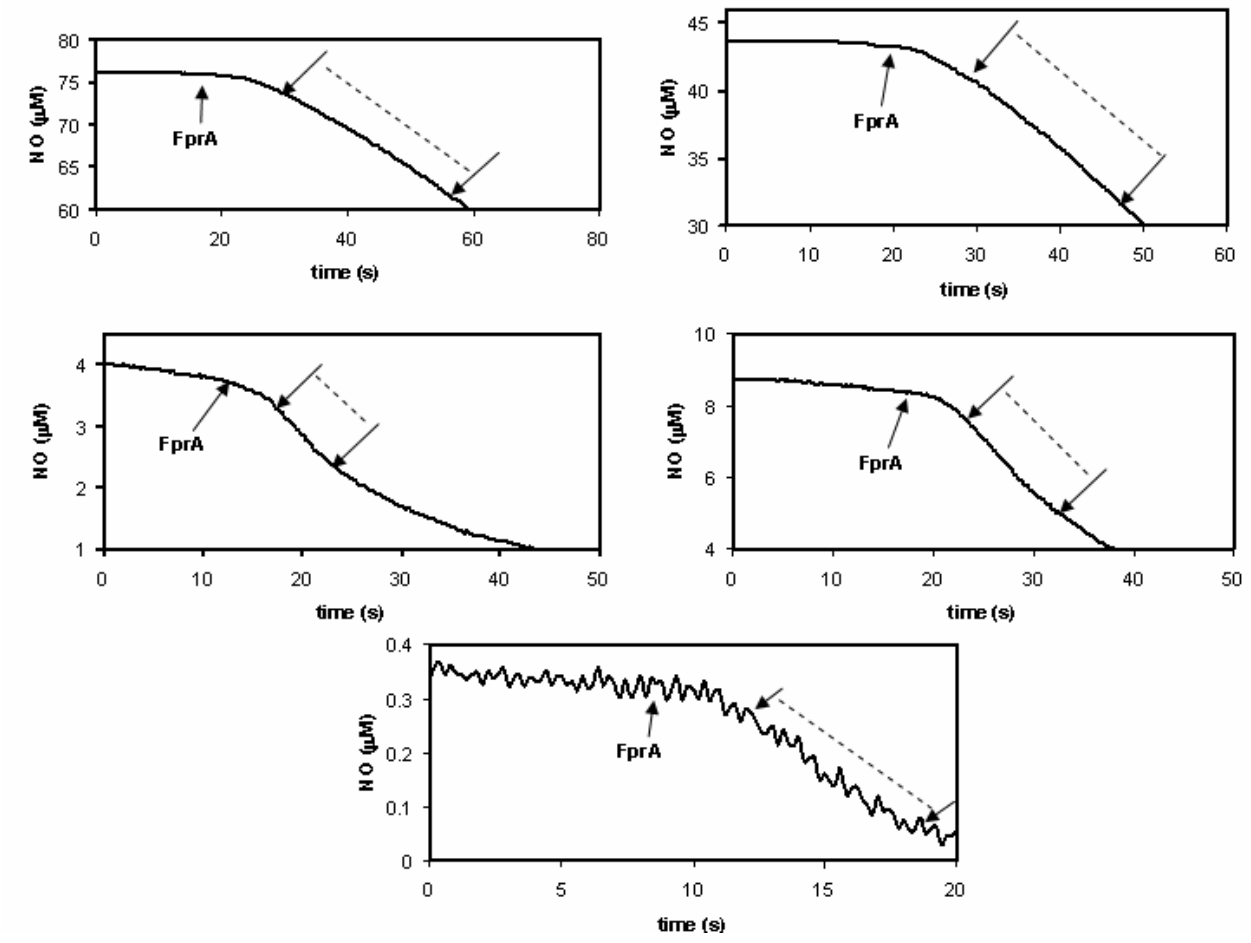

Figure 2.15. Traces illustrating NO consumption rates measured with an NO electrode at various initial NO concentrations, under conditions shown in Figure 2.14. Times of FprA addition are indicated with arrows. The intervals used to calculate rates are marked with dotted lines.

Complementation by M. thermoacetica FprA of E. coli ΔFlRd Strain Against NO Toxicity. The *E. coli* AG300 strain contains a disrupted FlRd gene. This strain was shown to be incapable of anaerobic growth in minimal media containing low micromolar levels of added NO, whereas the wild type strain under the same conditions showed little or no growth impairment.[13] As shown in Figure 2.16, IPTG-induced expression of the plasmid-borne *M. thermoacetica fprA* in strain AG300[pFprA-pCYB1] restored the anaerobic growth phenotype of cultures exposed to exogenous NO added either directly or from the NONOate. IPTG addition did not affect the growth rates in the absence of NO. If IPTG was not added, neither AG300[pFprA-pCYB1] nor the control strain, AG300[pCYB1], grew anaerobically in the presence of NO added to the levels listed in the legend to Figure 2.16.

Given the in vitro NO reductase activity of FprA, the logical inference from this growth complementation is that the level of intracellular NO is lowered due to the NO reductase activity of the heterologously expressed *M. thermoacetica* FprA. The lag phase in growth following addition of NO to the AG300[pFprA-pCYB1] cultures can be explained as the time required for induction of FprA and its lowering of the intracellular NO concentration to a tolerable level for growth. Since *M. thermoacetica* FprA by itself does not show NO consumption activity in vitro, but does show NADH:NO oxidoreductase activity when combined with Hrb, an endogenous *E. coli* enzyme most likely mimics Hrb's function as an NADH:FprA oxidoreductase. An analogous phenomenon occurred with *E. coli* FlRd. The gene adjacent to that encoding *E. coli* FlRd encodes a protein which functions as an NADH:FlRd oxidoreductase in vitro.[12] Disruption of this FlRd reductase gene resulted in somewhat lower intracellular NO consumption activity, but did not result in impaired anaerobic growth relative to wild type at micromolar levels of NO.[13] The FlRd reductase in strain AG300 could conceivably function as electron donor to the

heterologously expressed *M. thermoacetica* FprA. However, the *E. coli* FlRd reductase is not an Hrb homolog, nor does such a homolog exist in *E. coli*. The two domains of Hrb are instead reflected in separate modular fusions at the C-termini of two other FprAs, namely, the rubredoxin-like domain of *E. coli* FlRd and the FMN-binding domain of a cyanobacterial FprA.[3]

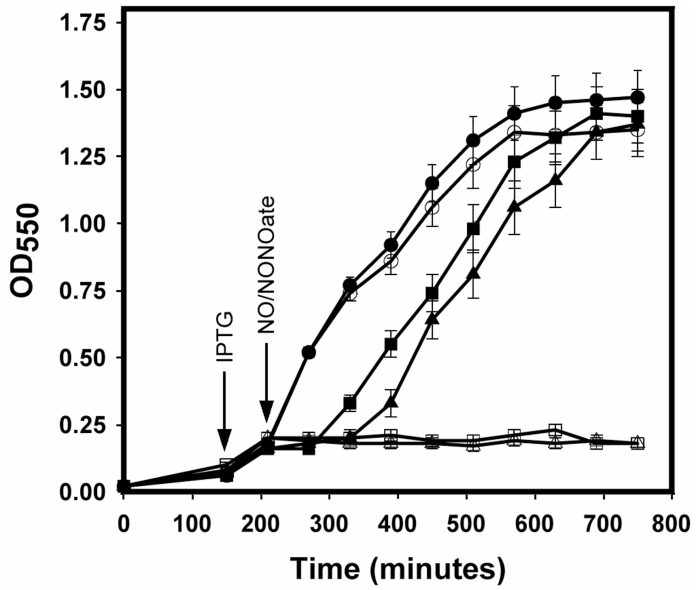

Figure 2.16. Restoration of anaerobic growth of *E. coli* AG300 in the presence of added NO by expression of plasmid-borne *M. thermoacetica fprA*. Cultures were grown in anaerobic minimal medium at 37 ºC as described in Materials and Methods. Filled symbols: strain AG300[pFprA-pCYB1]; open symbols: control strain AG300[pCYB1]. Circles: no NO added. Squares: NO added to a concentration of 7.2 μM; triangles: DEA NONOate added to a concentration of 5 μM. IPTG and NO/DEA NONOate were added at the times following inoculation indicated by the arrows. Each data point is the average of at least 4 independent growth experiments.

NO vs O_2 Reductase Function of FprA/Hrb. The relative NADH:NO oxidoreductase activities of *M. thermoacetica* Hrb/FprA NO determined in this work are similar to those reported for the *E. coli* FprA homolog, FlRd together with its FlRd reductase.[24] The turnover number (k_{cat}) for NADH:NO reductase activity of *M. thermoacetica* FprA at saturating Hrb, 48 s^{-1}, is somewhat higher than that reported for FlRd saturated with its reductase (8 s^{-1} on a monomer

basis), whereas the K_m for NO was reported to be < 1 μM for FlRd compared to 4 μM determined in this work for *M. thermoacetica* FprA.

Given the association of *M. thermoacetica fprA* and *hrb* with genes encoding oxidative stress protection proteins,[1] and the anaerobic growth requirement of *M. thermoacetica*, an oxidative or nitrosative stress protection function is more likely than a direct respiratory role for the respective O_2 or NO reductase activities of FprA/Hrb. Arguments in favor of an NO over an O_2 reductase function for *M. thermoacetica* FprA include its approximately 6-fold higher catalytic efficiency (k_{cat}/K_m) for NO vs O_2, its protection of a FlRd-deficient *E. coli* strain against the toxicity of micromolar levels of added NO (which notably occurred even without its presumed native electron donor, Hrb), and its progressive inactivation during O_2 reductase turnover but retention of activity during NO reductase turnover. This same pattern of inactivation and retention of activity was observed for *E. coli* FlRd both in vitro and in vivo.[12,13]

The present results show that both FprA and Hrb are expressed constitutively in *M. thermoacetica* under normal anaerobic growth conditions. While *M. thermoacetica* was reported to grow in liquid culture under low initial percentages of O_2, it failed to grow when the initial headspace O_2 was increased to 2.9 %,[5] which corresponds to a dissolved O_2 concentration that is approximately the same as Hrb/FprA's K_m for O_2 (26 μM) determined in this work. These observations further argue against an effective O_2-scavenging function for FprA.[5] *M. thermoacetica* could be exposed to NO as a consequence of its preference for nitrate as electron acceptor,[4] and a nitrate reductase activity has been detected in cell extracts.[25] Hrb/FprA shows no nitrate- or nitrite-dependent NADH consumption activity (Silaghi-Dumitrescu, R., Coulter, E. D., Kurtz, D. M., Jr., unpublished results). Alternatively, *M. thermoacetica* could be exposed to NO in its natural growth environment, presumed to be hot soil (with transient passage through

the mammalian intestine).[26,27] Hrb and FprA appear to be induced, by exposure of *M. thermoacetica* cultures to low-micromolar levels of NO (Das, A.; Kurtz, D. M., Jr.; Ljungdahl, L. G., unpublished observations). The results reported here demonstrate that *M. thermoacetica* Hrb/FprA is an efficient NO scavenger both *in vitro* and *in vivo*.

2.4 References:

(1) Das, A.; Coulter, E. D.; Kurtz, D. M., Jr; Ljungdahl, L. G. *J. Bacteriol.* **2001**, *183*, 1560-1567.

(2) Vadas, A.; Monbouquette, H. G.; Johnson, E.; Schroder, I. *J. Biol. Chem.* **1999**, *274*, 36715-36721.

(3) Vicente, J. B.; Gomes, C. M.; Wasserfallen, A.; Teixeira, M. *Biochem Biophys Res Commun* **2002**, *294*, 82-87.

(4) Seifritz, C.; Daniel, S. L.; Gossner, A.; Drake, H. L. *J. Bacteriol.* **1993**, *175*, 8008-8013.

(5) Karnholz, A.; Küsel, K.; Gossner, A.; Schramm, A.; Drake, H. L. *Appl. Environ. Microbiol.* **2002**, *68*, 1005-1009.

(6) Das, A.; Hugenholtz, J.; Van Halbeek, H.; Ljungdahl, L. G. *J. Bacteriol.* **1989**, *171*, 5823-5829.

(7) Sambrook, J.; Fritsch, E. F.; Maniatis, T. *Molecular cloning: a laboratory manual.*; 2nd ed.; Cold Spring Harbor Laboratory Press: Cold Spring Harbor, N.Y., 1990.

(8) Schagger, H.; von Jagow, G. *Analyt. Biochem.* **1987**, *166*, 368-379.

(9) Xiong, J.; Kurtz, D. M. J.; Ai, J.; Sanders-Loehr, J. *Biochemistry* **2000**, *39*, 5117-5125.

(10) Harlow, E.; Lane., D. *Antibodies: a laboratory manual*; Cold Spring Harbor Laboratory Press: Cold Spring Harbor, New York, 1988.

(11) Eby, D. M.; Beharry, Z. M.; Coulter, E. D.; Kurtz, D. M., Jr.; Neidle, E. L. *J. Bacteriol.* **2001**, *183*, 109-118.

(12) Gomes, C. M.; Vicente, J. B.; Wasserfallen, A.; Teixeira, M. *Biochemistry* **2000**, *39*, 16230-16237.

(13) Gardner, A. M.; Helmick, R. A.; Gardner, P. R. *J. Biol. Chem.* **2002**, *277*, 8172-8177.

(14) Solomon, E. I.; Brunold, T. C.; Davis, M. I.; Kemsley, J. N.; Lee, S.-K.; Lehnert, N.; Neese, F.; Skulan, A. J.; Yang, Y.-S.; Zhou, J. *Chem. Rev.* **2000**, *100*, 235-350.

(15) Frazão, C.; Silva, G.; Gomes, C. M.; Matias, P.; Coelho, R.; Sieker, L.; Macedo, S.; Liu, M. Y.; Oliveira, S.; Teixeira, M.; Xavier, A. V.; Rodrigues-Pousada, C.; Carrondo, M. A.; Le Gall, J. *Nat. Struct. Biol.* **2000**, *7*, 1041-1045.

(16) Chiu, H.-J.; Johnson, E.; Schroder, I.; Rees, D. C. *Structure* **2001**, *9*, 311-319.

(17) Eidsness, M. K.; Burden, A. E.; Richie, K. A.; Kurtz, D. M., Jr.; Scott, R. A.; Smith, E. T.; Ichiye, T.; Beard, B.; Min, T.; Kang, C. *Biochemistry* **1999**, *38*, 14803-14809.

(18) Eidsness, M. K.; Burden, A. E.; Richie, K. A.; Kurtz, D. M., Jr.; Scott, R. A.; Smith, E. T.; Ichiye, T.; Beard, B.; Min, T.; Kang, C. *Biochemistry* **2000**, *39*, 626.

(19) Jouanneau, Y.; Meyer, C.; Asso, M.; Guigliarelli, B.; Willison, J. C. *Eur. J. Biochem.* **2000**, *267*, 780-787.

(20) Zeng, Q.; Smith, E. T.; Kurtz, D. M. J.; Scott, R. A. *Inorg. Chim. Acta* **1996**, *242*, 245-251.

(21) Chen, L.; Liu, M. Y.; LeGall, J.; Fareleira, P.; Santos, H.; Xavier, A. V. *Biochem. Biophys. Res. Commun.* **1993**, *193*, 100-105.

(22) Girsch, P.; de Vries, S. *Biochim. Biophys. Acta* **1997**, *1318*, 202-216.

(23) Koutny, M.; Kucera, I. *Biochem. Biophys. Res. Commun.* **1999**, *262*, 562-564.

(24) Gomes, C. M.; Giuffre, A.; Forte, E.; Vicente, J. B.; Saraiva, L. M.; Brunori, M.; Teixeira, M. *J. Biol. Chem.* **2002**, *277*, 25273-25276.

(25) Arendsen, A. F.; Soliman, M. Q.; Ragsdale, S. W. *J. Bacteriol.* **1999**, *181*, 1489-1495.

(26) Breznak, J. A.; Kane, M. D. *FEMS Microbiol. Rev.* **1990**, *7*, 309-313.

(27) Drake, H. L.; Daniel, S. L. *Res. Microbiol.* **2004**, *155*, in press.

CHAPTER 3

A FLAVO-DIIRON PROTEIN FROM *DESULFOVIBRIO VULGARIS* WITH NITRIC OXIDE REDUCTASE AND OXIDASE ACTIVITIES

3.1. Introduction

A widespread class of bacterial and archaeal proteins, called FprA (type A flavoproteins) appear to harbor a novel type of active site, featuring a flavin in close contact with a non-heme, non-sulfur diiron site contributed from flavodoxin-like and metallo-β-lactamase-like domains, respectively.[1-3] An FprA homolog in the sulfate-reducing bacterium, *Desulfovibrio gigas*, named rubredoxin:oxygen oxidoreductase (ROO), was proposed to function as a dioxygen reductase based only on its *in vitro* oxidase activity.[4,5] More recently, *in vivo* evidence for a non-respiratory nitric oxide reductase (NOR) function was obtained for the FprA homolog, referred to as flavorubredoxin, from the facultative anaerobic bacterium, *E. coli*.[6] This non-respiratory NOR activity, i.e., catalyzing NO to N_2O reduction, protects *E. coli* against "nitrosative stress" under anaerobic growth conditions. Thus, expression of flavorubredoxin was induced by anaerobic exposure of *E. coli* to nitric oxide, flavorubredoxin knockout *E. coli* strains were more sensitive than wild-type strains to anaerobic nitric oxide exposure,[6] and expression of plasmid-borne flavorubredoxin restored nitric oxide resistance.[6-8] *E. coli* flavorubredoxin was reported to show both nitric oxide reductase and dioxygen reductase activities *in vitro*.[9,10] A five-gene cluster in

the anaerobic, acetogenic bacterium, *M. thermoacetica*, contains genes encoding an FprA together with oxidative stress protection proteins.[11] This gene clustering was initially taken to imply a dioxygen reductase function for FprA; however, efficient NOR activity, both *in vitr*o and *in vivo*, was subsequently demonstrated for *M. thermoacetica* FprA.[12] FprA homologs are found predominantly in air-sensitive microorganisms, often in multiple genomic copies. However, the generality of the NOR function for FprAs has not been established. *D. gigas* ROO, for example, has not been reported to have NOR activity.

The genome of the sulfate-reducing bacterium, *D. vulgaris,* encodes two FprA homologs, neither of which has been isolated. An amino acid sequence alignment of FprAs from *D. vulgaris, D. gigas* and *M. thermoacetica* (cf. Figure 3.1) reveals that the metallo-β-lactamase-like domain with its diiron ligand residues and the flavin-binding domain are conserved. Although not noted previously, one of these *D. vulgaris* FprA homologs (DvFprA1 in Figure 3.1) is upstream of and in close proximity to a gene encoding the so-called hybrid cluster (a.k.a., prismane) protein, HCP. HCP features an unusual iron-sulfur-oxygen cluster at its presumed active site.[13] The function of HCP has not been conclusively established. Expression of *E. coli* and *Morganella morganii* HCPs is induced by nitrate and nitrite, and *E. coli* HCP was reported to exhibit hydroxylamine reductase activity *in vitro* (catalyzing reduction of NH_2OH to NH_3 and H_2O).[13,14] The proximity of HCP and FprA genes in *D. vulgaris* is consistent with the involvement of the two proteins in nitrogen oxide metabolism. Unlike *M. thermoacetica*, *D. vulgaris* cannot grow using nitrate or nitrite as respiratory terminal electron acceptors.[15,16] *D. vulgaris* nevertheless contains and constitutively expresses a cytochrome *c* nitrite reductase (ccNIR), for which a detoxifying role in reducing nitrite as well as NO has been proposed.[15] It has alternatively been proposed that this ccNIR activity prevents inhibition of sulfate reduction

by nitrite.[17] HCP, FprA, and ccNIR may, thus, be members of a nitrosative stress protection system in *D. vulgaris.*

Based on its homology to *D. gigas* ROO, the second *D. vulgaris* FprA homolog (DvFprA2 in Figure 3.1) was proposed to be involved in oxidative stress protection, functioning as a dioxygen reductase.[17] As diagrammed in Figure 3.2, the DvFprA2 gene is found ~130 bp downstream of an *rbo/rub* operon encoding rubredoxin (Rub) and a 2-Fe superoxide reductase (Rbo). Both of these latter proteins are known to be involved in oxidative stress defense.[18-20] This situation is reminiscent of that found in *M. thermoacetica*, where an FprA gene is part of a five-gene cluster that also encodes the FprA reductase, Hrb, as well as Rub, Rbo, and rubrerythrin (another protein known to be involved in oxidative stress).[11] Northern blotting of *D. vulgaris* RNA probed with a DNA oligomer having the *rbo/rub* nucleotide sequence (i.e., the *fprA* region was not included in the probe) revealed a transcript of ~700-nt, a length consistent with that expected for an *rbo/rub* operon.[21] However, a minor transcript of ~3,000 nt was also observed in the same Northern blots. This larger size is consistent with an *rbo/rub/fprA* transcript.

```
M.thermoacetica FprA      MSQPVAITDGIYWVGAVDWNIRYFHGPAFSTHRGTTYNAYLIV-DDKTALVDTVYEPFKE
DvFpra1                   ---MRKIVESVYWVGAVDWDRRLFDSLVPLPD-GTTYNAYLVEGSEKTALIDAVDPDMVD
DvFpra2                   -MHPIEIKKDIFWVGVVDHNSRDFHGYSLSPQ-GTTYNAYVVK-DEKTVLFDTVKHDFTD
D.gigas ROO               -MQATKIIDGFHLVGAIDWNSRDFHGYTLSPM-GTTYNAYLVE-DEKTTLFDTVKAEYKG
                                * .... **.:* : * *..    .  *******::  .:**.*.*:*

M.thermoacetica FprA      ELIAKLKQIKDPVKLDYLVVNHTESDHAGAFPAIMELCPDAHVLCTQRAFDSLKAHYSHI
DvFpra1                   TLLGHLDGVE---KLDYVISQHAEQDHSGTIALVLDLYPEAKVVTNAKAKSMLMDLLLIP
DvFpra2                   TMLCRLSRVVEPCKIDYIVCNHLEPDHAGALPELIARCKPEKIFCSPMGLKAMEAHFDTT
D.gigas ROO               ELLCGIASVIDPKKIDYLVIQHLELDHAGALPALIEACQPEKIFTSSLGQKAMESHFHYK
                           ::  :  :    *:**:: :* * **:*::. ::      ::. .  . . :

M.thermoacetica FprA      DFNYTIVKTGTSVSLGKRSLTFIEAPMLHWPDSMFTYVPEEALLLPNDAFGQHIATSVRF
DvFpra1                   DDKFIVVGDGETLSLGDKTLTFILTPWVHWPETMSTYLAEDKILFSCDFFGSHIATSDLF
DvFpra2                   GWPVEVVKTGDSISIGKRTIHFVETRMLHWPDSMVSYIPEDKLLICNDAFGQNIASTERY
D.gigas ROO               DWPVQVVKHGETLSLGKRTVTFYETRMLHWPDSMVSWFADEKVLISNDIFGQNIAASERF
                          .    :*  * ::*:*.::: *  :  :***::* :::.:: :*:  * **.:**::  :

M.thermoacetica FprA      DDQVDAGLIMDEAAKYYANILMPFSNLITKKLDEIQKINLAIKTIAPSHGIIWR--KDPG
DvFpra1                   VRDQGR--VHEAAKRYFGEIMMPFRTIIAKNLEKLG--PYDIRMIAPSHGQIYD---SPG
DvFpra2                   ADEIDRSALFHAMKEYYHNIVLPFSPIVLKTLAQIEQLGLDIDMLAPDHGLIFRGYDDVK
D.gigas ROO               SDQIPVHTLERAMREYYANIVNPYAPQTLKAIETLVGAGVAPEFICPDHGVIFRGADQCT
                            :     :     .*: :*: *:     * :  :          :.*.** *:    .
```

```
M.thermoacetica FprA      RIIEAYARWAEGQGKAKAVIAYDTMWLSTEKMAHALMDGLVAGGCEVKLFKLSVSDRNDV
DvFpra1                   WIIDAYRDWVSGVAHNLVAFPFVSMHGSTRLMVDHLAAALSERDVRVELFNLAVTDIGKL
DvFpra2                   YALDTYRIFAEQKPQKRAVIVYDTMWHSTEKMASAIAEGLESVGVPTRVMWLKANHHSAV
D.gigas ROO               FAVQKYVEYAEQKPTNKVVIFYDSMWHSTEKMARVLAESFRDEGCTVKLMWCKACHHSQI
                            :: *  :..      ..: : :*  **. *.  :  .:   .  ..::   . . . :

M.thermoacetica FprA      IKEILDARAVLVGSPTINNDILPVVSPLLDDLVGLRPKNKVGLAFGAYGWGGGAQKILEE
DvFpra1                   AMSLVDAGTIVLGTPTVLAGPHPMAAYAAFLANALRPKAKYLSIVGSYGWGGKTVETLAG
DvFpra2                   MTELADCGAVLVGSPTHNNGILPAVAAMLTYMKGLRPQNRIGAAFGSFGWSGESVKSITE
D.gigas ROO               MSEISDAGAVIVGSPTHNNGILPYVAGTLQYIKGLRPQNKIGGAFGSFGWSGESTKVLAE
                            .: *. ::::*:**   .  * .:       .***: :    .*::**.* : : :

M.thermoacetica FprA      RLKAAKIELIAEPGPTVQWVPRGEDLQRCYELGRKIAARIAD-------
DvFpra1                   MIPNLKVEVLDPVLCKGLPTDDTYGALDRLADAIAAKHKESGFQR----
DvFpra2                   WLQSMGMETPVDP-VKVKHVPTHDTYRQCFEMGQAVGRALIELIEKCGG
D.gigas ROO               WLTGMGFDMPATP-VKVKNVPTHADYEQLKTMAQTIARALKAKLAA---
                           :    .:
```

Figure 3.1. ClustalW amino acid sequence alignment of *M. thermoacetica* FprA (Mt, accession number AAG00802), *D. gigas* ROO (Dg, AAG34792) and the two *D. vulgaris* FprA homologs, (Dv1, AAS96489, encoded upstream of hcp; Dv2, YP_012395, encoded downstream of rbo-rub). Diiron ligand residues in *D. gigas* ROO are marked with red stars, and residues involved in a flavin-binding signature are underlined. '*' indicates positions which have a single, fully conserved residue; ':' indicates that one of the following 'strong' groups is fully conserved: STA, NEQK, NHQK, NDEQ, QHRK, MILV, MILF, HY, FYW; '.' indicates that one of the following 'weaker' groups is fully conserved: CSA, ATV, SAG, STNK, STPA, SGND, SNDEQK, NDEQHK, NEQHRK, FVLIM, HFY.

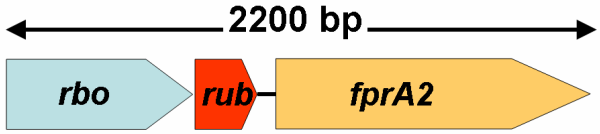

Figure 3.2. Potential *D. vulgaris rbo/rub/fprA2* operon. Distances are scaled to approximate lengths in bp.

Reported here are recombinant expression, isolation and characterization of DvFprA2. Similarly to the *M. thermoacetica* FprA, DvFprA2 exhibits anaerobic NOR activity both *in vivo* and *in vitro*, as well as dioxygen reductase activity *in vitro*. The latter but not the former activity leads to irreversible inactivation of the enzyme.

3.2 Materials and methods

Reagents and General Procedures. All solutions were prepared in deionized water. NADH, and NADPH (Sigma Chemical Co.) and protein molecular weight standards (Bio-Rad, Inc.) were used without further purification. Recombinant *D. vulgaris* rubredoxin was purified as

previously described.[18] Recombinant *M. thermoacetica* FprA was purified as described in Chapter 2. Molecular biology manipulations followed standard protocols.[22] DNA restriction and ligating enzymes were obtained from New England Biolabs, Inc. Stock solutions (25 mM) of DEA NONOate (diethylammonium (Z)-1-(N,N-diethylamino) diazen-1-ium-1,2-diolate, Cayman Chemicals, Inc.) were prepared in 0.01 M NaOH. DEA NONOate is stable at high pH but decomposes to release NO gas (1.5 mols NO/1 mol DEA NONOate) when added to assay mixtures at ~ pH 7. Where indicated, solutions were made anaerobic by repetitive vacuum/argon or N_2 gas exchange or extensive purging with argon or N_2 gas. Gaseous nitric oxide (98.5%) was purchased from Aldrich. The NO was purified by bubbling through 100 mL of a 10% KOH solution. The purified NO gas was used to prepare saturated NO solutions (~1.8 mM) by bubbling the gas through anaerobic deionized water for 15 minutes. Protein purity was judged by SDS-PAGE (15% polyacrylamide gels) and Coomassie blue staining.[23] Growth of *D. vulgaris* (Hildenborough) and isolation of chromosomal DNA therefrom was carried out by Dr. Kim Yong Ng in the Kurtz lab. Liquid cultures (4 L) of *D. vulgaris* were grown in medium C [24] at 37 ^{o}C in an anaerobic chamber (Coy Laboratory Products Inc.) containing a gas mixture of 5% (v/v) H_2, 10% (v/v) CO_2 and 85% (v/v) N_2. Cultures were harvested at late log phase growth (20 h). *D. vulgaris* strains were stored and maintained as liquid cultures in medium B[24] at 4 ^{o}C as previously described. Western blotting followed a standard procedure.[25] Chromosomal DNA of *D. vulgaris* and plasmid DNA were isolated and purified using a QIAamp DNA Mini Kit and QIAprep Spin Miniprep Kit from Qiagen Inc., Studio City, Calif., respectively. ESI protein mass spectrometry was performed at the University of Georgia Chemical and Biological Sciences Mass Spectrometry Facility on a Perkin Elmer Sciex API I plus quadrupole mass spectrometer. Antibodies against purified recombinant *D. vulgaris* FprA and Hrb were raised in rabbits at the

Animal Care and Use Facility at the University of Georgia and purified from serum by a standard procedure.[26]

D. vulgaris FprA Cloning, Overexpression and Purification. The N- and C-terminal PCR primers, incorporating *Nde*I and *Bam*HI restriction sites, respectively, DvFprAN [5`-acgacagccatATGCATCCTATCGAAATC-3`], and DvFprAC [5`-taatggatccCTAACCCCCCGCACTTTTC-3`], were used for PCR amplification and subsequent cloning of the DvFprA2 gene (that downstream of *rbo-rub*, designated DVU3185[17]) from *D. vulgaris* genomic DNA into both the pET-(21b+) (Novagen, Inc.) and pCYB1 (New England Biolabs) vectors, generating the respective plasmids pET-DvFprA (without the His-tag) and pCYB1-DvFprA. Overexpression and purification of DvFprA2 was identical to that described in Chapter 2 for *M. thermoacetica* FprA. As for *M. thermoacetica* FprA, the pET-DvFprA (non-His-tagged) plasmid was typically used for overexpression.

Hrb and Flavo-Hrb expression and characterization: Recombinant *M. thermoacetica* Hrb was expressed and purified as described in Chapter 2, under low-temperature (0-4 °C) and low-light conditions. However, a variant of Hrb, labeled flavo-Hrb, could be purified if no precautions were taken to avoid exposure to light and all manipulations were carried at room temperature. Flavo-Hrb eluted off the columns as a bright-yellow fraction, as opposed to full-size Hrb which was orange. Pale pink fractions, presumably containing the Hrb rubredoxin domain (cf. UV-vis absorption spectroscopy and gel-filtration), could also be identified alongside Flavo-Hrb. Flavo-Hrb was verified by SDS-PAGE, UV-vis absorption, mass spectrometry and N-terminal amino acid sequencing to consist of a truncated Hrb, lacking the rubredoxin domain and containing only flavin as a cofactor (molecular mass 17828 Da confirmed with mass spectrometry, indicating cleavage after residue T164, cf. Figure 2.1, Chapter 2, and an

MDTKALHTLTYGLXT N-terminal sequence). Flavo-Hrb did not catalyze FprA reduction by NADH, but did catalyze reduction of *D. vulgaris* rubredoxin by NADH, albeit at rates too slow to support a measurable NADH:FprA oxidoreductase activity.

Analytical Methods. Protein concentrations were determined using the Bio-Rad protein assay (Bio-Rad, Hercules, CA) with bovine serum albumin as the standard. Metal contents of Hrb and FprA were determined by inductively coupled plasma-atomic emission analysis at the University of Georgia Chemical Analysis Facility. Flavin was identified and quantitated as described previously.[11] Molar absorptivities were determined from the protein quantitations, and these values were subsequently used to calculate all protein concentrations from measured absorbances. N-terminal amino acid sequencing of Flavo-Hrb was performed at the University of Georgia Integrated Biotechnology Laboratories facility.

Enzymatic Assays. NADH-dependent oxidase (O_2-consumption) assays were monitored in air-saturated buffer by the rate of decreasing absorbance at 340 nm due to O_2-dependent NADH oxidation NADH-dependent NO reductase (NO consumption) activities were assayed anaerobically by monitoring the decrease in absorbance at 340 nm. NO, from an NO-saturated aqueous solution, was introduced into the anaerobic assay mixture in a 1-cm pathlength cell via a Hamilton gas-tight syringe and the rate of decrease in A_{340} due to NADH consumption was measured. Alternatively, the NADH-dependent NO reductase activity was monitored under the conditions described above, but measuring the decrease in NO concentration with a Clark-type NO-sensitive electrode (2mm diameter, WPI, Inc.). NO electrode measurements were performed with stirring inside an NO chamber (WPI, Inc.), where anaerobicity was maintained by continuously purging the headspace with nitrogen gas through a needle inserted into one of the two narrow ports. The second port was used for adding the reagents via Hamilton gas-tight

syringes. Appendix B shows a schematic diagram of this chamber, with details of the operation procedure. All assays were performed at pH 7.0 and room temperature, unless otherwise noted. The NO electrode was calibrated using a nitrite/iodide/H_2SO_4 mixture, as described in the NO electrode manual. Further details of the assay protocols, including component concentrations, are provided in the figure legends.

Spectroscopy. Ultraviolet-visible absorption spectra were obtained in 1-cm pathlength quartz cuvettes on a Shimadzu UV-2401PC scanning spectrophotometer.

FprA Complementation of E. coli Growth Sensitivity to NO. E. coli strain AG300, containing a disrupted FlRd gene, was kindly provided by Paul R. Gardner.[6] The anaerobic culture medium contained 60 mM K_2HPO_4, 33 mM KH_2PO_4, 7.6 mM $(NH_4)_2SO_4$, 1.7 mM sodium citrate, 1 mM $MgSO_4$, 10 μM $MnCl_2$, 10 μM thiamin hydrochloride, 2% potassium gluconate, 0.25% casamino acids, ampicilin (0.1 g/L) and chloramphenicol (0.1 g/L). For anaerobic growth, a protocol routinely employed by Amaresh Das for growing *M. thermoacetica* under anaerobic conditions was used, where the culture bottles are made anaerobic, sealed, and then used for growth without any need for maintaining an anaerobic environment around the bottles (i.e., an anaerobic chamber was *not* used at any point throughout these growth studies). Thus, the medium (in 1- or 2-liter Erlenmeyer flasks, covered with aluminum foil) was preheated for 10 minutes in an autoclave at 100 °C, then purged with N_2 for ~20 minutes (during which time the temperature dropped to ~50-60 °C). Twenty-five- or 100-mL volumes of this medium were transferred into narrow-neck culture bottles, so that the ratio of culture volume to head-space was 4:1. The bottles were purged with N_2 for 5-15 minutes, both *before* and *after* transferring the media. The bottles were then sealed by crimping with 1-cm thick rubber septa and autoclaved. At this point the culture medium and headspace in the bottles were assumed to be anaerobic and to remain so

throughout the growth study. All subsequent additions to these flasks (e.g., inoculation, induction, NO addition) were done with either disposable 1-mL syringes or Hamilton 50-µL gas-tight syringes without removing the septa. Ten-milliliter cultures of *E. coli* AG300 that had been transformed with either pCYB1 or pCYB1-pFprA were grown overnight with shaking in 15-mL Falcon tubes aerobically at 37 °C in LB medium containing ampicilin (0.1 g/L) and chloramphenicol (0.1 g/L). One-half-milliliters of these aerobic cultures were inoculated into 25 mL of the anaerobic culture medium in sealed bottles prepared as described above. The anaerobic cultures were grown without shaking at 37 °C until O.D. 550 nm ~0.6 (typically 8 hours to overnight), at which point 0.5 mL aliquots of these cultures were used to inoculate fresh 25-mL batches of anaerobic culture medium, which were then incubated without shaking at 37 °C until O.D. 550 nm ~0.6. This cycle was repeated a third time. At O.D. ~0.6, 1-mL aliquots of the third subcultures were used to inoculate 150-mL flasks each containing 100 mL of anaerobic culture medium. Results reported below were obtained with these 100-mL cultures. IPTG (0.05 mg/L) was added to each 100-mL culture at O.D. 550 nm ~0.1. Where required, aliquots of either an NO-saturated aqueous solution or 25 mM DEA NONOate were added to the 100-mL cultures 60 minutes after IPTG addition. Concentrations of added NO are given in the figure legends. Optical densities were measured by removing 1-mL aliquots of medium from the culture bottles, using sterile disposable 1-mL syringes.

3.3 Results and discussion

Expression of DvFprA2 in D. vulgaris. Western blots of *D. vulgaris* cells using antibodies raised against DvFprA2 (cf. Figure 3.3) show that this protein is constitutively expressed in *D. vulgaris* under anaerobic conditions using lactate as electron donor and sulfate as electron acceptor.[27] The

effect of nitric oxide or dioxygen on the level of FprA expression in *D. vulgaris* has not been reported and was not investigated in this work.

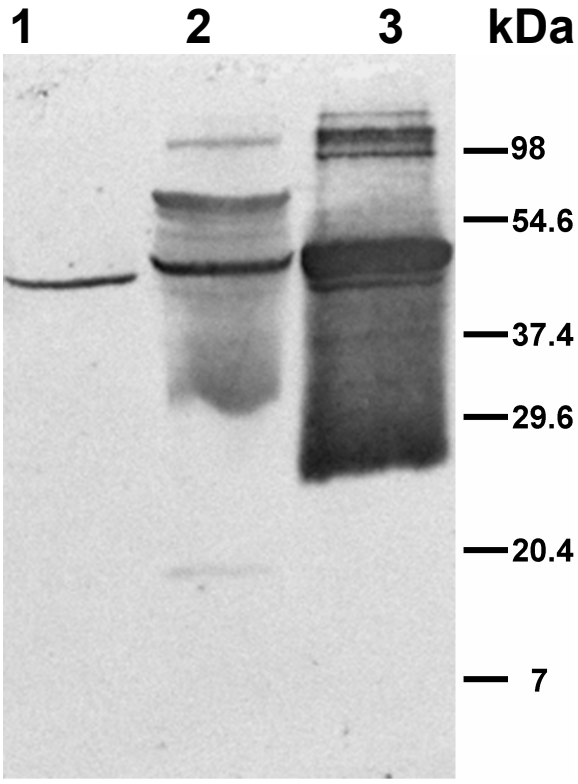

Figure 3.3. Western blot probed with antibodies raised against recombinant DvFprA2. Lane 1, purified recombinant DvFprA2; lane 2, *D. vulgaris* cell extract; lane 3, purified as-isolated *M. thermoacetica* FprA.

Recombinant DvFprA2 Overexpression, Purification, and Physicochemical Properties. All FprA and Hrb concentrations are expressed on a monomer basis, unless otherwise noted. Recombinant DvFprA2 was readily overexpressed in and isolated from *E. coli* under the same conditions and with similar yields as for *M. thermoacetica* FprA (cf. Chapter 2). Also paralleling the *M. thermoacetica* FprA, DvFprA2 was shown by gel filtration to be a homodimer in solution, whereas SDS-PAGE showed a monomer of molecular mass consistent with that calculated from the amino acid sequence (~45 kDa). However, unlike *M. thermoacetica*, but much like *D. gigas* ROO,[4,5] DvFprA2 co-purified with a sub-stoichiometric heme contaminant. The *D. gigas* ROO

crystal structure revealed no heme or obvious heme-binding site.[2] Attempts to remove the heme contaminant from the DvFprA2 preparations included anion/cation-exchange and hydrophobic chromatographies, ammonium sulfate precipitation, and mild acidic or basic treatment. None of these treatments succeeded in removing all of the heme. Figure 3.4 shows the UV-vis absorption spectrum of as-isolated DvFprA*2*, which is dominated (as in the case of *D. gigas* ROO[4,5]) by heme and flavin absorptions. Following heat-denaturation to release the protein-bound flavin,[28] an extinction coefficient of 24 mM homodimer^{-1}cm^{-1} was calculated for the flavin at 470 nm, essentially identical to that of *M. thermoacetica* FprA. Metal and flavin analysis confirmed a cofactor content of 0.7-0.9 FMN and 1.7-1.9 Fe per DvFprA2 monomer. Assuming ε_{420} = 100 mM^{-1} cm^{-1} for the heme contaminant, the estimated mol ratio of heme/flavin was ~0.3.

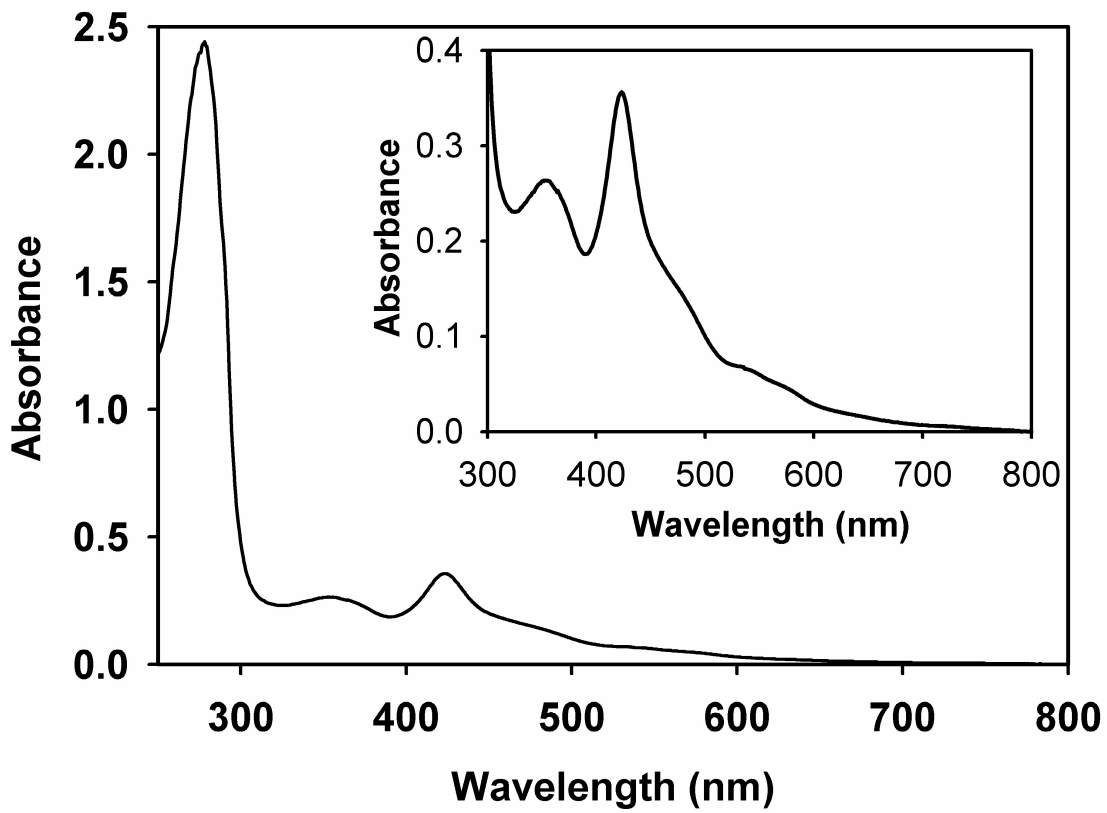

Figure 3.4. UV-vis absorption spectrum of as-isolated DvFprA2 in aerobic 50 mM MOPS pH 7.3.

Oxidase and Nitric Oxide Reductase Activities. As expected, the recombinant DvFprA2 exhibited both dioxygen reductase and NOR activities. Figures 3.5 or 3.6 show traces comparing NADH consumption rates of DvFprA2 vs. *M. thermoacetica* FprA in the presence of either nitric oxide (Figure 3.5) or dioxygen (Figure 3.6), using *M. thermoacetica* Hrb as the NADH:FprA oxidoreductase. For NOR activity (Figure 3.5) the NADH concentration decreased linearly with time (over periods where NADH concentration was not rate-limiting), whereas for dioxygen reductase activity (Figure 3.6) this decrease was non-linear and indicative of a progressive decrease in the rate of NADH consumption. Thus, DvFprA2, similarly to *M. thermoacetica* FprA, became inactivated when turning over as dioxygen reductase, but not when turning over as anaerobic NOR.

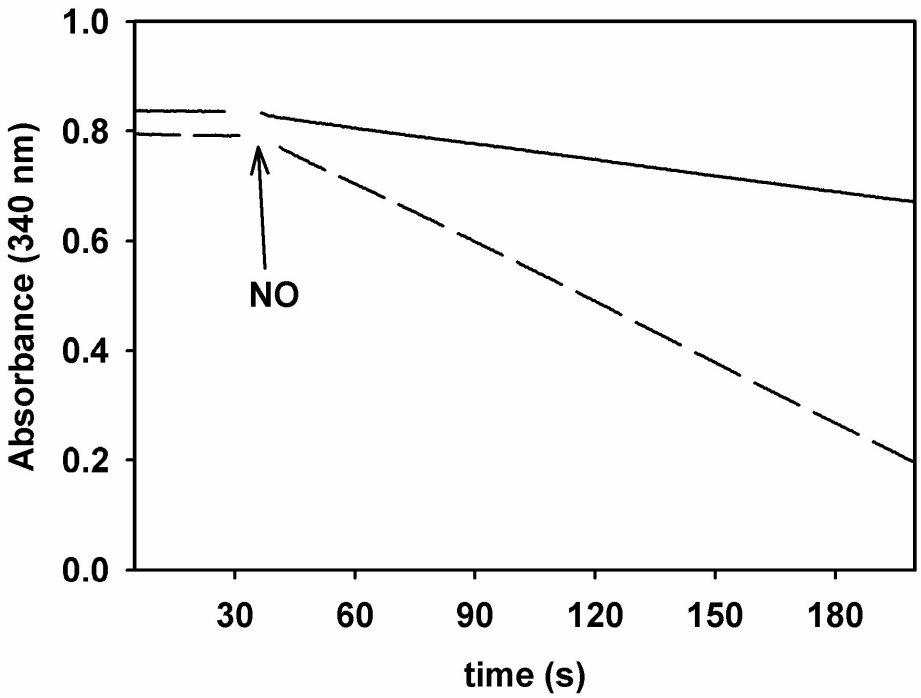

Figure 3.5. NOR activity of 1 μM DvFprA2 (solid line) or *M. thermoacetica* FprA (dashed line), monitored as the time course of NADH consumption (ΔA_{340}), in the presence of 1 μM *M. thermoacetica* Hrb and 160 μM NADH in anaerobic 50 mM MOPS, pH 7.0 at room temperature. NO (100 μM) was added at the time indicated by the arrow.

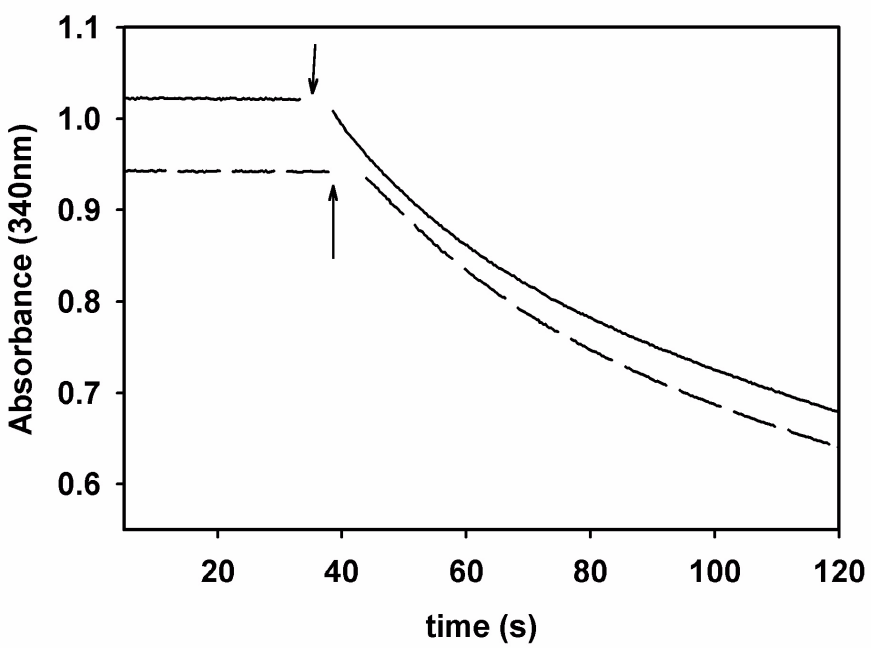

Figure 3.6. Dioxygen reductase activity of recombinant DvFprA2 (0.7 μM, solid line) and recombinant *M. thermoacetica* FprA (0.7 μM, dashed line) in the presence of 0.8 μM recombinant *M. thermoacetica* Hrb, monitored as time course of NADH consumption (ΔA_{340}) with 160 μM NADH in air-saturated 50 mM MOPS pH 7.0 at room temperature. Reactions were initiated by adding Hrb(which shows no dioxygen reductase activity on this scale) at times indicated by arrows.

As discussed above, the gene for DvFprA2 may be co-transcribed with that for rubredoxin in *D. vulgaris*,[17] suggesting that rubredoxin serves as a proximal electron donor to DvFprA2 *in vivo*. Consistent with this suggestion, Figure 3.7 shows that the reduced *D. vulgaris* rubredoxin - DvFprA2 combination functions as an NOR, for which the K_m for the DvFprA2-rubredoxin interaction is ~8 μM. For comparison, the K_m for the *M. thermoacetica* FprA - *M. thermoacetica* Hrb interaction (the genes for which are known to be co-transcribed[11]) is only slightly lower, ~2 μM (using either NO or O_2 as electron acceptor, cf. Chapter 2).[12]

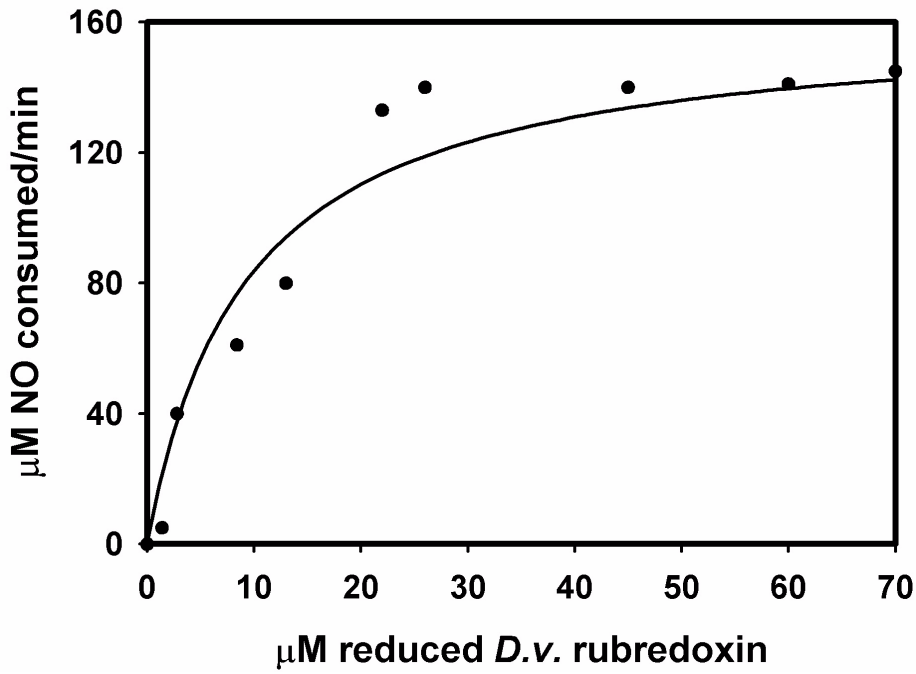

Figure 3.7. Michaelis-Menten plot illustrating DvFprA2-*D. vulgaris* rubredoxin interaction in the NOR assay in anaerobic 50 mM MOPS pH 7.0 at room temperature. Reduced rubredoxin from a 450 μM stock solution was added to an anaerobic NO chamber, which contained 120 nM DvFprA2 and 50 μM NO. NO consumption rates were monitored using an NO electrode. The reduced *D. vulgaris* rubredoxin stock solution was prepared by anaerobic reductive titration with NADH in the presence of 1 μM Flavo-Hrb. At the concentrations used here, Flavo-Hrb does not support FprA turnover, either in the presence or absence of rubredoxin. The fit of the Michaelis-Menten equation indicated by the solid trace was obtained using the parameters: K_m = 8 μM, k_{cat} = 22 s^{-1}.

Figure 3.8 shows that the DvFprA2-*M. thermoacetica* Hrb interaction during NOR turnover features a similarly low K_m (~8 μM) as for the DvFprA2-rubredoxin interaction. The similar K_m's presumably reflect the strong amino acid sequence and, therefore, structural similarity between the Hrb rubredoxin domain and the *D. vulgaris* rubredoxin (cf. Chapter 2). *M. thermoacetica* Hrb could, therefore, be conveniently used as an NADH:DvFprA2 oxidoreductase in a *saturating* manner.

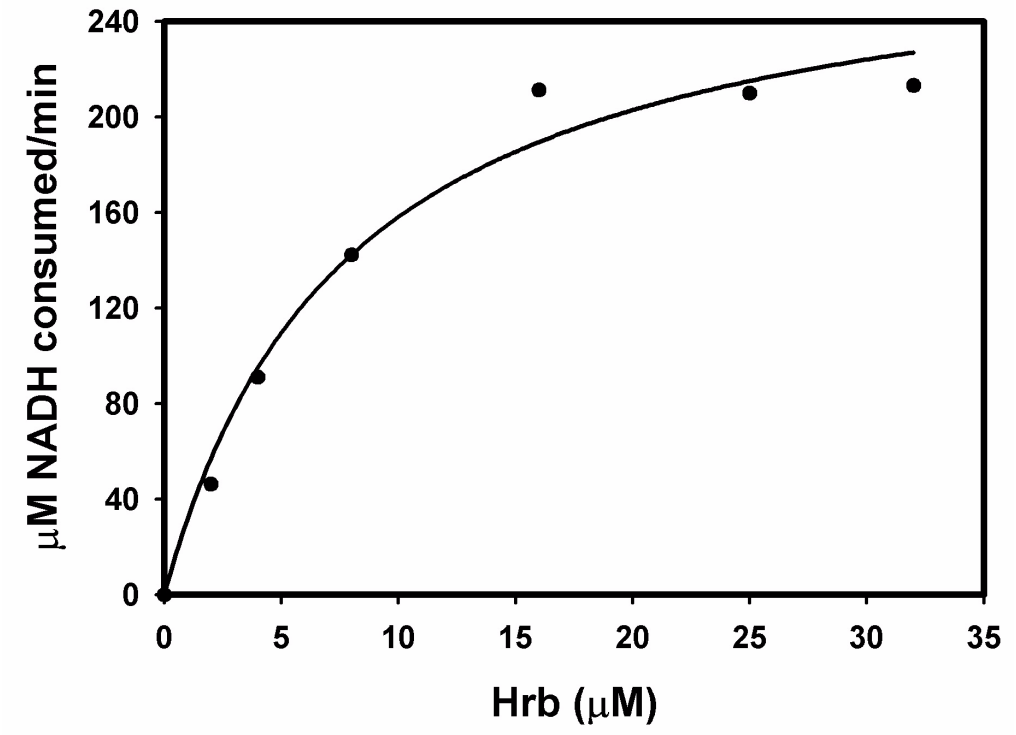

Figure 3.8. Michaelis-Menten plot illustrating DvFprA2-*M. thermoacetica* Hrb interaction in the NOR assay in anaerobic 50 mM MOPS pH 7.0 at room temperature with 250 nM DvFprA2, 160 μM NADH, and 100 μM NO. Reactions were initiated by adding FprA. Initial rates of NADH consumption are plotted. The fit indicated by the solid trace was obtained using the parameters: K_m = 8 μM, k_{cat} = 19 s^{-1}.

Figure 3.9 illustrates Michaelis-Menten plots for the dioxygen reductase and NOR activities of DvFprA2 in the presence of saturating *M. thermoacetica* Hrb. Table 3.1 lists the resulting kinetic parameters, along with those previously reported for other FprAs. The DvFprA2 K_m for dioxygen is the same within experimental uncertainty as that of *M. thermoacetica* FprA.[12] On the other hand the DvFprA2 K_m for NO is ~5 times higher than that measured for *M. thermoacetica* FprA.[12] The k_{cat}/K_m values for DvFprA2 NO- and O_2-reductase activities are essentially identical. A five-fold lower K_m for nitric oxide vs. dioxygen as well as inactivation during dioxygen reductase turnover were among the arguments used in favor of an NOR physiological function for *M. thermoacetica* FprA (cf. Chapter 2).[12] For DvFprA2, the K_m for

nitric oxide is only slightly smaller than that for dioxygen, but inactivation still occurred under dioxygen reductase but not NOR turnover. Based on this latter criterion, the *in vitro* kinetic data favor an NOR over a dioxygen reductase function for DvFprA2.

An improved fit for the DvFprA2 NOR activity in Figure 3.9 was obtained by adopting a kinetic scheme (Scheme 3.1) previously used to analyze *M. thermoacetica* FprA NOR turnover kinetics and which was adapted from that used for bacterial respiratory NORs that contain a binuclear heme:non-heme iron active site.[12,29,30] According to this scheme, at saturating levels of NADH and Hrb, reduction of two NO to N_2O occurs at a single reduced FprA active site (E_{red}).

$$E_{red} + NO \overset{K_1}{\rightleftharpoons} E_{red}\text{-}NO$$

$$E_{red}\text{-}NO + NO \overset{K_2}{\rightleftharpoons} E_{red}\text{-}(NO)_2$$

$$E_{red}\text{-}(NO)_2 \xrightarrow{k_{cat}} E_{ox} + N_2O$$

Scheme 3.1

The rate law applying to Scheme I is [29,30]:

$$v = (V_{max}[NO]^2)/(K_1+K_2[NO]+[NO]^2) \qquad (1),$$

where v is the initial velocity. Fits of equation 1 to the data plotted in Figure 3.9 yielded the dashed curve with parameters: k_{cat} = 12 s^{-1}, K_1 = 217 μM, K_2 = 3 μM. For *M. thermoacetica* FprA, K_1 and K_2 were 5 and 2 μM, respectively, i.e., very similar to each other. The drastic difference between K_1 and K_2 in DvFprA2 can either be assumed to be artifactual (especially given the error bars in Figure 3.9), or it may be due to a distinct structural and/or mechanistic difference between the two FprAs. Thus the apparent cooperativity in DvFprA2, where binding of the first NO molecule (K_1 = 217 μM) strongly increases the affinity for binding a second NO molecule (K_2 = 3 μM) could in principle be linked to the presence of the heme contaminant in D.

vulgaris, or, more likely, to a difference in diiron site structure and/or accessibility between the *M. thermoacetica* and *D. vulgaris* FprAs.

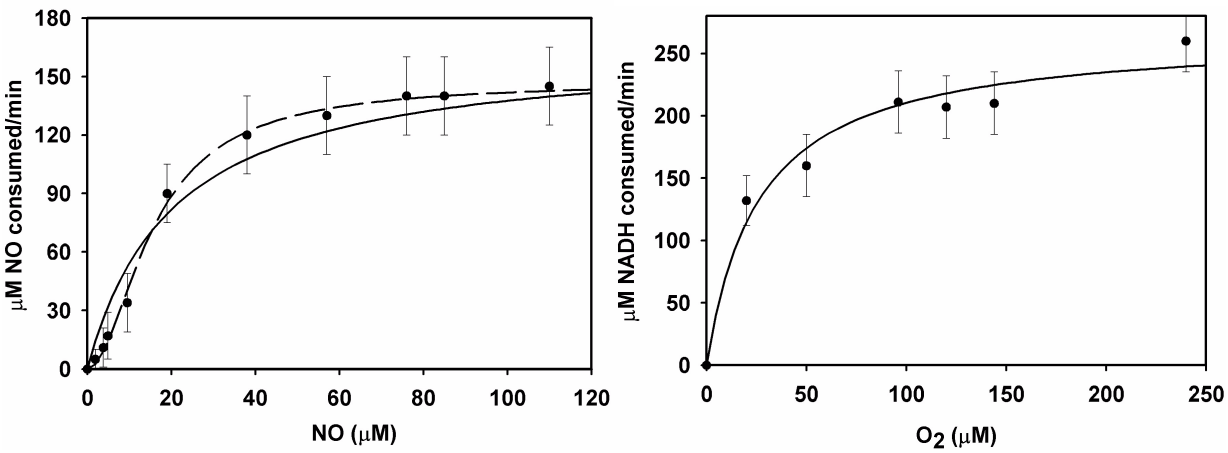

Figure 3.9. Michaelis-Menten plots comparing DvFprA2 NOR and dioxygen reductase activities at room temperature. Left: NOR assays in anaerobic 50 mM MOPS pH 7.0 with 230 nM DvFprA2, 170 μM NADH and 16 μM Hrb. Reactions were initiated by adding FprA. Nitric oxide reduction was monitored with an NO-sensitive electrode. The fit indicated by the solid trace was obtained using the parameters with respect to NO: K_m = 19 μM, k_{cat} = 12 s^{-1}, k_{cat}/K_m = 0.4 $\mu M^{-1}s^{-1}$. Right: dioxygen reductase activity in air-saturated 50 mM MOPS pH 7.0 with 170 μM NADH, 16 μM Hrb and 250 nM DvFprA2. Reactions were initiated by adding FprA, O_2-dependent NADH consumption was monitored at 340 nm. The fit to the Michaelis-Menten equation indicated by the solid trace was obtained using the parameters (with respect to O_2): K_m = 24 μM, k_{cat} = 9 s^{-1}, k_{cat}/K_m = 0.7 μM^{-1} s^{-1}. Error bars on each data point represent the range for three determinations.

Table 3.1. Comparison of steady-state kinetic parameters for oxidase and nitric oxide reductase activities of FprAs.

FprA source	substrate	K_m (μM)	k_{cat} (s^{-1})	k_{cat}/K_m (μM^{-1} s^{-1})
M. thermoacetica[a]	O_2	26	50	1.9
M. thermoacetica[a]	NO	5	48	9.6
D. vulgaris[b]	O_2	24	17	0.7
D. vulgaris[b]	NO	19	12	0.6
D. gigas[c]	O_2	N.R.	N.R.	N.R.
E. coli[d]	NO	<1	1	<1

[a]In 50 mM phosphate pH 7.0, room temperature with 10 μM Hrb, 10 nM FprA, cf. Chapter 2. [b]DvFprA2 in 50 mM MOPS pH 7.0, room temperature with 16 μM Hrb, 230 nM FprA. [c]ROO;

conditions not specified. Dioxygen reductase activities for "all FprAs" i.e., those available to Vicente et al (Ref. [31]) were reported to be identical, but exact values of Michaelis-Menten parameters were not reported (N.R.). [d]Flavorubredoxin in 50 mM Tris pH 7.6, room temperature with 1-7 μM reductase and 22.5 nM flavorubredoxin (ref. 9).

Expression of *M. thermoacetica* FprA was shown (cf. Chapter 2) to protect an *E. coli* flavorubredoxin knockout strain from NO-induced death, thus providing *in vivo* evidence for NOR activity of *M. thermoacetica* FprA, even in the absence of its putative native reductase, Hrb. Figure 3.10 shows that plasmid-borne expression of DvFprA2, presumably via its NOR activity, also restores anaerobic growth to the *E. coli* flavorubredoxin knockout strain exposed to nitric oxide.

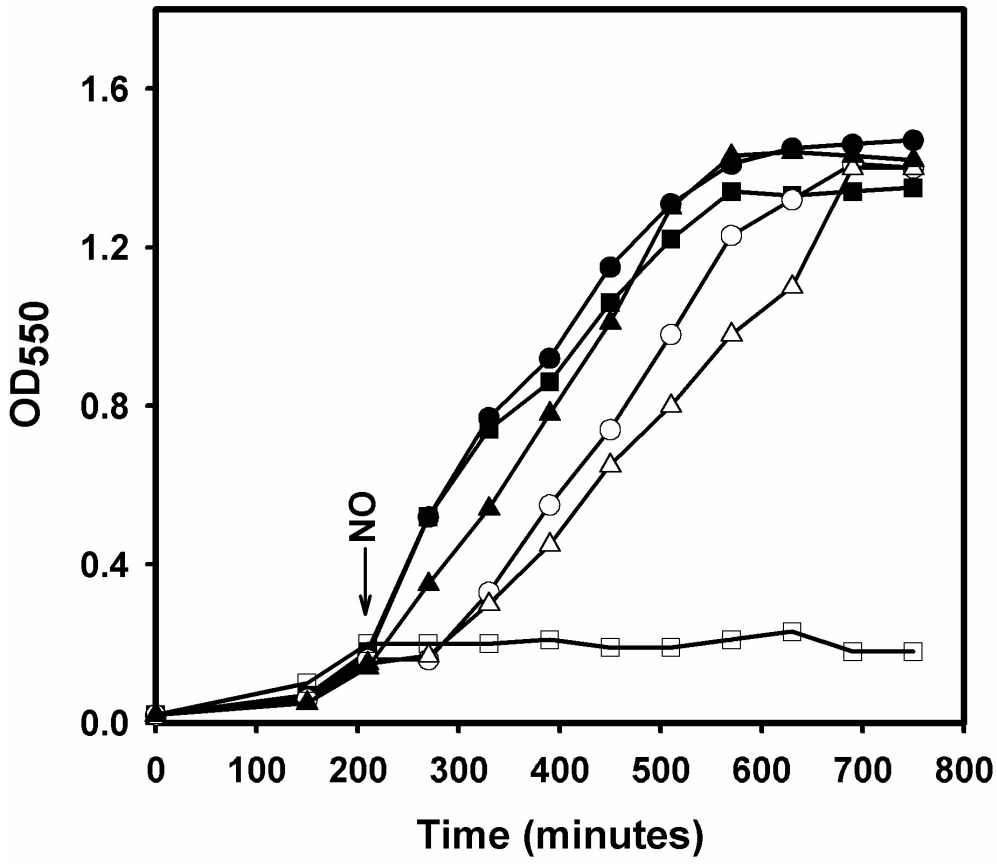

Figure 3.10. Restoration of anaerobic growth to *E. coli* AG300 (flavorubredoxin knockout strain) in the presence of exogenous nitric oxide by expression of the plasmid-borne *M. thermoacetica* FprA or DvFprA2 genes. Cultures were grown in anaerobic minimal medium at 37 ºC as described in Materials and Methods. IPTG was added at OD_{550} = 0.08-0.09. Circles: *E.*

coli AG300 + pCYB1-pFprA (expressing *M. thermoacetica* FprA). Triangles: *E. coli* AG300 + pCYB1-DvFprA (expressing DvFprA2). Squares: *E. coli* AG300 + pCYB1 (no FprA). Filled symbols: controls (no NO). Empty symbols: nitric oxide (7.5 μM) was added from a saturated aqueous stock solution, at the time indicated by the arrow.

The DvFprA2 cloned in this work, thus, appears to be a flavodiiron enzyme that catalyzes reduction of NO or O_2 equally efficiently *in vitro* based on initial rates, but which is irreversibly inactivated during dioxygen reductase turnover. DvFprA2 also appears to function as NOR *in vivo*, protecting an NO-sensitive *E. coli* strain even in the absence of its native reductase and probably at an intracellular NO concentration well below its estimated Michaelis-Menten K_m for NO (but, notably, above the 3 μM K_2 value derived for the sequential, non-Michaelis-Menten, mechanism of Scheme 3.1). Neither DvFprA2 nor any other FprA homolog characterized to date has been shown to act as a dioxygen reductase *in vivo*.

DvFprA2 is the first reported example of a flavo-diiron non-respiratory NOR from sulfate-reducing bacteria. DvFprA2 is likely to be structurally closely related to *D. gigas* ROO, for which dioxygen reductase but not NOR activity has been reported.[2-5,32,33] Based on the data reported here, however, it might be expected that *D. gigas* ROO would have a level of NOR activity similar to that of DvFprA2. A BLAST search reveals that the closest amino acid sequence homologs to DvFprA2 are a *D. desulfuricans* FprA (79% identity) and *D. gigas* ROO (57% identity, 72% similarity) – a similarity expected for these three closely-related species of sulfate-reducing bacteria.

The deduced amino acid sequence of the second *D. vulgaris* FprA homologue, DvFprA1 in Figure 3.1, the gene for which is upstream of the HCP gene, is 37% identical to that of DvFprA2. As shown schematically in Figure 3.11, the third genes both upstream and downstream from that encoding DvFprA1 are putative transposases, *orfA, orfB, iSDvu5*, which

include the inverted repeats normally required for transposase activity. Transposases are enzymes encoded within transposable DNA elements that are known to facilitate intra- and inter-genomic transfer of DNA. For example, transposases are responsible for transfer of antibiotic resistance genes across bacterial strains (it may be noteworthy in this regard that FprAs in fact contain a metallo β-lactamase-like domain[2]).[34] In addition to the DvFprA1 gene, genes encoding hybrid cluster protein, HCP, a GGDEF domain protein likely to be involved in signaling, and two unknown putative proteins (marked "?" in Figure 3.11) are found between the transposase elements. Transposases are not found near DvFprA2 or near FprAs from other sulfate-reducing bacteria. The presence of DvFprA1 together with the putative hydroxylamine reducing enzyme, HCP, between transposase elements suggests that these two proteins were inserted at this particular locus on the *D. vulgaris* genome together, possibly as an adaptation to increased nitrogen oxide stress. FprA and HCP genes are also found close to each other in the archaeon, *P. furiosus* (accession AE010189.1, www.ncbi.nlm.nih.gov), where putative HCP and FprA genes are separated by a gene encoding a putative protein of unknown function. In fact, the closest amino acid sequence homology to DvFprA1 is found in archaeal FprAs (59% identity with *Thermoanaerobacter tengcongensis*, 48% with *Methanothermobacter thermautotrophicus*, and 45% with *P. furiosus* FprAs). Perhaps connected to these observations, genomic analyses based on sequence similarities have lead to the proposal that both FprAs and HCPs have undergone lateral gene transfer among archaea and bacteria.[35] Approximately 10% of the FprA genes for which neighboring sequences are known, are found close to transposase genes (cf. Table 3.2). The most manifest case is that of *C. thermocellum*, where the genes immediately upstream and downstream of *one* of the FprAs encode transposases.

Figure 3.11. Schematic diagram of the DvFprA1 gene locus. Distances are scaled to approximate lengths in bp; the total length of the diagrammed DNA is approximately 6800 bp.

As exemplified by *M. thermoacetica* FprA, DvFprA2 and *D. gigas* ROO, approximately 22% of the FprA genes for which loci are known are found next to genes encoding proteins that are directly or indirectly implicated in oxidative stress protection (Rbo, Rbr, SOD, hemerythrin, ferric uptake protein, alkyl hydroperoxide reductase, thioredoxin reductase, or ferritin), and 16% of FprA genes are found next to a subset of these, namely, Rbo/SOR, Rbr, or SOD genes. For comparison, Table 3.2 shows the percentages for which genes encoding other types of proteins occur in close proximity (within ~5 genes) to FprA genes. The high percentage of FprA genes found near genes encoding proteins involved in nitrogen metabolism (29%) is consistent with involvement of these FprAs in detoxification of nitric oxide, which is a by-product of nitrogen metabolism (cf. Chapter 1). Data in Table 3.2 are also consistent with a possible role for FprAs in protecting NO- (or O_2-) sensitive enzymes such as hydrogenases[1] or iron-sulfur proteins involved in carbohydrate metabolism.[6] Significant percentages of FprA genes are also found close to genes involved in nucleic acid metabolism (replication, translation, transcription, and repair). A protective role may be invoked for FprAs in these cases too. Nineteen percent of FprA genes are found near cell wall biosynthesis-related genes. Cell wall biosynthesis involves nitrogen metabolism, but may also (much like replication) involve large changes in cell structure, and/or volumes, or exogenous stress. A significant percentage of FprAs is also found near genes encoding transport/translocation-related proteins (membrane channels, transporters, ATPases), some of which are involved in antibiotic trafficking, again linking FprA to a cellular stress factor. Nitric oxide was shown to be an endogenous signaling agent in cellular response to

pressure and heat shock in yeast (which contains no FprA homolog).[36] Similar nitric oxide-based signaling mechanisms in FprA-containing organisms have not been reported, but the close proximity of kinase genes to 16% of FprA genes would be consistent with such bacterial nitric oxide signaling. Finally, and probably most significantly, ~50% of the FprA genes occur in tandem with genes encoding proteins likely to function as reductases (rubredoxin, ferredoxin, or redox-active flavoproteins) - consistent with a redox function of the respective FprAs.

Table 3.2. Percentages of bacterial and archaeal genes found in close proximity (within ~5 genes upstream or downstream) of the 89 FprA genes whose loci were available in the NCBI database as of June 2004.[a]

Annotated functions of encoded flanking genes	Percentage
nitrogen metabolism (including nitrogen storage compounds and nitrogen oxides)	29%
amino acid metabolism	26%
helicases, topoisomerases, nucleases	29%
t-RNA or ribosomal proteins	21%
nucleotide synthesis	15 %
cell wall-related	19%
membrane channels, transporters, or ATPases	30%
kinases	16%
transposases	10%
hydrogenase	11%
carbohydrate metabolism	20%
rubredoxin, ferredoxin, or redox flavoprotein	50%

[a]Eight of these FprA genes occur in tandem, and percentages are calculated treating each "tandem" of FprAs as one single FprA (i.e., assuming 81 rather than 89 loci).

D. vulgaris FprA has recently been crystallized in an effort towards broadening our structural database of the FprA family and, thereby, understanding the factors governing NO vs. O_2 reactivity among this widespread class of flavo-diiron proteins.

3.4. References

(1) Wasserfallen, A.; Ragettli, S.; Jouanneau, Y.; Leisinger, T. *Eur. J. Biochem.* **1998**, *254*, 325-332.

(2) Frazão, C.; Silva, G.; Gomes, C. M.; Matias, P.; Coelho, R.; Sieker, L.; Macedo, S.; Liu, M. Y.; Oliveira, S.; Teixeira, M.; Xavier, A. V.; Rodrigues-Pousada, C.; Carrondo, M. A.; Le Gall, J. *Nat. Struct. Biol.* **2000**, *7*, 1041-1045.

(3) Gomes, C. M.; Frazao, C.; Xavier, A. V.; Legall, J.; Teixeira, M. *Protein Sci.* **2002**, *11*, 707-712.

(4) Chen, L.; Liu, M. Y.; LeGall, J.; Fareleira, P.; Santos, H.; Xavier, A. V. *Biochem. Biophys. Res. Commun.* **1993**, *193*, 100-105.

(5) Chen, L.; Liu, M. Y.; Legall, J.; Fareleira, P.; Santos, H.; Xavier, A. V. *Eur. J. Biochem.* **1993**, *216*, 443-448.

(6) Gardner, A. M.; Helmick, R. A.; Gardner, P. R. *J. Biol. Chem.* **2002**, *277*, 8172-8177.

(7) Sarti, P.; Fiori, P. L.; Forte, E.; Rappelli, P.; Teixeira, M.; Mastronicola, M.; Sanciu, G.; Giuffre, A.; Brunori, M. *Cell. Mol. Life Sci.* **2004**, *61*, 618-623.

(8) Mukhopadhyay, P.; Zheng, M.; Bedzyk, L. A.; Larossa, R. A.; Storz, G. *Proc. Natl. Acad. Sci. USA* **2004**, *101*, 745-750.

(9) Gomes, C. M.; Giuffre, A.; Forte, E.; Vicente, J. B.; Saraiva, L. M.; Brunori, M.; Teixeira, M. *J. Biol. Chem.* **2002**, *277*, 25273-25276.

(10) Gomes, C. M.; Vicente, J. B.; Wasserfallen, A.; Teixeira, M. *Biochemistry* **2000**, *39*, 16230-16237.

(11) Das, A.; Coulter, E. D.; Kurtz, D. M., Jr.; Ljungdahl, L. G. *J. Bacteriol.* **2001**, *183*, 1560-1567.

(12) Silaghi-Dumitrescu, R.; Coulter, E. D.; Das, A.; Ljungdahl, L. G.; Jameson, G. N.; Huynh, B. H.; Kurtz, D. M., Jr. *Biochemistry* **2003**, *42*, 2806-2815.

(13) Macedo, S.; Mitchell, E. P.; Romao, C. V.; Cooper, S. J.; Coelho, R.; Liu, M. Y.; Xavier, A. V.; LeGall, J.; Bailey, S.; Garner, C. D.; Hagen, W. R.; Teixeira, M.; Carrondo, M. A.; Lindley, P. *J. Biol. Inorg. Chem.* **2002**, *7*, 514-525.

(14) Wolfe, M.; Heo, J.; Garavelli, J. S.; Ludden, P. W. *J. Bacteriol.* **2002**, *184*, 5898-5902.

(15) Pereira, I. A. C.; LeGall, J.; Xavier, A. V.; Teixeira, M. *Biochim. Biophys. Acta* **2000**, *1481*, 119-130.

(16) Seifritz, C.; Daniel, S. L.; Gossner, A.; Drake, H. L. *J. Bacteriol.* **1993**, *175*, 8008-8013.

(17) Heidelberg, J. F.; Seshadri, R.; Haveman, S. A.; Hemme, C. L.; Paulsen, I. T.; Kolonay, J. F.; Eisen, J. A.; Ward, N.; Methe, B.; Brinkac, L. M.; Daugherty, S. C.; Deboy, R. T.; Dodson, R. J.; Durkin, A. S.; Madupu, R.; Nelson, W. C.; Sullivan, S. A.; Fouts, D.; Haft, D. H.; Selengut, J.; Peterson, J. D.; Davidsen, T. M.; Zafar, N.; Zhou, L.; Radune, D.; Dimitrov, G.; Hance, M.; Tran, K.; Khour, i. H.; Gill, J.; Utterback, T. R.; Feldblyum, T. V.; Wall, J.; Voordouw, G.; Fraser, C. M. *Nat. Biotechnol.* **2004**, *22*, 554-559.

(18) Coulter, E.; Kurtz, D. M., Jr. *Arch. Biochem. Biophys.* **2001**, *394*, 76-86.

(19) Kurtz, D. M., Jr.; Coulter, E. D. *Chemtracts Inorg. Chem.* **2001**, *14*, 407-435.

(20) Kurtz, D. M., Jr.; Coulter, E. *J. Biol. Inorg. Chem.* **2002**, *6.*, 653-658.

(21) Fu, R.; Voordouw, G. *Microbiology* **1997**, *143*, 1815-1826.

(22) Sambrook, J.; Fritsch, E. F.; Maniatis, T. *Molecular cloning: a laboratory manual.*; 2nd ed.; Cold Spring Harbor Laboratory Press: Cold Spring Harbor, N.Y., 1990.

(23) Schagger, H.; von Jagow, G. *Analyt. Biochem.* **1987**, *166*, 368-379.

(24) Postgate, J. R. *The sulfate-reducing bacteria*, Edn. 2, vol. 130, Cambridge University Press, London 1984.

(25) Xiong, J.; Kurtz, D. M., Jr.; Ai, J.; Sanders-Loehr, J. *Biochemistry* **2000**, *39*, 5117-5125.

(26) Harlow, E.; Lane., D. *Antibodies: a laboratory manual*; Cold Spring Harbor Laboratory Press: Cold Spring Harbor, New York, 1988.

(27) Ng, K. Y.; Vishwanathan, R.; Kurtz , D. M., Jr., *unpublished observations*.

(28) Chapman, S. K.; Reid, G. A. *Methods in Molecular Biology* **1999**, Vol. 131-Flavoprotein protocols, Humana Press, Totowa, NJ.

(29) Girsch, P.; de Vries, S. *Biochim. Biophys. Acta* **1997**, *1318*, 202-216.

(30) Koutny, M.; Kucera, I. *Biochem. Biophys. Res. Commun.* **1999**, *262*, 562-564.

(31) Vicente, J. B.; Gomes, C. M.; Wasserfallen, A.; Teixeira, M. *Biochem. Biophys. Res. Commun.* **2002**, *294*, 82-87.

(32) Gomes, C. M.; Silva, G.; Oliveira, S.; LeGall, J.; Liu, M. Y.; Xavier, A. V.; Rodrigues-Pousada, C.; Teixeira, M. *J. Biol. Chem.* **1997**, *272*, 22502-22508.

(33) Victor, B. L.; Vicente, J. B.; Rodrigues, R.; Solange, O.; Rodrigues-Pousada, C.; Frazao, C.; Gomes, C. M.; Teixeira, M.; Soares, C. *J. Biol. Inorg. Chem.* **2003**, *8*, 475-488.

(34) Heffron, F.; McCarthy, B. J.; Ohtsubo, H.; Ohtsubo, E. *Cell* **1979**, *18*, 1153-1163.

(35) Andersson, J. O.; Sjongren, A. M.; Davis, L. A. M.; Embley, T. M.; Roger, A. J. *Curr. Biol.* **2003**, *13*, 94-104.

(36) Domitrovic, T.; Palhano, F. L.; Barja-Fidalgo, C.; DeFreitas, M.; Orlando, M. T. D.; Fernandes, P. M. B. *FEMS Yeast Res.* **2003**, *1560*, 1-6.

CHAPTER 4

ELECTRON TRANSFER MECHANISM AND AN UNPRECEDENTED RUBREDOXIN - NITRIC OXIDE ADDUCT IN *MOORELLA THERMOACETICA* HIGH-MOLECULAR WEIGHT RUBREDOXIN (HRB)

4.1. Introduction

Chapter 2 presented the initial characterization of a flavo-diiron protein, FprA, and its reductase, Hrb, as a novel nitric oxide reductase (NOR) system involved in nitrosative stress defense in *Moorella thermoacetica*. FprA features two cofactors, a flavin adenine dinucleotide (FMN) and a diiron site, with the latter likely to be the site of NO reduction. The reductase, Hrb, also features a unique combination of two cofactors, namely an FMN and an [$Fe(Cys)_4$] rubredoxin-type site. An electron flow pathway was established *in vitro*, from NADH to NO, as follows: **NADH** $\rightarrow$ FMN**(Hrb)** $\rightarrow$ [$Fe(Cys)_4$]**(Hrb)** $\rightarrow$ FMN**(FprA)** $\rightarrow$ diiron**(FprA)** $\rightarrow$ **NO**. The proposed electron-flow pathway from Hrb to FprA was based on, among other things, the inability of Zn-substituted Hrb to support NOR turnover even though NADH could still reduce the Hrb FMN rapidly and completely.[1] The net reaction catalyzed in this system is

$$2NO + NADH + H^+ \rightarrow N_2O + H_2O + NAD^+ \qquad 4.1$$

The FprA/Hrb system was also found to catalyze the four-electron reduction of O_2 to H_2O by NADH, during which FprA became irreversibly inactivated. This oxidase reactivity was found to be less efficient than NOR activity by the same enzymatic system, and *in vivo* evidence for an

NO-reductase function of FprAs in *E. coli*,[2] *T. vaginalis*,[3] and *M. thermoacetica*[1] has been reported. In the case of *M. thermoacetica* FprA/Hrb, the steady-state kinetics were found to be consistent with NO reduction occurring at the FprA diiron site according to Scheme 4.1.

Scheme 4.1

$$E_{red} + NO \overset{K_1}{\rightleftharpoons} E_{red}\text{-}NO$$

$$E_{red}\text{-}NO + NO \overset{K_2}{\rightleftharpoons} E_{red}\text{-}(NO)_2$$

$$E_{red}\text{-}(NO)_2 \xrightarrow{k_{cat}} E_{ox} + N_2O$$

With the exception of the steady-state kinetics data reported in Chapter 2, the mechanism of NO reduction by FprAs remains largely unexplored.[1] The present chapter describes kinetics and spectroscopic experiments aimed at understanding the details of the mechanism of nitric oxide reduction by the *M. thermoacetica* FprA-Hrb couple, focusing on the role of Hrb.

4.2. Materials and methods

Reagents and General Procedures. All solutions were prepared in deionized water. NADH, NADPH (Sigma Chemical Co.) and protein molecular weight standards (Bio-Rad, Inc.) were used without further purification. Stock solutions (25 mM) of DEA NONOate (diethylammonium (Z)-1-(N,N-diethylamino) diazen-1-ium-1,2-diolate, Cayman Chemicals, Inc.) were prepared in 0.01 M NaOH. DEA NONOate is stable at high pH but decomposes to release NO gas (1.5 mols NO/1 mol DEA NONOate) when added to assay mixtures at ~ pH 7. Where indicated, solutions were made anaerobic by repetitive vacuum/argon or N_2 gas exchange or extensive purging with argon or N_2 gas. Gaseous nitric oxide (98.5%) was purchased from Aldrich. The NO was purified by bubbling through 100 mL of a 10% KOH solution. The

purified NO gas was used to prepare saturated NO solutions (~1.8 mM in water) by bubbling the gas through anaerobic deionized water for 15 minutes. Nitric oxide concentrations in Hrb-NO mixtures were measured with a Clark-type NO-sensitive electrode (2mm diameter, WPI, Inc.) with stirring in an argon-purged NO Chamber (WPI, Inc.) calibrated and manipulated as previously described.[1] Protein purity was judged by SDS-PAGE (15% polyacrylamide gels) and Coomassie blue staining.[4] The recombinant proteins, *M. thermoacetica* FprA,[1] *M. thermoacetica* Hrb,[1] *P. furiosus* rubredoxin[5] and *D. vulgaris* rubredoxin-like protein, Rdl,[6] were obtained as previously described.

Spectroscopy. Room-temperature ultraviolet-visible absorption spectra were obtained in 1-cm pathlength quartz cuvettes on a Shimadzu UV-2401PC scanning spectrophotometer. EPR spectra were recorded on a Bruker ESP-300E spectrometer equipped with an ER-4116 dual-mode cavity and an Oxford Instruments ESR-9 flow cryostat, using 200-μL sample volumes. The WINEPR v. 2.11 (Bruker Instruments) and EPRQUANT (written by Dr. Andrew Kowal in the Johnsosn group at the University of Georgia) programs, access to which was kindly provided by Dr. Richard Conover, were used for EPR data manipulation and quantitation.

For the oxidized (as isolated) Hrb, NADH-reduced Hrb, and reduced Hrb+NO EPR spectra, samples contained 100 μM Hrb. Hrb (200 μM) was reduced in anaerobic 50 mM MOPS pH 7.0 inside a Vacuum Atmospheres glove box with stoichiometric NADH at room temperature. For the "Hrb+NO" sample, 100 μL reduced Hrb were transferred to an EPR tube, which was sealed with a tight-fitting septum and removed from the glove box. Aqueous NO-saturated solution (100 μL of 1.8 mM NO) was then added via a syringe at room temperature, and then the sample was immediately frozen in liquid nitrogen. For the "NADH-reduced"

sample, the reduced Hrb was diluted to 100 μM with anaerobic 50 mM MOPS pH 7.0 rather than with aqueous NO.

UV-vis absorption spectra at cryogenic temperatures were recorded on solutions placed in a custom-made Dewar cuvette (cf. Figure 4.1). The Dewar cuvette, which was designed by Dr. Irene Kung in the Kurtz group and fabricated by the UGA glass-blowing shop, was equipped with optical quality quartz windows and a 2-cm pathlength. The cuvette contained an extension that was sealed with a rubber or silicon septum, and the headspace was maintained under positive argon pressure. The solution in the cuvette was cooled to -40 °C using a dry ice/isopropanol bath[7,8] in the surrounding chamber. A thermometer was placed inside the dry ice/isopropanol bath, and the temperature was adjusted by adding dry ice or room-temperature isopropanol, as required. The Dewar was placed in a specially constructed plexiglass bracket to which fiber-optic cables leading to an Ocean Optics USB2000 UV-vis spectrometer were attached. UV-vis absorption spectra were recorded using the computer-driven Ocean Optics spectrometer. A concentrated solution of anaerobic as-isolated Hrb in 25 mM MOPS pH 7.3 was added to ~ 4 mL of the anaerobic cryo-solvent, which consisted of 5:3:2 by volume, aqueous 100 mM sodium cacodylate pH 6.5:ethylene glycol:methanol that had been cooled at 0 °C. After mixing, the temperature was lowered to -40 °C. Addition of the protein to the cryo-solvent was performed at 0 °C rather than at room temperature since previous experiments with *M. thermoacetica* FprA and *D. vulgaris* SOR had indicated that these proteins would precipitate (denature) at room temperature but not at 0 °C or below, in the cryo-solvents used in Figure 4.2. Cacodylate was used as a buffer due to the relatively small temperature dependence of its pK_a. Thus, the pH of a sodium cacodylate buffer solution increases by only 0.65-0.85 units on lowering the temperature from 23 °C to -40 °C, whereas the pH of a Tris buffer solution increases by 2.25-2.7 units upon

lowering the temperature over the same range.[7] Cacodylate, ethylene glycol and methanol do not affect the Hrb optical absorption spectrum, nor do they inhibit the NOR activity of *M. thermoacetica* Hrb-FprA.

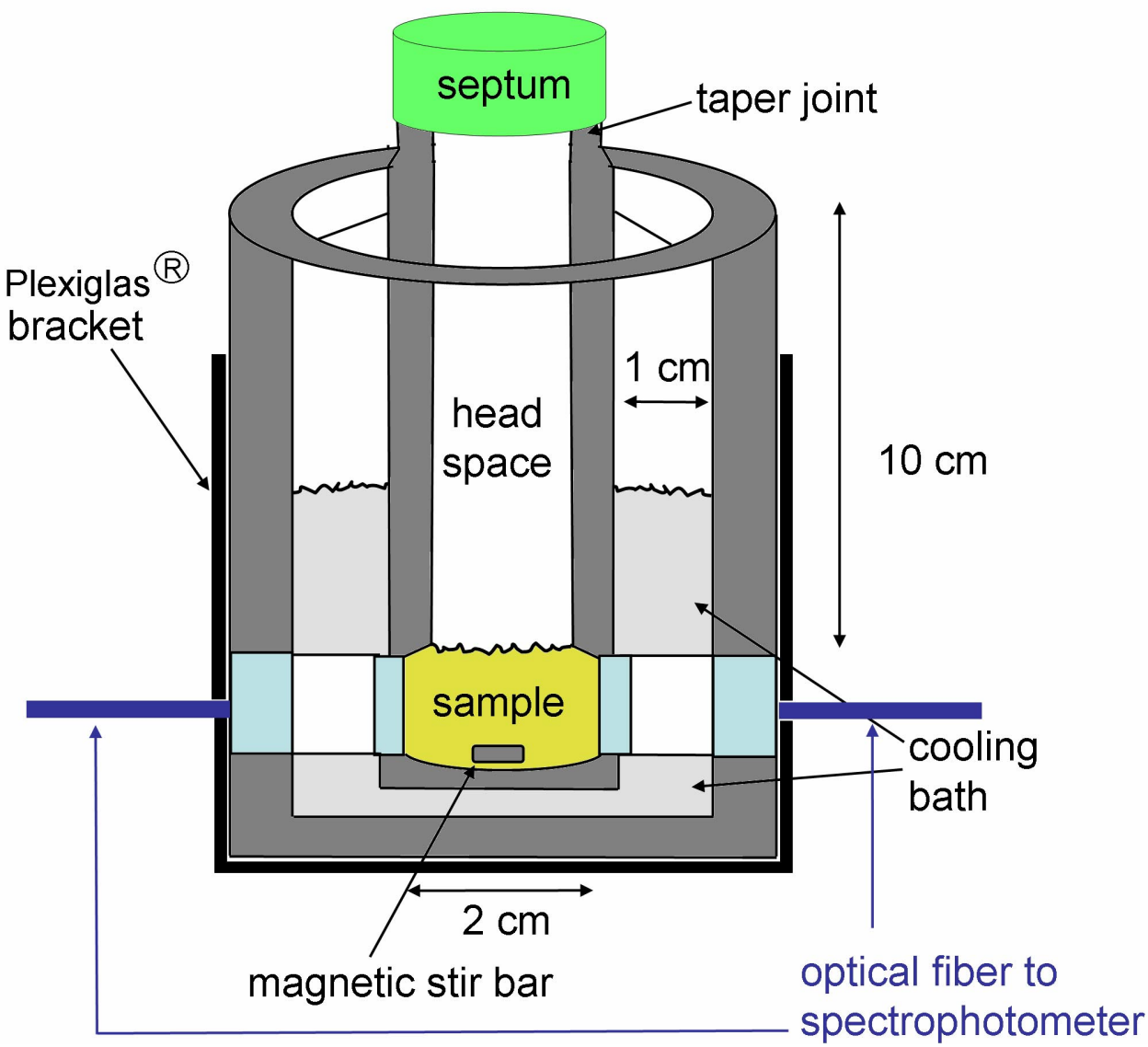

Figure 4.1. Schematic diagram (cross-section) of the custom-made Dewar cuvette used for recording cryogenic UV-vis spectra. Optical quality quartz windows are shown in cyan, the rest of the Dewar vessel, made of borosilicate glass, is shown in dark grey. Drawing is not to scale, but relevant dimensions are indicated.

Stopped-flow spectrophotometric experiments were carried out on an Applied Photophysics SX.18MV-R instrument. Stopped-flow data analysis and fitting was performed

with the Pro-Kineticist program v. 1.06 (Applied Photophysics, Ltd.). Experimental conditions are given in figure legends.

Homolog Modeling, Docking. Docking was performed using the rigid-body Dock module within Sybyl 6.7 (Tripos, Inc.) at the UGA SVMGL facility. PDB files were prepared by removing water molecules, adding protons, and adding Gasteiger-Hückel charges. The DOCK module was used to manually dock Hrb onto FprA. Homology modelling was performed using SwissModel.[9]

4.3. Results and discussion

All Hrb and FprA concentrations in figure legends refer to monomers and are given immediately *after* mixing.

Electron Transfer Mechanism of Hrb. As reported in Chapter 2, NADH can stoichiometrically reduce both the FMN and $[Fe(SCys)_4]$ cofactors of Hrb (cf. Figure 2.9). Under equilibrium titration conditions, NADH reduces the Hrb FMN by two electrons, but no reduction of the FMN is observed until the rubredoxin-type $[Fe(SCys)_4]$ site has been reduced. This behavior is consistent with the respective reduction potentials previously measured for the two cofactors at pH 7 (vs. NHE): -120 mV for the FMN/$FMNH_2$, and -30 mV for the $[Fe^{3+/2+}(SCys)_4]$.[1] While hydride transfer from NADH to flavin is ubiquitous in biochemistry, no hydride and/or electron transfer directly from NADH to iron-sulfur centers has to our knowledge been reported. The optical titration data in Figure 2.9 (Chapter 2) were, therefore, interpreted as due to NADH's reduction of the Hrb FMN, which then rapidly donates its electrons to the $[Fe(SCys)_4]$ site. Figures 4.2 and 4.3 show *direct* evidence for an **NADH** $\rightarrow$ FMN**(Hrb)** $\rightarrow$ $[Fe(Cys)_4]$**(Hrb)** electron flow pathway. Anaerobic mixing of excess NADH with as-isolated (oxidized) Hrb either in a stopped-flow instrument at room-temperature or at -40 °C in an aqueous ethylene

glycol:methanol cryo-solvent, results in almost instantaneous and complete FMN reduction, followed by a slower electron transfer to the [Fe(SCys)$_4$] site. In both the low-temperature and stopped-flow experiments, with the exception of the first one or two traces recorded after mixing, which show absorption due residual oxidized FMN flavin, only rubredoxin-type [Fe(SCys)$_4$] spectral features with λ_{max} ~490 nm and 550 nm are distinguishable, as can be seen by comparison with the reference spectra in Figure 4.2 inset. In the low-temperature experiment, a weak absorption at ~630 nm which forms and disappears at intermediate times after mixing, is likely due to a neutral (protonated) semiquinone form of the Hrb FMN.[10,11] This semiquinone is the expected product when a two-electron reduced Hrb FMN (optically silent) transfers one of its electrons to reduce the [Fe^{3+}(SCys)$_4$] site. Alternatively, the FMN semiquinone may also form via comproportionation from oxidized and two-electron reduced Hrb FMN.

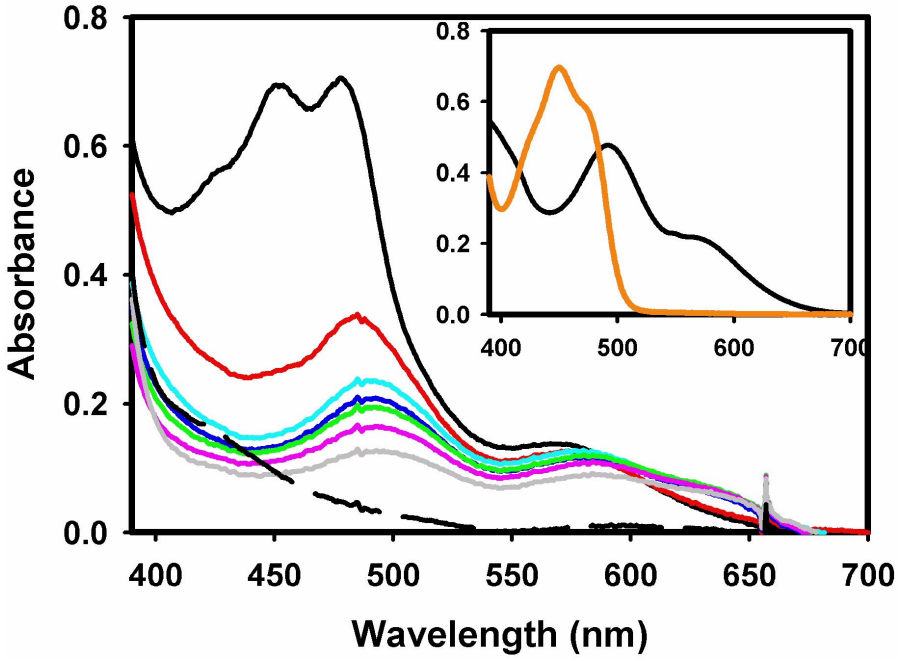

Figure 4.2. UV-vis absorption spectral time course for the anaerobic reaction of as-isolated *M. thermoacetica* Hrb (22 µM) with NADH at -40 °C in a cryo-solvent comprised of 50% aqueous 100 mM cacodylate pH 6.5, 30% ethylene glycol, 20% methanol by volume. NADH (350 µM)

was added at -40 °C from a 100 mM stock solution in water: methanol (1:1 v/v). Spectral traces are color coded as: black, as-isolated Hrb; red, 10 seconds after adding NADH at -40 °C; other colors, 0.5, 1, 2, 3 and 5 minutes after mixing, from highest to lowest A_{490}; dashed trace,10 minutes after mixing. No further spectral changes occurred after 10 minutes. The inset shows spectra of oxidized *P. furiosus* rubredoxin (black trace) and iron-devoid (Zn-substituted) *M. thermoacetica* Hrb (orange).

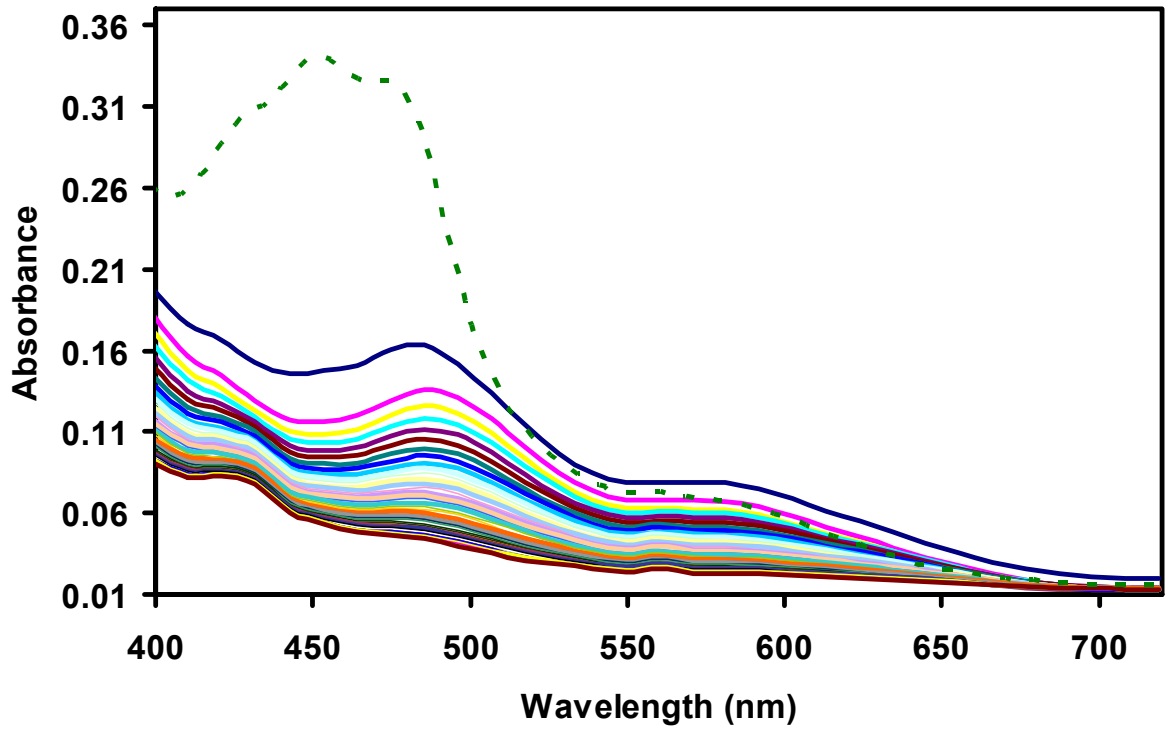

Figure 4.3. UV-vis absorption spectra collected over the first 255 ms (solid traces, from highest to lowest A_{490} in ~8-ms increments) after anaerobic stopped-flow mixing of as-isolated *M. thermoacetica* Hrb (20 μM) with NADH (400 μM) in anaerobic 50 mM MOPS pH 7.0 at room temperature. The green dashed trace shows the "control" spectrum of as-isolated *M. thermoacetica* Hrb (20 μM) mixed with anaerobic buffer in the absence of NADH 2 s after mixing (spectrum identical to that observed 2 ms after mixing).

The oxidized Hrb+NADH stopped-flow data in Figure 4.3 is well fitted using an A → B → C model, as shown in Figure 4.4, with the rates of the successive reaction steps estimated to be 125 s^{-1} and 11 s^{-1}, respectively. Calculated A, B and C component spectra from a global fit of trace absorption spectral time course are shown in Figure 4.4 (inset). Based on these component spectra, the initial rapid step, A→ B, represents the two-electron reduction of the FMN by

NADH. In agreement with this initial fast rate (and with the cryogenic spectral time course in Figure 4.2), most of the FMN absorbance in Figure 4.3 disappears within the mixing time, and the first recorded stopped-flow spectrum resembles that of oxidized rubredoxin (cf. inset to Figure 4.2). The subsequent slower step, B → C, then describes reduction of the Hrb [Fe(SCys)$_4$] site. Thus, in the Figure 4.4 inset the calculated A component absorption spectrum resembles that of as-isolated Hrb, the calculated B component spectrum resembles that of the Hrb [Fe^{3+}(SCys)$_4$],[1] and the calculated C component spectrum is identical to that of fully-reduced Hrb (cf. Figures 4.2, 4.3). The weak, relatively narrow absorption features at ~420 nm and 560 nm in all the component spectra are attributed to a heme contaminant.

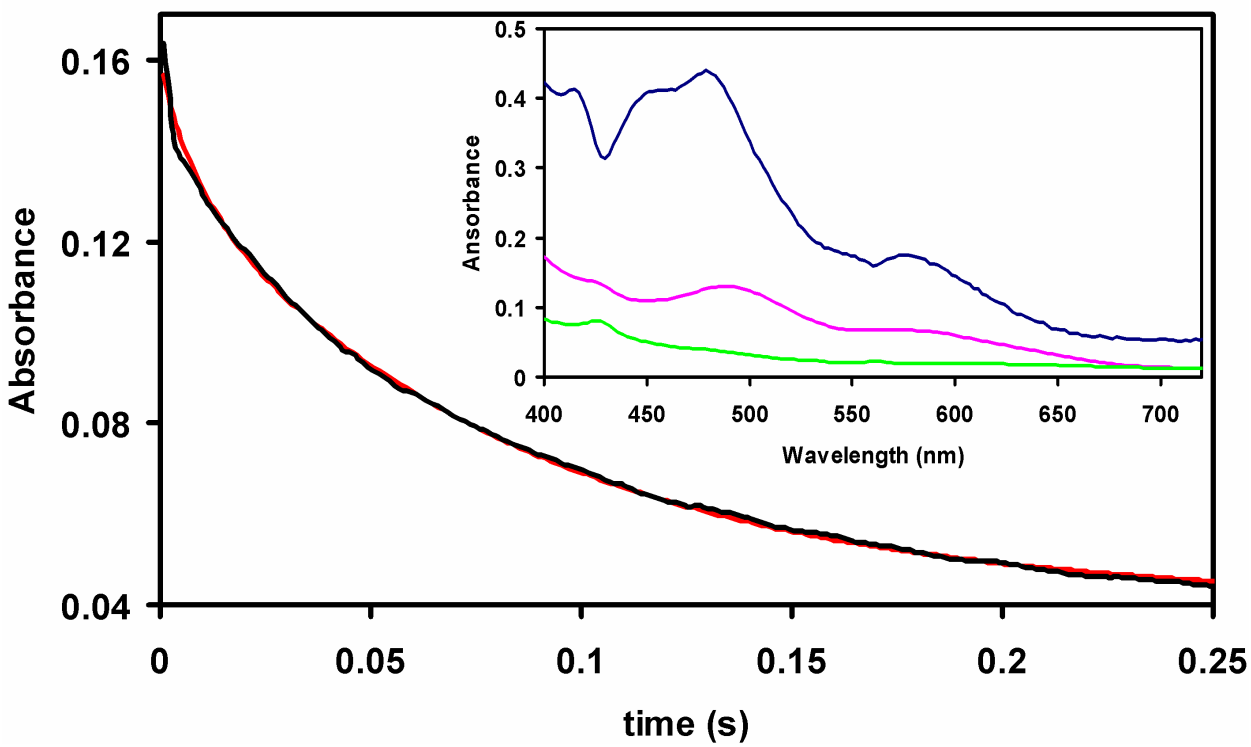

Figure 4.4. Black trace: absorbance time course at 485 nm after anaerobic stopped-flow mixing of as-isolated *M. thermoacetica* Hrb (20 μM) with NADH (400 μM) in 50 mM MOPS pH 7.0 at room temperature. Red trace: calculated absorbance time course, assuming an A → B → C model with k_1 = 125 s^{-1} and k_2 = 11 s^{-1}. Inset: calculated spectra for the A (blue), B (pink) and C (green) component species used in the fit. The spectra shown were obtained assuming initial relative concentrations 0.1, 0.9 and 0.0 for A, B, and C, respectively ("initial" refers to the first

collected spectrum, top blue trace in Figure 4.3). Calculations assuming other values for the initial concentrations of A, B and C resulted in shapes of the A component spectrum that were less similar to the as-isolated, oxidized, Hrb.

The fitted kinetic trace shown in Figure 4.4 does not perfectly reproduce the shape of the experimental kinetic time course for the first few milliseconds (left-most side of the time-course plot). Addition of a third reaction step in the fitting procedure, generating an A $\rightarrow$ B $\rightarrow$ C $\rightarrow$ D model with k_1 = 465 s^{-1}, k_2 = 29 s^{-1} and k_3 = 8 s^{-1}, improved the agreement between calculated and experimental data, as shown in Figure 4.5. In this improved fit, the calculated spectra of the starting component, A, final component, D, and first intermediate, B, (inset to Figure 4.5) are similar to those obtained from the A $\rightarrow$ B $\rightarrow$ C model in Figure 4.4. The calculated absorption spectrum of the "extra" intermediate component, C, in the Figure 4.5 inset, seems to be simply an average of the "fully-reduced" final spectrum (green traces in Figures 4.4 and 4.5 insets) with the "$[Fe^{3+}(SCys)_4]$-only" spectrum (pink traces in Figures 4.4 and 4.5 insets), casting some doubt on the need to invoke a four-species model vs. a three-species model to explain the Hrb-NADH stopped-flow kinetics.

The initial spectra in Figures 4.2 and 4.3 following mixing with NADH represent a novel, transient form of Hrb, containing a predominantly two-electron reduced FMN and an oxidized $[Fe(SCys)_4]$ site. A subsequent intermediate, containing a reduced $[Fe(SCys)_4]$ site and a one-electron reduced flavin (i.e., a flavin semiquinone) may be inferred from the 630-nm feature in Figure 4.2, although this semiquinone could also arise via comproportionation of reduced and oxidized Hrb FMN. On the other hand, the first spectrum recorded after stopped-flow mixing of Hrb with NADH in Figure 4.3 shows a broad increase in absorption in the 520-750 nm region compared to that of the oxidized Hrb. This increased absorption is consistent with the presence of an NADH:$FMN_{oxidized}$ charge-transfer complex. For reference, Figure 4.6 shows the optical

absorption spectrum of the NADH:$FMN_{oxidized}$ charge-transfer complex of another electron-transport flavoprotein, phthalate dioxygenase reductase (PDR).[11] Like Hrb, PDR contains two redox centers: a solvent-exposed FMN and a dinuclear iron-sulfur cluster; the spectra shown are obtained on a truncated PDR, lacking the iron-sulfur cluster domain. The calculated component A spectrum from the Hrb stopped-flow experiments (cf. Figures 4.4 and 4.5) appears to contain features consistent with an NADH:$FMN_{oxidized}$ charge-transfer complex, superimposed on absorption spectral features characteristic of the [$Fe^{3+}(SCys)_4$] site. The spectrum of the subsequent NAD^+:$FMN_{reduced}$ charge-transfer complex of PDR in Figure 4.6, characterized by a steadily rising absorption above 550 nm, is not evident in any of the spectra of Figures 4.2-4.5.

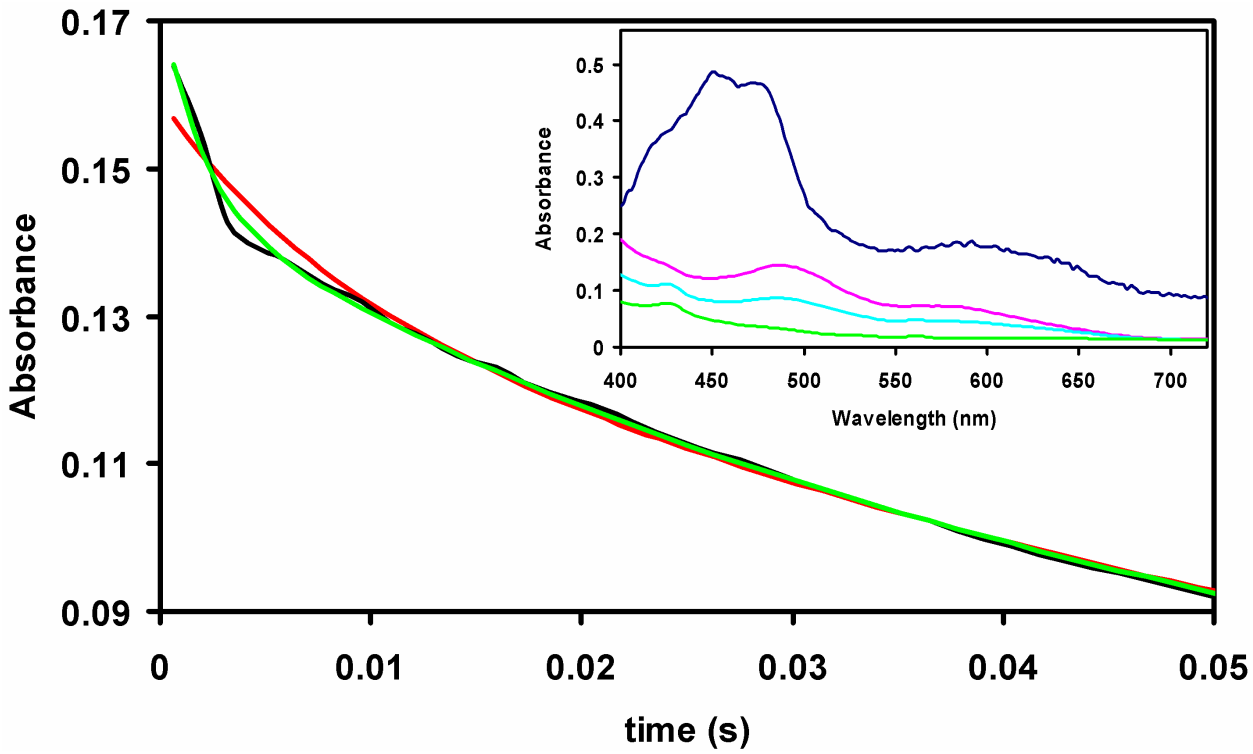

Figure 4.5. Black trace: same absorbance time course at 485 nm as in Figure 4.4, but with only the first 50 ms of the time course shown, to illustrate the improved fit in a three-reaction kinetic model. Red trace: calculated absorption time course for the A → B → C model (same as in Figure 4.4). Green trace: calculated absorbance time course assuming an A → B → C → D model, with k_1 = 465 s^{-1}, k_2 = 29 s^{-1} and k_3 = 8 s^{-1}. Inset: calculated UV-vis absorption spectra for

the A (blue), B (pink), C (cyan) and D (green) species used in the fit. The spectra shown were obtained assuming initial relative concentrations 0.2, 0.2, 0.6 and 0.0 for components A, B, C and D, respectively in the top (blue) spectrum of Figure 4.3. Calculations assuming other values for the initial concentrations of A-D resulted in shapes of the A component spectrum that were less similar to the as-isolated, oxidized, Hrb.

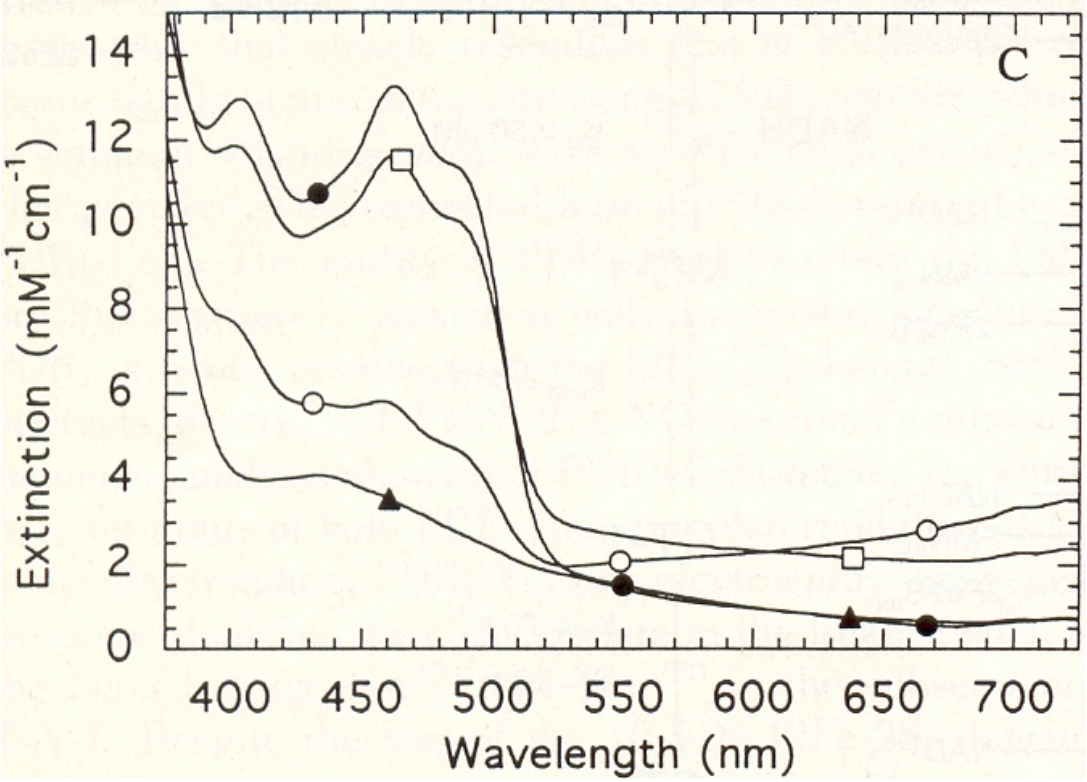

Figure 4.6. UV-vis absorption spectra of species detected upon stopped-flow mixing of oxidized truncated PDR with NADH under anaerobic conditions (reproduced from Ref. 11). Filled circles: oxidized PDR; squares: NADH:$FMN_{oxidized}$ charge-transfer complex; empty circles: NAD^+:$FMN_{reduced}$ charge transfer complex; triangles: reduced PDR.

The fit in Figure 4.4 suggests that full reduction of Hrb by excess NADH involves a step with $k \sim 11$ s^{-1}, ~5 times slower than the 50 s^{-1} k_{cat} value determined from Hrb-FprA NOR turnover experiments.[1] This slow step in the NADH+Hrb experiments cannot, therefore, be a part of the normal NADH-Hrb-FprA NOR (or dioxygen reductase) catalytic cycle. The fit in Figure 4.4 shoes that this slow step represents reduction of the $[Fe^{3+}(SCys)_4]$ site (presumably via

intramolecular electron transfer from $FMN_{reduced}$), a step previously shown to be essential for Hrb-FprA turnover (because Zn-substituted Hrb was inactive).[1] The stopped-flow data can be reconciled with the turnover data by assuming that upon docking of Hrb onto FprA, conformational changes and/or changes in polarity around the $[Fe(SCys)_4]$ site lead to a more efficient electron transfer from the Hrb FMN to the Hrb $[Fe(SCys)_4]$ site than observed in the single-turnover NADH-Hrb stopped-flow experiment. A second explanation may be invoked by assuming the three-reaction model of Figure 4.5. According to this model, reduction of part of the Hrb $[Fe(SCys)_4]$ sites does in fact occur at ~30 s^{-1}, a rate closer to the k_{cat} for NOR turnover. The slower phase, at 8 s^{-1} in Figure 4.5, may be due to reduction of a small fraction of Hrb $[Fe(SCys)_4]$ sites which belong to Hrb molecules depleted in flavin. Indeed, slightly sub-stoichiometric amounts of FMN were reported for the as-isolated Hrb.[1]

In the FprA-Hrb system electrons flow from a two-electron reductant, NADH, to a two-electron oxidized diiron site in FprA, i.e., a net *two-electron process*. The $[Fe(SCys)_4]$ site, however, can cycle only between Fe(III) and Fe(II), i.e., a one-electron process. This two-electron/one-electron switch is also present in *E. coli* flavorubredoxin which contains a covalently attached rubredoxin-like $[Fe(SCys)_4]$ domain.[12] Similarly, genetic and *in vitro* evidence favors rubredoxin as the proximal electron donor to *D. gigas* ROO[13] and, as described in Chapter 3, *D. vulgaris* FprA. However, Chapters 2 and 3 describe results showing that FprAs from two heterologous sources (*M .thermoacetica* and *D. vulgaris*) function efficiently in *E. coli*, even in the absence of their proposed physiological proximal electron donors (Hrb or rubredoxin, respectively). Moreover, the *E. coli* flavorubredoxin appears to function efficiently in a mutant strain that is unable to express the flavorubredoxin reductase, which is itself a flavoprotein.[2] It is,

therefore, unclear why nature chose the two-electron → one-electron → two-electron pathway for Hrb→FprA.

An Hrb-NO adduct. While examining the redox properties of Hrb, it was noticed that both dioxygen and NO (FprA substrates) are able to oxidize Hrb in the absence of FprA. Reoxidation by dioxygen was complete within a few seconds, thus accounting for the low (" background") level of aerobic NADH consumption shown by Hrb, especially in concentrations >1 μM (at room temperature, and apparently independent of buffer and pH in the range of 5-10). Such low "oxidase" activity is in fact expected of any oxygen-sensitive redox protein. NO was also observed to oxidize the Hrb FMN, but this reaction is apparently slow enough to prevent any detectable NOR turnover of Hrb at concentrations as high as 10 μM (using saturating NADH and 100 μM NO) at room temperature in the pH range 5-10.

In what was initially intended as a control experiment, the EPR spectrum of NO-treated reduced Hrb was recorded after freezing. Surprisingly, as shown in Figure 4.7, the bulk of the EPR-active iron in the sample appears to be part of a g ~ 4.0 signal, the unmistakable signature of a $S = 3/2$ non-heme $\{FeNO\}^7$ complex.[14,15] [14-36] Integration of the EPR signals (taking the as-isolated Hrb ferric EPR signal as reference) indeed suggests that in the NO-reacted Hrb sample, ~55% of the $[Fe(SCys)_4]$ is $S = 3/2$ $\{FeNO\}^7$ (g = 3.92, 2.0) and ~10% is ferric (g = 4.3, 9.5). Such NO reactivity has not been documented for any rubredoxin. Analogous EPR experiments (spectra not shown) confirm that reduced *P. furiosus* rubredoxin (Rd) and *D. vulgaris* rubredoxin-like protein (Rdl)[6] do not form any EPR-active NO adducts under conditions similar to those of Figure 4.5 (Rd and Rdl at 200 μM were reduced anaerobically with stoichiometric NADH and a 0.1 μM Hrb). Rather, a slow reoxidation of Rd and Rdl was observed over the course of several minutes to an hour. The optical absorption spectra of the NO-treated

rubredoxins after exposing to air were identical to those of the as-isolated (oxidized) proteins, suggesting that NO does not destroy the [Fe(SCys)$_4$] site.

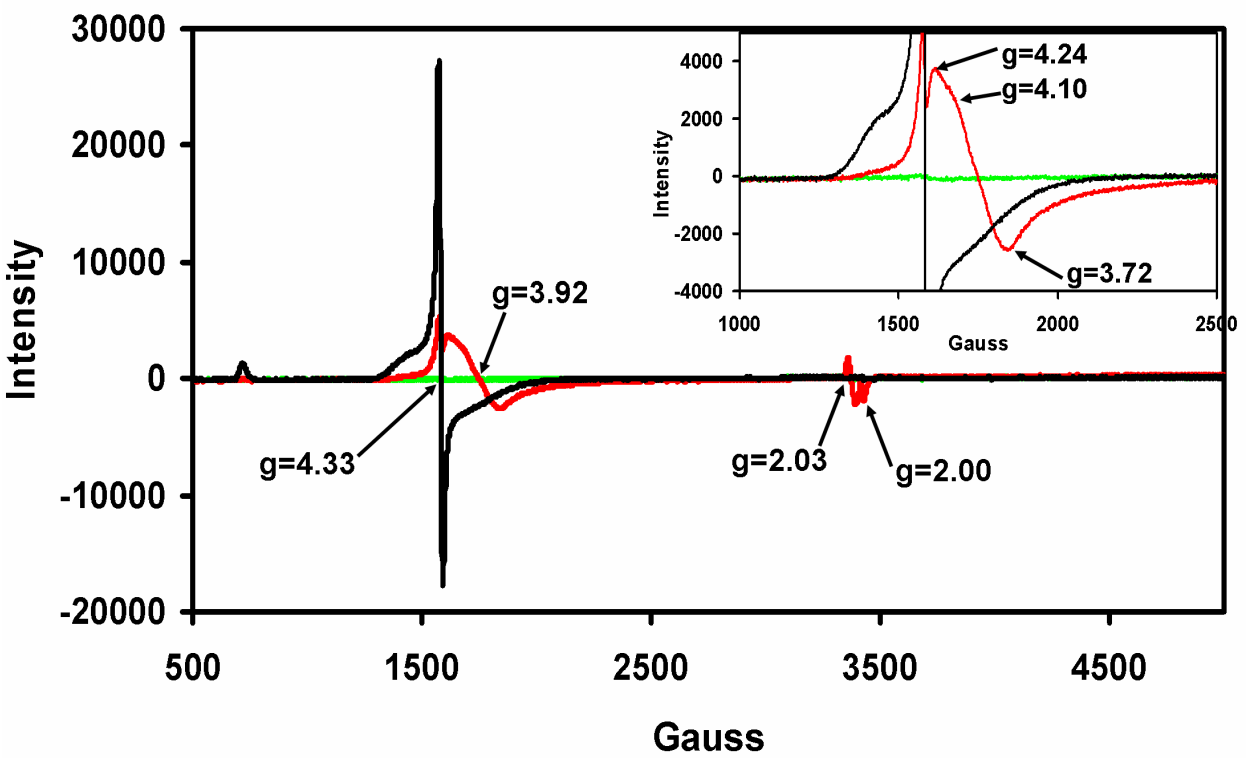

Figure 4.7. EPR spectra of as-isolated (black trace), NADH-reduced (green trace) and NADH-reduced+NO (red trace) *M. thermoacetica* Hrb (cf. Materials and methods). EPR conditions: temperature 4 K; microwave power 2mW, microwave frequency 9.60 GHz, modulation amplitude 6.366 G.

As-isolated recombinant Hrb is labile and undergoes cleavage with slow destruction of the rubredoxin domain when exposed to air, light, and room temperature.[1] From this point of view, one may argue that the Hrb-NO adduct forms upon reaction of NO with a *damaged* Hrb. The UV-vis absorption spectra in Figure 4.8 indicate, however, that the formation of reduced Hrb-NO complex is reversible, and that its decay and [Fe(SCys)$_4$] reoxidation are catalyzed by FprA. This behavior is that expected from an intact, functional, rather than damaged Hrb. Thus, an anaerobic sample of Hrb was reduced with stoichiometric NADH, then treated with excess NO; upon mixing the contents of the cuvette, the Hrb FMN appeared to have reoxidized, along

with a small fraction of the Hrb [Fe(SCys)$_4$] site. Upon addition of a catalytic amount of FprA, complete reoxidation of the Hrb [Fe(SCys)$_4$] site could be visualized from the UV-vis absorption spectrum. Notably, addition of *Zn-substituted* FprA did not bring about oxidation of the NO-treated Hrb [Fe(SCys)$_4$] site, suggesting that the decay of the Hrb-NO adduct requires a *functional diiron site* in FprA.

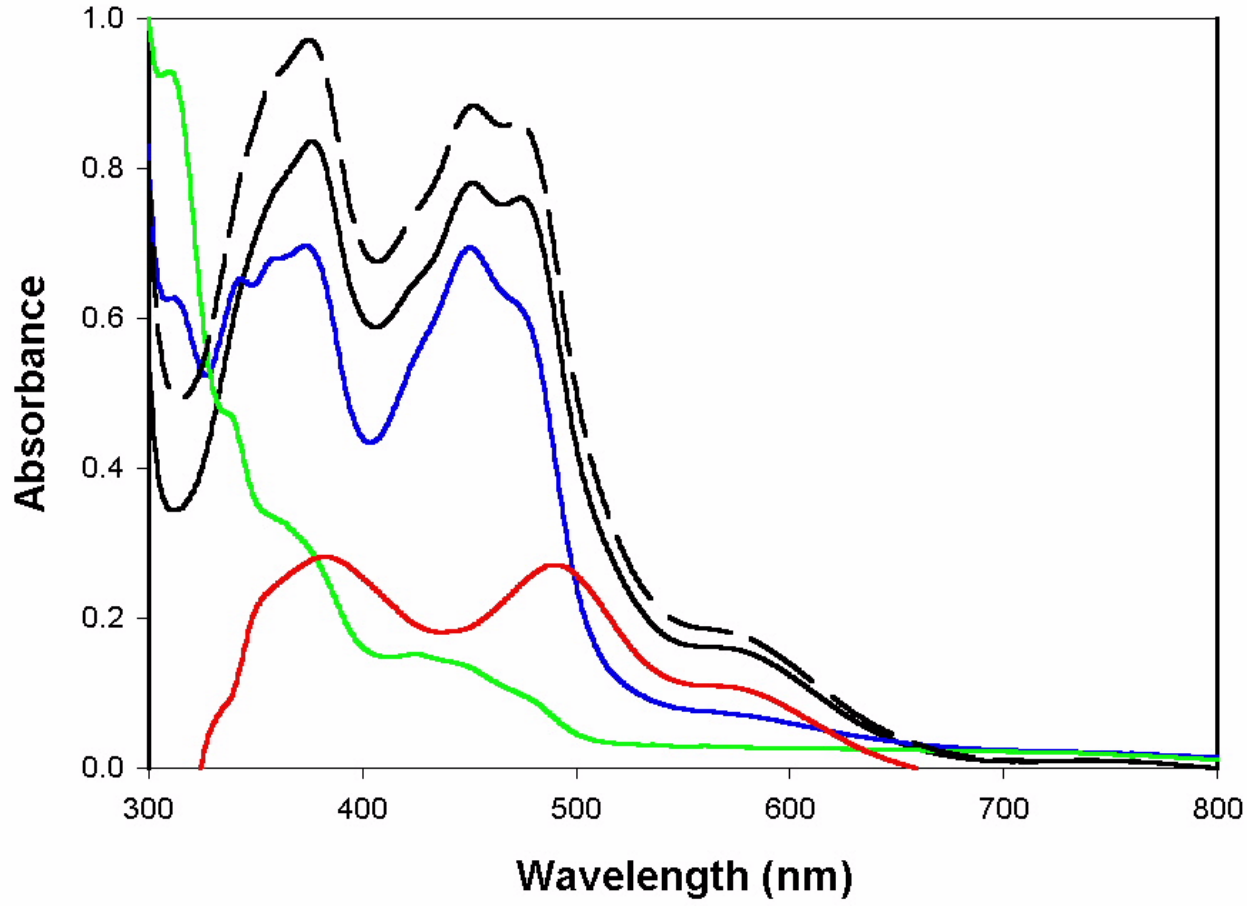

Figure 4.8. UV-vis absorption spectral monitoring of the anaerobic reaction of reduced *M. thermoacetica* Hrb with NO in 50 mM MOPS pH 7.0 at room temperature. Black solid trace: as-isolated Hrb (47 μM). Green trace: Hrb anaerobically reduced with stoichiometric NADH. Blue trace: after addition of NO (250 μM) and Zn-substituted FprA (2 μM) to the NADH-reduced Hrb. Black dashed trace: same as blue trace, but after adding 2 μM iron-containing FprA. Red trace: difference spectrum, dashed minus blue traces.

The EPR and UV-vis absorption experiments are thus consistent with a reversible Hrb $[Fe^{2+}(SCys)_4]$-NO adduct being formed at Hrb concentrations in the range 40-100 μM. Could such complexes also occur *in vivo*, allowing Hrb to act as an FprA-dependent NO scavenger? The experiments illustrated in Figure 4.7 and 4.8 use Hrb and NO concentrations that are much higher than are likely to occur intracellularly and, therefore, do not address this question directly. However, the data in Table 4.1 shows that distinct differences in NO concentrations were detected using an NO electrode when mixing reduced or oxidized Hrb (in concentrations as low as 6 μM) with equimolar or excess NO solution (note that when substoichiometric NADH relative to Hrb is added only the $[Fe(SCys)_4]$ site gets reduced). These differences may correspond to (sub-stoichiometric) Hrb-NO adduct formation from reduced Hrb even at low micromolar (close to physiologically relevant) Hrb and NO concentrations – suggesting that the Hrb-NO adduct may form *in vivo*.

The nature of the Hrb-NO adduct remains unclear. The $[Fe(SCys)_4]$ sites of typical rubredoxins feature a robust tetrahedral geometry in both oxidized and reduced forms and are not known to bind a fifth ligand.[5,37-39] In particular, the present experiments confirm that reduced rubredoxins themselves do not generate EPR-active NO adducts. It may be inferred that in Hrb, NO binding to the $[Fe^{2+}(SCys)_4]$ is facilitated by an increased flexibility of the protein backbone around the iron site, and/or by reversible dissociation of one of the cysteinate ligands from the iron. The structure of Hrb is unknown, but given the high amino acid sequence homology and similar reduction potentials between the Hrb $[Fe(SCys)_4]$ domain and those of canonical rubredoxins (cf. Figure 2.1, Chapter 2), the structural basis of the unique NO reactivity of the Hrb $[Fe(SCys)_4]$ site remains unclear.

Table 4.1. Measured NO concentrations[a] after anaerobically mixing as-isolated Hrb with NADH and NO (in that order) in 1 mL of 50 mM MOPS pH 7.0 at room temperature.

Hrb	NADH added	Reduced Hrb [$Fe(Cys)_4$]	NO added	NO detected	% Hrb-NO
19 μM	none	0 μM	57 μM	57 μM	-
	9.5 μM	9.5 μM	57 μM	50.7 μM	33 %
9.6 μM	none	0 μM	28.8 μM	28.8 μM	-
	4.8 μM	9.6 μM	28.8 μM	24.9 μM	41 %
13 μM	None	0 μM	57 μM	57 μM	-
	9.5 μM	13 μM	57 μM	44 μM	100 %
12.6 μM	none	0 μM	19.2 μM	19.2 μM	-
	6.3 μM	12.6 μM	19.2 μM	7.5 μM	92 %
	3.1 μM	6.3 μM	19.2 μM	12.5 μM	105 %
12.6 μM	none	0 μM	12.6 μM	12.6 μM	-
	6.3	12.6	12.6 μM	9.5 μM	25%

[a]using the NO electrode, cf. Materials and Methods.

A homology model was generated for *M. thermoacetica* Hrb, based on the crystal structures of *Archaeoglobus fulgidus* ferric reductase, PDB code 1I0R (the amino acid sequence of which is homologous to the Hrb flavo domain, and which, like Hrb, is a homodimer) and *Pyrococcus furiosus* rubredoxin, PDB code 1BRF, (modeling the Hrb rubredoxin domain). A ~15 residue stretch that could not be modeled (and is likely to constitute a random coil) connects the flavo and rubredoxin domains in Hrb. This unmodeled connection allows the two domains of the Hrb model to be positioned in a large number of relative orientations with the minimum iron-to-FMN distance being ~12 Å. An Hrb model featuring such a short Fe-FMN distance was docked onto *M. thermoacetica* FprA (which was itself a homology model, built using the crystal structure of *D. gigas* ROO, pdb code 1E5D). The best docking position (shown in Figure 4.9) allowed a minimum Hrb-FprA surface-to-surface distance of 3 Å and an Hrb-iron to FprA-FMN

distance of ~20 Å. The latter distance is probably too long for efficient electron transfer, but may in principle become shorter, depending on the exact orientation of the rubredoxin domain within Hrb. A previously reported docking model of *D. gigas* rubredoxin to *D. gigas* ROO showed preferential binding of the [Fe(SCys)$_4$] site close to the FprA FMN.[13] The FMN-to-[Fe(SCys)$_4$] distance for the *D. gigas* ROO-rubredoxin docking was not explicitly reported, but the authors did note that the [Fe(SCys)$_4$] site of the rubredoxin was not in direct contact with the ROO surface, which implies an ROO-FMN-to-[Fe(SCys)$_4$] distance similar to that estimated from the *M. thermoacetica* Hrb-FprA docking. The Hrb [Fe(SCys)$_4$] site was reported to have a reduction potential more than 80 mV more positive than the FprA FMN, which seems inconsistent with the demonstrated efficient electron transfer between Hrb and FprA during turnover.[1] Also, as shown in this Chapter, reduction of the Hrb [Fe(SCys)$_4$] site by NADH in a stopped-flow single-turnover experiment may be too slow to be consistent with efficient electron transfer from Hrb to FprA. Docking of Hrb on FprA results in a distinct change in the environment around the otherwise solvent-exposed Hrb [Fe(SCys)$_4$] domain, which becomes buried between the Hrb FMN domain and the FprA. This change in solvent accessibility (polarity) could affect the [Fe(SCys)$_4$] redox properties and possibly allow a more efficient electron transfer from [Fe(SCys)$_4$] to FprA. The presence of the Hrb [Fe(SCys)$_4$] site near the FprA FMN and implicitly near the diiron site which is less than 4 Å from the FMN (Cf. Chapter 6), may also be important if indeed Hrb forms an NO adduct *in vivo*. It raises the intriguing possibility that the Hrb [Fe(SCys)$_4$] site delivers not only electrons, but also the substrate, NO, to the FprA flavo-diiron site.

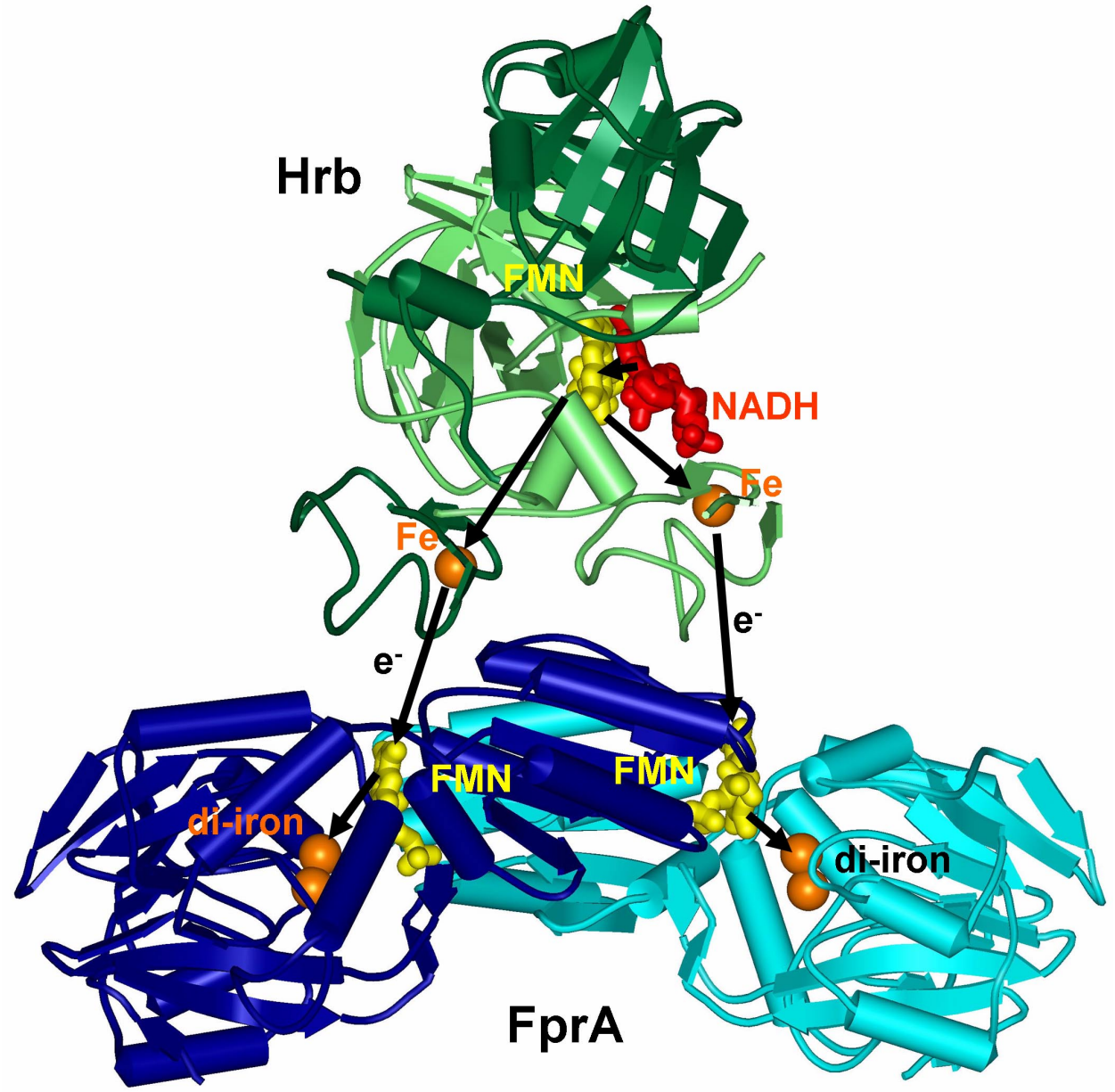

Figure 4.9. Proposed structure for the *M. thermoacetica* Hrb-FprA complex, predicted from homology modelling and docking. The two monomers of the Hrb homodimer are shown in different shades of green. The two monomers of the FprA homodimer are shown in different shades of blue. Iron is shown in orange, FMN in yellow, NADH in red. Arrows indicate the verified electron flow pathway: NADH → Hrb-FMN → Hrb-[Fe(SCys)$_4$] → FprA-FMN → FprA-diiron site.[1]

4.4. References

(1) Silaghi-Dumitrescu, R.; Coulter, E. D.; Das, A.; Ljungdahl, L. G.; Jameson, G. N.; Huynh, B. H.; Kurtz, D. M., Jr. *Biochemistry* **2003**, *42*, 2806-2815.

(2) Gardner, A. M.; Helmick, R. A.; Gardner, P. R. *J. Biol. Chem.* **2002**, *277*, 8172-8177.

(3) Sarti, P.; Fiori, P. L.; Forte, E.; Rappelli, P.; Teixeira, M.; Mastronicola, M.; Sanciu, G.; Giuffre, A.; Brunori, M. *Cell. Mol. Life Sci.* **2004**, *61*, 618-623.

(4) Schagger, H.; von Jagow, G. *Analyt. Biochem.* **1987**, *166*, 368-379.

(5) Eidsness, M. K.; Richie, K. A.; Burden, A. E.; Kurtz, D. M., Jr.; Scott, R. A. *Biochemistry* **1997**, *36*, 10406-10413.

(6) Lumppio, H.; Shenvi, N.; Summers, A.; Voordouw, G.; Kurtz, D. M., Jr. *J. Bacteriol.* **2001**, *183*, 101-108.

(7) Douzou, P. *Cryobiochemistry*; Academic Press: London, 1977.

(8) Armarego, W. L.; Perrin, D. D. *Purification of Laboratory Chemicals*, Butterworth Heinemann, Oxford, 1998.

(9) Schwede, T.; Kopp, J.; Guex, N.; Peitsch, M. C. *Nucleic Acids Res.* **2003**, *31*, 3381-3385.

(10) Chapman, S. K.; Reid, G. A. *Methods in Molecular Biology*, Vol. 131-Flavoprotein protocols, Humana Press, Totowa, NJ, 1999.

(11) Gassner, G. T.; Ludwig, M. L.; Gatti, D. L.; Correll, C. C.; Ballou, D. P. *FASEB J.* **1995**, *9*, 1411-1418.

(12) Gomes, C. M.; Vicente, J. B.; Wasserfallen, A.; Teixeira, M. *Biochemistry* **2000**, *39*, 16230-16237.

(13) Victor, B. L.; Vicente, J. B.; Rodrigues, R.; Solange, O.; Rodrigues-Pousada, C.; Frazao, C.; Gomes, C. M.; Teixeira, M.; Soares, C. *J. Biol. Inorg. Chem.* **2003**, *8*, 475-488.

(14) Brown, C. A.; Pavlovski, M. A.; Westre, T. E.; Zhang, Y.; Hedman, B.; Hodgson, K. O.; Solomon, E. I. *J. Am. Chem. Soc.* **1995**, *117*, 715-732.

(15) Jackson, T. A.; Yikilmaz, E.; Miller, A. F.; Brunold, T. C. *J. Am. Chem. Soc.* **2003**, *125*, 10833-10845.

(16) Butler, A. R.; Megson, I. L. *Chem. Rev.* **2002**, *102*, 1155-1166.

(17) Chiou, Y.-M.; Que, L., Jr. *Inorg. Chem.* **1995**, *34*, 3270-3278.

(18) Clay, M. D.; Cosper, C. A.; Jenney, F. E.; Adams, M. W. W.; Johnson, M. K. *Proc. Natl. Acad. Sci. USA* **2003**, *100*, 3796-3801.

(19) Cooper, C. E. *Biochim. Biophys. Acta* **1999**, *1411*, 290-309.

(20) Coufal, D. E.; Tavares, P.; Pereira, A. S.; Huynh, B. H.; Lippard, S. J. *Biochemistry* **1999**, *38*, 4504-4513.

(21) Ford, P. C.; Lorkovic, I. M. *Chem.Rev.* **2002**, *102*, 993-1018.

(22) Feig, A. L.; Bautista, M. T.; Lippard, S. J. *Inorg. Chem.* **1996**, *35*, 6892-6898.

(23) Haskin, C. J.; Ravi, N.; Lynch, J. B.; Munck, R.; Que, L., Jr. *Biochemistry* **1995**, *34*, 11090-11098.

(24) Hayton, T. W.; Legzdins, P.; Sharp, W. B. *Chem. Rev.* **2002**, *102*, 935-992.

(25) Hendriks, J.; Oubrie, A.; Castresana, J.; Urbani, A.; Gemeinhardt, S.; Saraste, M. *Biochim. Biophys. Acta* **2000**, *1459*, 266-273.

(26) Hodges, K. D.; Wollman, R. G.; Kessel, S. L.; Hendrickson, D. N.; Van Derveer, D. G.; Barefield, E. K. *J. Am. Chem. Soc.* **1979**, *101*, 906-917.

(27) Kelm, M. *Biochim. Biophys. Acta* **1999**, *1411*, 273-289.

(28) LeBrun, N. E.; Andrews, S. C.; Moore, G. R.; Thomson, A. J. *Biochem. J.* **1997**, *326*, 173-179.

(29) Li, M.; Bonnet, D.; Bill, E.; Neese, F.; Weyhermuller, T.; Blum, N.; Sellman, D.; Wieghardt, K. *Inorg. Chem.* **2002**, *41*, 3444-3456.

(30) Lopes, L. G. F.; Sousa, E. H. S.; Miranda, J. C. V.; Oliveira, C. P.; Carvalho, I. M. M.; Batista, A. A.; Ellena, J. J.; Castellano, E. E.; Nascimento, O. R.; Moreira, I. S. *J. Chem. Soc., Dalton Trans.* **2002**, 1903-1906.

(31) Pohl, K.; Wieghardt, K.; Nuber, B.; Weiss, J. *J. Chem. Soc., Dalton Trans.* **1987**, 187.

(32) Ray, M.; Golombek, A. P.; Hendrich, M. P.; Glenn, P. A. Y.; Liable-Sands, L. M.; Rheingold, A. L.; Borovik, A. S. *Inorg. Chem.* **1999**, *38*, 3110-3115.

(33) Roach, P. L.; Clifton, I. J.; Hensgens, C. M.; Shibata, N.; Schofield, C. J.; Hajdu, J.; Baldwin, J. E. *Nature* **1997**, 827.

(34) Wasser, I. M.; de Vries, S.; Moenne-Loccoz, P.; Schroeder, I.; Karlin, K. D. *Chem. Rev.* **2002**, *102*, 1201-1234.

(35) Yang, T.-C.; Wolfe, M.; Neibergall, M. B.; Mekmouche, Y.; Lipscomb, J. D.; Hoffman, B. M. *J. Am. Chem. Soc.* **2003**, *125*, 2034-2035.

(36) Zhang, Z.; Ren, J.; Harlos, K.; McKinnon, C. H.; Clifton, I. J.; Schofield, C. J. *FEBS Lett.* **2002**, *517*, 7-12.

(37) Eidsness, M. K.; Burden, A. E.; Richie, K. A.; Kurtz, D. M., Jr.; Scott, R. A.; Smith, E. T.; Ichiye, T.; Beard, B.; Min, T.; Kang, C. *Biochemistry* **1999**, *38*, 14803-14809.

(38) Eidsness, M. K.; Burden, A. E.; Richie, K. A.; Kurtz, D. M., Jr.; Scott, R. A.; Smith, E. T.; Ichiye, T.; Beard, B.; Min, T.; Kang, C. *Biochemistry* **2000**, *39*, 626.

(39) Min, T.; Ergenekan, C. E.; Eidsness, M. K.; Ichiye, T.; Kang, C. *Protein Sci.* **2001**, *10*, 613-621.

CHAPTER 5

NITRIC OXIDE ADDUCTS OF *MOORELLA THERMOACETICA* FPRA, A FLAVO-DIIRON NON-RESPIRATORY NITRIC OXIDE REDUCTASE

5.1. Introduction

The homodimeric flavo-diiron protein, FprA, and its reductase, Hrb, have been shown to function as a novel non-respiratory nitric oxide reductase (NOR) involved in nitrosative stress defense in the anaerobic, acetogenic bacterium, *Moorella thermoacetica*.[1] The net reaction catalyzed in this system is:

$$2NO + NADH + H^+ \rightarrow N_2O + H_2O + NAD^+ \qquad 5.1.$$

The FprA/Hrb system also catalyzes the four-electron reduction of O_2 to H_2O by NADH *in vitro*, but this dioxygen reductase activity is less efficient than the NOR activity and results in irreversible inactivation of the FprA. Transcription of the FprA gene from the anaerobic bacterium, *C. perfringens*, has recently been shown to be induced by exposure of the bacterial cultures to air.[2] However, *in vivo* evidence for an NOR function of FprAs in *E. coli*, [3-5] and in *T. vaginalis*[6] has been reported.

For the *M. thermoacetica* Hrb/FprA, the steady-state kinetics for NOR activity were found to be consistent with NO reduction occurring at the FprA diiron site according to Scheme 5.1.[1]

$$E_{red} + NO \overset{K_1}{\rightleftharpoons} E_{red}\text{-}NO$$

$$E_{red}\text{-}NO + NO \overset{K_2}{\rightleftharpoons} E_{red}\text{-}(NO)_2$$

$$E_{red}\text{-}(NO)_2 \xrightarrow{k_{cat}} E_{ox} + N_2O$$

Scheme 5.1

The di-zinc substituted *M. thermoacetica* FprA was inactive as an NOR (or dioxygen reductase), implicating the diiron site as the center of NO (and O_2) reduction. Otherwise, the mechanism of NO reduction by FprAs remains largely unexplored.[1] Upon manual mixing of the dithionite-reduced *E. coli* FprA homologue, flavorubredoxin,[7] with NO, an EPR signal consistent with an S = 1/2 state (g = 2.04 and 2.002) was detected. This signal was ascribed to a hemerythrin-type diferrous mono-NO adduct (cf. Chapter 1), although alternative interpretations, such as a mixed-valent Fe(II)-Fe(III) state or matrix-bound NO, cannot be excluded. This S = 1/2 flavorubredoxin species appeared to be relatively stable at room temperature, so that its involvement as a transient intermediate in the rapid, catalytic NO reduction at the diiron site is unlikely.

Based on the (mostly indirect) information available to date (cf. Chapters 1 and 2 and Scheme 5.1), a di-NO adduct is likely to be involved in catalytic NO reduction by FprA, as shown in Scheme 5.2.

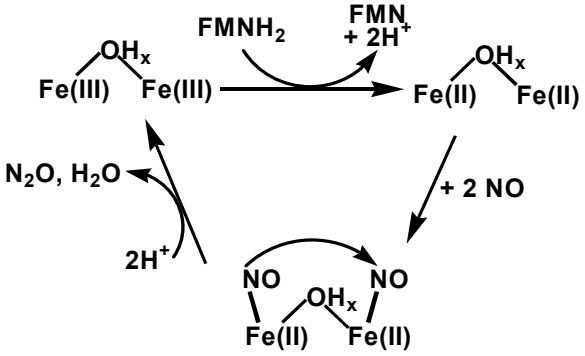

Scheme 5.2

The present chapter describes the use of stopped-flow, cryogenic, and rapid-freeze-quench (RFQ) techniques to identify and characterize transient nitric oxide adducts of *M. thermoacetica* FprA and the insights these adducts provide into the mechanism of NOR activity.

5.2. Materials and methods

Reagents and General Procedures. All solutions were prepared in deionized water. NADH, NADPH, 3-[[tris(Hydroxymethyl)methyl]amino]propanesulfonic acid (TAPS) (Sigma Chemical Co.), N-morpholinoethanesulfonic acid (MOPS) (Fisher) and ethylene glycol (J.T. Baker) were used without further purification. Stock solutions (25 mM) of DEA NONOate (diethylammonium (Z)-1-(N,N-diethylamino) diazen-1-ium-1,2-diolate, Cayman Chemicals, Inc.) were prepared in 0.01 M NaOH. DEA NONOate is stable at high pH but decomposes to release NO gas (1.5 mols NO/1 mol DEA NONOate) when added to assay mixtures at ~ pH 7. Where indicated, solutions were made anaerobic by repetitive vacuum/argon or N_2 gas exchange or extensive purging with argon or N_2 gas. Gaseous nitric oxide (98.5%) was purchased from Aldrich. The NO was purified by bubbling through 100 mL of a 10% KOH solution. The purified NO gas was used to prepare saturated NO solutions (~1.8 mM in water, or 12 mM in ethanol) by bubbling the gas through either anaerobic deionized water or ethanol for 15 minutes. NO concentrations were measured with an NO electrode (World Precision Instruments, Inc.). *M. thermoacetica* FprA (including ^{57}Fe-labeled His-tagged FprA) and *M. thermoacetica* Hrb were obtained as previously described.[1] Previously determined molar absorptivities[1] were used to calculate all protein concentrations from measured absorbances. NADH-dependent oxidase (O_2 consumption) and NADH-dependent NOR (NO consumption) activities of Hrb/FprA were monitored as previously described.[1] FprA and Hrb concentrations refer to monomers.

Unless otherwise specified, "reduced FprA" refers to the state containing a two-electron reduced FMN and a diferrous diiron site. Reduced FprA or Zn-FprA for all experiments was generated at room temperature under anaerobic conditions by reductive titration with either NADH in the presence of 0.5-1 μM Hrb or sodium dithionite of 20-200 μM FprA for UV-vis absorption and EPR experiments, or 1-2 mM FprA and 5-10 μM Hrb for Mössbauer and RFQ experiments. Anaerobic conditions were ensured either by working inside an anaerobic chamber (Coy Laboratory Products, Inc.) or Vacuum Atmospheres, Inc. glove box (<1 ppm O_2), or by performing the titration inside a rubber septum-sealed argon-purged cuvette and adding reductant via a gas-tight syringe. Where necessary, excess reducing agent was removed by concentration/dilution cycles in 10-kDa-cutoff centrifugal concentrators inside the Vacuum Atmospheres glove box. Lower concentrations (10-100 μM) of reduced FprA could be generated via anaerobic photoreduction in the presence of 50 mM Tris pH 7 and 1 μM 5-deazaflavin,[8] and the protein thus generated yielded stopped-flow results indistinguishable from those of NADH/Hrb-reduced FprA. Photoreduction was achieved in sealed 1-mL quartz cuvettes, placed in an ice-water bath using a slide projector as the source of photons. However, this method of reduction proved to be convenient only for Zn-substituted FprA, where photoreduction took ~20 minutes. Complete photoreduction of iron-containing FprA took several hours.

Spectroscopy. Room-temperature ultraviolet-visible absorption spectra were obtained in 1-cm pathlength quartz cuvettes on a Shimadzu UV-2401PC scanning spectrophotometer. EPR spectra were recorded on a Bruker ESP-300E spectrometer equipped with an ER-4116 dual-mode cavity and an Oxford Instruments ESR-9 flow cryostat, using 200-μL sample volumes. The SPECCONV, WINEPR v. 2.11 (Bruker), and EPRQUANT programs (access to which was kindly provided by Dr. Richard Conover at the University of Georgia) were used for EPR data

manipulation and quantitation. For spin quantitation, the EPR signal centered at g = 4.3 of as-isolated *M. thermoacetica* Hrb was used as the standard. Mössbauer spectra were recorded in the laboratory of Professor Vincent Huynh at the Department of Physics at Emory University by Dr. Ricardo Garcia on either a weak-field spectrometer with a Janis 8DT variable temperature cryostat or a strong-field spectrometer furnished with CNDT/SC Super-Varitemp cryostat encasing an 8T superconducting magnet. Both spectrometers operate in a constant acceleration mode in transmission geometry. The zero velocity of the spectra refers to the centroid of a room temperature spectrum of metallic iron foil. The Mössbauer spectra were analyzed using the WMOSS program (WEB Research Co. Edina, MN) based on a spin Hamiltonian formalism conventionally used for Mössbauer analysis. Mössbauer spectroscopy employed as-isolated ^{57}Fe-enriched His-tagged FprA. UV-vis absorption spectral time courses following stopped-flow mixing were carried out on an Applied Photophysics SX.18MV-R instrument at room temperature. Stopped-flow data analysis and fitting was performed with the program Pro-Kineticist v. 1.06 (Applied Photophysics, Ltd.). Other experimental conditions are given in the figure legends.

Cryogenic Temperature Reactions. FprA was reduced anaerobically at room temperature with excess NADH (15 mM) and 10 μM Hrb in the buffers specified in figure legends, after which the excess NADH was removed by repeated concentrations/dilutions in a centrifugal concentrator. Anaerobic ethylene glycol was then added to these reduced FprA solutions to achieve either 2:3 or 1:1 (v/v) buffer:ethylene glycol. The temperatures of these solutions of reduced FprA in cryosolvent were then lowered to and maintained at -40 to -60 °C in dry ice/isopropanol baths[9,10] in Dewar vessels. Reaction vessels were whenever possible maintained sealed with rubber septa under positive argon pressure via a needle connected to an argon tank. For EPR samples, 200-μL

volumes of reduced FprA (at concentrations and in cryosolvents indicated in the figure legends) that had been prepared at room temperature in the anaerobic Vacuum Atmospheres box were loaded into EPR tubes, which were then sealed with tight-fitting rubber septa. These tubes were removed from the anaerobic box and placed in low-temperature baths (dry ice-isopropanol, -40°C) for 10 minutes. Nitric oxide was then added from a 12 mM anaerobic ethanolic stock solution via a Hamilton syringe, the 22-gauge needle of which was long enough to reach inside the protein solution. The immersed needle was allowed to equilibrate (cool) inside the EPR tube before delivering the NO solution. Mixing was then achieved with the EPR tube still immersed in the dry ice/isopropanol bath by syringe rotation and gentle movements of the syringe plunger, after which the samples were immediately frozen in liquid nitrogen. The mixed solutions contained 5% ethanol by volume. When necessary, EPR samples were "annealed" by removing the tubes from liquid nitrogen and either placing them in the dry ice/isopropanol bath or warming to and incubating at room temperature for various times listed in the figure legends. Cryogenically "NO-reacted" Mössbauer samples were prepared following the same protocol described for the EPR samples except that the reduced FprA (400 μL) was placed inside a Mössbauer sample cup, which was then placed inside a septum-sealed 15-mL Falcon tube and maintained under positive argon pressure when not inside the anaerobic Vacuum Atmospheres box. UV-vis absorption spectra at cryogenic temperatures were recorded on 4-mL FprA solutions placed in a custom-made Dewar cuvette (cf. Figure 4.1, Chapter 4) equipped with optical quality quartz windows and a 2-cm pathlength. The cuvette contained an extension that was sealed with a rubber or silicon septum, and the headspace was maintained under positive argon pressure. The solution in the cuvette was cooled to -40 °C using a dry ice/isopropanol bath[9,10] in the surrounding chamber. A thermometer was placed inside the dry ice/isopropanol bath, and the

temperature was adjusted by adding dry ice or room-temperature isopropanol, as required. The Dewar was placed in a specially constructed Plexiglas® bracket to which fiber-optic cables leading to an Ocean Optics, Inc. USB2000 UV-vis spectrometer were attached. UV-vis absorption spectra were recorded using the computer-driven Ocean Optics spectrometer.

Rapid Freeze-Quench EPR and Mössbauer Experiments. The apparatus and procedures used to prepare and measure the rapid freeze-quench EPR and Mössbauer samples are described elsewhere.[11-13] Reaction and spectrometer conditions are given in the figure legends. FprA for these experiments was reduced anaerobically with 10 mM sodium dithionite; excess dithionite and dithionite byproducts were then removed by repeated concentrations and dilutions in 50 mM MOPS pH 7 using centrifugal concentrators inside an anaerobic Vaccum Atmospheres glove box. The RFQ sequence consisted of mixing NO-saturated ethanol (measured to contain 12 mM NO with an NO electrode) with NO-saturated water (measured to contain 1.8 mM NO), at room temperature in a 1:2 (v/v) ratio, with the resulting mixture being further mixed, in a 3:2 (v/v) ratio, with an anaerobic solution of 1.33 mM reduced ^{57}Fe-enriched His-tagged FprA. This mixing yielded a concentration of diiron sites of 0.5 mM and an approximate FprA active site:NO molar stoichiometry of 1:4, i.e., enough NO for a "single turnover" of the four-electron reduced FprA. The RFQ-mixed solution contained 18 vol. % ethanol.

Site-Directed Mutagenesis. Genes encoding H25F and Y195F variants of the *M. thermoacetica* FprA in plasmid, pHisFprA, encoding the histidine-tagged FprA, were generated using the QuikChange site-directed mutagenesis kit (Stratagene) following the procedures described in the product manual. The following primers were used (with the variant codon in italics): H25F, C CGC TAC TTC *TTC* GGT CCC GCT TTT TCC; Y195F, GAG GCG GCC AAG *TTC* TAT GCC AAT ATT CTC. For each primer, the complement was generated automatically by the

manufacturer (Integrated DNA Technologies) using standard nucleotide pairing. The variant codons in the resulting plasmids pH25F-FprA and pY195F-FprA were verified by sequence analysis of the plasmids at the University of Georgia Integrated Biotechnology Laboratories. The variant FprAs were expressed and purified following the protocols previously described for "wild-type" histidine-tagged *M. thermoacetica* FprA (cf. Chapter 2).[1]

5.3. Results and discussion

All FprA and Hrb concentrations refer to monomers. In figure legends, concentrations of all reactants are given immediately *after* mixing.

Manual Mixing EPR and Mössbauer Experiments. The Mössbauer spectrum of NADH/Hrb-reduced ^{57}Fe-enriched *M. thermoacetica* FprA (cf. Figure 5.1) confirms the presence of a diferrous FprA site. The Mössbauer data are consistent with two types of high-spin ferrous sites, A and B, which together account for ~70% of the iron in the sample (the remainder being mostly the previously reported antiferromagnetically-coupled diferric sites[1]). Spectra collected at 6 Tesla (not shown) suggest that the site A iron is part of an antiferromagnetically coupled diferrous site, whereas essentially no coupling could be detected for B - consistent with mononuclear iron or with a diiron site containing magnetically uncoupled ferrous centers, possibly due to loss of the solvent bridge present in the diferric state.[1] The relative ratios of the A and B ferrous forms varied from preparation to preparation and did not appear to be influenced by pH in the range 6 – 9 (data not shown).

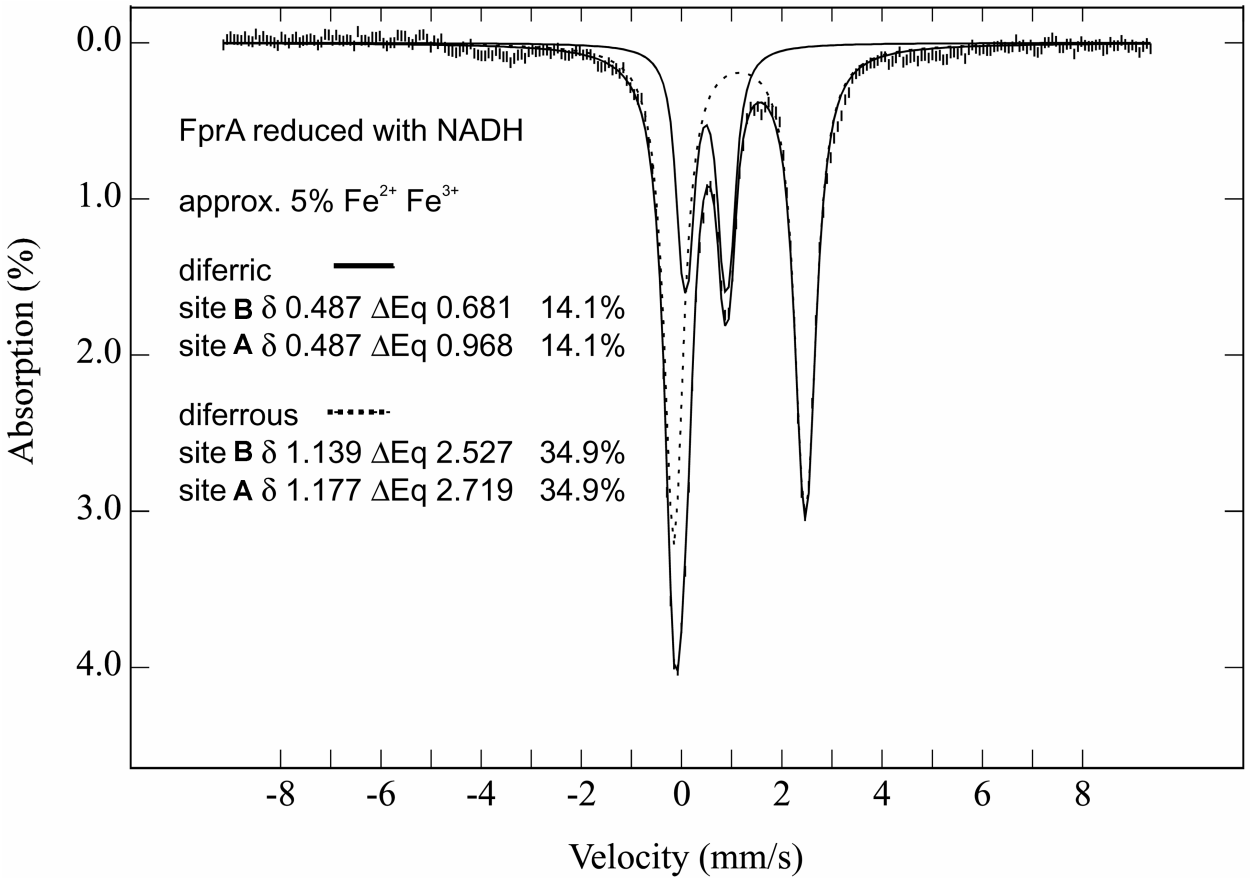

Figure 5.1. Mössbauer spectrum recorded at 4.2 K in a magnetic field of 50 mT oriented parallel to the γ-ray beam of ^{57}Fe-enriched *M. thermoacetica* FprA (1 mM) reduced with stoichiometric NADH in the presence of 5 μM Hrb in anaerobic 50 mM MOPS pH 7.0 after 15 minutes of reaction at room temperature. Experimental data are shown as hash marks, and fits are shown as solid and dotted lines, as indicated in the inset.

Approximately 5% of the iron in the sample of Figure 5.1 was present as S = 1/2 Fe(II)-Fe(III) mixed-valent diiron sites, and similarly low percentages of mixed-valent diiron sites were present in other NADH/Hrb-reduced Mössbauer samples (not shown). The EPR spectra in Figure 5.2 show that incomplete reduction of FprA by NADH/Hrb resulted in a weak EPR signal with g-values ~1.9, 1.85 and 1.79 (red trace in Figure 5.2), consistent with an S = 1/2 Fe(II)-Fe(III) site.[14] For the red trace in Figure 5.2 this signal amounted to ~50 μM spins or ~25% of the FprA diiron sites present in this particular sample. Attempts to produce quantitative amounts of this

mixed-valent EPR signal by reductive titration of *M. thermoacetica* FprA (gray traces in Figure 5.2) failed, suggesting that the mixed-valent state is relatively unstable. Mixed-valent states of diiron sites have not been reported for other FprAs. The intense narrow signal at g = 2.005 is attributable to the FprA FMN semiquinone, and its double integration reveals a steady increase in intensity, from 10 μM (5 % of active sites) in the sample obtained with 0.3 reducing equivalents, to 110 μM (55 % of active sites) in the sample obtained with 3 reducing equivalents. The broader g = 2.039 signal, which is well defined only in the red trace shown in Figure 5.2, may be due to a mixed-valent diiron site in a different state/conformation than the one giving rise to the g ~ 1.9, 1.85 and 1.79 signals. The g = 4.3 signal accounted for 3-9 μM (1-5 % of the active sites), which is likely due to contributions from the rubredoxin site of the FprA:NADH oxidoreductase, Hrb, present at 1 μM, and/or to non-specifically-bound iron.

An EPR spectrum of anaerobically reduced FprA mixed with the NO donor, DEA NONoate (cf. Figure 5.3) featured a g ~ 4.0 signal consistent with an $S = 3/2$ $\{FeNO\}^7$ center,[15-17] and a g = 1.97 signal typical of "matrix" NO. By analogy with similar complexes detected in other diiron proteins,[15-17] the g ~ 4.0 feature could be due to a damaged FprA active site, containing only one iron atom. Reaction of NO with a magnetically coupled diferrous site would have been expected to generate either an integer-spin and presumably EPR-silent species (di-ferrous di-NO), or a hemerythrin-type $S = 1/2$ mono-NO adduct ($[Fe^{II},\{FeNO\}^7]$, cf. Chapter 1) with much lower g values.[18,19] The g ~ 4.0 signal corresponds to a spin concentration of ~10 μM or ~5% of the FprA diiron sites present in the sample, assuming one $\{FeNO\}^7$ site per protein monomer.

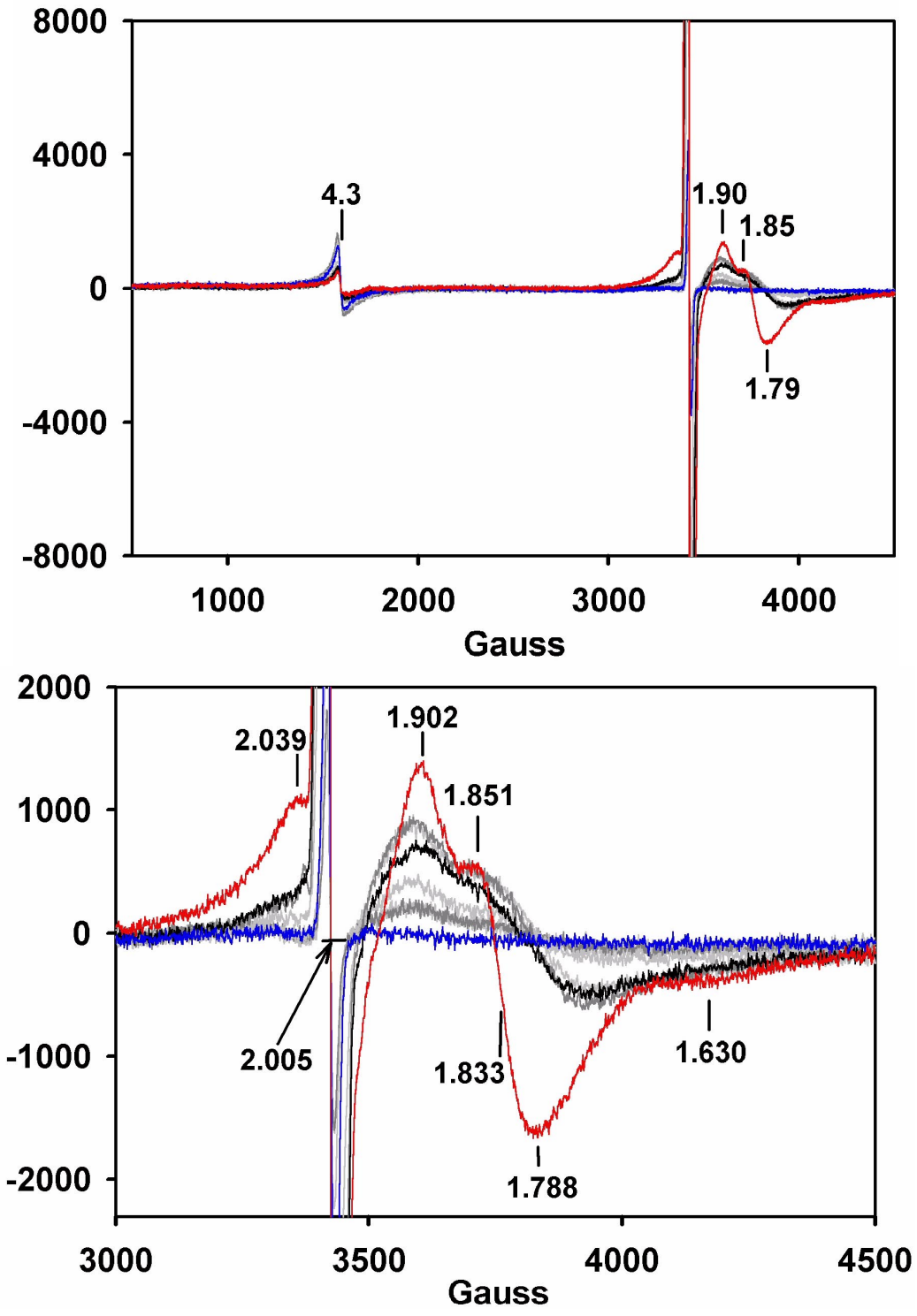

Figure 5.2. EPR spectra illustrating a signal from a probable mixed-valent (Fe^{II},Fe^{III}) FprA diiron site. Bottom panel shows details of the g ~ 2 region. Blue trace: as-isolated FprA (200 μM,

in 50 mM MOPS pH 7.0). Red trace: as-isolated FprA (200 μM) + 1.5 reducing equivalents (NADH) with 1 μM Hrb in anaerobic 50 mM MOPS pH 7.0. The reaction was allowed to proceed for 10 minutes at room temperature before freezing in liquid nitrogen. Gray traces: spectra obtained following the same procedure and under the same conditions as for the red trace but with a different FprA preparation (200 μM), using reducing equivalents (in the form of NADH) in the following approximate amounts (approximate yields of mixed-valent signal given in μM): 0.3 (4 μM), 0.6 (4 μM), 1, (8 μM), 1.5 (18 μM), 2 (17 μM) and 3 (11 μM). EPR conditions: temperature 4 K; microwave power 2 mW, microwave frequency 9.60 GHz, modulation amplitude 6.366 G. g-values are listed in the figure.

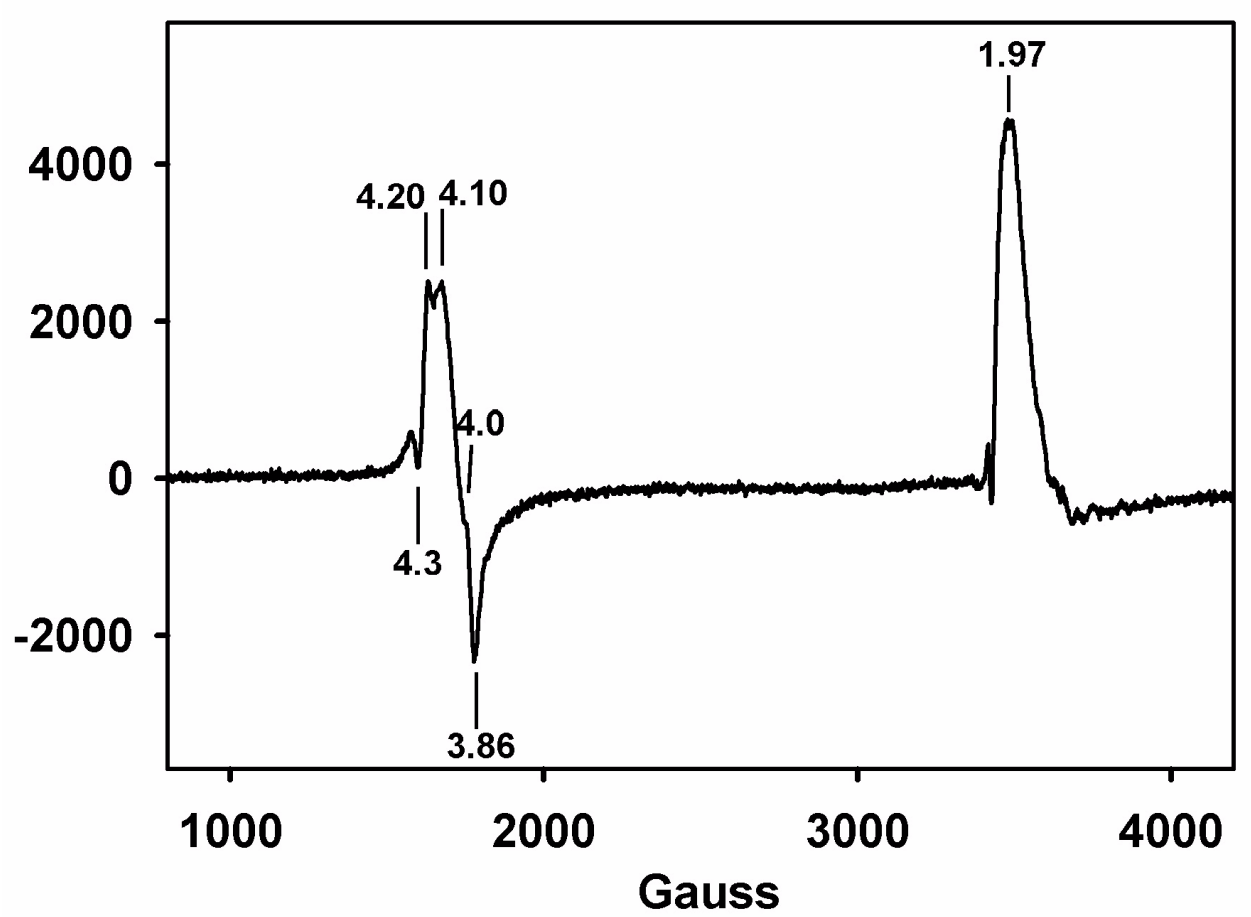

Figure 5.3. EPR spectrum of anaerobic NADH/Hrb-reduced FprA (200 μM) reacted with 0.8 mM NO (generated i*n situ* from DEA NONoate) in 50 mM MOPS pH 7.3 after 30 minutes of reaction at room temperature and freezing in liquid nitrogen. EPR conditions: temperature, 3.7 K; microwave power, 2 mW; microwave frequency, 9.60 GHz; modulation amplitude, 6.366 G. g-values are listed in the figure.

The same reaction with DEA NONoate was carried out on an ^{57}Fe-enriched FprA sample and analyzed by Mössbauer spectroscopy (cf. Figure 5.4). As expected, most of the iron (~72%)

in this sample was reoxidized to the antiferromagnetically coupled diferric state. This result constitutes the first *direct* evidence that NO can reoxidize the diferrous FprA active site. Approximately 20% of the iron was found in the form of $S = 3/2$ $\{FeNO\}^7$ centers, consistent with the EPR experiment in Figure 5.3. A minor portion (8%) of the iron was found in a diamagnetic $[\{FeNO\}^7]_2$ state, resulting from antiferromagnetic coupling between two $S = 3/2$ $\{FeNO\}^7$ centers. The latter adduct is reminiscent of those characterized for methane monooxygenase and ribonucleotide reductase (cf. Chapter 1);[15,16] in those cases, decay of such diamagnetic NO species was accompanied by N_2O formation. The diamagnetic FprA $[\{FeNO\}^7]_2$ species may, thus, be an intermediate en route to N_2O formation catalyzed by FprA. The fact that uncoupled ferrous or ferric absorptions did not accompany the $S = 3/2$ $\{FeNO\}^7$ absorption is consistent only with di-$\{FeNO\}^7$ sites in which the two $S = 3/2$ centers are not magnetically coupled.

In contrast to the NONOate experiments of Figures 5.3 and 5.4, EPR spectra of reduced FprA anaerobically mixed with NO-saturated water at room temperature and then frozen did not reveal any EPR-active species other than the flavin semiquinone present in almost all FprA preparations (spectra not shown). On the other hand, EPR monitoring of reactions of reduced FprA with NO in a cryosolvent at -40 °C (cf. Figures 5.5-5.7), in the pH range 6.2-8.8, *did* show the $S = 3/2$ $\{FeNO\}^7$ signal. This pH range was used because the FprA/Hrb couple is active as an NOR between pH 6 and 7, but is essentially inactive at pH 8.8. No other EPR-detectable species were apparent, except for the $g \sim 1.97$ "matrix" NO signal and a free radical signal with a peak-to-trough distance of 14 G, consistent with a deprotonated FMN semiquinone, similar to those seen in other (non-NO reacted) FprA samples.[20] The $g \sim 4.0$ signal remained unchanged upon annealing to -40 °C and refreezing, but disappeared after annealing the sample to room

temperature. This disappearance was not compensated by any new features in the spectrum, such as a g ~ 4.3 signal characteristic of a mononuclear high-spin ferric center. Furthermore, the EPR spectra of as-isolated FprA, as well as of a control sample, that was NADH/Hrb-reduced, cooled to -40 °C and then air-oxidized at room temperature in the absence of NO did not contain any significant features characteristic of a mononuclear ferric site. These results suggest that the diiron site is not irreversibly damaged by any of the steps involved in the cryoreduction/reoxidation experiment (i.e., reduction, cryosolvent addition, NO addition, reoxidation, annealing, warming). The g ~ 4.0 signal is thus likely to arise from an *intact diiron site*. Quantitation of the g ~ 4.0 signal reveals that, at its maximum, the g ~ 4.0 species is present at ~27 μM (7% of the FprA diiron sites, assuming that the $S = 3/2$ $\{FeNO\}^7$ adducts occur in pairs rather than one per FprA site) at pH 6.2, 29 μM (7.5%) at pH 7, and 33 μM (9%) at pH 8.8. The g ~ 4.0 signal is most likely due to a magnetically non-coupled diiron site where the two $S = 3/2$ $\{FeNO\}^7$ centers act as isolated paramagnets. This explanation is consistent with the Mössbauer spectrum in Figure 5.4. A less likely possibility is that the g ~ 4.0 species represents a novel type of diiron-NO adduct, such as with a bridging NO ligand. The g = 1.94 signal is due to non-metal-bound, "matrix" NO; its shape is not consistent with the mixed-valent EPR signal shown in Figure 5.2.

The shape of the g ~ 4.0 signal is essentially the same at pH 6.2 and pH 7, a pH range where FprA is active as NOR, but is slightly different at pH 8.8 where FprA is inactive. These differences can be seen in the superpositioned spectra in Figure 5.8. The differences between the pH 8.8 and lower-pH spectra are evident in the relative ratios of intensities at g = 4.20 vs. g = 4.09, as well as at g = 3.93 vs. g = 3.86. These differences may be ascribed to two different Fe-

NO adducts/conformations in the sample. These shapes are also different from that of the g ~ 4.0 signal generated with NONOate (Figure 5.3).

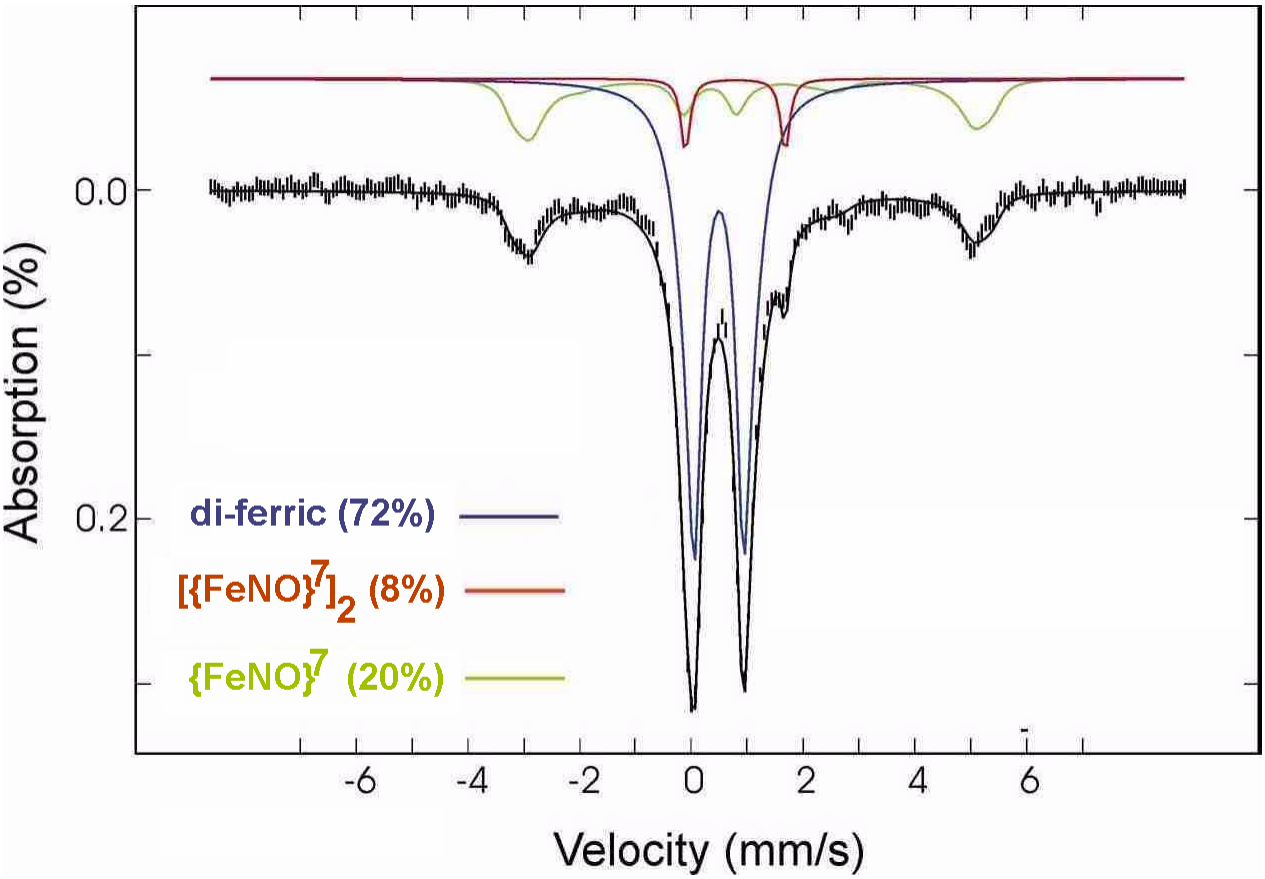

Figure 5.4. Mössbauer spectrum (hash marks) of ^{57}Fe-enriched NADH/Hrb-reduced FprA (1mM) after anaerobically reacting with NO (4 mM, generated *in situ* from DEA NONoate) in 50 mM MOPS pH 7 at room temperature for 45 minutes. The black solid line overlaying the experimental spectrum is the weighted sum of the three spectral components indicated in color. The spectrum was recorded at 4.2 K in a magnetic field of 50 mT oriented parallel to the γ-ray beam. The parameters for the dinitrosyl species are $\delta = 0.79$ mm/s and $\Delta EQ = 1.78$ mm/s.

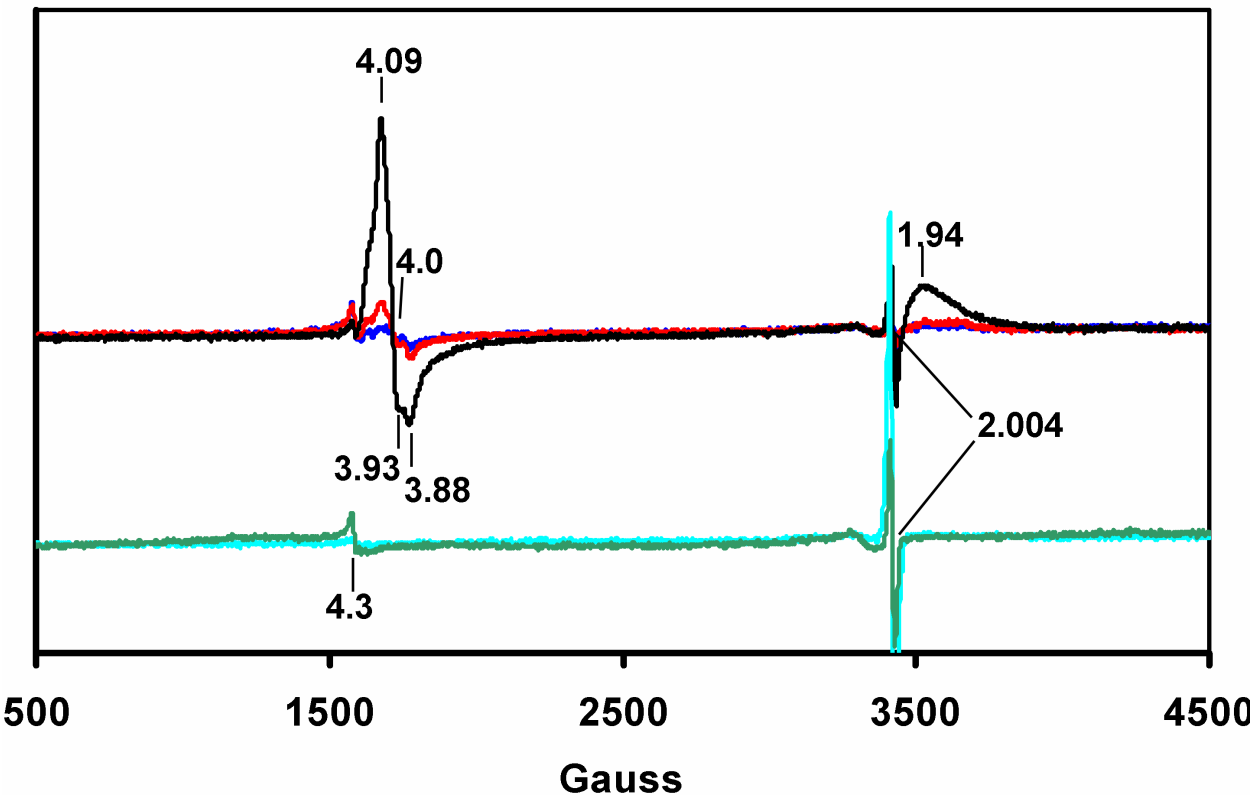

Figure 5.5. EPR spectra following mixing of NADH/Hrb-reduced FprA (200 µM FprA, 1 µM Hrb) with NO (1 mM) from an ethanol stock at -40 °C in 1:1 (v/v) aqueous 50 mM MOPS pH 7.0: ethylene glycol (5 % vol. ethanol after mixing). Black trace, immediately after mixing (this spectrum was not affected by subsequent incubation at -40 °C for up to 15 minutes); red trace, after thawing the sample anaerobically at room temperature and then immediately freezing in liquid nitrogen; blue trace: after equilibrating the sample at room temperature aerobically (i.e., septum was removed, sample was pipetted up and down several times with a Pasteur pipette, and after 5 minutes was re-frozen in liquid nitrogen). Offset for clarity are shown "control" spectra of the anaerobic reduced sample before adding NO (cyan trace), and of oxidized FprA in the same cryosolvent (green trace; prepared under aerobic conditions). EPR conditions: temperature, 4.0 K; microwave power, 2 mW; microwave frequency, 9.60 GHz; modulation amplitude, 6.366 G. g-values are listed in the figure.

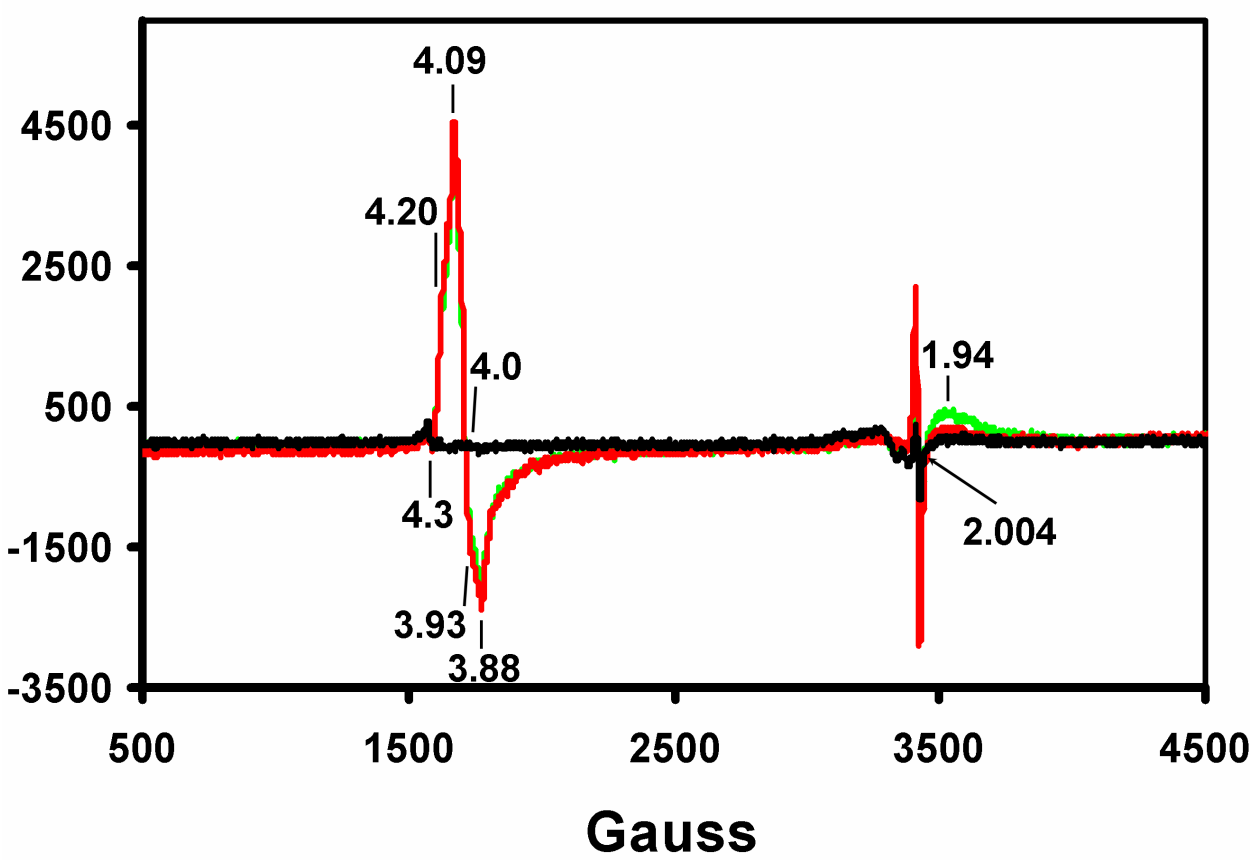

Figure 5.6. EPR spectra following mixing of NADH/Hrb-reduced FprA (200 µM FprA, 1 µM Hrb) with NO (1 mM) from an ethanol stock at -40 °C in 1:1 (v/v) aqueous at sodium phosphate pH 6.2: ethylene glycol (5 % vol. ethanol after mixing). Red trace: immediately after mixing; green trace: after incubation at -40 °C for 5 minutes and re-freezing in liquid nitrogen. Black trace: after equilibrating aerobically at room temperature, as described in the Figure 5.5 legend. EPR conditions: temperature, 4.0 K; microwave power, 2 mW; microwave frequency, 9.60 GHz; modulation amplitude, 6.366 G. g-values are listed in the figure.

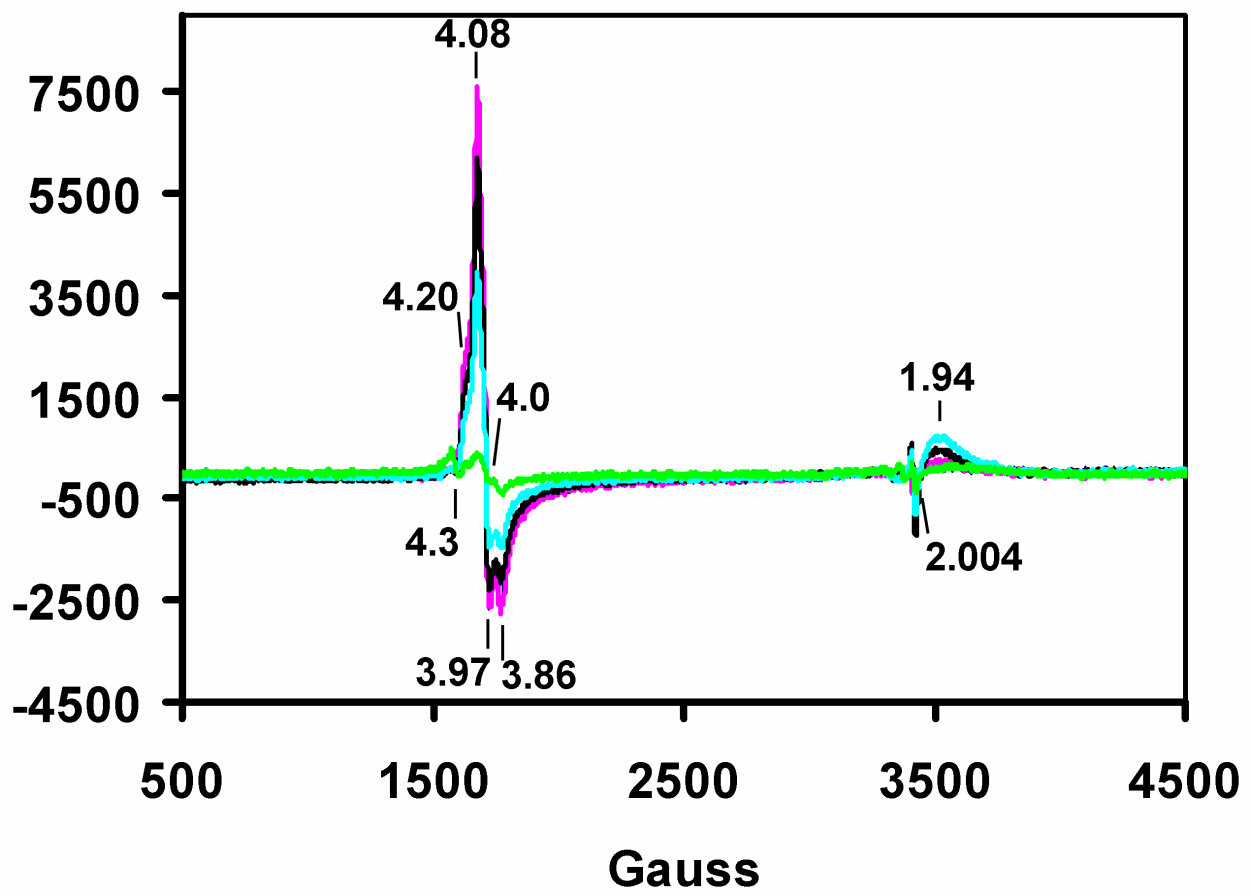

Figure 5.7. EPR spectra following mixing of NADH/Hrb-reduced FprA (200 µM FprA, 1 µM Hrb) with NO (1 mM) from an ethanol stock at -40 °C in 1:1 (v/v) aqueous 50 mM TAPS pH 8.8 : ethylene glycol (5 % vol. ethanol after mixing). Cyan trace, immediately after mixing; black trace, after incubating at -40°C for 5 minutes; pink trace, after incubating at -40 °C for 40 more minutes (spectra recorded after incubating for 15 or 30 minutes showed intensities intermediate between those of pink and black traces); green trace, spectrum after thawing the sample aerobically at room temperature as described in Figure 5.5 legend. EPR conditions: temperature, 4.0 K; microwave power, 2 mW; microwave frequency, 9.60 GHz; modulation amplitude, 6.366 G. g-values are listed in the figure.

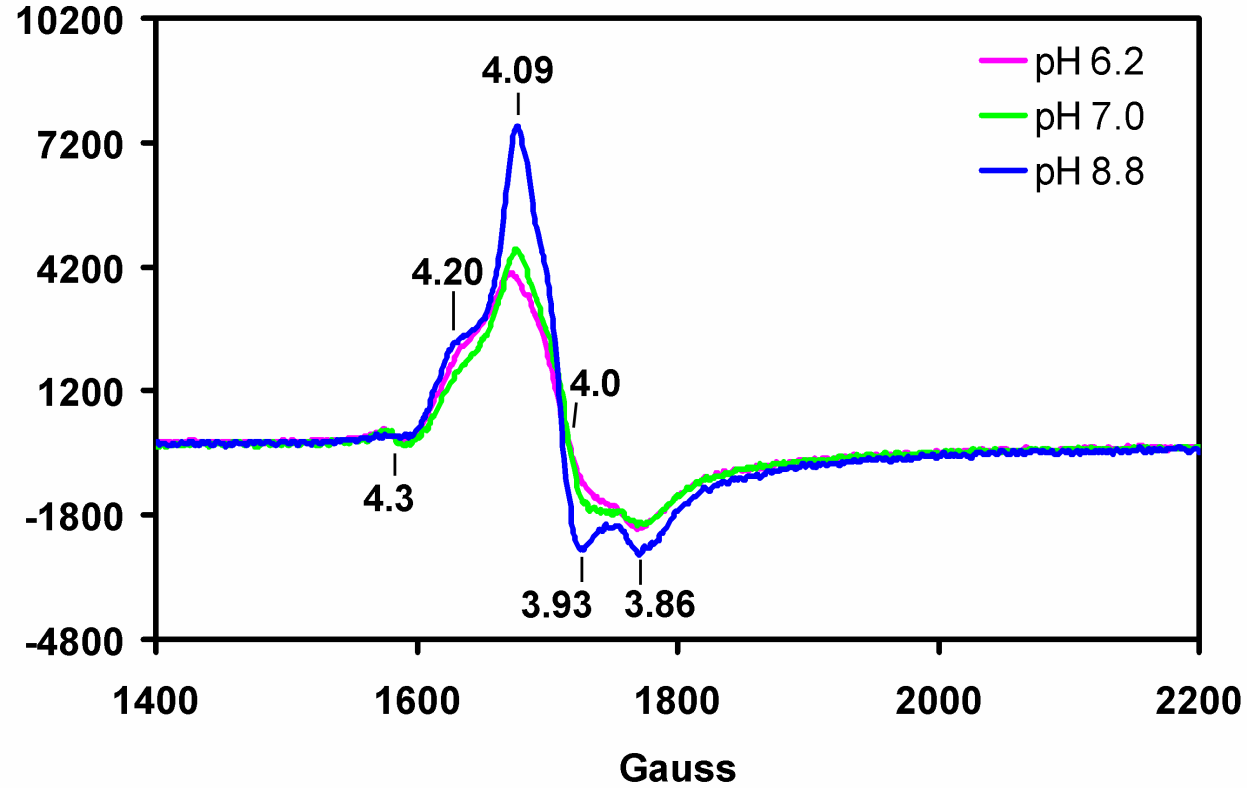

Figure 5.8. Horizontally expanded g ~ 4.0 regions of the EPR spectra collected immediately after mixing reduced FprA with NO in 1:1 (v/v) aqueous buffer:ethylene glycol at –40 °C at three different pHs (reproduced from Figures 5.5-5.7). g-values are listed in the figure.

The crystal structure of the *D. gigas* FprA homologue, named ROO,[21] revealed the presence of a tyrosine and a histidine in close proximity to the active site but not ligated to iron (cf. Figure 5.9). These two residues appeared to hydrogen-bond to an ill-defined electron density above the diiron site, which was proposed to be a dioxygen molecule. The equivalent residues in *M. thermoacetica* FprA are Y195 and H25. Figures 5.10 and 5.11 show EPR spectra collected at 4K after mixing reduced H25F or Y195F FprA variants with NO under the same cryogenic conditions as used for wild-type FprA in Figure 5.5 (pH 7.0, -40 °C). The variant FprAs gave somewhat higher yields of the g ~ 4.0 signal compared to the wild-type (9% of total diiron sites for H25F, 24% in Y195F, compared to 7.5% in wild-type FprA). As shown in Figure 5.12, the shape of the g ~ 4.0 signal is affected by the substitution of Y195 and H25 by phenylalanine, as

expected if the nitrosyl adduct indeed forms at the diiron site. These differences can be seen in the relative ratios of intensities at g = 4.20 vs. g = 4.09, as well as at g = 3.93 vs. g = 3.86. Also, the Y195F FprA variant develops a feature at g = 3.67 which is absent from the corresponding spectra of the wild-type and from the H25F FprA variant spectrum. The fact that the g ~ 4.0 EPR signal in Figures 5.10 and 5.11 disappears (albeit more slowly than with wild-type) upon warming to room temperature without concomitant development of a g ~ 4.3 signal suggests that the NO adducts in these variants are not due to diiron sites that have lost one iron. These data thus confirm that the "mononuclear" EPR signal seen with FprA is due to the diiron site. Consistent with the differences seen in the g ~ 4.0 EPR signal, the H25F and Y195F variants were significantly less active as NORs compared to wild-type *M. thermoacetica* FprA (cf. Chapter 6).

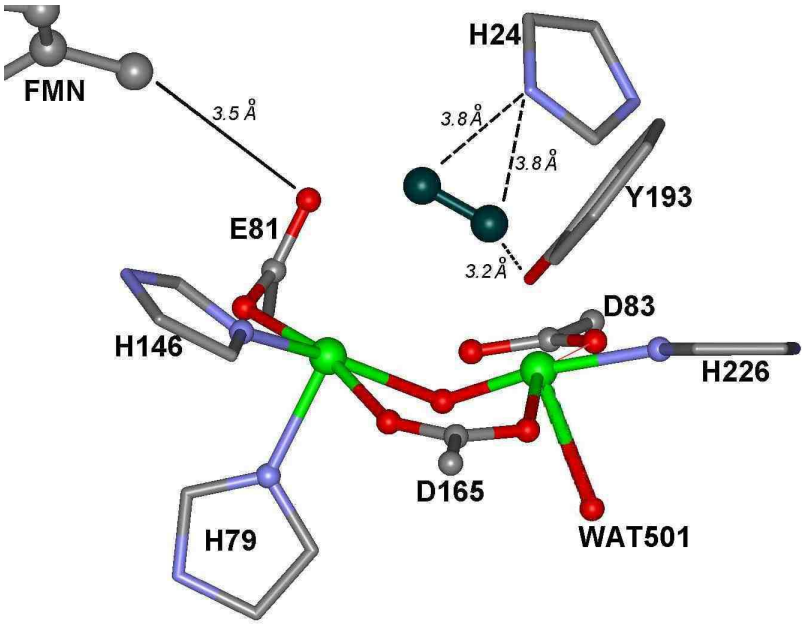

Figure 5.9. View of the *D. gigas* ROO diiron site, showing proximal residues, H24 and Y193. Drawn from coordinates in PDB ID 1E5D.

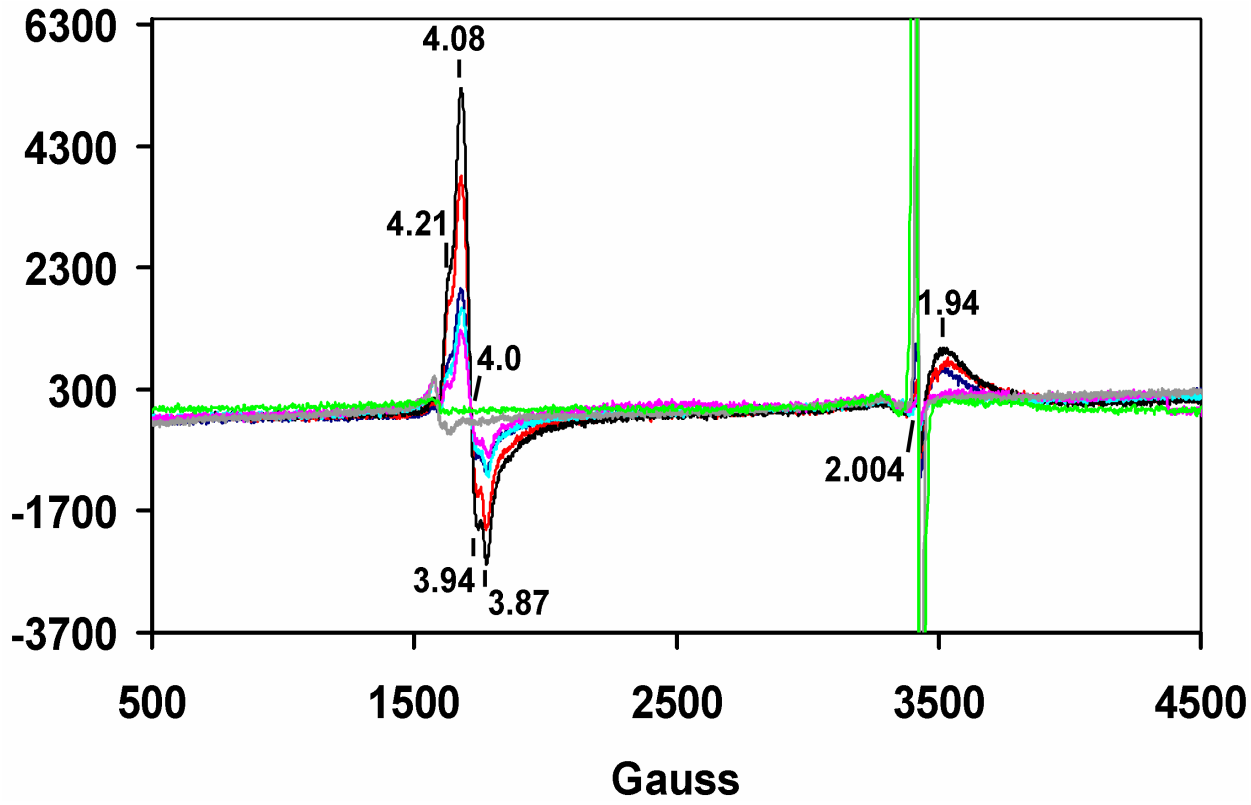

Figure 5.10. EPR spectra following mixing of NADH/Hrb-reduced H25F-FprA (200 µM FprA, 1 µM Hrb) with NO (1 mM) from an ethanol stock at -40 °C in 1:1 (v/v) aqueous at 50 mM MOPS pH 7.0:ethylene glycol (5 % vol. ethanol after mixing). Dark blue trace, immediately after mixing; red trace, after incubation at -40 °C for 5 minutes; black trace, after incubation at -40°C for 15 minutes; cyan trace, after thawing anaerobically at room temperature and immediately refreezing; pink trace, after equilibrating anaerobically at room temperature; gray trace, after equilibrating aerobically at room temperature for 5 minutes. Green trace shows "control" spectrum of reduced H25F-FprA, before adding NO. EPR conditions: temperature, 4.0 K; microwave power, 2 mW; microwave frequency, 9.60 GHz; modulation amplitude, 6.366 G. g-values are listed in the figure.

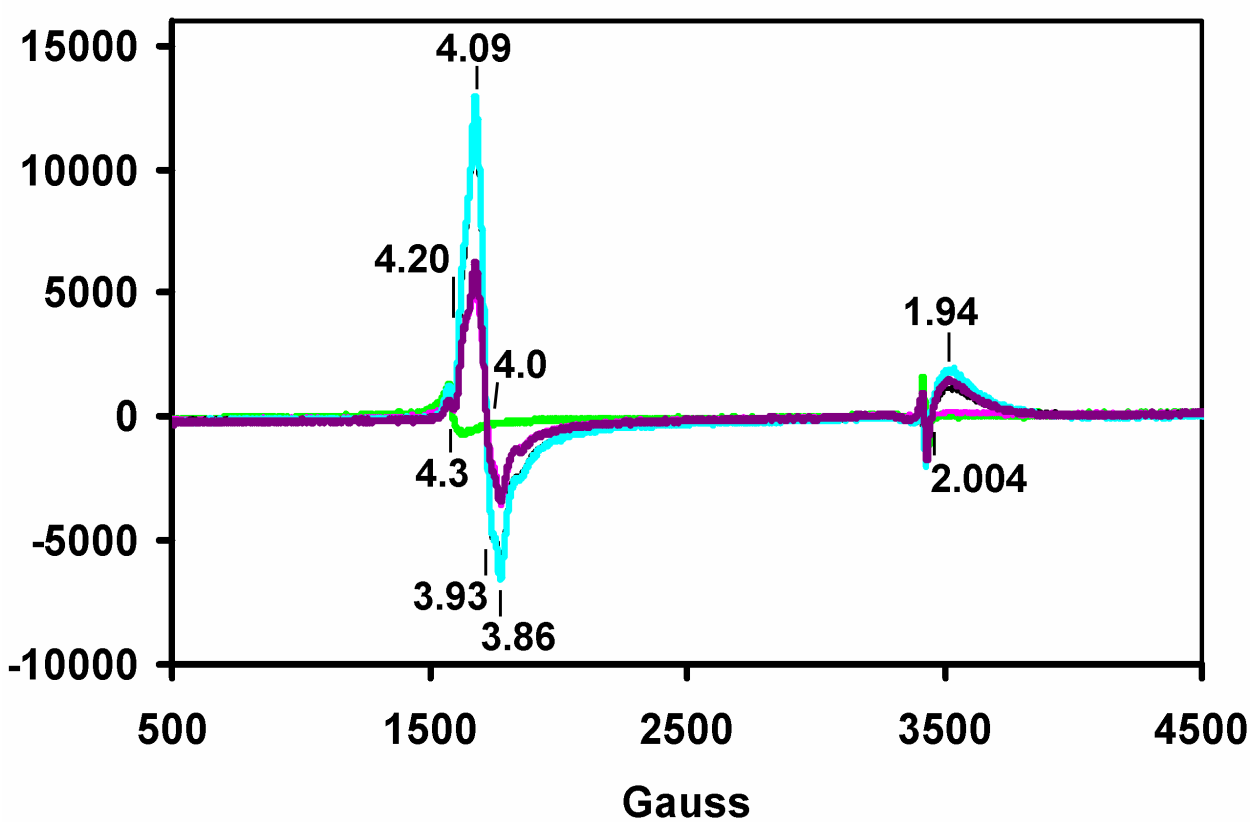

Figure 5.11. EPR spectra following mixing of NADH/Hrb-reduced Y195F-FprA (200 µM FprA, 1 µM Hrb) with NO (1 mM) from an ethanol stock at -40 °C in 1:1 (v/v) aqueous at 50 mM MOPS pH 7.0:ethylene glycol (5 % vol. ethanol after mixing). Pink trace, immediately after mixing; cyan trace, after annealing at -40 °C for 5 minutes; black trace (superimposed on cyan in the g = 4.0 region), after annealing at -40 °C for 15 minutes; dark pink trace, after thawing the sample anaerobically at room temperature and immediately refreezing; green trace, after equilibrating the sample aerobically at room temperature. EPR conditions: temperature, 4.0 K; microwave power, 2 mW; microwave frequency, 9.60 GHz; modulation amplitude, 6.366 G. g-values are listed in the figure.

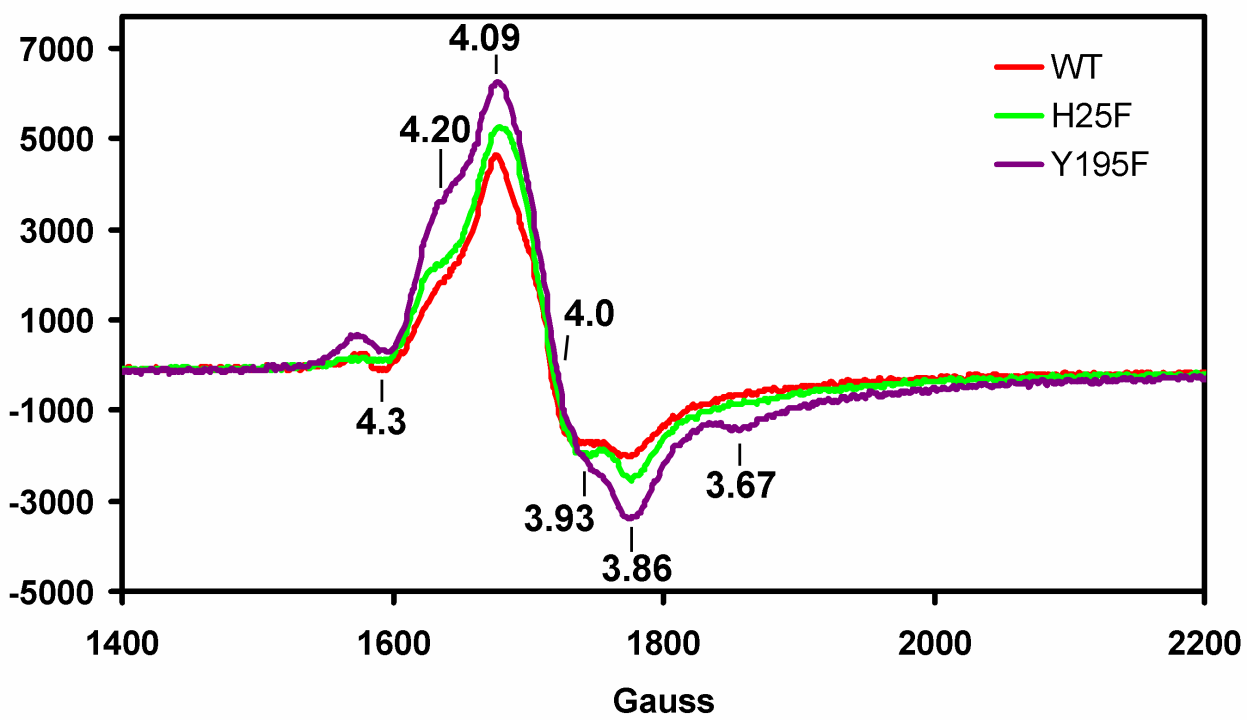

Figure 5.12. Horizontally expanded g ~ 4.0 regions of the EPR spectra of wild-type (WT), H25F and Y195F FprA, collected immediately after mixing the reduced FprA with NO, at –40 °C. Spectra are reproduced from Figures 5.5, 5.10, and 5.11, respectively. g-values are listed in the figure.

Figure 5.13 illustrates the Mössbauer spectrum of an experiment paralleling the EPR experiment shown in Figure 5.5. The top trace illustrates the spectrum of anaerobic NADH/Hrb-reduced FprA in a 1:1 (v/v) mixture of ethylene glycol and aqueous pH 7 buffer. This sample contained the same two forms of the diferrous site, A (66%) and B (25%) as shown in Figure 5.1, with small amounts of diferric (2%) and mixed-valent (4%) sites. The A and B forms are, thus, not affected by the presence or absence of ethylene glycol. The Figure 5.13 (top) sample was then thawed to -50 °C anaerobically in a septum-sealed 15-mL container, and NO was added from an ethanolic stock via a gas-tight syringe, to a final concentration of 4 mM. Within 20 seconds after the NO addition, the sample was frozen in liquid nitrogen. The Mössbauer spectrum of this sample (middle trace in Figure 5.13) is almost identical to that of the reduced untreated sample, i.e., it still contained approximately the same percentages of A and B diferrous

sites. This NO-treated sample was, therefore, thawed to -40 °C in a septum-sealed 15-mL container, and allowed to remain at this temperature for 15 minutes while the headspace was exchanged with pure NO gas via a stainless steel needle inserted through the septum. After ~10 minutes at -40 °C, gaseous NO was gently bubbled through the sample for approximately one minute, and the sample was re-frozen in liquid nitrogen. The Mössbauer spectrum of this "extensively NO-reacted" sample (bottom trace in Figure 5.13) illustrates that NO has reacted and/or oxidized the majority of the diferrous sites. Thus, the proportion of components A and B decreased from 66% and 25%, respectively, in the reduced sample, to 11% and 15%, respectively, in the extensively NO-reacted sample. Corresponding to the amount of ferrous A that has disappeared upon reoxidation (66% $\rightarrow$ 11%), 10% of the iron in the extensively NO-reacted sample is now in the diferric state and 50% is in the S = 1/2 mixed-valent (semi-met) form. On the other hand, corresponding to the amount of ferrous B that has disappeared upon reoxidation (25% $\rightarrow$ 15%), 11% of the sample is now in a S = 3/2 $\{FeNO\}^7$ state similar to that illustrated in Figure 5.4. The connection between ferrous B and S = 3/2 $\{FeNO\}^7$ is reinforced by the fact that both states contain non-coupled iron, as opposed to the ferrous A and diferric states which contain antiferromagnetically coupled iron. Thus, due to its lower percentage decrease, it appears that the B ferrous form is significantly more slowly reacting with NO than is the A form. Besides being slower, reoxidation of the B diferrous sites also appears to lead to the S = 3/2 $\{FeNO\}^7$ state, which in other diiron proteins has been identified to be unproductive towards N_2O formation.[15-17,22] However, the EPR experiments in Figures 5.5-5.7 indicate that the S = 3/2 $\{FeNO\}^7$ adduct of reduced FprA is *not* due to a mononuclear (damaged) form of the diiron site, in contrast to conclusions reached from Mössbauer and EPR spectra of NO-reacted diferrous methane monooxygenase and ribonucleotide reductase.[15-17,22]

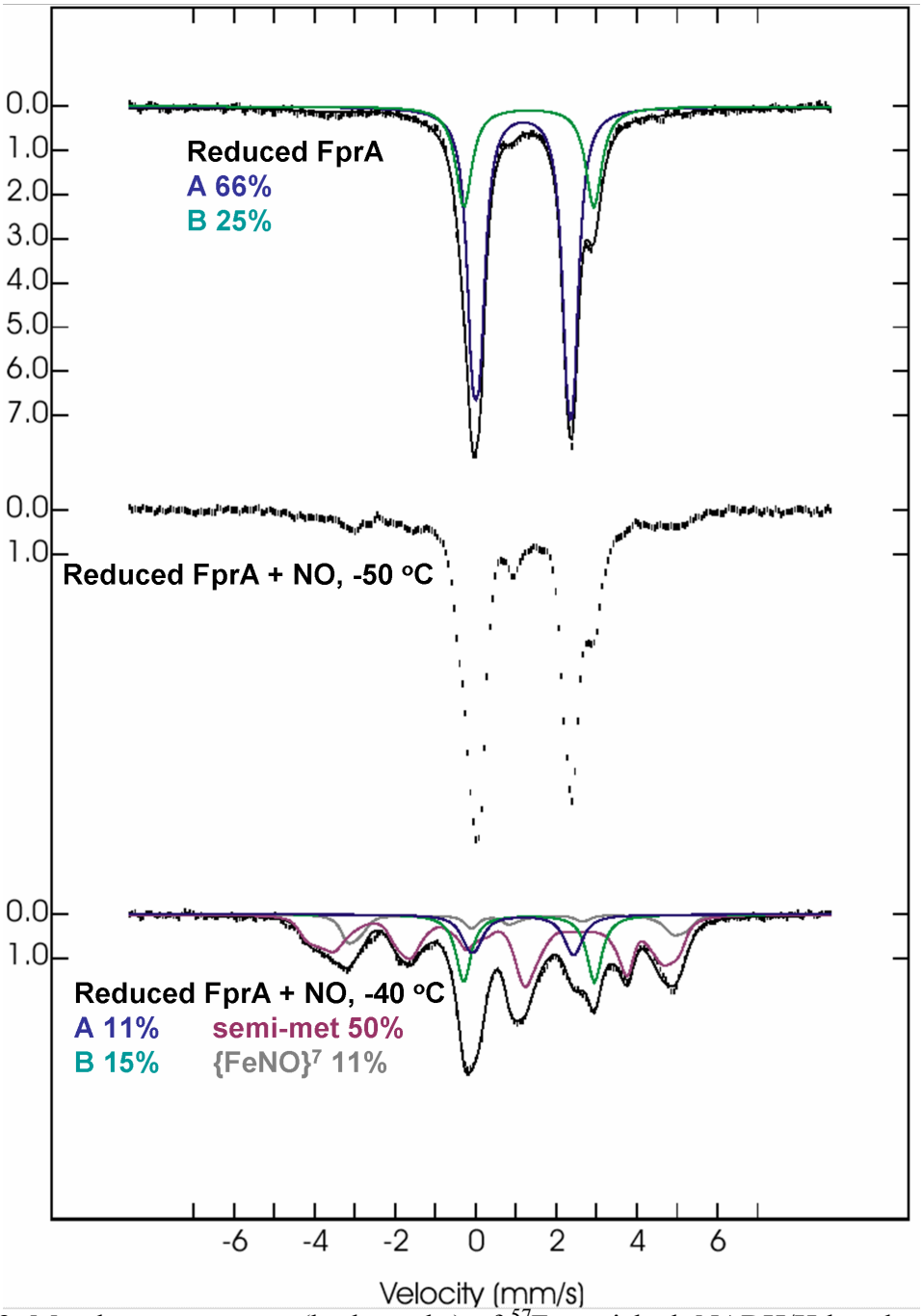

Figure 5.13. Mössbauer spectrum (hash marks) of ^{57}Fe-enriched, NADH/Hrb-reduced FprA (1 mM FprA, 10 μM Hrb) after anaerobically reacting with NO from an ethanolic stock at -50 °C or -40 °C in a 1:1 (v/v) mixture of ethylene glycol:50 mM MOPS pH 7 (20% ethanol after mixing). Black solid lines overlaying the experimental spectra are weighted sums of the three spectral components indicated in colors. The spectra were recorded at 4.2 K in a magnetic field of 50 mT oriented parallel to the γ-ray beam. Top spectrum: reduced FprA. Middle spectrum: reduced FprA, reacted with stoichiometric NO at -50 °C, cf. text. Bottom spectrum: Same sample, exposed to excess gaseous NO at -40 °C for 15 minutes.

Stopped-flow UV-vis absorption spectroscopy. Figure 5.14 shows the absorption spectral time course following anaerobic stopped-flow mixing of reduced FprA with excess NO. A uniform increase in absorbance across the 300-750 nm range is seen in the collected UV-vis absorption spectra, consistent with oxidation of the reduced FprA FMN. Most of this absorbance increase occurred within the mixing dead time (1-2 msec), whereas under the same conditions as in Figure 5.14 Zn-substituted FprA did not react with NO at all in the time-frame used for the stopped-flow experiment and the reduced FMN was instead oxidized by NO over the course of several minutes.

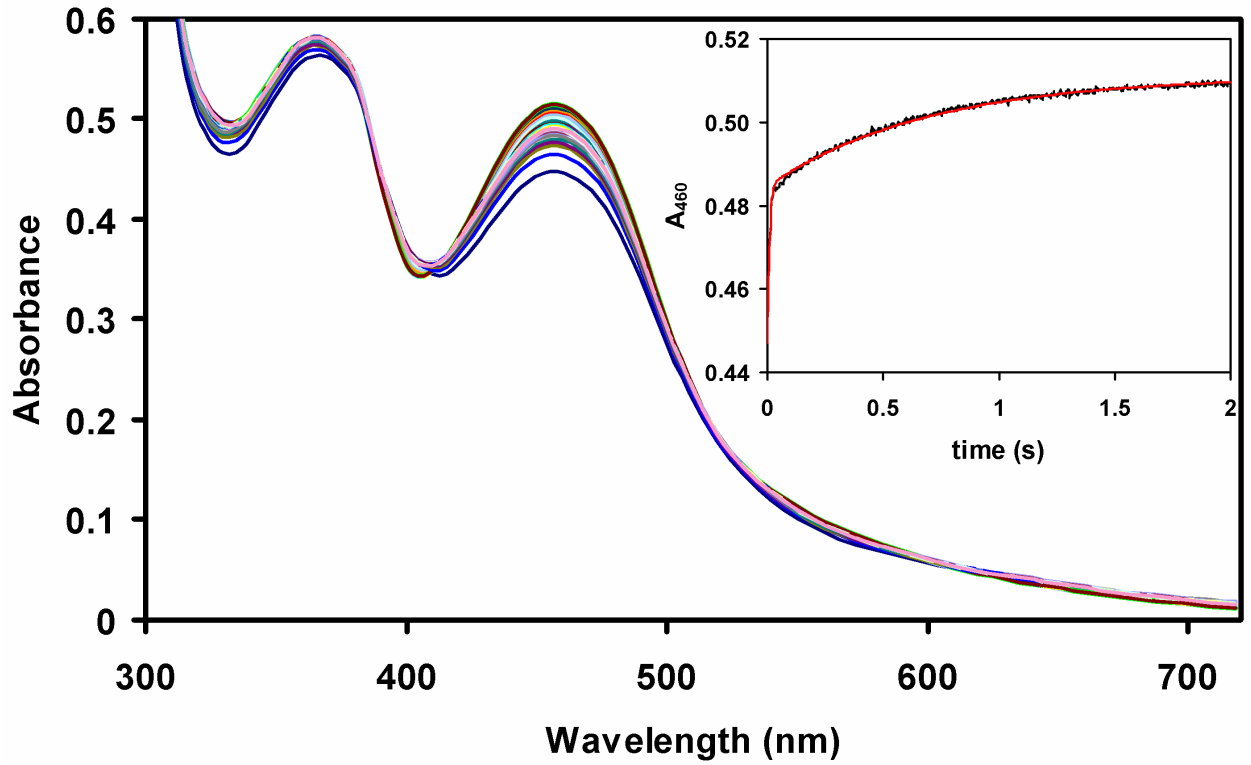

Figure 5.14. UV-vis absorption spectral time course following anaerobic stopped-flow mixing of dithionite-reduced *M. thermoacetica* FprA (43 μM) with NO (900 μM) in 50 mM MOPS pH 7.0 at room temperature. Spectra were collected every ~2.7 msec following mixing. Inset shows the absorbance time-course at 460 nm (black trace) and a kinetic fit (red trace) assuming an A → B → C reaction sequence with k_1 = 130 s^{-1} and k_2 = 1.4 s^{-1}.

The absorbance time course in Figure 5.14 is interpreted as due to an A → B → C reaction sequence in which the majority of component A is consumed within the stopped-flow mixing dead time (1-2 ms). Calculated A, B and C component spectra from global fits of absorption spectral time course are shown in Figure 5.15. Although the calculated component spectrum C reproduces very well that of the fully-oxidized FprA, the exact shapes of the calculated component A and B spectra are strongly dependent on the initial fractions assumed for A, B, and C in the first spectrum recorded after mixing. Considering that all the experimental spectra collected following stopped-flow mixing are almost identical to that of the as-isolated (oxidized) FprA, speculations on the exact shape and composition of the A and B component spectra may not be meaningful. The calculated spectrum of component A contains features at ~650, 480 and 350 nm, which are consistent with flavin and/or iron-nitric oxide species. A synthetic diferrous-dinitrosyl compound ($[\{FeNO\}^7]_2$) (UV-vis absorption spectrum shown in Figure 5.16, Panel A) was reported to feature absorption maxima at 620 nm (broad, $\varepsilon \sim 600\ M^{-1}cm^{-1}$), 520 nm ($\varepsilon \sim 400\ M^{-1}cm^{-1}$), and 330 nm ($\varepsilon \sim 28000\ M^{-1}cm^{-1}$, presumably with contributions from alkoxide and benzimidazole → Fe(III) ligand-to-metal charge transfer).[23] For comparison, oxidized FMN features $\varepsilon \sim 12000\ M^{-1}cm^{-1}$ at 460 and 380 nm. FMN neutral (protonated) semiquinones absorb at ~ 600 nm ($\varepsilon \sim 2000\ M^{-1}cm^{-1}$); typical UV-vis absorption spectra of anionic and neutral semiquinones are illustrated for comparison in Figure 5.16, Panel B.[20] FprA was previously reported to form an anionic, (not neutral) semiquinone, which did not feature absorption maxima above 600 nm.[1]

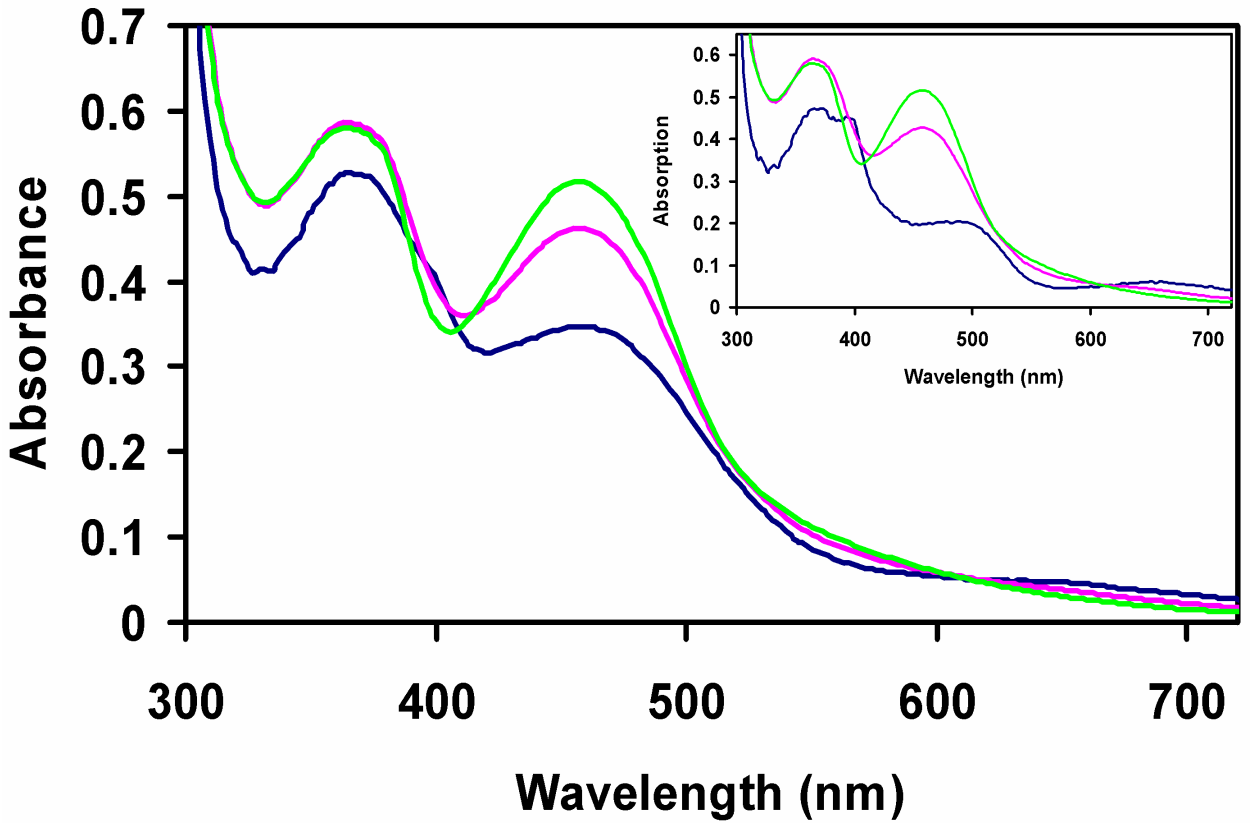

Figure 5.15. Calculated A (blue trace), B (pink trace) and C (green trace) component spectra, assuming different fractions for A (0.4 in main panel, 0.2 in inset), B (0.1 in main panel, 0.1 in inset) and C (0.5 in main panel, 0.7 in inset) in the first spectrum recorded after mixing in Figure 5.14.

A

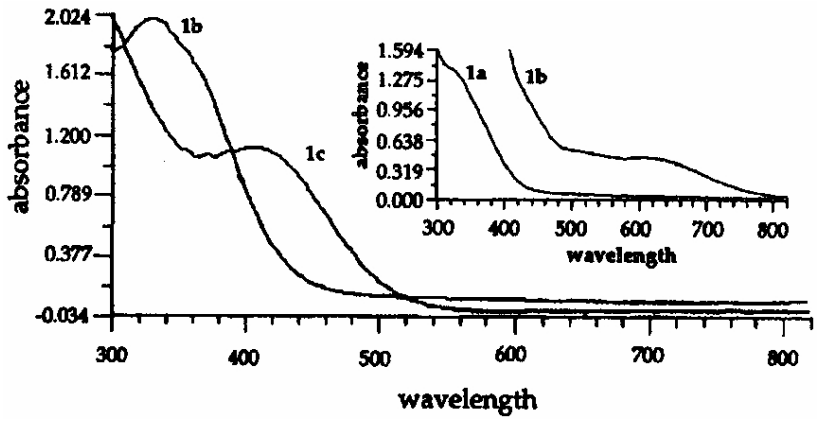

B

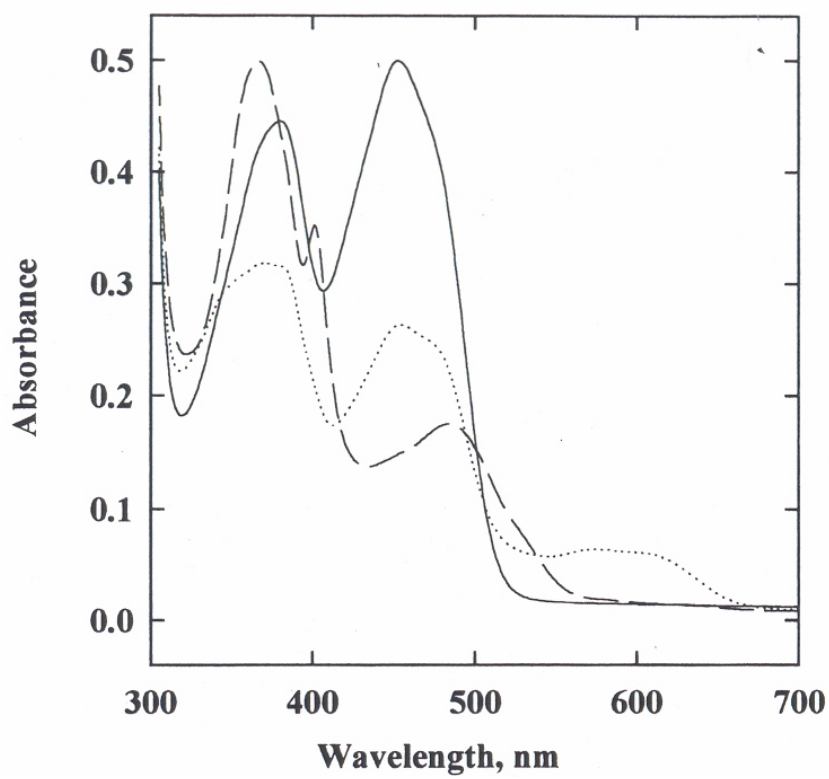

Figure 5.16. Panel A: UV-vis absorption spectrum of a synthetic diferrous-dinitrosyl $[\{FeNO\}^7]_2$ complex in acetonitrile (trace annotated 1b). Spectra are reproduced from Ref. 23 Panel B: UV-vis absorption spectra of oxidized (solid trace), neutral (dotted trace) and anionic (dashed trace) semiquinone froms of the flavoprotein, glucose oxidase. Spectra are reproduced from Ref. 20.

Perhaps as expected from the low-micromolar K_m for the FprA-NO interaction (2-5 μM) determined from steady-state turnover (cf. Chapter 2), results essentially identical to those in Figure 5.14 were obtained using NO concentrations in the range 25-900 μM.

Paralleling the stopped-flow experiment in Figure 5.14, the reaction of reduced FprA with NO was monitored in a cryo-solvent, 3:2 (v/v) ethylene glycol:100 mM sodium phosphate pH 6.1, at -60 °C (cf. Figure 5.16). As expected, reoxidation was dramatically slowed down compared to room temperature, taking minutes, rather than milliseconds. Qualitatively similar results were obtained in cryo-solvents with other aqueous components (cacodylate pH 6.2, MOPS pH 7) and 1:1 ethylene glycol: aqueous buffer, at -40 °C. A monotonous reoxidation of the flavin is apparent in the increasing absorbance at ~460 nm. On the other hand, the absorbance at ~ 350 nm appears to transiently increase and then decrease in the range where a diferrous-dinitrosyl adduct would be expected to absorb.[23] These absorption changes in the 350-nm region are not seen in the UV-vis stopped-flow experiment but are consistent with the detection of iron-nitrosyl adducts in the EPR cryogenic experiments shown in Figures 5.5-5.7 and 5.13. Alternatively, the absorption changes at ~350 nm may be assigned to an anionic FMN semiquinone (cf. Figure 5.16), which is also consistent with the data in Figures 5.5-5.7. No ~650 nm absorption, as implied from fits to the stopped-flow spectra (Figure 5.15) is evident from the spectra of Figure 5.17.

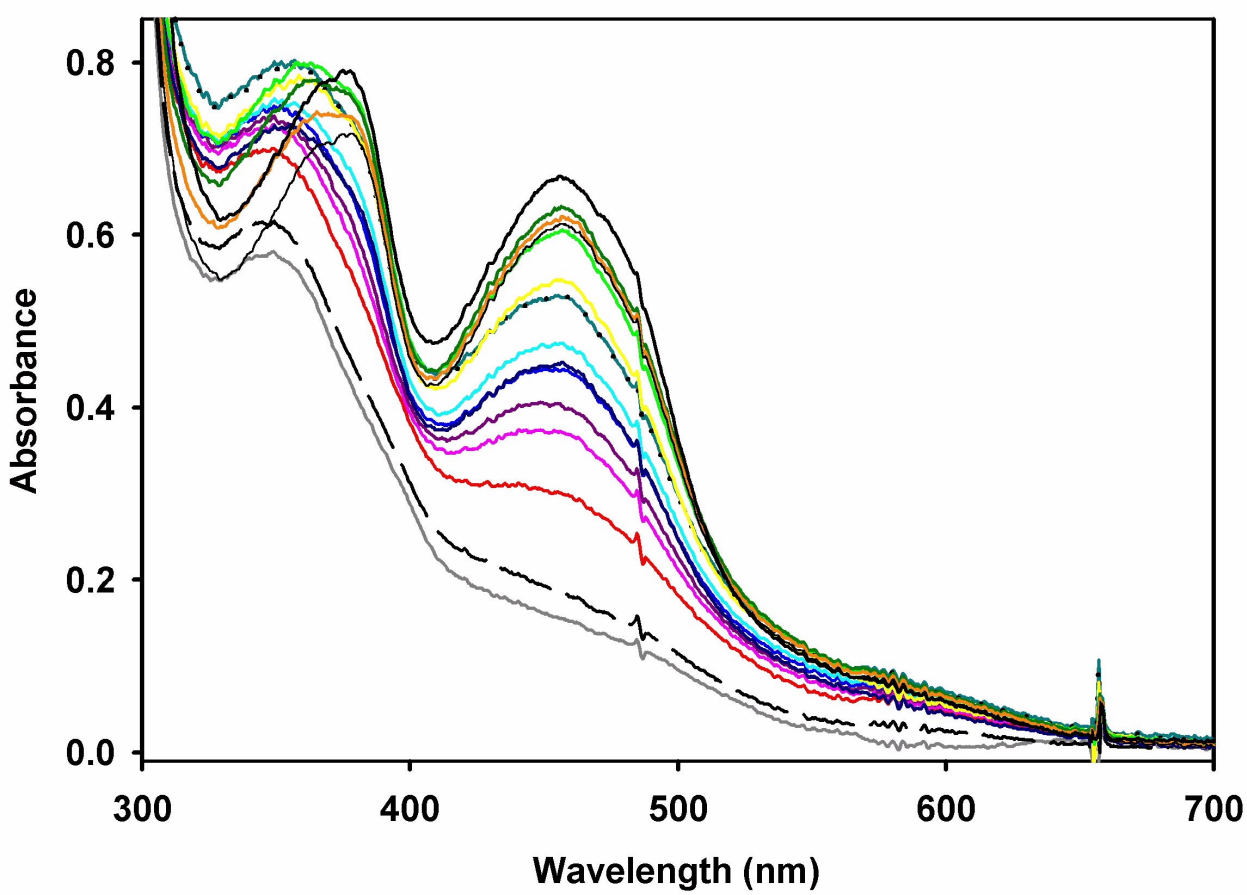

Figure 5.17. Optical absorption spectral time course following anaerobic mixing of NADH/Hrb-reduced FprA with NO at -60 °C. Gray trace: spectrum after adding the anaerobically-reduced FprA (from a 150-μM stock solution in aqueous 25 mM MOPS pH 7.3) into the Dewar cuvette containing 3:2 (v/v) ethylene glycol:100 mM sodium phosphate pH 6.1 at room temperature to give an FprA concentration of 15 μM and cooling to -50 °C. Dashed black trace: after cooling to -60 °C. Red trace: same solution as dashed black trace, immediately after adding 150 μM NO at -60 °C (NO added from a 12 mM anaerobic ethanolic stock; ethanol concentration after mixing: ~2 vol. %). Pink trace: 2 minutes after red trace at -60 °C. Dark pink: 4 minutes after red trace at -60 °C. Blue trace: 6 minutes after red trace, and 150 μM more NO added at -60 °C (ethanol concentration after mixing: 4 vol. %). Cyan trace: 4 minutes after blue trace at -60 °C. Dark blue trace: 11 minutes after blue trace at -60 °C. Dotted black trace: 16 minutes after blue trace at -60 °C. Yellow trace: 33 minutes after blue trace, and warmed to -50 °C. Light green trace: 40 minutes after blue trace, at -45 °C. Dark green trace: 60 minutes after blue trace, -30 °C. Orange trace: 80 minutes, -25 °C. Thin black trace: 90 minutes, -17 °C. Solid black trace: air-exposed, +15 °C.

RFQ Mössbauer and EPR spectroscopy. EPR spectra collected after RFQ mixing of reduced FprA with stoichiometric amounts of NO at room temperature are shown in Figure 5.18.

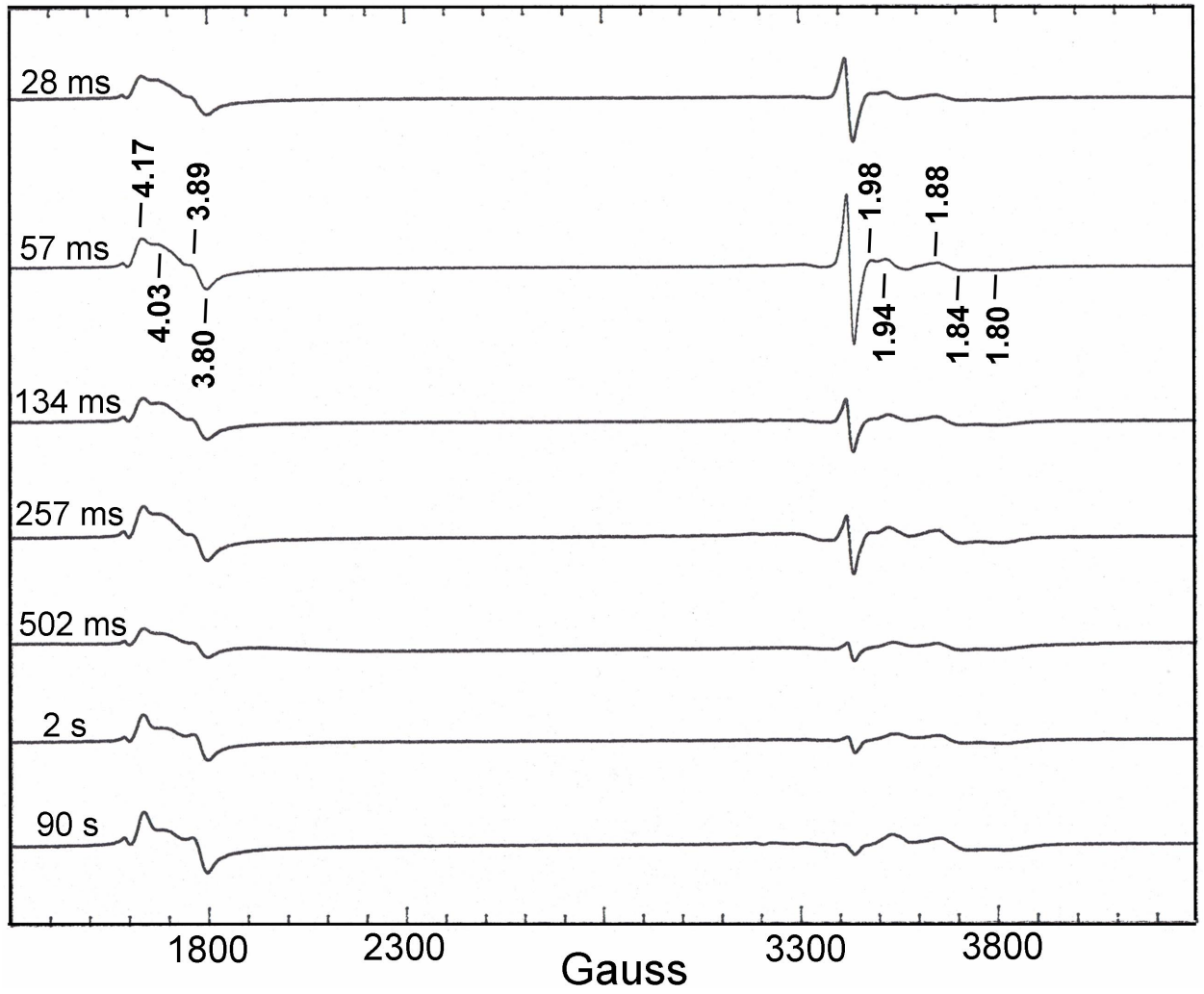

Figure 5.18. EPR spectra obtained after RFQ mixing of dithionite-reduced *M. thermoacetica* FprA (0.5 mM diiron sites) with NO (2 mM) in 50 mM MOPS pH 7 (ethanol concentration after mixing: 18 vol. %) at room temperature. EPR conditions: temperature - 12 K, microwave power - 2mW, microwave frequency - 9.60 GHz. g-values are listed above and below the 57-ms trace.

The EPR signal at ~1700 G (g ~ 4.0) is reminiscent of the S = 3/2 $\{FeNO\}^7$ EPR signal previously recorded in room-temperature and cryogenic reactions of reduced FprA manually mixed with NO (Figures 5.3-5.7); the shape of the S = 3/2 signal in Figure 5.18 is distorted from those in Figures 5.3-5.7, which may be due to recording of the RFQ EPR spectra at 12 K vs. 4 K for the spectra in Figures 5.3-5.7. In the cryogenic EPR experiments, the g ~ 4.0 signal decayed over the course of several minutes. Consistent with this long life-time, and incompatible with

turnover number of 50 s^{-1} measured for FprA NOR activity (for which any catalytically competent species should have disappeared within ~20 ms after mixing),[1] the RFQ-EPR spectra show a lifetime of the $S = 3/2$ signal at room temperature of ≥ 90 s. The presence of the mixed-valent diiron signal centered at ~3600 G in similar amounts at all time points suggests that this form is also not catalytically competent. The sharp free radical signal at g~2 can be identified as the anionic FMN semiquinone of FprA, by virtue of its peak-to-through distance of 14 G (identical to that previously measured in several non-RFQ FprA EPR samples). Based on the relative intensities of the very sharp semiquinone and relatively broader iron-based EPR signals, it can be concluded that the semiquinone is present in very low concentrations.

Analogous RFQ Mössbauer spectra recorded for the 28 ms, 57 ms, 2 s and 90 s RFQ time points are shown in Figure 5.19 and Figure 5.20 shows the time courses of the relative concentrations of the species determined to be present in these samples. In addition to the EPR-active species illustrated in Figure 5.18, the RFQ Mössbauer spectra reveal the presence a diferrous-dinitrosyl adduct, similar to that previously detected in the NONOate manual mixing experiment of Figure 5.4. This adduct accounts for ~40% of the RFQ sample at 28 ms, and its concentration decreases with time – unlike the concentration of the $S = 3/2$ $\{FeNO\}^7$ "mononuclear" species. The decrease in diferrous-dinitrosyl concentration is paralleled by formation of diferric sites, suggesting a direct conversion of diferrous dinitrosyl to diferric. The presence of these NO adducts of FprA in the RFQ samples is at first perplexing, given the expectation based on the k_{cat} from NO turnover[1] that complete reoxidation of FprA by NO would occur within 20 ms, i.e., within the mixing dead-time of the RFQ instrument. On the other hand, the FprA-NO RFQ results parallel well those previously reported on the reaction of NO with diferrous methane monooxygenase or ribonucleotide reductase.[15-17,22] There, too, a relatively

stable $S = 3/2$ $\{FeNO\}^7$ "mononuclear" species was detected alongside a diferrous dinitrosyl species whose decay could be correlated with formation of diferric sites and production of N_2O.

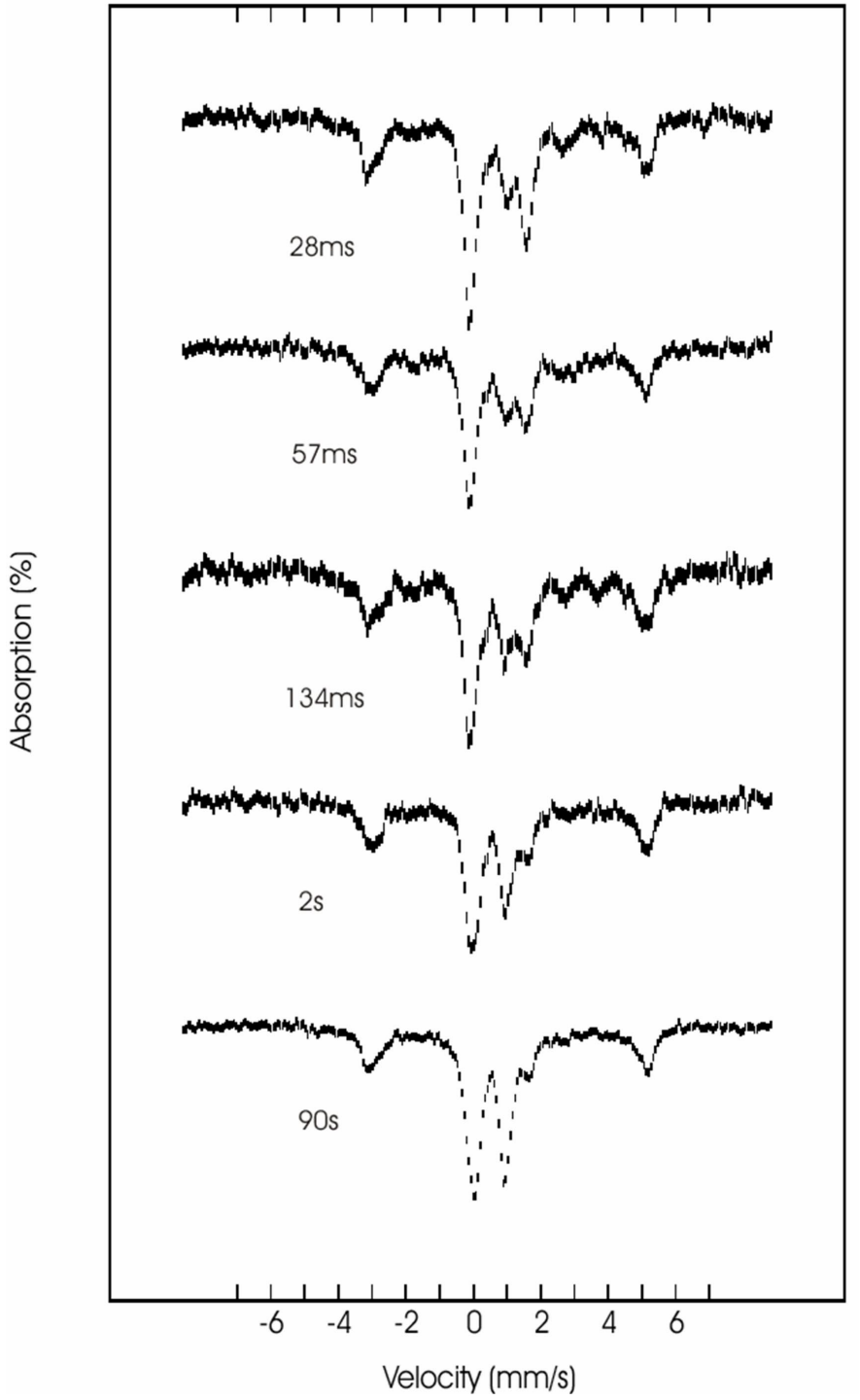

Figure 5.19. Mössbauer spectra obtained at various times after RFQ mixing of dithionite-reduced *M. thermoacetica* FprA (0.5 mM diiron sites) with NO (2 mM) in 50 mM MOPS pH 7

(ethanol concentration after mixing: 18 vol. %) at room temperature. The spectra were recorded at 4.2 K in a magnetic field of 50 mT oriented parallel to the γ-ray beam.

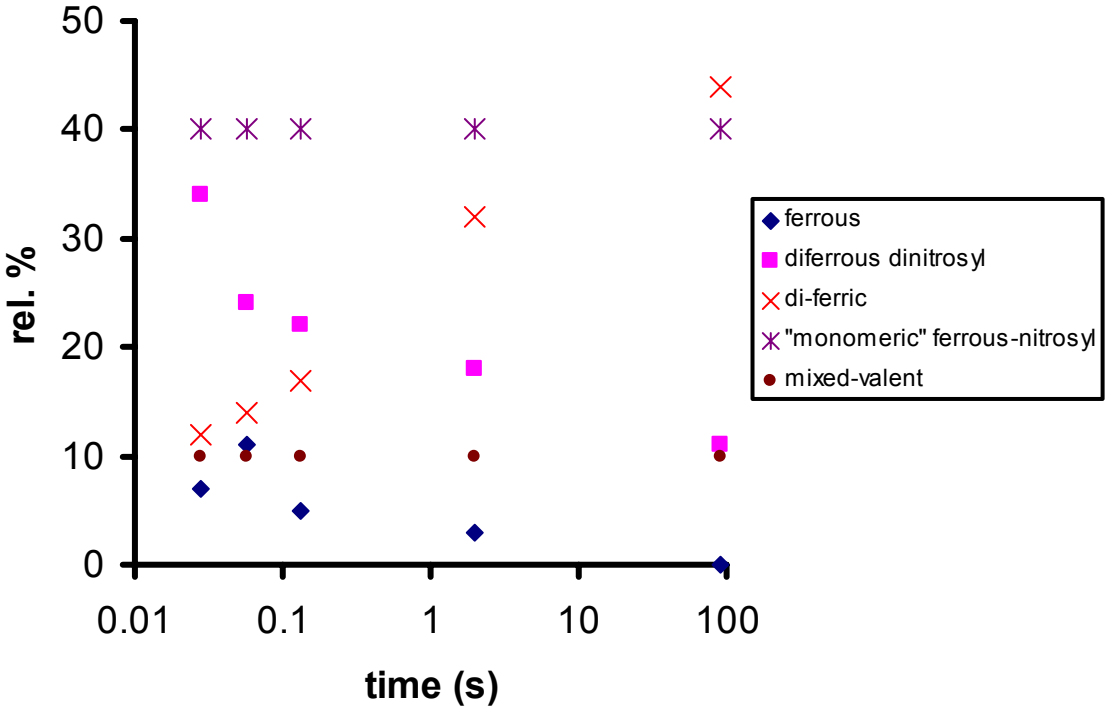

Figure 5.20. Time dependence of the calculated concentrations of species present in the RFQ Mössbauer spectra of Figure 5.19.

The RFQ observations can be rationalized by the reaction scheme shown in Figure 5.21. Formation of diferrous-dinitrosyl adducts and oxidation of the 4-electron reduced FprA to the 2-electron reduced FprA is proposed to be fast (>130 s^{-1}) and thus compatible with the measured k_{cat} of 50 s^{-1}.[1] Oxidation of the 2-electron reduced form to the fully oxidized form is on the other hand proposed to be relatively slow and to occur in single-turnover experiments, but not during catalytic turnover. The diferrous-dinitrosyl intermediates proposed in Figure 5.21 may be in the antiferromagnetically coupled $S = 0$ form and/or the non-coupled $S = 3/2$ $\{FeNO\}^7$ form. The FMN-oxidized $S = 0$ diferrous nitrosyl species appears more reactive than the FMN-oxidized $S =$

3/2 species; the former decays to diferric, whereas the latter remains unchanged during the course of the RFQ experiment (cf. Figures 5.18-5.20). On the other hand, reduction of both the *S* = 0 and *S* = 3/2 nitrosyl intermediates by the reduced FprA FMN is assumed to be efficient and compatible with turnover, accounting for the 130 s^{-1} phase seen in stopped-flow UV-vis absorption spectra (cf. Figures 5.14 and 5.15), where component A would contain a diferrous-dinitrosyl adduct and reduced FMN, and component B would contain a diferrous-dinitrosyl and oxidized FMN. The mechanism shown in Figure 5.21 is in agreement with the steady state NOR kinetics of *M. thermoacetica* FprA, summarized in Scheme 5.1, which requires binding of two NO molecules to the active site prior to product (N_2O) formation.

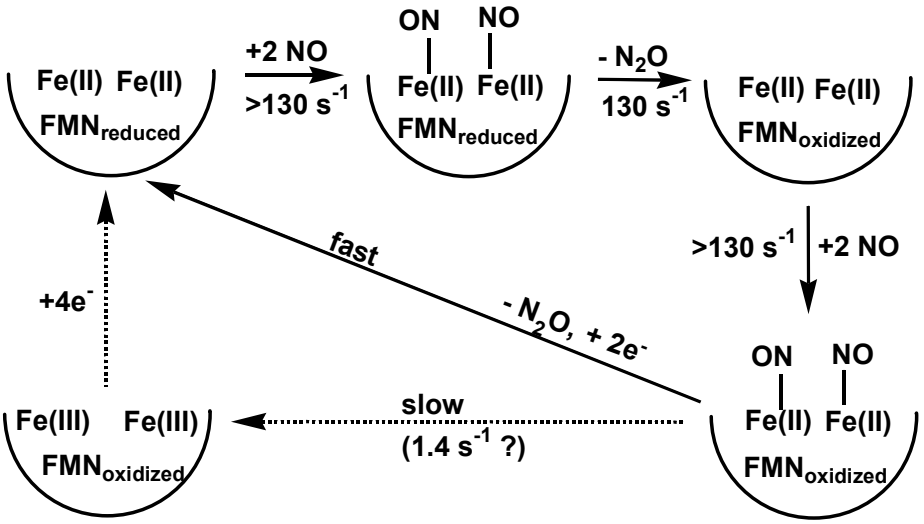

Figure 5.21. Proposed reaction scheme for catalytic turnover and single-turnover FprA-NO experiments. Steps shown with solid arrows are proposed to take place during both catalytic and single turnover, while those shown with dashed arrows are proposed to take place only in single-turnover experiments. Protons and proton donors are omitted for simplicity.

The much faster decay of the diferrous-dinitrosyl species in the presence of a reduced vs. oxidized FprA FMN is proposed to be due to the fact that N_2O release is triggered by reduction of the diferrous-dinitrosyl site by the reduced FMN. This reduction would transiently generate a "super-reduced" $[\{FeNO\}^8]_2$ or $[\{FeNO\}^7,\{FeNO\}^8]$ species, which is expected to be extremely

short-lived and, therefore, to not accumulate to detectable concentrations in stopped-flow or RFQ experiments. Such super-reduction may be facilitated by the fact that the iron in the $[\{FeNO\}^7]_2$ species should have a distinct Fe(III) character[23,24] thus mimicking the diferric site which the FprA FMN efficiently reduces. $\{FeNO\}^8$ species have also been invoked as intermediates in the catalytic reduction of nitric oxide by the hemoproteins, P450nor and cytochrome *c* nitrite reductase,[25-27] and non-heme $\{FeNO\}^8$ species are also known.[28] The absence of a proximal, low-potential electron donor to the diiron sites of ribonucleotide reductase and methane monooxygenase is consistent with the slow and sub-stoichiometric release of N_2O from their diferrous-dinitrosyl adducts.[15,16]

Decay of the FprA dinitrosyl species, regardless of its spin and oxidation state, is expected to occur via N-N bond formation to yield a hyponitrite, $N_2O_2^{2-}$, intermediate, following a paradigm set forth for the heme-containing NOR, P450nor.[25] Further decay of this hyponitrite intermediate to N_2O and H_2O is expected to be extremely fast under physiological conditions,[25,29] and may be catalyzed by proton-donating residues H25 and Y195 in the NO binding pocket above the diiron site of *M. thermoacetica* FprA, an issue which is further addressed in Chapter 6.

The above experiments provide the first reported detection of NO adducts that may participate in FprA's NOR activity. The key feature that allows FprA to perform efficient NO reduction compared to other non-heme diiron proteins is proposed to be the presence of a nearby flavin, which serves to "super-reduce" the $[\{FeNO\}^7]_2$ intermediate.

5.4. References

(1) Silaghi-Dumitrescu, R.; Coulter, E. D.; Das, A.; Ljungdahl, L. G.; Jameson, G. N.; Huynh, B. H.; Kurtz, D. M., Jr. *Biochemistry* **2003**, *42*, 2806-2815.

(2) Jean, D.; Briolat, V.; Reysset, G. *Microbiology* **2004**, *150*, 1649-1659.

(3) Gardner, A. M.; Helmick, R. A.; Gardner, P. R. *J. Biol. Chem.* **2002**, *277*, 8172-8177.
(4) daCosta, P.; Teixeira, M.; Saraiva, L. *FEMS Microbiology Lett.* **2003**, *218*, 385-393.
(5) Hutchings, M. I.; Mandhana, N.; Spiro, S. *J. Bacteriol.* **2002**, *184*, 4640-4643.
(6) Sarti, P.; Fiori, P. L.; Forte, E.; Rappelli, P.; Teixeira, M.; Mastronicola, M.; Sanciu, G.; Giuffre, A.; Brunori, M. *Cell. Mol. Life Sci.* **2004**, *61*, 618-623.
(7) Gomes, C. M.; Giuffre, A.; Forte, E.; Vicente, J. B.; Saraiva, L. M.; Brunori, M.; Teixeira, M. *J. Biol. Chem.* **2002**, *277*, 25273-25276.
(8) Eidsness, M. K.; Burden, A. E.; Richie, K. A.; Kurtz, D. M., Jr.; Scott, R. A.; Smith, E. T.; Ichiye, T.; Beard, B.; Min, T.; Kang, C. *Biochemistry* **1999**, *38*, 14803-14809.
(9) Douzou, P. *Cryobiochemistry*; Academic Press: London, 1977.
(10) Armarego, W. L.; Perrin, D. D. *Purification of Laboratory Chemicals*, Butterworth Heinemann, Oxford, 1998.
(11) Baldwin, J.; Krebs, C.; Ley, B. A.; Edmondson, D. E.; Huynh, B. H.; Bollinger Jr., J. M. *J. Am. Chem. Soc.* **2000**, *122*, 12195-12206.
(12) Krebs, C.; Chen, S.; Baldwin, J.; Ley, B. A.; Patel, U.; Edmondson, D. E.; Huynh, B. H.; Bollinger Jr., J. M. *J. Am. Chem. Soc.* **2000**, *122*, 12207-12219.
(13) Ravi, N.; Bollinger Jr., J. M.; Huynh, B. H.; Edmondson, D. E.; Stubbe, J. *J. Am. Chem. Soc.* **1994**, *116*, 8007-8014.
(14) Smoukov, S. K.; Davydov, R. M.; Doan, P. E.; Sturgeon, B.; Kung, I. Y.; Hoffman, B. M.; Kurtz, D. M., Jr. *Biochemistry* **2003**, *42*, 6201-6208.
(15) Coufal, D. E.; Tavares, P.; Pereira, A. S.; Huynh, B. H.; Lippard, S. J. *Biochemistry* **1999**, *38*, 4504-4513.
(16) Haskin, C. J.; Ravi, N.; Lynch, J. B.; Munck, R.; Que, L., Jr. *Biochemistry* **1995**, *34*, 11090-11098.
(17) LeBrun, N. E.; Andrews, S. C.; Moore, G. R.; Thomson, A. J. *Biochem. J.* **1997**, *326*, 173-179.
(18) Nocek, J. M.; Kurtz, D. M., Jr.; Sage, J. T.; Xia, Y. M.; Debrunner, P.; Shiemke, A. K.; Sanders-Loehr, J.; Loehr, T. M. *Biochemistry* **1988**, *27*, 1014-1024.
(19) Rodriguez, J. H.; Xia, Y. M.; Debrunner, P. G. *J. Am. Chem.Soc.* **1999**, *121*, 7846-7863.
(20) Chapman, S. K.; Reid, G. A. *Methods in Molecular Biology*, Vol. 131-Flavoprotein protocols, Humana Press, Totowa, NJ, 1999.

(21) Frazão, C.; Silva, G.; Gomes, C. M.; Matias, P.; Coelho, R.; Sieker, L.; Macedo, S.; Liu, M. Y.; Oliveira, S.; Teixeira, M.; Xavier, A. V.; Rodrigues-Pousada, C.; Carrondo, M. A.; Le Gall, J. *Nat. Struct. Biol.* **2000**, *7*, 1041-1045.

(22) Wallar, B. J.; Lipscomb, J. D. *Chem. Rev.* **1996**, *96*, 2625-2657.

(23) Feig, A. L.; Bautista, M. T.; Lippard, S. J. *Inorg. Chem.* **1996**, *35*, 6892-6898.

(24) Brown, C. A.; Pavlovski, M. A.; Westre, T. E.; Zhang, Y.; Hedman, B.; Hodgson, K. O.; Solomon, E. I. *J. Am. Chem. Soc.* **1995**, *117*, 715-732.

(25) Silaghi-Dumitrescu, R. *Eur. J. Inorg. Chem.* **2003**, 1048-1052.

(26) Harris, D. L. *Int. J. Quantum Chem.* **2002**, *88*, 133-200.

(27) Einsle, O.; Messerschmidt, A.; Huber, R.; Kroneck, P. M. H.; Neese, F. *J. Am. Chem. Soc.* **2002**, *124*, 11737-11745.

(28) Garcia-Serres, R. G.; Grapperhaus, C. A.; Bothe, E.; Bill, E.; Weyhermuller, T.; Neese, F.; Wieghardt, K. *J. Am. Chem. Soc.* **2004**, *126*, 5138-5153.

(29) Trogler, W. C. *Coord. Chem. Rev.* **1999**, *187*, 303-327.

CHAPTER 6

CRYSTAL STRUCTURES OF *MOORELLA THERMOACETICA* FPRA. NOVEL DIIRON SITE STRUCTURE AND MECHANISTIC INSIGHTS INTO A NON-RESPIRATORY NITRIC OXIDE REDUCTASE

6.1. Introduction

Chapters 2 and 5 described the nitric oxide reductase (NOR) activity (reaction NOR) of the *Moorella thermoacetica* flavo-diiron protein, FprA.[1] These investigations led to the proposal of a mechanism for NOR catalysis involving a diferrous dinitrosyl adduct of the diiron site, as shown in Scheme 6.1. Evidence for diferrous dinitrosyl adducts and a role for the reduced FprA FMN in triggering the reductive decay of this intermediate has been proposed in Chapter 5.

$$\mathbf{NADH + H^+ + 2NO \rightarrow N_2O + H_2O + NAD^+} \qquad \mathbf{(NOR)}$$

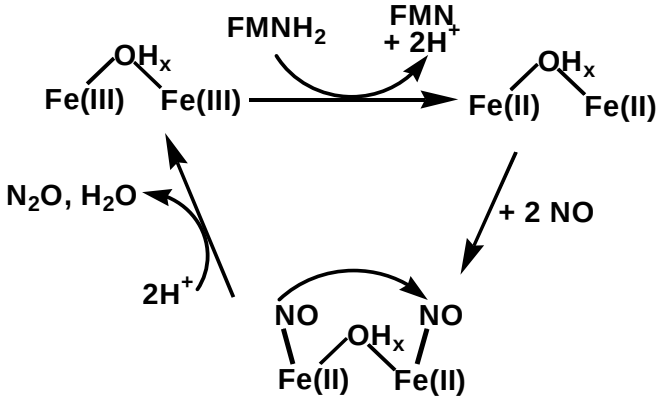

Scheme 6.1

This chapter describes the crystal structure of *M. thermoacetica* FprA. Comparison with the previously reported crystal structure of *D. gigas* ROO,[2] an FprA homolog which is proposed to be an O_2 reductase rather than NOR, reveals conserved features as well as significant differences between the diiron sites in the two proteins. Crystal structures are reported for the oxidized ("as-isolated"), reduced and reduced, NO-reacted *M. thermoacetica* FprA. The implications of the crystallographic results for the mechanism of NO reduction at the FprA active site and possible reasons for the apparently different catalytic activity of *D. gigas* ROO are discussed.

6.2. Materials and methods

Reagents and General Procedures. All solutions were prepared in deionized water. NADH, NADPH, PEG (Sigma Chemical Co.), DEA NONOate (diethylammonium (Z)-1-(N,N-diethylamino) diazen-1-ium-1,2-diolate, Cayman Chemicals, Inc.) were used without further purification. All protein concentrations are expressed in monomers. Histidine (His)-tagged and non-His-tagged recombinant *M. thermoacetica* FprA and recombinant *M. thermoacetica* Hrb (the NADH:FprA oxidoreductase) were obtained as previously described and used without further purification.[1] UV-vis absorption spectra of FprA crystals were recorded in melting point capillaries using a QDI1000 UV-vis-NIR microspectrophotometer (Craic Technologies, Inc.). NADH-dependent O_2-reductase (O_2 consumption) and NADH-dependent NOR (NO consumption) activities were monitored as previously described.[1]

FprA Crystallization. FprA solutions used for crystallization were invariably 1 mM in monomer in 25 mM MOPS pH 7.3. For non-His-tagged FprA preliminary screenings were performed using both sitting drop and batch methods with the following commercial reagent sets: Wizard I, Wizard II (Decode, Inc.), Crystal Screen 1, Crystal-Screen 2, Peg-Ion Screen, and MembFac

(Hampton Res.). The crystals eventually used for data collection were obtained from batch crystallization in melting-point capillaries at room temperature by layering 10 μL of the precipitant (200 mM zinc acetate, 50 mM sodium cacodylate pH 6.5, 5% isopropanol) with 10 μL of the oxidized (as-isolated) FprA solution. Diffraction quality crystals typically formed within 7 to 10 days. Typical crystals of as-isolated FprA and their UV-vis absorption spectrum are shown in Figure 6.1. This spectrum is similar to that recorded for the same FprA in solution prior to crystallization and is distinctly different from that of the Zn-substituted *M. thermoacetica* FprA. For iron-containing FprA, the absorbance in the range 300-380 nm is higher than that at 450 nm (A_{320}/A_{450} = 1.24, comparable to 1.29 for the crystalline FprA), whereas the opposite is true for the zinc-substituted FprA (A_{320}/A_{450} = 0.45). The spectrum of the FprA crystal indicates that, although present at 100 mM in the mother liquor, zinc has not displaced iron in the FprA active site. Similar crystals were obtained using a slightly different precipitant: 200 mM zinc acetate, 100 mM sodium acetate pH 4.5, and 10% PEG 3000. FprA crystals obtained as described above suffered visible damage when flash-frozen either by dipping into liquid nitrogen or by sudden exposure to a stream of nitrogen gas cooled to -185 °C. Ethylene glycol was, therefore, employed as cryoprotectant. To this end, crystals were progressively soaked for ~20 minutes in mother liquor (i.e., 1:1 (v/v) 25 mM MOPS pH 7.3:precipitant) containing ethylene glycol in 5% increments, up to 20%.

Using identical methodologies and reagents as described above, His-tagged FprA was found to crystallize using a different precipitant: 20 % PEG 3350 with either 200 mM sodium sulfate, lithium citrate, or sodium citrate. Even when cryoprotected by progressive soaking in ethylene glycol as described above for the wild-type protein, His-tagged FprA crystals did not diffract to any higher resolution than non-His-tagged FprA crystals; the unit cell adopted the

same space group as non-His-tagged FprA crystals. Therefore, His-tagged FprA crystals were not further investigated.

Anaerobic solutions of reduced FprA for crystallization screening were generated inside an anaerobic chamber (Coy Laporatory Products, Inc.) with an atmosphere containing 85% N_2, 10% CO_2, 5% H_2 and routinely <1 ppm O_2. The FprA was reduced in solution using 5 mM NADH and 10 μM Hrb. Hrb and excess NADH were not removed after reduction in an attempt to limit oxidation of FprA by trace amounts of dioxygen that might be present inside the anaerobic chamber. Anaerobic screening for crystallization of NADH/Hrb-reduced FprA was performed by the batch method in capillaries using identical procedures and commercial reagent sets (with the exception of MembFac) as described above for as-isolated FprA, but in an Echoterm incubator (Torrey Pines Scientific) at 7 °C inside the anaerobic Coy chamber. The best crystals were obtained using the following precipitant: 100 mM sodium citrate pH 5.6, 200 mM sodium/potassium tartrate, 2 M ammonium sulfate. These crystals diffracted to slightly lower resolution than did those of the as-isolated FprA, while displaying the same large unit cell. Therefore, the crystals that were used to solve the reduced FprA structure were prepared by reduction of the as-isolated FprA crystals. This reduction was readily achieved at room temperature inside the Coy chamber without any apparent damage to the crystals by adding a few crystals of sodium dithionite to ethylene glycol-treated, as-isolated FprA crystals that were sitting in a well of a 9-well glass plate containing 200 μL of mother liquor (containing the pH 6.5 precipitant and 20% vol. ethylene glycol). Upon treatment with dithionite, the FprA crystals changed within a few minutes from orange-brown to colorless.

For reaction with NO, the dithionite-reduced crystals in the Coy chamber were soaked for 20 minutes in anaerobic dithionite-free mother liquor (containing the pH 6.5 precipitant and 20%

vol. ethylene glycol) and then treated with a few grains of the NO-releasing agent, DEA-NONoate at room temperature. This treatment resulted in rapid reoxidation of the crystalline FprA, manifested as a change in color from clear to orange-brown. These reduced and reduced, NO-treated FprA crystals, maintained under the anaerobic mother liquor on a tape-covered glass plate, were removed from the Coy chamber, mounted on loops and flash-frozen by dipping in liquid nitrogen. The time elapsed from opening the Coy chamber to flash-freezing the crystals was less then one minute, and the crystals were at all times covered in mother liquor containing either excess sodium dithionite or NO (from the DEA NONOate). When mounted on the diffractometer for data collection, the dithionite-reduced crystals prepared as described above were still colorless.

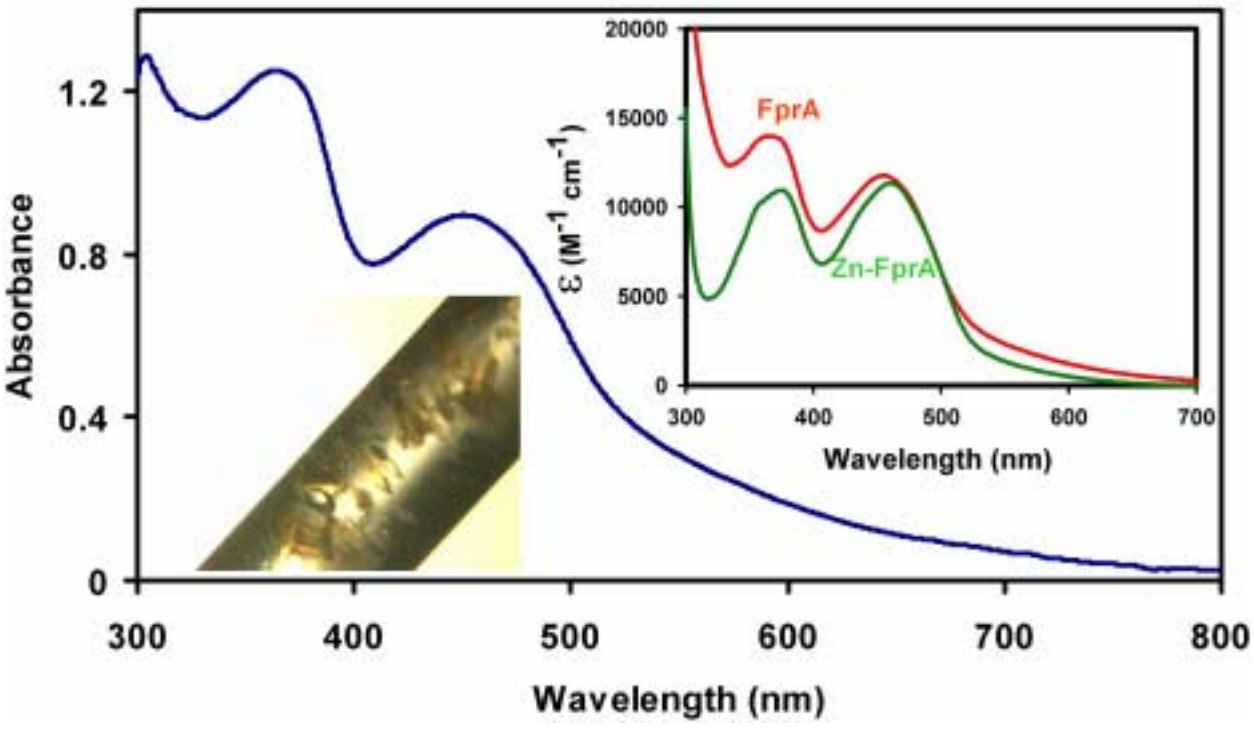

Figure 6.1. UV-vis absorption spectrum of as-isolated *M. thermoacetica* FprA crystals recorded in mother liquor (containing pH 6.5 precipitant). Lower left inset: photograph of as-isolated *M. thermoacetica* FprA crystals in mother liquor. Top right inset: solution UV-vis absorption spectrum of as-isolated (iron-containing) *M. thermoacetica* FprA and Zn-containing FprA in solution (from Ref. 1).

X-ray Diffraction Data Collection and Structure Determination. All X-ray diffraction data used for model building were acquired at -175 °C at the Advanced Light Source, Berkeley CA, on beamline 5.0.2 (X-ray wavelength, 0.97 Å). Two approaches were taken to obtain phases. First, a poly-alanine model of the *D. gigas* ROO crystal structure (PDB ID 1E5D) was used for molecular replacement. Second, a redundant (760 degrees of data) data set was collected at the University of Georgia on a Rigaku RU-200 rotating anode equipped with Osmic focusing mirrors and a R-axisIIc image plate detector using the oxidized crystals at -195 °C (X-ray wavelength, 1.54 Å). Although these latter experiments provided diffraction data to only 3.5-Å nominal resolution, they were sufficient for single anomalous dispersion (SAD), from which eight potential iron positions were identified in the asymmetric unit. A reasonable solution for the phases was obtained by molecular replacement that was in good agreement with the iron positions. During model building and refinement, the iron positions and the entire polypeptide were placed before the addition of the FMN cofactor or any water molecules. The oxidized (as-isolated) structure was refined first and the iron/peptide coordinates were used as a starting point for model building and refinement of the reduced and NO-treated FprA diffraction data sets. In the latter cases the peptide structure was modeled and refined prior to the addition of the FMN and water molecules. Subsequent rounds (15 for the initial oxidized structure, 3 each for the dithionite-reduced and NO-reacted structures) of model building and refinement were performed using the programs O[3] and CNS.[4] Figures were generated using the programs Molscript,[5] Xtalview,[6] Viewerlite (Accelrys, Inc), Pymol (DeLano Scientific LLC), and Raster3D.[7]

Table 1. Data collection and refinement statistics.

Data Set	λ(Å)	Resolution range (Å)	Completeness (%)	R_{sym} [a]
Oxidized	1.0	50.0-3.0	99.9(99.6)[b]	0.042(0.17)
Reduced	1.0	50.0-2.8	99.9(99.3)	0.049(0.26)
NO-treated	1.0	50.0-2.8	99.9(96.0)	0.047(0.19)

Model	Oxidized	Reduced	NO-Treated
Space group	$P4_32_12$	$P4_32_12$	$P4_32_12$
Unit cell dimensions (Å)	a=b=159.6, c=276.7	a=b=159.6, c=278.1	a=b=160.3, c=279.1
Refinement resolution (Å)	50.0-3.0	50.0-2.8	50.0-2.8
Unique reflections	71,781	88,890	89,051
R_{cryst} (%)	21.6	22.6	22.3
R_{free} (%)	25.9	24.5	24.5
Protein atoms	12,460	12,460	12,460
Cofactor/non-protein atoms	152	160	144
Water atoms	61	132	282
RMS deviations from ideality			
Bond distances	0.006	0.014	0.009
Bond angles	1.42	1.91	1.62
B-factors (Å^2)			
Average	55.9	52.9	64.6
Minimum	12.3	30.8	37.2
Maximum	132.8	200.0	152.0

[a] $R_{sym} = \sum_{hkl}[\sum_I(|I_{hkl,I} - \langle I_{hkl}\rangle|)] / \sum_{hkl,I}\langle I_{hkl}\rangle$, where I_{hkl} is the intensity of an individual measurement of the reflection with indices hkl and $\langle I_{hkl}\rangle$ is the mean intensity of that reflection. [b] The numbers in parenthesis refer to the outer resolution bin used in data processing.

Site-Directed Mutagenesis. Plasmids encoding site-directed variants of *M. thermoacetica* FprA were constructed using the plasmid, pFprA (non-His-tagged),[8] as template and the QuikChange site-directed mutagenesis kit (Stratagene) following the procedures described in the product manual. The primers used are listed for the corresponding variant (with the variant codon in italics): H86A, C GAA AGC GAT *GCT* GCC GGC GCC TTC CC; R391stop, GC TAC GAG CTG GGC *TGA* AAA ATC GCA GCG CGC; R391G, K392E, GC TAC GAG CTG GGC *GGA GAA* ATC GCA GCG CGC; R391E, K392E, GC TAC GAG CTG GGC *GAG GAA* ATC GCA GCG CGC; R391E, GC TAC GAG CTG GGC *GAG* AAA ATC GCA GCG CGC; H25F, C CGC TAC TTC *TTC* GGT CCC GCT TTT TCC; Y195F, GAG GCG GCC AAG *TTC* TAT GCC AAT ATT CTC. The primer complements were generated automatically by the

manufacturer (Integrated DNA Technologies) using standard nucleotide pairing. The variant codons in the resulting plasmids pH25F-FprA, pY195F-FprA, pH86A-FprA, pR391stop-FprA, pR391G,K392E-FprA, pR391E, K392E-FprA, pR391E-FprA were verified by sequence analysis of the plasmids at the University of Georgia Integrated Biotechnology Laboratories. The variant FprAs were expressed and purified following the protocol previously described for wild-type recombinant *M. thermoacetica* FprA.[1]

6.3. Results

The crystal structures of three forms of *M. thermoacetica* FprA obtained using pH 6.5 precipitant are reported: oxidized (as-isolated, resolution 3.0Å), anaerobic dithionite-reduced (reduced, resolution 2.8Å), and anaerobic dithionite-reduced, nitric oxide-reoxidized (NO-reacted, resolution 2.8 Å). The crystal structure of as-isolated FprA obtained using a pH 4.5 precipitant (resolution 3 Å) was identical (including diiron ligands) to that at obtained using the pH 6.5 precipitant, and is not further discussed.

Tertiary and Quaternary Structures. The crystal structure of the *M. thermoacetica* FprA reveals a "head-to-tail" homodimer with two active sites consisting of the diiron site of one monomer in close contact with the FMN of the second monomer (cf. Figure 6.2). As shown in Figure 6.3 the *M. thermoacetica* FprA tertiary and quaternary structures and the placement of cofactors are very similar to those reported for *D. gigas* ROO[2]. No difference in the quaternary or tertiary structures were observed among the as-isolated, reduced and NO-reacted forms of FprA.

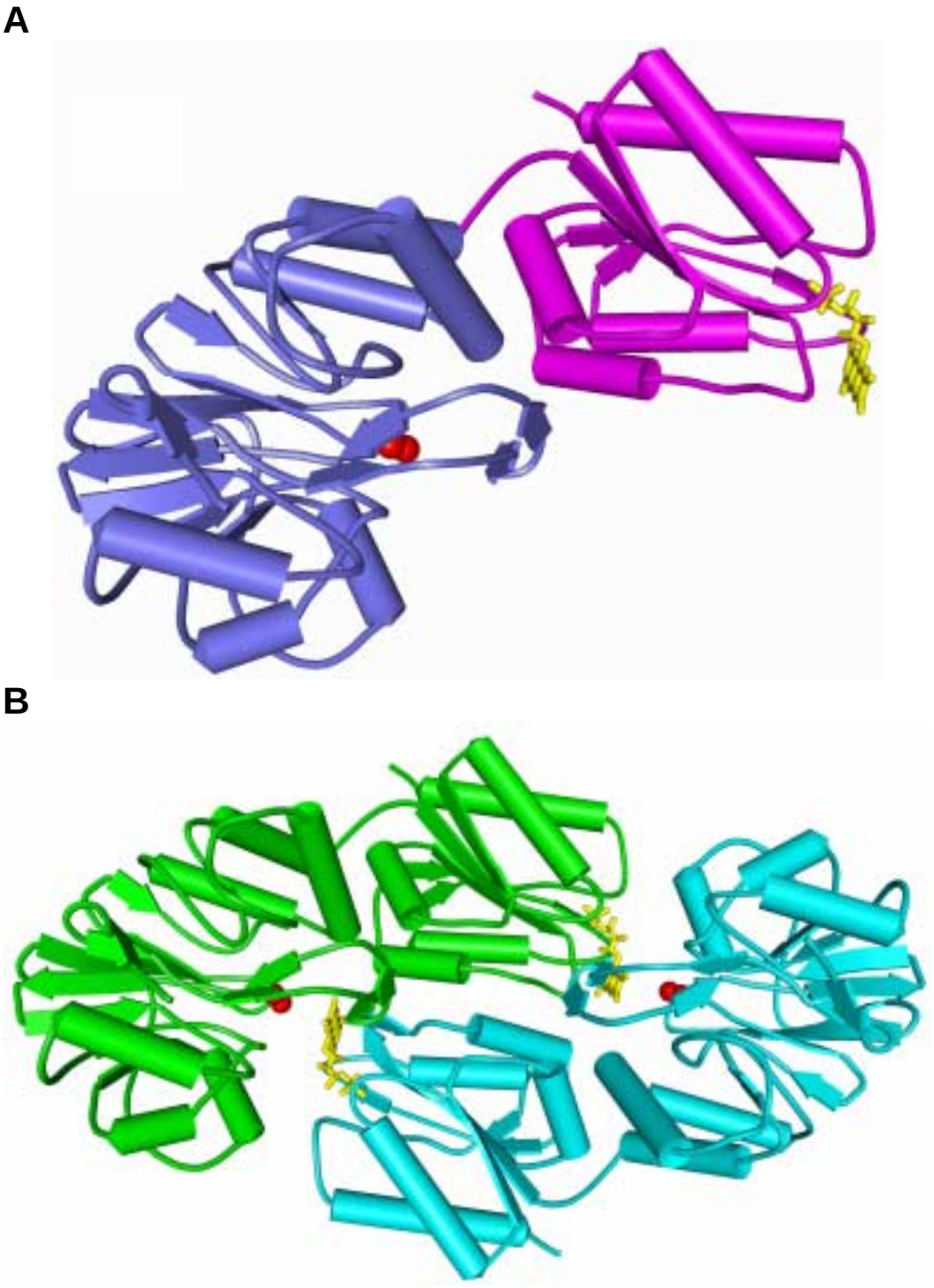

Figure 6.2. Representations of the FprA monomer (Panel A) and homodimer (panel B) in crystalline *M. thermoacetica* FprA. Cylinders represent helical regions, arrowed ribbons represent β-sheet regions. The FprA monomer has the β-lactamase-like domain highlighted in blue and the flavodoxin-like domain in pink. The homodimer has one monomer colored in green and the other cyan. Iron atoms are shown as red spheres, and FMN is shown as yellow sticks.

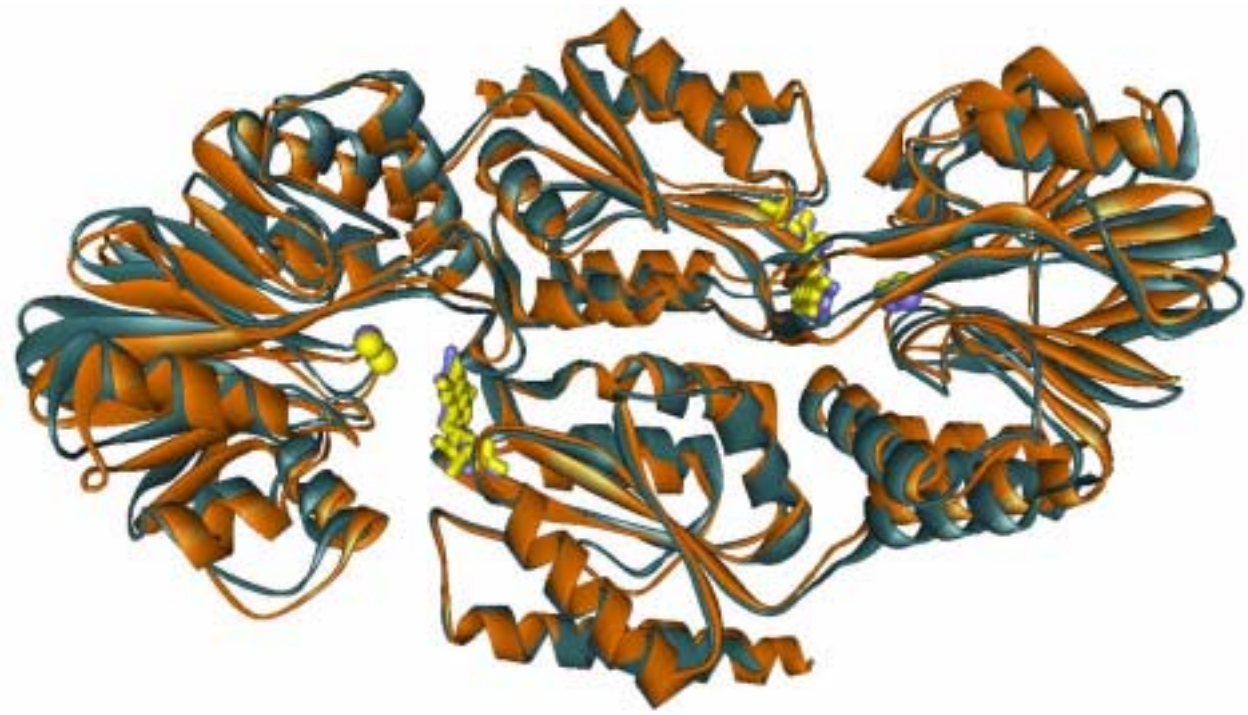

Figure 6.3. Superposition of the *D. gigas* ROO (orange, pdb file 1E5D) and as-isolated *M. thermoacetica* FprA (blue, this work) homodimers, in ribbon representations viewed along the pseudo two-fold rotational axis. Diiron and FMN cofactors are shown in sphere and stick representations, respectively (purple for *M. thermoacetica* FprA, yellow for *D. gigas* ROO). Superposition was performed in Swiss-pdb Viewer, giving a calculated root mean square displacement of 1.87 Å for backbone atoms.

However, as shown in Figure 6.4, the *M. thermoacetica* FprA unit cell contains two homodimers, as opposed to the single homodimer found in the unit cell of *D. gigas* ROO.[2] The association between the two *M. thermoacetica* homodimers, involving the β-lactamase-like domain of one homodimer and the flavodoxin domain of the other homodimer, appears to involve a very limited portion of the protein and presumably has no physiological relevance. In solution *M. thermoacetica* FprA is found to be a homodimer by gel-filtration with no evidence for a tetramer (or any higher oligomers). Site-directed mutagenesis of two residues involved in this inter-homodimer interaction, R391 and K392, to either a stop codon or glutamate (cf.

Materials and Methods), resulted in protein that either expressed as inclusion body or did not crystallize under any of the conditions used to screen wild-type *M. thermoacetica* FprA.

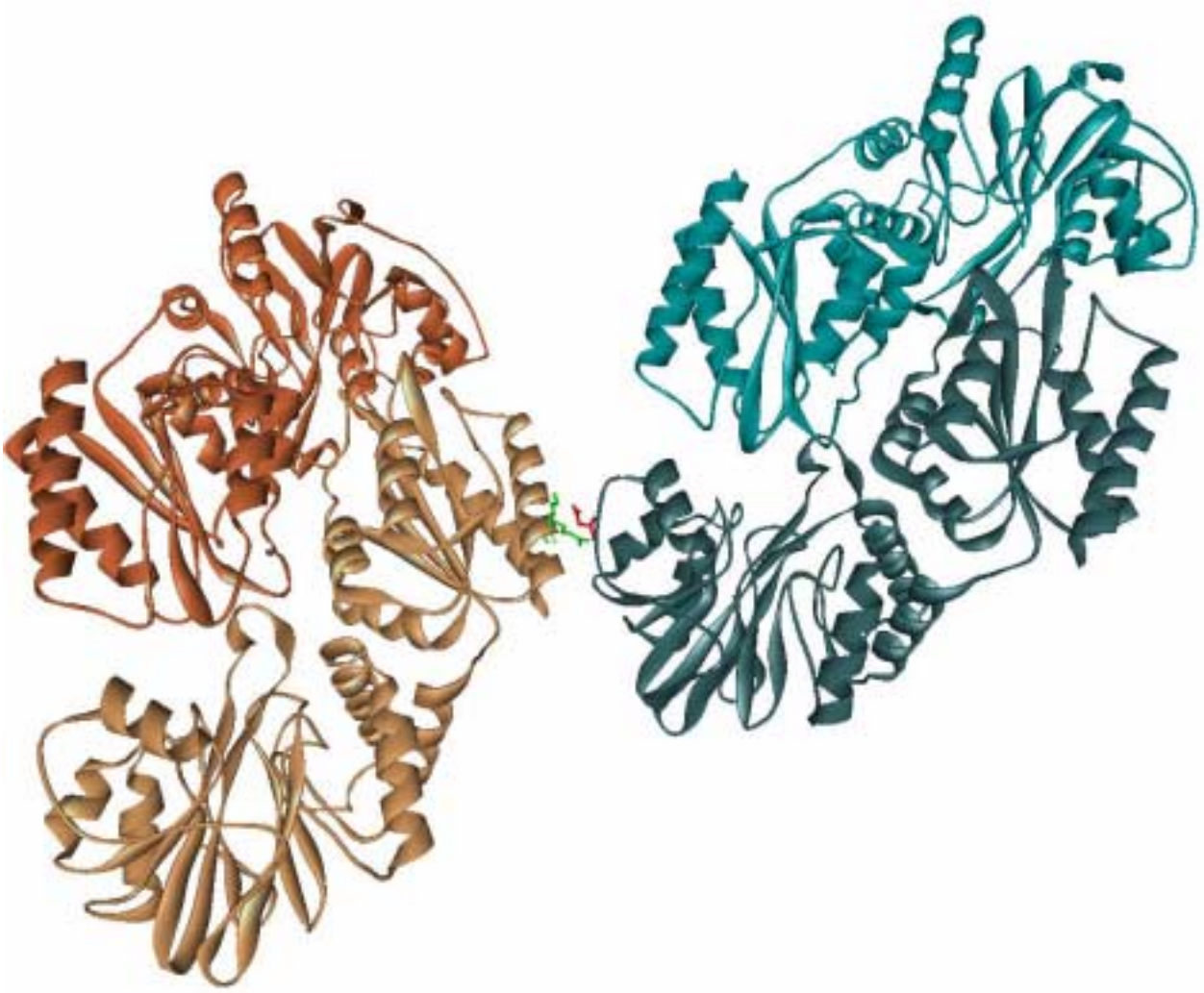

Figure 6.4. Ribbon representation of protein molecules in the *M. thermoacetica* FprA asymmetric unit. The two homodimers are shown in blue and orange, respectively, with different shades for each monomer. Residues R391 and K392 (green) of one monomer, and D120 (red) of the other monomer at the dimer-dimer interface are shown in wireframe representation.

Figure 6.5 illustrates an interaction between FprA monomers belonging to different unit cells. As confirmed by anomalous scattering data collected at 0.97 Å, this interaction is mediated by Zn^{2+}, which was present in the crystallization solutions at 200 mM. Residues S2 and D60 of one monomer are part of a zinc site that also involves residues D275 and H271 of another

symmetry related molecule. Although *M. thermoacetica* FprA crystals could be obtained under a number of different conditions, a divalent cation (most often Zn^{2+}) at 100-200 mM was always required. Neither NOR nor O_2 reductase activities of as-isolated (i.e., iron-containing) FprA are Zn^{2+}-dependent, nor did added Zn^{2+} salts up to 200 mM inhibit these activities (data not shown).

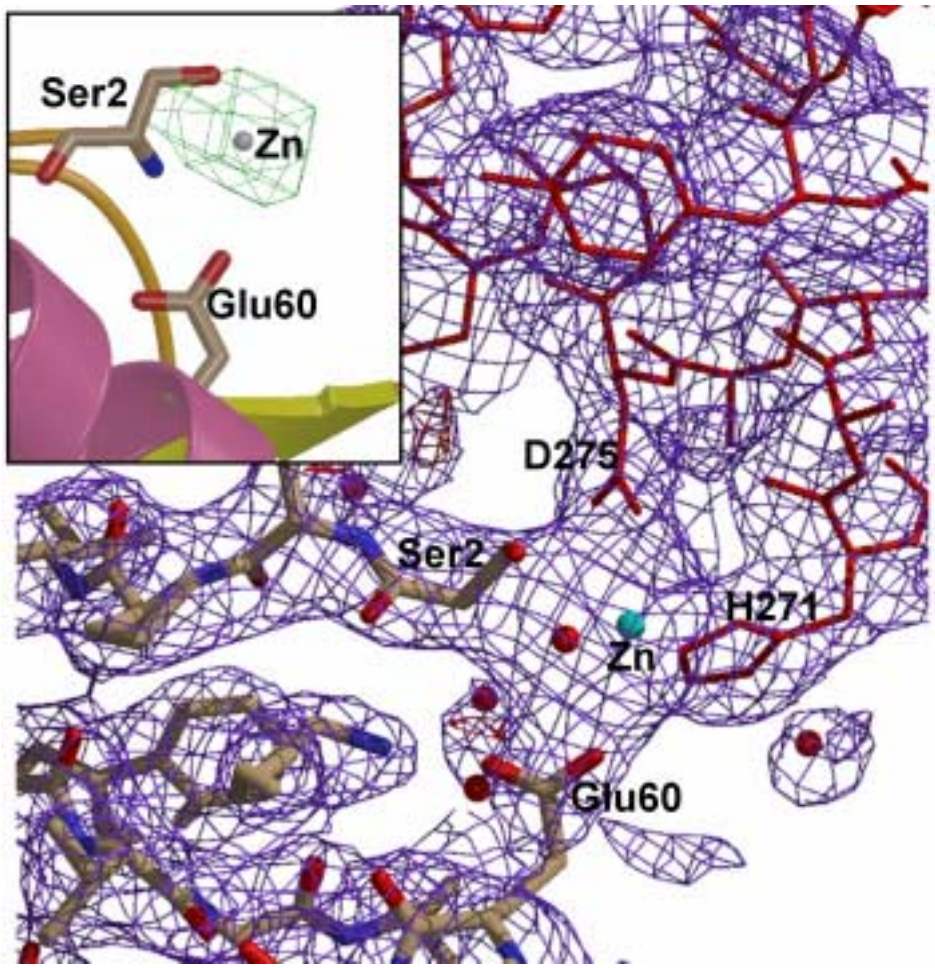

Figure 6.5. Interaction between monomers belonging to different unit cells in *M. thermoacetica* FprA crystals. Zn^{2+} is shown as cyan sphere. A portion of one FprA monomer is shown as sticks in CPK colors and the other as red wireframe. Water molecules are shown as red spheres. $2F_O$-F_C composite omit map with simulated annealing is contoured at 3σ. Inset shows anomalous scattering data collected at 0.97 Å, contoured at 10 σ and superimposed over the Zn site.

FMN binding site. As is the case for *D. gigas* ROO,[2] the FMN cofactor in *M. thermoacetica* FprA is found at the interface between the two monomers of the homodimer (cf. Figures 6.2 and

6.3). As shown in Figure 6.6, the O=C-NH-C=O portion of the FMN isoalloxazinic ring is visible from the outer surface of the protein in a space filling representation of the *M. thermoacetica* FprA homodimer. Steric crowding by the protein on both sides of the isoalloxazinic ring plane effectively precludes direct interaction with NADH, which typically involves aromatic ring stacking between the nicotinamide and the FMN. This structural feature explains why NADH does not directly reduce the FprA FMN.[1] Figure 6.7 shows that most of the residues in close contact with the FMN belong to one monomer. Four residues from the second monomer are also in close contact with the FMN. These latter residues are at or near the diiron site: E83, H148 (diiron ligands), H25 (substrate binding pocket, see below), and W149 (in close contact with H148). The presence of several aromatic residues between the FMN and the diiron site, namely, W376, W149, W347, H25, and H148, is likely to provide multiple, extremely efficient electron-transfer pathways between the FMN and diiron site. The shortest distance between the FMN and diiron site atoms is <4 Å and occurs between the non-iron-bound oxygen of the E83 carboxylate ligand and an FMN methyl group (cf. Figure 6.7).

As expected, there are mainly two types of interaction between the FMN and the FprA polypeptide: hydrophobic around the FMN aromatic system and hydrophilic around the FMN phosphorylated sugar. There appear to be no strong hydrogen bonding interactions at the aza atoms in the FMN aromatic ring, and these aza atoms are inaccessible to solvent. The non-protic FMN environment is consistent with one-electron reduction of the FMN in FprA yielding the non-protonated semiquinone.[1] Further reduction of this non-protonated semiquinone would require protonation in order to avoid formation of an energetically unfavorable dianionic isoalloxazinic ring. This reduction of the FprA semiquinone was shown to be slow (taking

several minutes at room temperature and incompatible with NOR enzymatic turnover) unless stoichiometric amounts of the NADH:FprA oxidoreductase, Hrb, were present.[1]

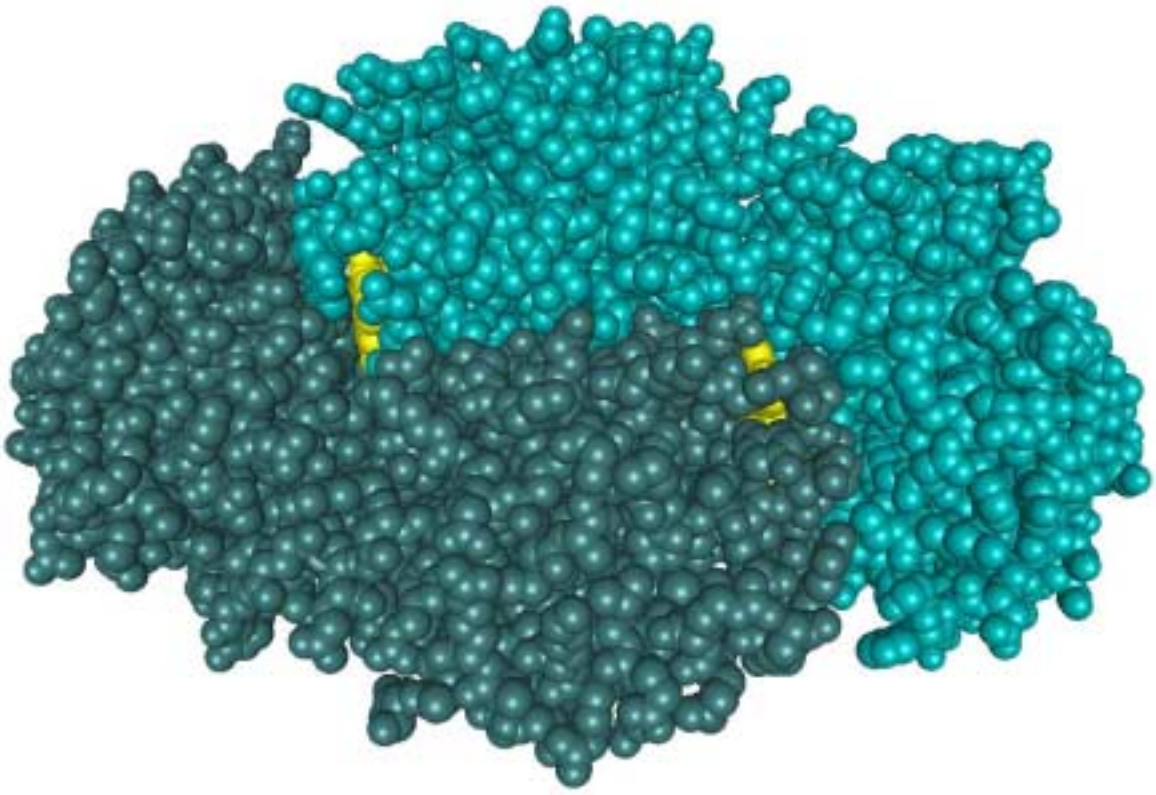

Figure 6.6. Space filling representation of the FprA homodimer viewed along the pseudo two-fold rotational axis with monomers colored different shades of blue. FMN atoms are shown in yellow.

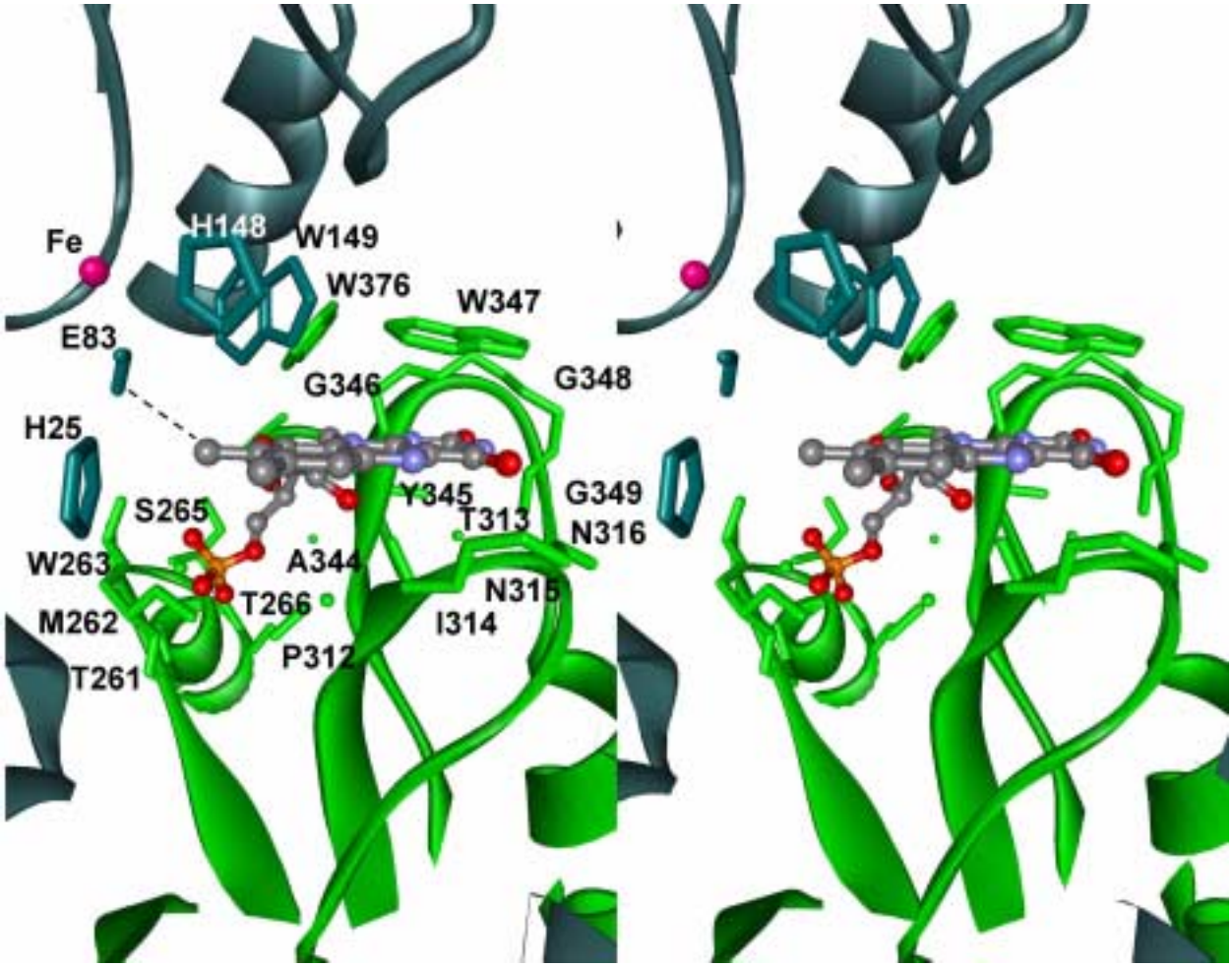

Figure 6.7. Stereo view of the FMN binding site in *M. thermoacetica* FprA. The FMN is shown in ball-and-stick representation and CPK colored. The protein is shown in ribbon representation with the two monomers colored in blue and green, respectively. Iron is shown as pink sphere. Residues 4.5 Å (or less) away from the flavin are shown in wireframe representation. Dashed line indicates the closest atomic contact between flavin (C8 methyl) and diiron site ligand E83 (non-iron-bound oxygen atom of the carboxylate side-chain).

Diiron site. Figure 6.8 shows the diiron site and the anomalous scattering for data collected at 1.54 Å on as-isolated FprA crystals. The presence of a significant anomalous scattering signal at this wavelength, together with the absence of an 1.54-Å anomalous scattering signal from the putative Zn^{2+}-occupied site in Figure 6.5, are consistent with the two metals in Figure 6.8 being iron.

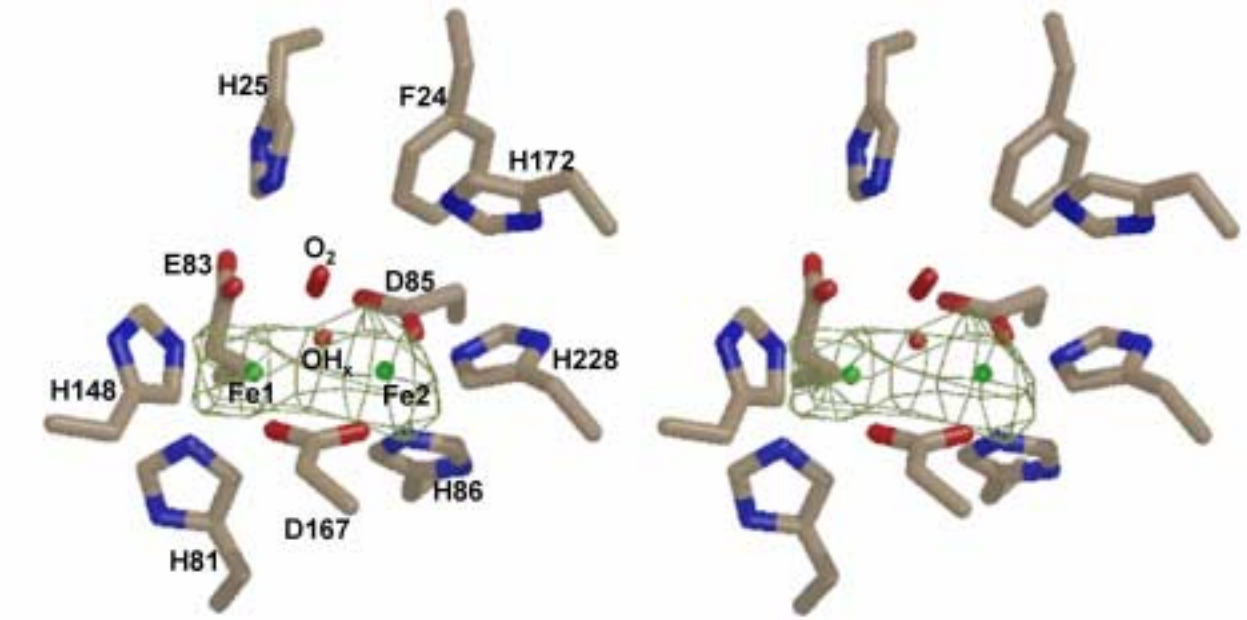

Figure 6.8. Anomalous scattering signal contoured at 8σ for data collected at 1.54 Å superimposed over a cross-eyed stereo view of model for the active site of as-isolated *M. thermoacetica* FprA. Color coding: carbon, tan; oxygen, red; nitrogen, blue; iron, green; α-helices, pink; β-sheets, yellow.

Figure 6.9 shows a superposition of the *D. gigas* ROO[2] and as-isolated *M. thermoacetica* FprA active sites, together with a schematic depiction of the diiron coordination sphere in the latter protein. Table 6.2 compares the iron-ligand and iron-iron distances in the two proteins. The X-ray diffraction data for all three *M. thermoacetica* FprA crystal structures (as-isolated, reduced, NO-reacted) are consistent with the presence of a solvent bridge between the two iron atoms. The resolutions of these structures are too low to provide evidence for protonation states of this bridge (i.e., oxo, hydroxo, or aquo). A hydroxo bridge was previously inferred for the as-isolated *M. thermoacetica* FprA in solution, based on UV-vis absorption and Mössbauer spectroscopies.[1] A solvent bridge between the irons was also included in the crystal structure of D. gigas ROO.[2]

The amino acid residues furnishing diiron ligands are homologous to and appear to occupy similar positions as those in *D. gigas* ROO *with the notable exception of H86*. The analogous residue, H84, in ROO appears to have swung away from the iron in ROO and is replaced by a solvent ligand (WAT501 in Figure 6.9). Figure 6.10 shows a composite omit map focusing on electron density around H86, which confirms that its side chain is within ligating distance of Fe2 in *M. thermoacetica* FprA. The ligation of H86 does not appear to be redox-dependent, since H86 remains a ligand in the as-isolated, reduced, and NO-reacted *M. thermoacetica* FprA crystals. An H86A variant of *M. thermoacetica* FprA was expressed in *E. coli* only as inclusion bodies – consistent with a strong structural role for H86 in *M. thermoacetica* FprA. The apparent de-ligation of the H86 homolog in ROO is unlikely to be pH-dependent, since the ROO crystals were obtained at pH ~ 6,[2] which is within the range of the pH 4.5 - 6.5 precipitants used to obtain the *M. thermoacetica* FprA crystals. Both iron atoms in the diiron site of *M. thermoacetica* FprA are five-coordinate (cf. Figure 6.9) with the unoccupied sixth coordination positions approximately trans to H81 and H86. These empty coordination positions could serve to bind NO. In the *D. gigas* ROO crystal structure, the analogous coordination positions of the two irons trans to H81 and WAT501 were also empty and inferred to be involved in substrate (O_2) binding.[2]

As shown in Figure 6.8 and 6.9, several residues line a pocket above the two unoccupied iron coordination positions of the diiron site. The position of the pocket residue, Y195 (Y193 in ROO), is well conserved. On the other hand, H25 (H24 in ROO) and F24 (F23 in ROO) appear displaced, presumably due to the presence of the "extra" Y26 in ROO. Residue H172, substituted by N170 in ROO, is placed next to Y195. Together, H25, Y195 and H172 appear to form a network of hydrogen-bonding/proton donating residues which may be important in catalysis.

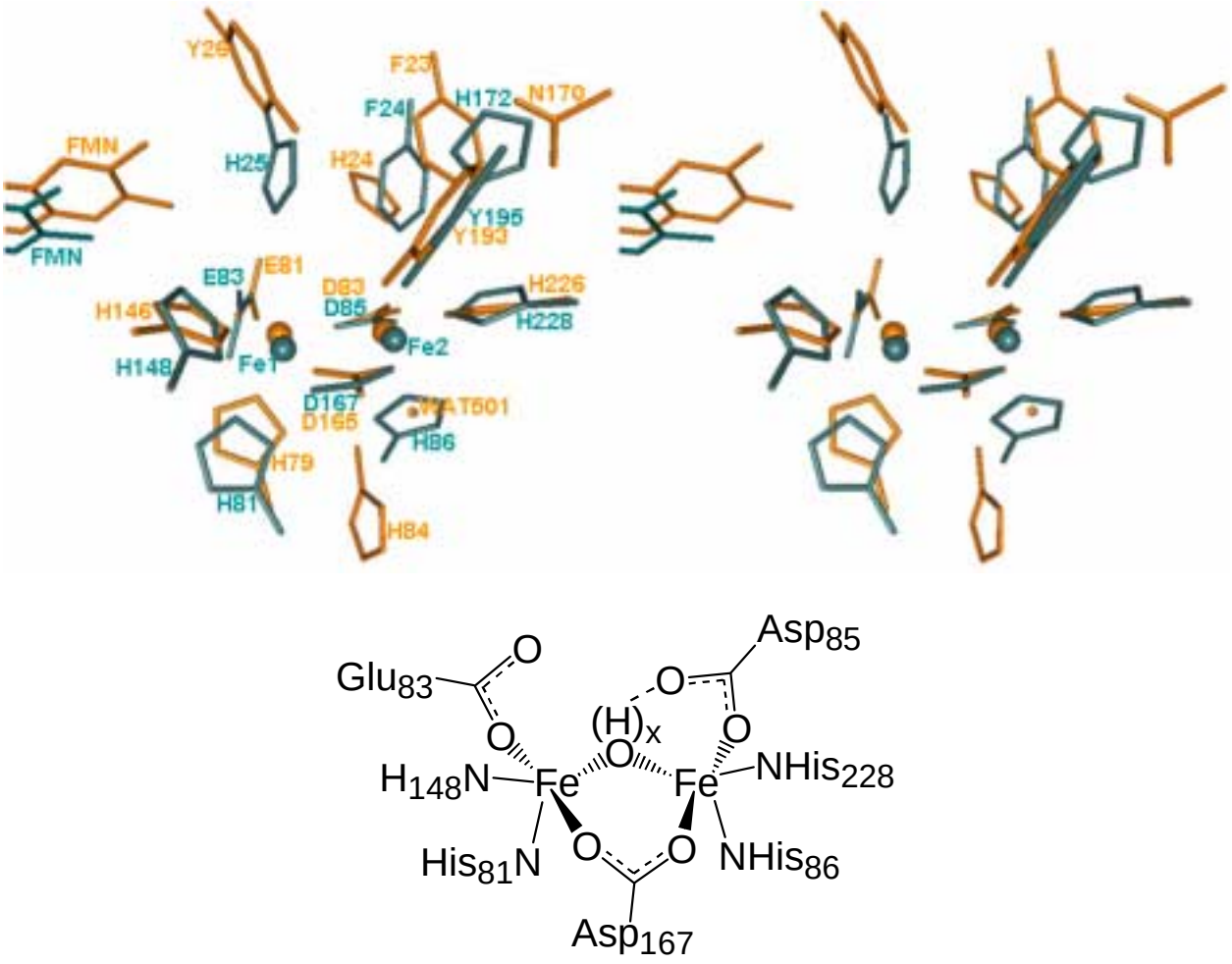

Figure 6.9. Top panel: cross-eyed stereo view of the *D. gigas* ROO (orange, PDB code 1E5D) and *M. thermoacetica* FprA (blue) diiron sites and surrounding residues from the same superposition of the two proteins shown in Figure 6.3. Iron atoms are shown as spheres. Bottom panel: schematic depiction of the diiron coordination sphere in *M. thermoacetica* FprA.

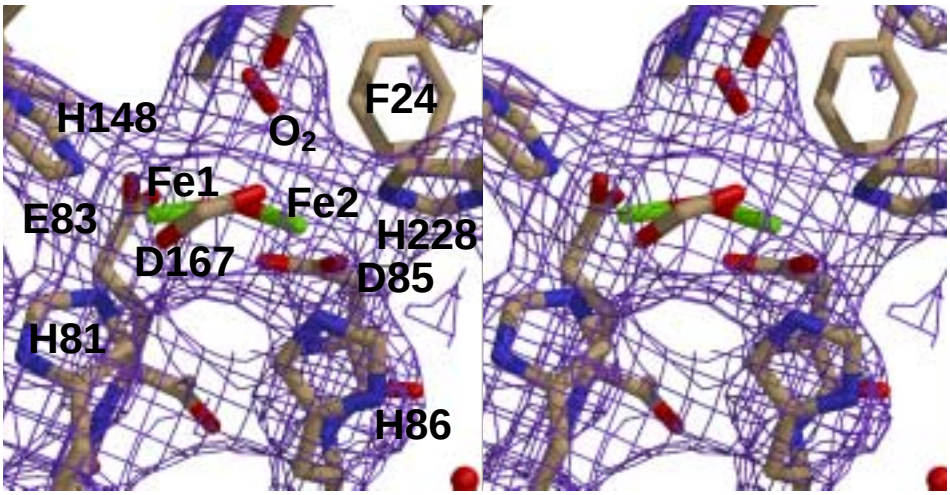

Figure 6.10. Cross-eyed stereo view of model and $2F_O$-F_C composite omit map with simulated annealing for the diiron site in as-isolated *M. thermoacetica* FprA crystals. The composite omit map was generated using the simulated annealing protocol with 5 % of the model being omitted at a time. The atoms are colored as described in Figure 6.8 and the composite omit map is contoured at 1.5 σ.

Table 6.2. Iron-ligand and iron-iron interatomic distances (Å) for *M. thermoacetica* FprA (this work) and *D. gigas* ROO (Ref. 2).

Distances[a]	*D. gigas* ROO	*M. thermoacetica* FprA		
	as-isolated	as-isolated	reduced	NO-reacted
Fe1-Fe2	3.36, 3.37	3.30, 3.31, 3.31, 3.34	3.28, 3.35, 3.23, 3.46	3.23, 3.33, 3.33, 3.57
Fe1-E83 OE1	2.04, 2.04	2.25, 2.74, 1.94, 1.91	2.31, 2.30, 2.29, 2.01	2.33, 2.19, 2.08, 1.83
Fe1-H148 NE2	2.08, 2.08	2.24, 2.06, 2.34, 2.23	2.33, 2.35, 2.47, 2.34	2.42, 2.40, 2.49, 2.29
Fe1-H81 NE2	2.14, 2.13	2.67, 2.43, 2.44, 2.37	2.44, 2.39, 2.33, 2.37	2.36, 2.33, 2.19, 2.38
Fe1-D167 OD2	1.93, 1.93	2.04, 2.16, 2.03, 2.05	2.17, 2.29, 2.12, 2.08	2.16, 2.30, 2.10, 2.17
Fe1-O_{solv}[b]	2.25, 2.26	2.04, 2.04, 2.04, 2.05	2.03, 2.03, 2.02, 2.06	1.98, 2.00, 2.00, 2.03
Fe2-D85 OD2	2.32, 2.33	2.19, 2.11, 2.12, 2.23	2.32, 2.16, 2.32, 2.22	2.27, 2.04, 2.09, 2.08
Fe2-H228 NE2	2.02, 2.02	1.98, 2.11, 2.01, 2.05	2.13, 2.16, 2.11, 2.15	2.24, 2.17, 1.99, 2.11
Fe2-H86 NE2[c]	5.99, 5.96 *2.43, 2.59*	2.09, 2.06, 2.28, 2.21	2.25, 2.18, 2.35, 2.22	2.14, 2.17, 2.36, 2.21
Fe2-D167 OD1	2.05, 2.06	2.09, 1.95, 2.05, 2.17	2.26, 2.37, 2.32, 2.31	2.30, 2.30, 2.24, 2.36
Fe2-O_{solv}[c]	1.75, 1.76	2.03, 2.03, 2.03, 2.04	2.05, 2.03, 2.02, 2.05	2.00, 2.00, 1.95, 2.04
Fe1-X[d]	2.73, 3.11	2.99, 3.31, 3.06, 2.91	3.19, 3.24, 3.02, 3.18	3.54, 3.45, 3.21, 3.25
Fe2-X[d]	2.60, 2.61	2.92, 2.57, 3.17, 2.37	2.66, 2.78, 3.56, 3.41	3.21, 3.06, 3.24, 3.09

[a]Residue numbering as in *M. thermoacetica* FprA. Distances are listed for each monomer in the asymmetric unit in the order A, B, C, D. [b]Distance to the bridging solvent molecule. [c]Shown in italics is the distance between Fe2 and its WAT501 solvent ligand in *D. gigas* ROO. [d]Distance to the closest atom of the exogenous ligand, "X" = O_2, ethylene glycol, or water (see text).

As shown in Table 6.2, the average Fe1-Fe2 distance in the as-isolated *M. thermoacetica* FprA crystals is 3.2 Å, which is slightly shorter than the corresponding 3.4 Å previously reported in the crystal structure of *D. gigas* ROO.[2] In order to ascertain that the Fe1-Fe2 distance in *M. thermoacetica* FprA did not significantly increase upon reduction, fits of the data on the reduced FprA were attempted to models having significantly longer or shorter Fe1-Fe2 distances. When an Fe1-Fe2 distance of 2.9 Å was assumed in the model, a strong peak developed between the two irons in the $1F_O$-F_C composite omit map (Figure 6.11, left), suggesting that such a model places too much electron density in this area. Conversely, when a fixed Fe1-Fe2 distance of 3.8 Å was used in the model (Figure 6.11, right), similar peaks developed outside the diiron site in the 1*F*o-*F*c difference map, suggesting that such a structure places too much electron density along the Fe1-Fe2 axis on the outer edges of the diiron site. These fits are thus consistent with the average 3.3-Å Fe1-Fe2 distance for reduced (presumably diferrous) *M. thermoacetica* FprA listed in Table 6.2. Similarly, the NO-reacted (presumably diferric) FprA shows an average Fe1-Fe2 distance of 3.4 Å.

The 2.5-Å resolution crystal structure of the as-isolated (presumably diferric) *D. gigas* ROO showed electron density above the diiron site, which was tentatively interpreted as a dioxygen molecule.[2] A similar density (but less well-defined, due to the slightly lower resolution) was present in the maps from the as-isolated *M. thermoacetica* FprA crystal (cf. Figure 6.10). As shown in Figure 6.12, the electron density map from reduced *M. thermoacetica* FprA crystals also shows such "extra" density above the diiron site. In this case, this electron density could be better fit as an ethylene glycol than as a diatomic molecule. This modelling is consistent with the usage of ethylene glycol as cryoprotectant when freezing the crystals. The closest atoms of the modeled ethylene glycol are too far away to furnish ligands to Fe1 or Fe2

(cf. Table 6.2), but could be within hydrogen-bonding distance of His25 NE2. The cis conformation of the modeled ethylene glycol is not unusual in protein crystals.[9,10] The best fit to the electron density has the C-C bond axis of the ethylene glycol approximately perpendicular to the Fe1-Fe2 axis. Remarkably, as shown in Figure 6.13, the electron density modeled as ethylene glycol disappeared almost completely in the NO-reacted crystals. The residual electron density above the diiron site in the NO-reacted crystals is more consistent with a solvent molecule hydrogen-bonded to the bridging solvent ligand. This change in electron density above the diiron site is consistent with displacement of ethylene glycol by NO, followed by reduction of NO at the diiron site with the product of this reduction (N_2O) leaving the site before the crystal was frozen. The diiron site in Figure 6.13 should thus be in the diferric state.

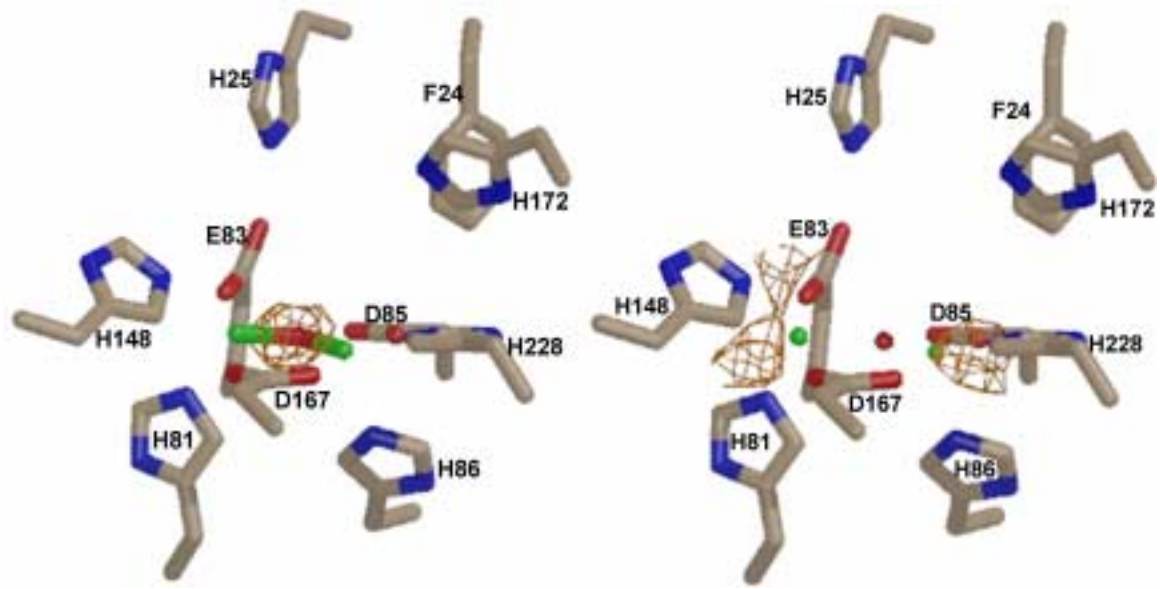

Figure 6.11. Left: $1F_O$-F_C composite omit map contoured at -3σ for reduced *M. thermoacetica* FprA crystals with the Fe1-Fe2 distance fixed at 2.9 Å in the calculated map. Right: $1F_O$-F_C map contoured at -4σ for the reduced FprA crystals with the Fe1-Fe2 distance fixed at 3.8 Å in the calculated map. Maps are superimposed on the model for the diiron site.

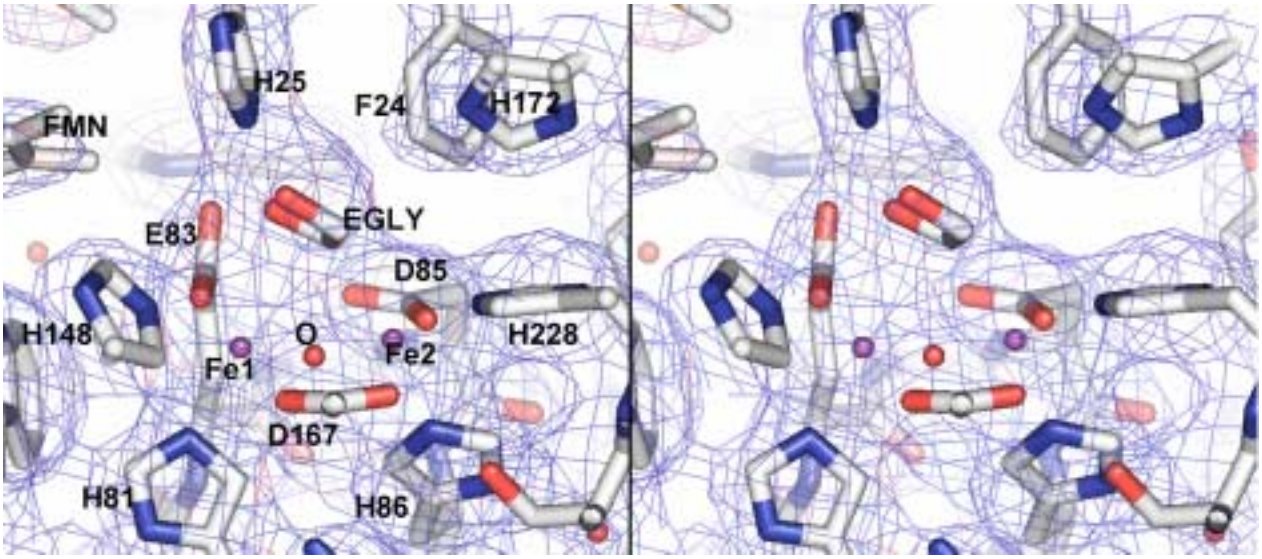

Figure 6.12. Cross-eyed stereo view of model and $2F_O$-F_C composite omit map with simulated annealing for the reduced *M. thermoacetica* FprA diiron site superimposed on a model including ethylene glycol (labeled EGLY). Color coding: carbon, white; nitrogen, blue; oxygen, red; iron, purple.

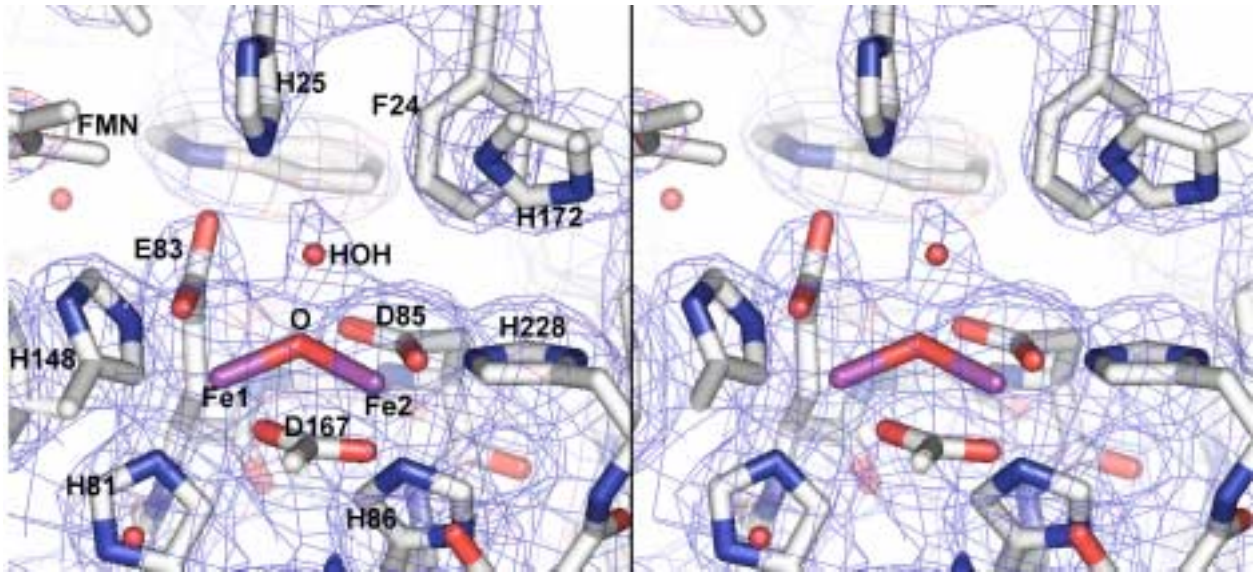

Figure 6.13. Cross-eyed stereo view of model and $2F_O$-F_C composite omit map with simulated annealing for the NO-reacted *M. thermoacetica* FprA active site, showing the solvent molecule that has replaced the ethylene glycol upon treatment of the dithionite-reduced crystals with NO. Color coding: carbon, white; nitrogen, blue; oxygen, red; iron, purple.

The putative O_2, ethylene glycol or solvent occupancy above the FprA diiron site suggests that the pocket could also be occupied by NO. Figure 6.14, Panel A, shows space filling models of this pocket, and Panels B and C illustrate that the pocket is indeed large enough to accommodate two NO molecules in at least two possible conformations. Figure 6.14, Panel B, shows a diferrous dinitrosyl model in which each NO molecule is N-coordinated terminally to one iron with Fe-N-O angles of 144°, Fe-NO distances of 1.75 Å, N-O distances of 1.16 Å and N---N distance between the coordinated NO's of 2.80 Å. These parameters mimic the known structure of a previously described synthetic diferrous dinitrosyl complex.[11] Figure 6.14, Panel C, shows a diferrous mono-nitrosyl model with one NO coordinated to one iron as described for the diferrous dinitrosyl and a second non-coordinating NO sitting above the diiron site in a "near-attack conformation", ~ 3Å away (N---N distance) from the coordinated NO. The pocket above the diiron site appears to sterically accommodate these adducts very well. The closest residues to the NOs in either model are H25, Y195, H172 and F24 with side-chain atoms ~3 Å from either atom of the two NOs (cf. Figure 6.14). The presence of the H25 Nε and Y195 phenolic OH atoms within hydrogen-bonding distance from the NO is consistent with involvement of these residues in NOR catalysis, verified by site-directed mutagenesis (see below). Rotation of either (or both) coordinated NO molecules around the Fe-NO axes at a fixed Fe-N-O angle of 144° appears to be sterically permitted. Although the diferrous-mononitrosyl model in Figure 6.14 (bottom right) depicts the coordinated NO bound to the iron atom closer to the FMN, the reversed situation (with NO bound to the other iron) is also sterically possible in the model.

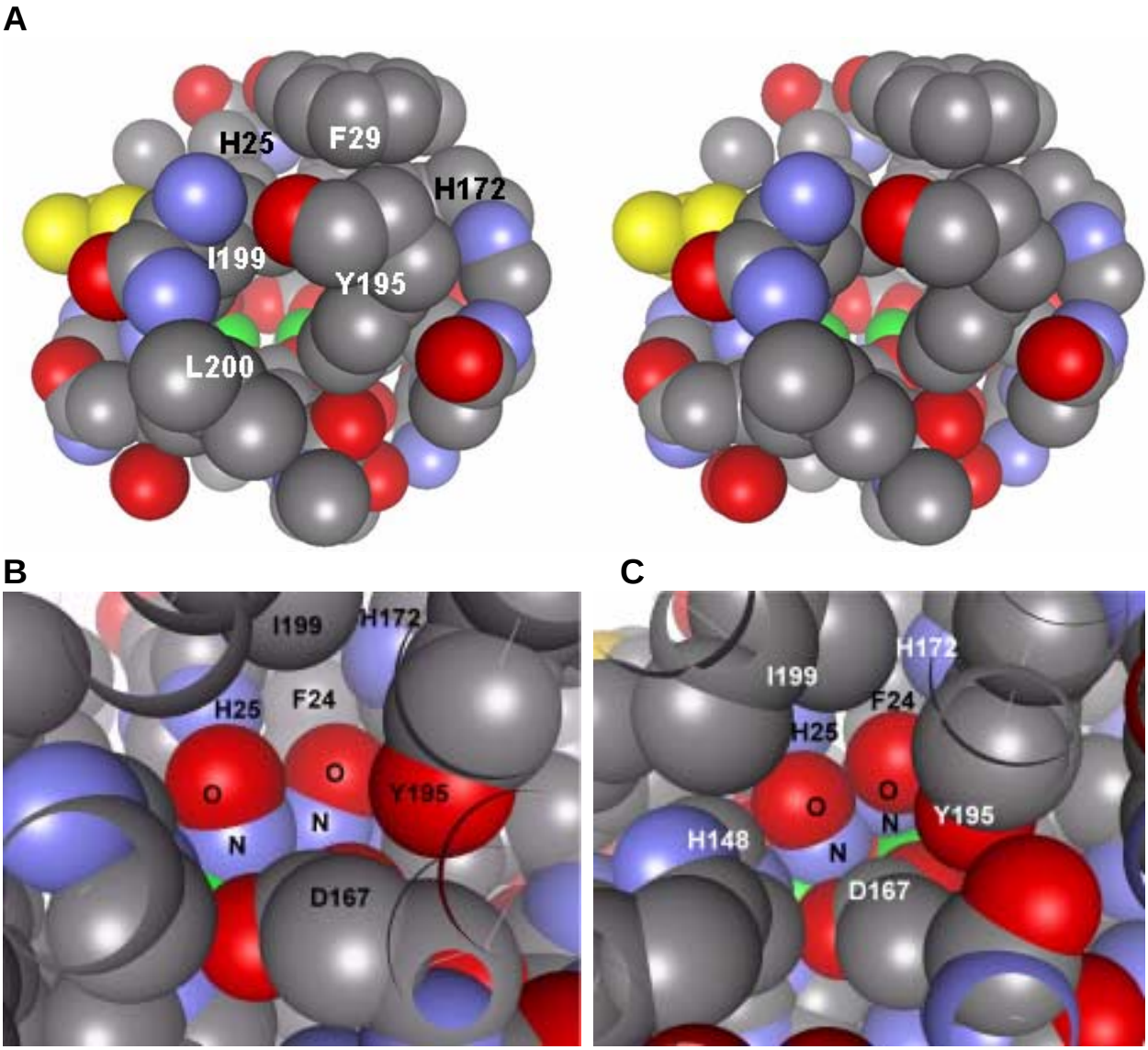

Figure 6.14. Panel A: cross-eyed stereo view of space-filling representation of the substrate-binding cavity in the reduced *M. thermoacetica* FprA structure (with ethylene glycol omitted for clarity). Panel B: diferrous dinitrosyl model. Panel C: diferrous mononitrosyl model with one NO coordinated to iron and the other NO 2.6 Å away from the closest iron atom. Atoms are color-coded as: iron, green; oxygen, red; nitrogen, blue; carbon, gray; FMN, yellow.

Channels Leading to the Active Site. The active site of *M. thermoacetica* FprA is designed to sterically limit access of larger molecules to the diiron site while allowing entry and egress of small molecules, such as substrate (NO, O_2) and products (N_2O, H_2O) to the "substrate-binding cavity" above the diiron site. Figures 6.15 and 6.16 illustrate that this substrate-binding cavity is

accessible from the surface of the protein via four long (10-17 Å) narrow channels. The walls of these channels feature atom-to-atom distances as low as ~5 Å, implying an effective van der Waals diameter as low as 2 Å which appears barely wide enough to allow efficient (on a *catalytic* time scale) passage of small/linear molecules, such as the FprA substrate(s)/products. Similar channels are present in the *D. gigas* ROO crystal structure.[2] These channels do not appear to be occupied in any of the *M. thermoacetica* FprA or *D. gigas* ROO structures.

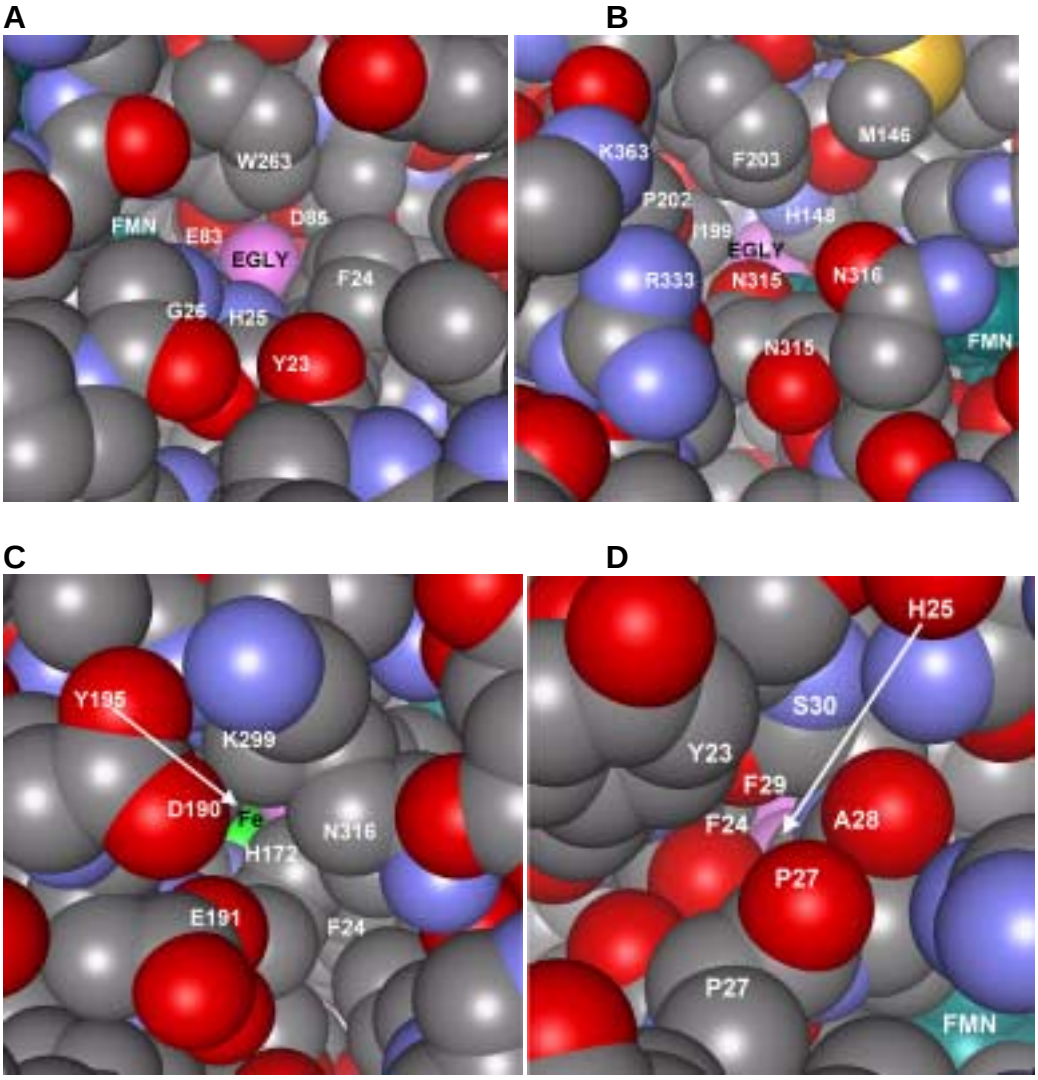

Figure 6.15. Views of four channels connecting the protein surface with the substrate-binding cavity above the diiron site in the reduced *M. thermoacetica* FprA crystal structure. Color codings are: carbon-gray, oxygen-red, nitrogen-blue, sulfur-yellow, iron-green, ethylene glycol

(EGLY)-pink, FMN-cyan. Approximate surface-to-iron channel lengths are: 10 Å (**A**), 11 Å (**B**), 17 Å (**C**), and 14 Å (**D**).

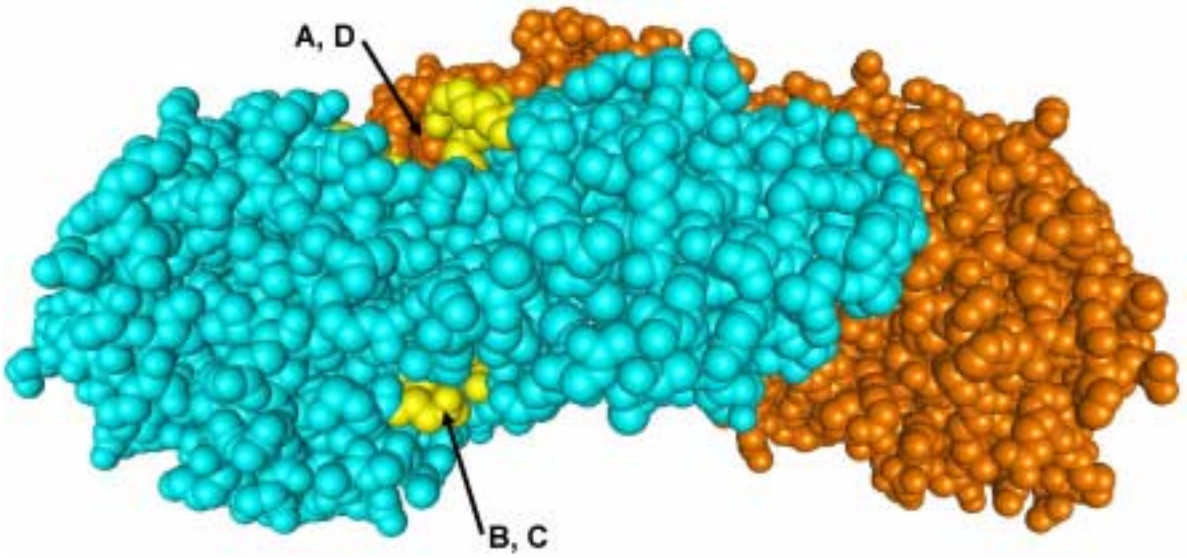

Figure 6.16. Space-filling view of the *M. thermoacetica* FprA homodimer (with the monomers colored cyan and orange) illustrating the locations of the four channels shown in Figure 6.15 leading from the surface of the protein to one of the diiron sites. Residues labeled in Figure 6.15 are colored yellow.

Evidence for involvement of H25 and Y195 in NOR catalysis. With respect to the importance of the pocket residues, H25 and Y195, for NO reduction by *M. thermoacetica* FprA, Figure 6.17 shows that the H25F and Y195F variants of *M. thermoacetica* FprA exhibit decreased NOR activities, and that this decrease is due to a decrease in k_{cat}, rather than in K_M, relative to wild-type FprA. Both variants had a K_M of 7 μM compared to 4 μM for wild-type, whereas the k_{cat} was 7 s^{-1} for Y195F and 1.4 s^{-1} for H25F, compared to 48 s^{-1} for wild-type.[1] Thus, Y195 and H25 are likely involved in the rate-limiting step of NO reduction at the FprA active site, presumably via proton donation.

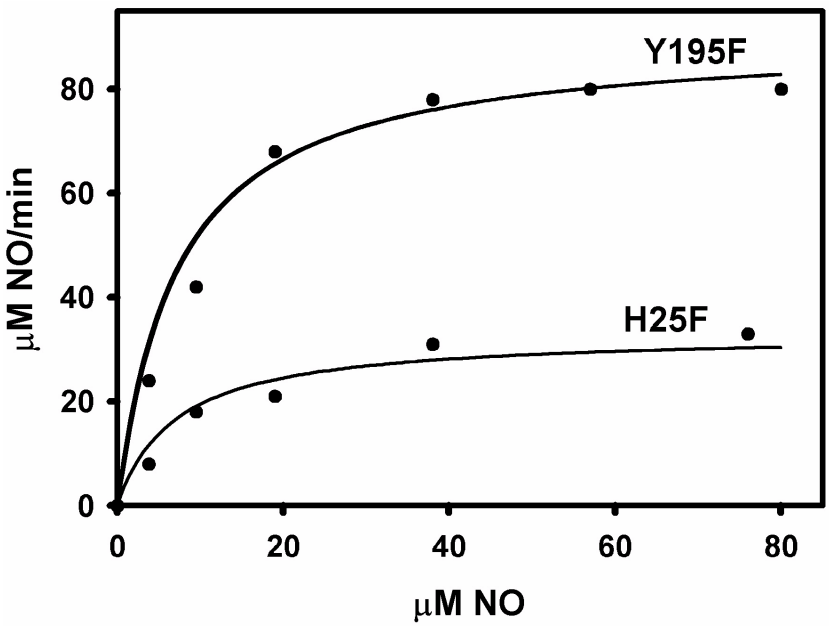

Figure 6.17. NO concentration dependence of NADH:NO oxidoreductase activity of *M. thermoacetica* Hrb + FprA variants H25F and Y195F at saturating Hrb and NADH. Assay solutions contained 10 μM Hrb, 160 μM NADH and either 190 nM Y195F FprA or 400 nM H25F in 50 mM phosphate pH 7. All rates were measured at room temperature (~23 ºC). The solid traces represent fits of the experimental data to the Michaelis-Menten equation using parameters listed in the text.

6.4. Functional implications

Published data have been interpreted to suggest that *D. gigas* ROO is a dioxygen reductase,[2] while *M. thermoacetica* FprA appears more likely to be an NOR.[1] Although the reactivity of *D. gigas* ROO with NO has not been reported, an FprA from *D. vulgaris*, which is taxonomically closely related to *D. gigas*, has been described in Chapter 3 to act as both NOR and O_2-reductase. Both *M. thermoacetica* FprA and *D. vulgaris* FprA appear to competently protect an NO-hypersensitive *E. coli* strain from NO-induced death (Cf. Chapters 2,3). A similar NOR activity may be thus be expected for *D. gigas* ROO. As shown by the sequence alignment in Figure 3.2, the residues lining the substrate-binding pocket of *D. vulgaris* FprA are very similar to those of *D. gigas* ROO. Appendix C provides a detailed discussion on the degree to

which the active site residues, including the diiron ligands and the pocket residues are conserved in the ~ 100 FprA sequences known to date.

The models of Figure 6.14 illustrate that binding of two nitric oxide molecules at the *M. thermoacetica* FprA active site, according to the mechanism shown in Scheme 6.1, is sterically feasible. The fact that Fe1 and Fe2 at the *M. thermoacetica* FprA diiron site do not move away from each other upon their reduction and are maintained at ~ 3.3 Å is consistent with nitric oxide reduction to N_2O via a diferrous dinitrosyl mechanism. By contrast, reduction of diferric sites to diferrous in other non-heme diiron proteins with histidine and carboxylate ligands, such as rubrerythrin and ribonucleotide reductase, results in lengthening of the Fe-Fe distance by up to ~0.7 Å, to ~ 4 Å in the diferrous state.[12,13] Perhaps symptomatically, these other diiron proteins catalyze *O-O bond-breaking*, and not the *bond-forming* NOR reaction. The ribonucleotide reductase diferrous site binds dioxygen and reductively cleaves the O-O bond.[13] Similarly, the rubrerythrin diferrous site reductively cleaves the O-O bond in H_2O_2.[12] Although the diferrous site in ribonucleotide reductase does form a diferrous dinitrosyl adduct, it only slowly and non-catalytically decomposes to release N_2O, consistent with the ~3.9 Å Fe-Fe distance in the diferrous state.[14] Nitric oxide adducts of rubrerythrin have not been reported. Although the Fe-Fe distance in methane monooxygenase, a diiron enzyme whose catalytic cycle involves reductive O-O bond cleavage and subsequent O-C bond forming, does not vary by more than 0.2 Å between the diferric and diferrous states, the coordination geometry of both irons does change significantly upon diferrous $\leftrightarrow$ diferric inter-conversion.[15] Compared to ribonucleotide reductase, rubrerythrin, and methane monooxygenase, the retention of the coordination environment and Fe1-Fe2 bond distance upon reduction of the *M. thermoacetica* FprA diiron site argues against a dioxygen reductase function for FprA.[1] The fact that FprAs do in fact reduce O_2,

but in a less efficient manner than NO,[1] is paralleled by the similarities that the two classes of respiratory NORs, discussed in Chapter 1, share with dioxygen-activating enzymes. P450nor structurally resembles the P450 monooxygenases, while bacterial respiratory NORs structurally resemble cytochrome *c* oxidases.[16-18] Bacterial respiratory NORs do in fact exhibit oxidase activity, but with a $k_{cat} \sim 5$ times lower than that for nitric oxide.[19] P450nor has not been reported to exhibit oxidase or monooxygenase activity, possibly due to the very polar, solvent-exposed active site of P450nor[20] preventing efficient binding of the non-polar dioxygen molecule. The *M. thermoacetica*[1], *D. vulgaris* (cf. Chapter 3) and *E. coli*[21] FprAs inactivate when turning over as oxidases The apparent loss of the H84 diiron ligand in the *D. gigas* ROO crystal structure could be a consequence of ROO's inactivation following adventitious oxidase turn-over during the early stages of isolation and purification from the *D. gigas* cell extract.

The M. thermoacetica FprA crystal structure data reported herein provide new insight into the structural mechanisms used for fine-tuning the protein functions of non-heme diiron sites for dioxygen activation vs. the nitric oxide reduction.

6.5. References

(1) Silaghi-Dumitrescu, R.; Coulter, E. D.; Das, A.; Ljungdahl, L. G.; Jameson, G. N.; Huynh, B. H.; Kurtz, D. M., Jr. *Biochemistry* **2003**, *42*, 2806-2815.

(2) Frazão, C.; Silva, G.; Gomes, C. M.; Matias, P.; Coelho, R.; Sieker, L.; Macedo, S.; Liu, M. Y.; Oliveira, S.; Teixeira, M.; Xavier, A. V.; Rodrigues-Pousada, C.; Carrondo, M. A.; Le Gall, J. *Nat. Struct. Biol.* **2000**, *7*, 1041-1045.

(3) Jones, T. A.; Zou, J. Y.; Cowan, S. W.; Kjeldgaard. *Acta Crystallogr. A* **1991**, *47 (Pt 2)*, 110-119.

(4) Brunger, A. T.; Adams, P. D.; Clore, G. M.; DeLano, W. L.; Gros, P.; Grosse-Kunstleve, R. W.; Jiang, J. S.; Kuszewski, J.; Nilges, M.; Pannu, N. S.; Read, R. J.; Rice, L. M.; Simonson, T.; Warren, G. L. *Acta Crystallogr. D* **1998**, *54 (Pt 5)*, 905-921.

(5) Kraulis, P. J. *J. Appl. Crystallogr.* **1991**, *24*, 945-949.

(6) McRee, D. E. *J. Struct. Biol.* **1999**, *125*, 156-165.

(7) Merritt, E. A.; Bacon, D. J. *Methods Enzymol.* **1997**, *277*, 505-524.

(8) Das, A.; Coulter, E. D.; Kurtz, D. M., Jr.; Ljungdahl, L. G. *J. Bacteriol.* **2001**, *183*, 1560-1567.

(9) Laskowski, R. A.; Hutchinson, E. G.; Michie, A. D.; Wallace, A. C.; Jones, M. L.; Thornton, J. M. *Trends Biochem. Sci.* **1997**, *22*, 488-490.

(10) Kadziola, A.; Abe, J.; Svensson, B.; Haser, R. *J. Mol. Biol.* **1994**, *239*, 104-121.

(11) Feig, A. L.; Bautista, M. T.; Lippard, S. J. *Inorg. Chem.* **1996**, *35*, 6892-6898.

(12) Jin, S.; Kurtz , D. M., Jr.; Liu, Z. J.; Rose, J.; Wang, B. C. *J. Am. Chem. Soc.* **2002**, *124*, 9845-9855.

(13) Voegtli, W. C.; Sommerhalter, M.; Saleh, L.; Baldwin, J.; Bollinger Jr., J. M.; Rosenzweig, A. C. *J. Am. Chem. Soc.* **2003**, *125*, 15822.

(14) Haskin, C. J.; Ravi, N.; Lynch, J. B.; Munck, R.; Que, L., Jr. *Biochemistry* **1995**, *34*, 11090-11098.

(15) Whittington, D. A.; Lippard, S. J. *J. Am. Chem. Soc.* **2001**, *123*, 827-838.

(16) Hendriks, J.; Oubrie, A.; Castresana, J.; Urbani, A.; Gemeinhardt, S.; Saraste, M. *Biochim. Biophys. Acta* **2000**, *1459*, 266-273.

(17) Silaghi-Dumitrescu, R. *Eur. J. Inorg. Chem.* **2003**, 1048-1052.

(18) Silaghi-Dumitrescu, R.; Silaghi-Dumitrescu, I. *Rev. Roum. Chim.* **2004**, *3-4*, 257-268.

(19) Wasser, I. M.; de Vries, S.; Moenne-Loccoz, P.; Schroeder, I.; Karlin, K. D. *Chem. Rev.* **2002**, *102*, 1201-1234.

(20) Shimizu, H.; Obayashi, E.; Gomi, Y.; Arakawa, H.; Park, S.-Y.; Nakamura, H.; Adachi, S.-i.; Shoun, H.; Shiro, Y. *J. Biol. Chem.* **2000**, *275*, 4816-4826.

(21) Gardner, A. M.; Helmick, R. A.; Gardner, P. R. *J. Biol. Chem.* **2002**, *277*, 8172-8177.

APPENDIX A

This Appendix shows a CLUSTAL X (1.81)[1] multiple amino sequence alignment with alignment quality curve (gray bar graphs at the bottom of each 50-residue stretch of aligned sequences) of the ~ 100 FprA sequences in the NCBI database as of May, 2004. The amino acid sequences of *D. gigas* ROO and *M. thermoacetica* FprA, for which crystal structures are available (cf. Chapter 6 and Ref. 2), are highlighted in yellow. Shown in red are amino acid residues serving as diiron ligands in *Moorella thermoacetica* FprA. Shown in blue are amino acid residues defining the substrate-binding cavity in *M. thermoacetica* FprA, as discussed in Chapter 6 and Appendix C.

		50
Methanosarcinamazei	--	
Methanosarcinabarkeri	--	
Methanosarcinaacetivorans_C2A	--	
Methanosarcinabarkeri_3_	--	
P.furiosusDSM3638_1_	--	
fprA-1[A.fulgidusDSM4304]	--	
FprA3[M.thermautotrophicus	--	
Thermoanaerobactertengcongensi	--	
PorphyromonasgingivalisW83	--	
BacteroidesthetaiotaomicronVPI	--	
FusobacteriumATCC25586_1_	--	
FusobacteriumATCC49256	--	
FusobacteriumATCC25586_2_	--	
FusobacteriumATCC49256_2_	--	
Clostr.tetaniE88_4_	--	
P.abyssi	--	
P.horikoshii	--	
P.furiosusDSM3638_2_	--	
Thermotogamaritima	--	
Shigella	--	
E.coli/O157_H7	--	
E.coli/O6/FlRd	--	
E.coli/K12	--	
E.coli/unknown	--	
S.typhimuriumLT2	--	
Salmonella	--	
gi|44480963|gb|EAJ57255.1|	--	
Anophelesgambiae	--	
E.coli_unknown_	--	
V.vulnificusYJ016	--	
V.vulnificusCMCP6	--	
Clostr.tetaniE88	--	
M.thermoacetica/fprA	--	
MethanosarcinaacetivoransC2A	--	
Methanosarcinabarkeri_2_	--	
Methanococcusmaripaludis_2_	--	
Methanococcusmaripaludis_3_	--	
Methanococcusjannaschii_2_	--	
M.thermoautotrophicum_DeltaH_	--	
FprA1/M.thermautotrophicus	--	
Methanothermobactermarburgensi	--	
FprA_II_Methanothermobacter	--	
Geobactermetallireducens	--	
GeobactersulfurreducensPCA	--	
DesulfovibriodesulfuricansG20	--	
D.gigas	--	
Methanococcusmaripaludis	--	
Methanococcusjannaschii	--	
Methanococcusjannaschii_3_	--	
fprA-2/A.fulgidusDSM4304	MSPHPFHTFNFQQVLFTARVSDDVVVVVKNLVHLLANFLQLLQGFLPLKM	
Giardiaintestinalis	--	
Spironucleusbarkhanus	--	
Trichomonasvaginalis	--	
Clostr.tetaniE88_2_	--	
Clostr.perfringens_3_	--	
Clostr.thermocellumATCC27405	--	
Clostr.perfringens_1_	--	
Clostr.perfringens_2_	--	
ChlorobiumtepidumTLS	--	
Clostr.acetobutylicum	--	
Clostr.tetaniE88_3_	--	
Clostr.acetobutylicum_2_	--	
Rhodobactercapsulatus_1_	--	
Rhodobactercapsulatus_2_	--	
Rhodobactersphaeroides	--	
Dechloromonasaromatica	--	
Wolinellasuccinogenes	--	
Nostocpunctiforme_1_	--	
NostocPCC7120_2_	--	
Nostocpunctiforme_3_	--	

```
NostocPCC7120_4_                  -------------------------------------------------- 50
TrichodesmiumerythraeumIMS101     --------------------------------------------------
SynechocystisPCC6803_1_           --------------------------------------------------
Gloeobacterviolaceus              --------------------------------------------------
NostocPCC7120_1_                  --------------------------------------------------
Nostocpunctiforme_5_              --------------------------------------------------
SynechocystisPCC6803_2_           --------------------------------------------------
Thermosynechococcuselongatus      --------------------------------------------------
SynechococcusWH8102               --------------------------------------------------
gi|44454558|gb|EAJ38476.1|        --------------------------------------------------
gi|44083259|gb|EAH03645.1|        --------------------------------------------------
ProchlorococcusmarinusMIT9313     --------------------------------------------------
ProchlorococcusmarinusCCMP1375    --------------------------------------------------
gi|43719610|gb|EAF14811.1|        --------------------------------------------------
gi|42845529|gb|EAA90143.1|        --------------------------------------------------
gi|44500849|gb|EAJ70075.1|        --------------------------------------------------
ProchlorococcusmarinusCCMP1378    --------------------------------------------------
gi|42832038|gb|EAA83473.1|        --------------------------------------------------
gi|44305658|gb|EAI33747.1|        --------------------------------------------------
gi|44606330|gb|EAK43227.1|        --------------------------------------------------
gi|44126537|gb|EAH26947.1|        --------------------------------------------------
gi|44102955|gb|EAH14255.1|        --------------------------------------------------
Nostocpunctiforme_2_              --------------------------------------------------
NostocPCC7120_3_                  --------------------------------------------------
SynechocystisPCC6803_3_           --------------------------------------------------
Nostocpunctiforme_4_              --------------------------------------------------
NostocPCC7120_5_                  --------------------------------------------------
Treponema                         --------------------------------------------------
                                  ==================================================

                                                                                  100
Methanosarcinamazei               -----------------------------------------MGMKNMKNY
Methanosarcinabarkeri             ----------------------------------------------MDIY
Methanosarcinaacetivorans_C2A     ----------------------MYRILVHFILRVNDSEESWRKSMEIY
Methanosarcinabarkeri_3_          --------------------------------------------------
P.furiosusDSM3638_1_              ----------------------------------------------------M
fprA-1[A.fulgidusDSM4304]         --------------------------------------------------
FprA3[M.thermautotrophicus        ---------------------------------------------------M
Thermoanaerobactertengcongensi    ---------------------------------------------------M
PorphyromonasgingivalisW83        ----------------------------------------------------MY
BacteroidesthetaiotaomicronVPI    ----------------------------------------------------ME
FusobacteriumATCC25586_1_         ----------------------------------------------------MY
FusobacteriumATCC49256            ----------------------------------------------------D
FusobacteriumATCC25586_2_         ----------------------------------------------------MH
FusobacteriumATCC49256_2_         ----------------------------------------------------MH
Clostr.tetaniE88_4_               ----------------------------------------------------MY
P.abyssi                          ----------------------------------------------MVKV
P.horikoshii                      ----------------------------------------MCMVKV
P.furiosusDSM3638_2_              ----------------------------------------------MPKV
Thermotogamaritima                ----------------------------------------------MPKI
Shigella                          --------------------------------------------------
E.coli/O157_H7                    --------------------------------------------------
E.coli/O6/FlRd                    --------------------------------------------------
E.coli/K12                        --------------------------------------------------
E.coli/unknown                    --------------------------------------------------
S.typhimuriumLT2                  --------------------------------------------------
Salmonella                        --------------------------------------------------
gi|44480963|gb|EAJ57255.1|        --------------------------------------------------
Anophelesgambiae                  --------------------------------------------------
E.coli_unknown_                   --------------------------------------------------
V.vulnificusYJ016                 --------------------------------------------------
V.vulnificusCMCP6                 --------------------------------------------------
Clostr.tetaniE88                  --------------------------------------------------
M.thermoacetica/fprA              ----------------------------------------------MS
MethanosarcinaacetivoransC2A      -----------------------------------------MGDMETEKTD
Methanosarcinabarkeri_2_          --------------------------------------------------
Methanococcusmaripaludis_2_       ----------------------------------------------MKA
Methanococcusmaripaludis_3_       ----------------------------------------------MKA
Methanococcusjannaschii_2_        ----------------------------------------MKKYES
```

```
M.thermoautotrophicum_DeltaH_       ----------------------------------------------MKA100
FprA1/M.thermautotrophicus          ---------------------------------------MCGDIMKA
Methanothermobactermarburgensi      ----------------------------------------------MKA
FprA_II_Methanothermobacter         ---------------------------------------MVFNMKA
Geobactermetallireducens            ----------------------------------------------MPV
GeobactersulfurreducensPCA          -----------------------------------------------M
DesulfovibriodesulfuricansG20       -----------------------------------------------M
D.gigas                             -----------------------------------------------M
Methanococcusmaripaludis            ------------------------------------------------
Methanococcusjannaschii             ----------------------------------------------MIL
Methanococcusjannaschii_3_          ---------------------------------------------MVKY
fprA-2/A.fulgidusDSM4304            VDPNFEVHGCPKPHSFKSFRFFLRLILHSELKNSKIERKFYRRGNEVNHM
Giardiaintestinalis                 ------------------------------------MSSKPKYV
Spironucleusbarkhanus               ------------------------------------------------
Trichomonasvaginalis                ---------------------------------MLSTSSARSFSALDL
Clostr.tetaniE88_2_                 ---------------------------------------MGVINMM
Clostr.perfringens_3_               ----------------------------------------------MN
Clostr.thermocellumATCC27405        ------------------------------------------------
Clostr.perfringens_1_               -----------------------------------------------M
Clostr.perfringens_2_               ------------------------------------------------
ChlorobiumtepidumTLS                ----------------------------------------MTDN
Clostr.acetobutylicum               -----------------------------------------------M
Clostr.tetaniE88_3_                 ---------------------------------------MIGGYNM
Clostr.acetobutylicum_2_            -----------------------------------------------M
Rhodobactercapsulatus_1_            ----------------------------MSVPPFTIRPAAPRLDGPT
Rhodobactercapsulatus_2_            ------------------------------------------------
Rhodobactersphaeroides              ------------------------------------MPPLP----AE
Dechloromonasaromatica              ----------------------------------------MAAAAITD
Wolinellasuccinogenes               ------------------------------------------------
Nostocpunctiforme_1_                ----------------------------MVAIA-------ENVQHRLTI
NostocPCC7120_2_                    ----------------------------MVSMSTTGNAHTENVQHRLTV
Nostocpunctiforme_3_                ----------------------------MVALT-------EKTEKRLTI
NostocPCC7120_4_                    ----------------------------MVALT-------EKTEKRLTI
TrichodesmiumerythraeumIMS101       ----------------------------MVAIT-------DPVKNRLTI
SynechocystisPCC6803_1_             ----------------------------MFTTP-------LPPQKRLST
Gloeobacterviolaceus                ----------------------------MQQT----------IQKRLTV
NostocPCC7120_1_                    ----------------------------MVALT--EDTQANANIGRLTV
Nostocpunctiforme_5_                ------------------------------------------------
SynechocystisPCC6803_2_             ----------------------------MVTLI--DSPTSAAVQPRLTL
Thermosynechococcuselongatus        ---------------------------------MAVTITKRPPRLTL
SynechococcusWH8102                 ------------------------------------MVVAAAAPKLSL
gi|44454558|gb|EAJ38476.1|          ------------------------------------MVVAPAAPKLSL
gi|44083259|gb|EAH03645.1|          ------------------------------------------------
ProchlorococcusmarinusMIT9313       ----------------------------MNVASKDTTVTTASTAPRLSL
ProchlorococcusmarinusCCMP1375      ----------------------------MSTNSRAVIEQKITSPRLSL
gi|43719610|gb|EAF14811.1|          ------------------------------------------------
gi|42845529|gb|EAA90143.1|          ----------------------------MVFTESTALENQKGDTPKLSL
gi|44500849|gb|EAJ70075.1|          ----------------------------MITSSKTNTSDINKVEQKLSV
ProchlorococcusmarinusCCMP1378      ----------------------------MITSAKTSSSEMNKVEQKLSV
gi|42832038|gb|EAA83473.1|          ------------------------------------------------
gi|44305658|gb|EAI33747.1|          ----------------------------MIASAETSNSKLAQTNNKLTV
gi|44606330|gb|EAK43227.1|          ----------------------------MIASARTSNSKLAQTNNKLTV
gi|44126537|gb|EAH26947.1|          ---------------------------------------TNNKLTV
gi|44102955|gb|EAH14255.1|          ------------------------------------------------
Nostocpunctiforme_2_                ------------------------MPNSPLLTEVIMSVATLTPNHSRDV
NostocPCC7120_3_                    ---------------------------------MTIATSS--RPRDV
SynechocystisPCC6803_3_             -------------------MISPIGGLSQALHSPSDSIFVAS--LPRDI
Nostocpunctiforme_4_                ---------------------------------MTNS--KPRDV
NostocPCC7120_5_                    ---------------------------------MSDS--KPRDV
Treponema                           -----------------------------------------------M
```

```
                                                                                150
Methanosarcinamazei                 NIPEIARN----------------VFWVGAKDWNRRMFDA-LIPLPQGT
Methanosarcinabarkeri               SVPEIAKD----------------VFWVGAKDWSRRMFDA-LVPLPQGT
Methanosarcinaacetivorans_C2A       NIPEIARN----------------VFGVGSKDWNRRIFDS-LIPLPEGT
Methanosarcinabarkeri_3_            ------------------------------------------------
P.furiosusDSM3638_1_                KSVKLLDG----------------VYWVGVKDWSRRIFDS-LIPLPEGT
fprA-1[A.fulgidusDSM4304]           ------------------------------------------------
```

```
FprA3[M.thermautotrophicus          TAKRIADG----------------VYYTGTIDWDRRTFDE-LVTLPRGT150
Thermoanaerobactertengcongensi      KAMVIKPG----------------VSKIGAVHWERRLFDS-LIPLPDGT
PorphyromonasgingivalisW83          QVPQVTDS----------------VYYVGVNDRSKSLFEN-MWPLPYGV
BacteroidesthetaiotaomicronVPI      QKTRIKGN----------------VHYVGVNDRNKHRFEA-LWPLPYGV
FusobacteriumATCC25586_1_           CCTKINDD----------------IIWIGINDRKTERFEN-YIPLDNGV
FusobacteriumATCC49256              SYRANRDD----------------IIWIGVNDRKTERFEN-YIPLDNGI
FusobacteriumATCC25586_2_           NVRKITED----------------LYWIGANDRRLALFEN-IHPIPEGV
FusobacteriumATCC49256_2_           NVRNITED----------------LYWIGANDRRLALFEN-IHPIPEGV
Clostr.tetaniE88_4_                 CVRKITED----------------LYWVGGNDRRLALFEN-IHPIPKGV
P.abyssi                            WIEKLLEEPE--------------LYLLRVDDDRIRYFEA-TWDIPEGI
P.horikoshii                        WVEKLLDEPE--------------LYILRLDDSEIKHFEA-AWSIPEGI
P.furiosusDSM3638_2_                WIEKLTEDME--------------LYLIRVDDDQIKYFEA-AWDIPEGI
Thermotogamaritima                  WTERIFDDPE--------------IYVLRIDDDRIRYFEA-VWEIPEGI
Shigella                            MSIVVKNN----------------IHWVGQRDWEVRDFHGTEYKTLRGS
E.coli/O157_H7                      MSIVVKNN----------------IHWVGQRDWEVRDFHGTEYKTLRGS
E.coli/O6/FlRd                      MSIVVKNN----------------IHWVGQRDWEVRDFHGTEYKTLRGS
E.coli/K12                          MSIVVKNN----------------IHWVGQRDWEVRDFHGTEYKTLRGS
E.coli/unknown                      ----------------------------------------|---|------
S.typhimuriumLT2                    MSILVKNN----------------IHWVGQRDWEVRDFHGTEYKTLRGS
Salmonella                          MSILVKNN----------------IHWVGQRDWEVRDFHGTEYKTLRGS
gi|44480963|gb|EAJ57255.1|          MSIHVKNN----------------IHWVGQRDWEVRDFHGTEYKTHKGT
Anophelesgambiae                    ------------------------------DWEVRDFHGTEYKTHKGT
E.coli_unknown_                     MSIVVKNN----------------IHWVGQRDWEVRDFHGTEYKTLRGS
V.vulnificusYJ016                   MTIHVKNN----------------IHWVGQRDWEVQDFHGTEYKMTKGT
V.vulnificusCMCP6                   MTIHVKNN----------------IHWVGQRDWEVQDFHGTEYKMTKGT
Clostr.tetaniE88                    MSFKVTNK----------------VTWVGKIDWELRRFHGDEYSTHRGT
M.thermoacetica/fprA                QPVAITDG----------------IYWVGAVDWNIRYFHGPAFSTHRGT
MethanosarcinaacetivoransC2A        GAVEIARG----------------VYWVGAIDWNGRDFHG--FTTPGGT
Methanosarcinabarkeri_2_            ----------------------------------------|---|------
Methanococcusmaripaludis_2_         DAVKISEG----------------VYWVGTYDWDIRSYHG--YTLKG-T
Methanococcusmaripaludis_3_         DAVKISEG----------------VYWVGTYDWDIRSYHG--YTLKG-T
Methanococcusjannaschii_2_          RRSKIADG----------------VYWVGVLDWDIRMYHG--YTLKG-T
M.thermoautotrophicum_DeltaH_       RAEKIADG----------------LYWTGVLDWDIRNYHG--YTLQG-T
FprA1/M.thermautotrophicus          RAEKIADG----------------LYWTGVLDWDIRNYHG--YTLQG-T
Methanothermobactermarburgensi      AAKRISDG----------------VYWTGVLDWDLRNYHG--YTLQG-T
FprA_II_Methanothermobacter         DAVKIADG----------------VYWVGVMDWDIRSYHG--YTLGG-T
Geobactermetallireducens            KAVEIKKD----------------IYWVGAVDWAVRDFHG-YET-PRGT
GeobactersulfurreducensPCA          KAVEIKQG----------------VFWVGAVDWAVRDFHG-YET-PRGT
DesulfovibriodesulfuricansG20       QAARIISSKTHTQDETMKALEIKKDVFWVGAVDYDSRDFHG-YSLSPQGT
D.gigas                             QATKIIDG----------------FHLVGAIDWNSRDFHG-YTLSPMGT
Methanococcusmaripaludis            MAVTLKEG----------------VYWVGAIDWNIREFHG-YET-KDGS
Methanococcusjannaschii             MVLEIKNG----------------IYWVGVIDWEIRDFHG-YGT-PYGS
Methanococcusjannaschii_3_          MVLKIKDN----------------IYCMSFIEWKIKEYRG-LDI-EKGT
fprA-2/A.fulgidusDSM4304            KPVELKDG----------------VFWVGAIDWDERDFHN-FVT-ARGL
Giardiaintestinalis                 QDQEMIPG----------------VYWVGIVDWMVRIFHG--YHTDEGS
Spironucleusbarkhanus               NPQPMLDD----------------IHWVGIVDWAVRIFHG--YHTDEGS
Trichomonasvaginalis                GVTKVADD----------------VLWIGVNDWDLREFHS--MQSPVGT
Clostr.tetaniE88_2_                 KNVIIKEK----------------IYLVGKIDDRDVPFHR--LTLTKGT
Clostr.perfringens_3_               KEIKLRND----------------IYSVGVIDNRPVPFHR--LILEKGT
Clostr.thermocellumATCC27405        ----------------------------------------|---|------
Clostr.perfringens_1_               NYLEVKKD----------------IYWVGSLDPELRVFDI-IMYTPYGT
Clostr.perfringens_2_               ----------------------------------------|---MYTPYGT
ChlorobiumtepidumTLS                KILPITDD----------------VSWIGVLDPGLITFDI-VMETKYGT
Clostr.acetobutylicum               SAEKLCEN----------------VYWVGVKDQKLRVFDI-IMNTKKGS
Clostr.tetaniE88_3_                 SSFKIRDN----------------IYSVGVKDPDLRVFDI-IMETNGGT
Clostr.acetobutylicum_2_            PAIKIKDN----------------IFSVGVLNPSLRIFDI-IMKTEYGT
Rhodobactercapsulatus_1_            GPVAVAPG----------------VHWVGALDPGLRNFDV-ILKTANGT
Rhodobactercapsulatus_2_            ----------------------------------------|---|------
Rhodobactersphaeroides              GPVEIVPG----------------VHWIGAFDPGLRSFDT-LMKTANGT
Dechloromonasaromatica              SAVEIAPG----------------VHWVGALDPHLRSFDI-ILKTANGT
Wolinellasuccinogenes               MRTLLAPS----------------VHWVGVKDPELAIFDI-VVPTEHGT
Nostocpunctiforme_1_                QTVEIAPN----------------TTAIRSLDWDRDRFDI-EFGLQNGT
NostocPCC7120_2_                    ETVEIAPN----------------TTAIRCLDWDRDRFDI-EFGLQNGT
Nostocpunctiforme_3_                QTVEIAQE----------------TTAIRSLDWDRDRFDI-EFGLQNGT
NostocPCC7120_4_                    QTADIAQD----------------TTAIRSLDWERDRFDI-EFGLQNGT
TrichodesmiumerythraeumIMS101       ETNKIASD----------------TMAIRSLDWDRDRFDI-EFGLQNGT
SynechocystisPCC6803_1_             QTEAIAKN----------------ITAIRSLDWDRDRFDI-EFGLQNGT
Gloeobacterviolaceus                QSGAVAPE----------------TVAMRCLDWDRDRFDI-EFGLQNGT
NostocPCC7120_1_                    QTVEIADE----------------TTAIRCLDWDRERFDI-EFGLRNGT
Nostocpunctiforme_5_                ----------------------------------------|---|------
SynechocystisPCC6803_2_             QTADIAAH----------------TTAIRCLDWDRDRFDI-EFELRHGT
```

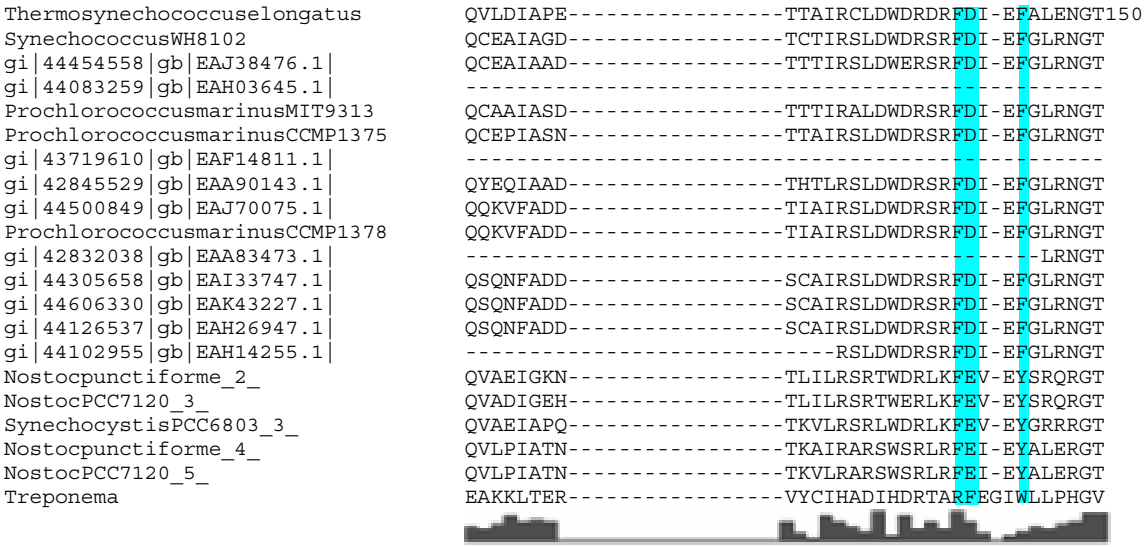
Thermosynechococcuselongatus QVLDIAPE----------TTAIRCLDWDRDRFDI-EFALENGT150
SynechococcusWH8102 QCEAIAGD----------TCTIRSLDWDRSRFDI-EFGLRNGT
gi|44454558|gb|EAJ38476.1| QCEAIAAD----------TTTIRSLDWERSRFDI-EFGLRNGT
gi|44083259|gb|EAH03645.1| ----------
ProchlorococcusmarinusMIT9313 QCAAIASD----------TTTIRALDWDRSRFDI-EFGLRNGT
ProchlorococcusmarinusCCMP1375 QCEPIASN----------TTAIRSLDWDRSRFDI-EFGLRNGT
gi|43719610|gb|EAF14811.1| ----------
gi|42845529|gb|EAA90143.1| QYEQIAAD----------THTLRSLDWDRSRFDI-EFGLRNGT
gi|44500849|gb|EAJ70075.1| QQKVFADD----------TIAIRSLDWDRSRFDI-EFGLRNGT
ProchlorococcusmarinusCCMP1378 QQKVFADD----------TIAIRSLDWDRSRFDI-EFGLRNGT
gi|42832038|gb|EAA83473.1| ----------LRNGT
gi|44305658|gb|EAI33747.1| QSQNFADD----------SCAIRSLDWDRSRFDI-EFGLRNGT
gi|44606330|gb|EAK43227.1| QSQNFADD----------SCAIRSLDWDRSRFDI-EFGLRNGT
gi|44126537|gb|EAH26947.1| QSQNFADD----------SCAIRSLDWDRSRFDI-EFGLRNGT
gi|44102955|gb|EAH14255.1| ----------RSLDWDRSRFDI-EFGLRNGT
Nostocpunctiforme_2_ QVAEIGKN----------TLILRSRTWDRLKFEV-EYSRQRGT
NostocPCC7120_3_ QVADIGEH----------TLILRSRTWERLKFEV-EYSRQRGT
SynechocystisPCC6803_3_ QVAEIAPQ----------TKVLRSRLWDRLKFEV-EYGRRRGT
Nostocpunctiforme_4_ QVLPIATN----------TKAIRARSWSRLRFEI-EYALERGT
NostocPCC7120_5_ QVLPIATN----------TKVLRARSWSRLRFEI-EYALERGT
Treponema EAKKLTER----------VYCIHADIHDRTARFEGIWLLPHGV

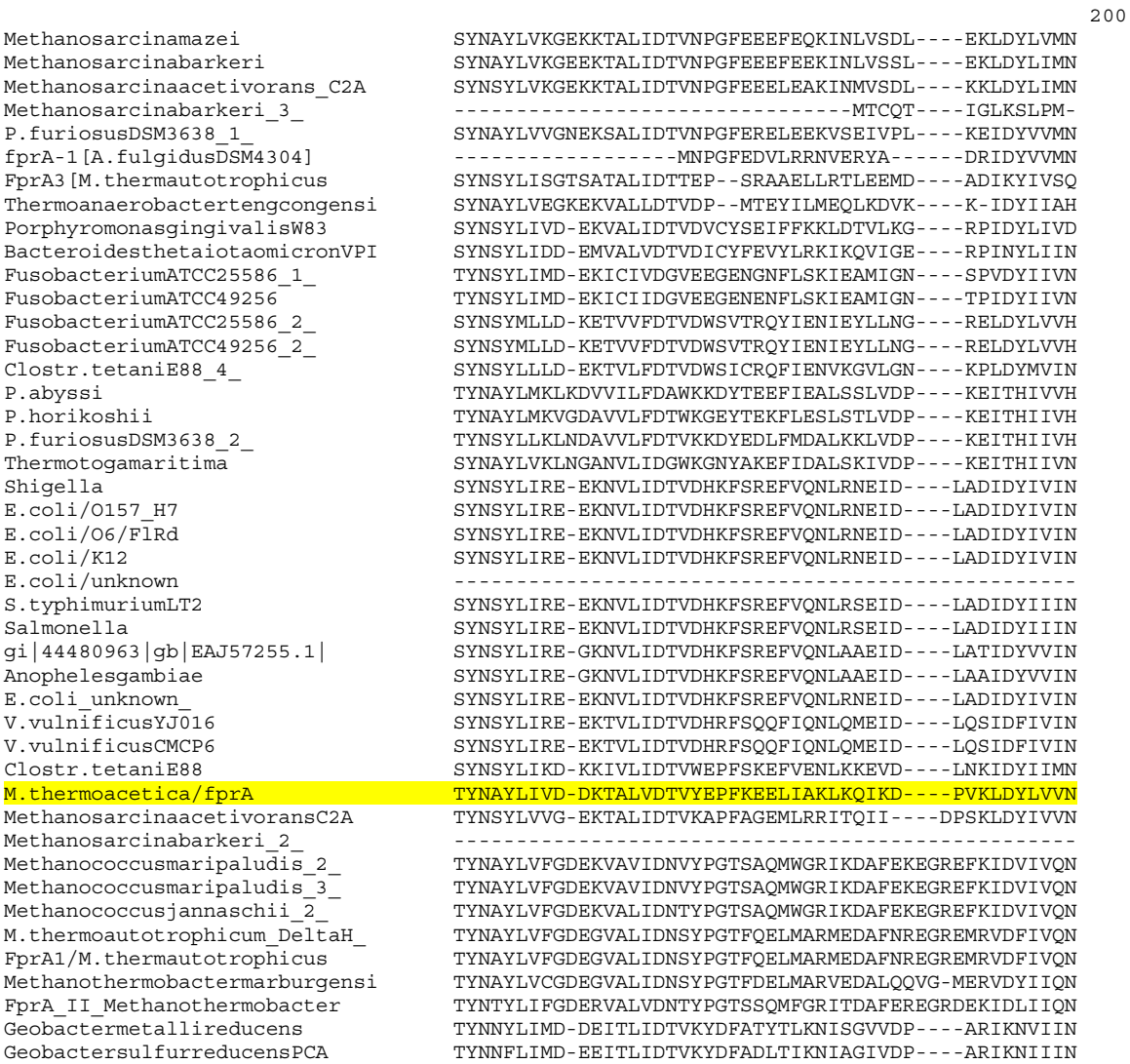
200
Methanosarcinamazei SYNAYLVKGEKKTALIDTVNPGFEEEFEQKINLVSDL----EKLDYLVMN
Methanosarcinabarkeri SYNAYLVKGEEKTALIDTVNPGFEEEFEEKINLVSSL----EKLDYLIMN
Methanosarcinaacetivorans_C2A SYNSYLVKGEKKTALIDTVNPGFEEELEAKINMVSDL----KKLDYLIMN
Methanosarcinabarkeri_3_ ----------MTCQT----IGLKSLPM-
P.furiosusDSM3638_1_ SYNAYLVVGNEKSALIDTVNPGFERELEEKVSEIVPL----KEIDYVVMN
fprA-1[A.fulgidusDSM4304] ----------MNPGFEDVLRRNVERYA------DRIDYVVMN
FprA3[M.thermautotrophicus SYNSYLISGTSATALIDTTEP--SRAAELLRTLEEMD----ADIKYIVSQ
Thermoanaerobactertengcongensi SYNAYLVEGKEKVALLDTVDP--MTEYILMEQLKDVK----K-IDYIIAH
PorphyromonasgingivalisW83 SYNSYLIVD-EKVALIDTVDVCYSEIFFKKLDTVLKG----RPIDYLIVD
BacteroidesthetaiotaomicronVPI SYNSYLIDD-EMVALVDTVDICYFEVYLRKIKQVIGE----RPINYLIIN
FusobacteriumATCC25586_1_ TYNSYLIMD-EKICIVDGVEEGENGNFLSKIEAMIGN----SPVDYIIVN
FusobacteriumATCC49256 TYNSYLIMD-EKICIIDGVEEGENENFLSKIEAMIGN----TPIDYIIVN
FusobacteriumATCC25586_2_ SYNSYMLLD-KETVVFDTVDWSVTRQYIENIEYLLNG----RELDYLVVH
FusobacteriumATCC49256_2_ SYNSYMLLD-KETVVFDTVDWSVTRQYIENIEYLLNG----RELDYLVVH
Clostr.tetaniE88_4_ SYNSYLLLD-EKTVLFDTVDWSICRQFIENVKGVLGN----KPLDYMVIN
P.abyssi TYNAYLMKLKDVVILFDAWKKDYTEEFIEALSSLVDP----KEITHIVVH
P.horikoshii TYNAYLMKVGDAVVLFDTWKGEYTEKFLESLSTLVDP----KEITHIIVH
P.furiosusDSM3638_2_ TYNSYLLKLNDAVVLFDTVKKDYEDLFMDALKKLVDP----KEITHIIVH
Thermotogamaritima SYNAYLVKLNGANVLIDGWKGNYAKEFIDALSKIVDP----KEITHIIVN
Shigella SYNSYLIRE-EKNVLIDTVDHKFSREFVQNLRNEID----LADIDYIVIN
E.coli/O157_H7 SYNSYLIRE-EKNVLIDTVDHKFSREFVQNLRNEID----LADIDYIVIN
E.coli/O6/FlRd SYNSYLIRE-EKNVLIDTVDHKFSREFVQNLRNEID----LADIDYIVIN
E.coli/K12 SYNSYLIRE-EKNVLIDTVDHKFSREFVQNLRNEID----LADIDYIVIN
E.coli/unknown ----------
S.typhimuriumLT2 SYNSYLIRE-EKNVLIDTVDHKFSREFVQNLRSEID----LADIDYIIIN
Salmonella SYNSYLIRE-EKNVLIDTVDHKFSREFVQNLRSEID----LADIDYIIIN
gi|44480963|gb|EAJ57255.1| SYNSYLIRE-GKNVLIDTVDHKFSREFVQNLAAEID----LATIDYVVIN
Anophelesgambiae SYNSYLIRE-GKNVLIDTVDHKFSREFVQNLAAEID----LAAIDYVVIN
E.coli_unknown_ SYNSYLIRE-EKNVLIDTVDHKFSREFVQNLRNEID----LADIDYIVIN
V.vulnificusYJ016 SYNSYLIRE-EKTVLIDTVDHRFSQQFIQNLQMEID----LQSIDFIVIN
V.vulnificusCMCP6 SYNSYLIRE-EKTVLIDTVDHRFSQQFIQNLQMEID----LQSIDFIVIN
Clostr.tetaniE88 SYNSYLIKD-KKIVLIDTVWEPFSKEFVENLKKEVD----LNKIDYIIMN
M.thermoacetica/fprA TYNAYLIVD-DKTALVDTVYEPFKEELIAKLKQIKD----PVKLDYLVVN
MethanosarcinaacetivoransC2A TYNSYLVVG-EKTALIDTVKAPFAGEMLRRITQII----DPSKLDYIVVN
Methanosarcinabarkeri_2_ ----------
Methanococcusmaripaludis_2_ TYNAYLVFGDEKVAVIDNVYPGTSAQMWGRIKDAFEKEGREFKIDVIVQN
Methanococcusmaripaludis_3_ TYNAYLVFGDEKVAVIDNVYPGTSAQMWGRIKDAFEKEGREFKIDVIVQN
Methanococcusjannaschii_2_ TYNAYLVFGDEKVALIDNTYPGTSAQMWGRIKDAFEKEGREFKIDVIVQN
M.thermoautotrophicum_DeltaH_ TYNAYLVFGDEGVALIDNSYPGTFQELMARMEDAFNREGREMRVDFIVQN
FprA1/M.thermautotrophicus TYNAYLVFGDEGVALIDNSYPGTFQELMARMEDAFNREGREMRVDFIVQN
Methanothermobactermarburgensi TYNAYLVCGDEGVALIDNSYPGTFDELMARVEDALQQVG-MERVDYIIQN
FprA_II_Methanothermobacter TYNTYLIFGDERVALVDNTYPGTSSQMFGRITDAFEREGRDEKIDLIIQN
Geobactermetallireducens TYNNYLIMD-DEITLIDTVKYDFATYTLKNISGVVDP----ARIKNVIIN
GeobactersulfurreducensPCA TYNNFLIMD-EEITLIDTVKYDFADLTIKNIAGIVDP----ARIKNIIIN

```
DesulfovibriodesulfuricansG20       TYNAYVVKD-EKTVLFDNVKEGFLPTMLCRLSQVTEL----EKIDYIVCN200
D.gigas                             TYNAYLVED-EKTTLFDTVKAEYKGELLCGIASVIDP----KKIDYLVIQ
Methanococcusmaripaludis            SYNSYLIED-EKIVLIDTVKKYLFDEFYGRIKKVVDP----EKIDYIVVN
Methanococcusjannaschii             TYNSYLIKD-KKNVLIDTAKDYMFNELIYGISKFIDP----KDLDYIIVN
Methanococcusjannaschii_3_          TYNSYLILD-KNNVIIDTTRIKYFDELLSYLKDVAN-----LKLDYIISN
fprA-2/A.fulgidusDSM4304            TYNSYLIVD-DKVVLVDTVKHKFVKESMERIRKLVDP----SQIDYVIVN
Giardiaintestinalis                 SYNSYFIDD-ECPTVIDSVKYPFAEEWLSRIAACCP----LDKIKYVVMN
Spironucleusbarkhanus               SYNSYLIMD-EQPTLIDSVKYPFVQEHLERIQAVCA----LDKIKFIIMN
Trichomonasvaginalis                SYNSYLIQS-SEPTIVDAVKYTMAHAWIDRLKSIGGDD--LKGIKRIIVQ
Clostr.tetaniE88_2_                 TYNSYLLLT-EKPTIIDTVDISFGREYIQSLKNLIDL----DKIQYIVIN
Clostr.perfringens_3_               TYNSYLLKT-RKPTVIDTVDLIYTKDFLNNLKEIIDL----KDISYIVIN
Clostr.thermocellumATCC27405        ------------------MDIEFGKEYVDNLSKIIDP----ENIEYIVIN
Clostr.perfringens_1_               TYNSYVVKGSEKIAVFETVKEKCFDDYLSKLNSLG---IDPKSIDYIVVD
Clostr.perfringens_2_               TYNSYVVKGSEKTAIFETVKAEFFDQYIARLKDLG---VEPSEIDYIVVS
ChlorobiumtepidumTLS                TYNSYFIN-AEKKTVVETTKVKFWPTYIEKLKKV----VNPEEIEYIIVD
Clostr.acetobutylicum               TYNSYLIN-DDKVAIIDTVKDGFYDEFLKSIKSV----IGDKKVDYIVVQ
Clostr.tetaniE88_3_                 TYNSYLID-DEKVAIIDTVKDGFYDKFYSNIKEV----IGERKVDYIIVQ
Clostr.acetobutylicum_2_            SYNAYLIK-GKKNVLIDTVHGRFFDEYLENIKSV----IDPSSIDYVIMN
Rhodobactercapsulatus_1_            TYNAYAVRGSEGVAVIDTVKAEFAGDFFARLEAV----ARYDEIRLIVLN
Rhodobactercapsulatus_2_            --------------MIDTVKAEFAGDFFARLEAV----ARYDEIRLIVLN
Rhodobactersphaeroides              SYNAYTVRGAAGVAVIDTVHADHAETFFARLEAV----ARYDEITQIVLN
Dechloromonasaromatica              SYNSYVVRGDNGVAIIDTVKENFADDFFRRLESV----AEYEEITTIVLN
Wolinellasuccinogenes               TYNSYLIQGSEKCALIDTSKANFSKEYFTHLEKH----LPLQKIDYIVVQ
Nostocpunctiforme_1_                TYNSYLIR-GEQTVLIDTSHQKFRDLYLETLKGL----VNPKTIDYIIVS
NostocPCC7120_2_                    TYNSYLIR-GEQTVLVDTSHQKFRQLYLETLKGL----INPKAIDYIIVS
Nostocpunctiforme_3_                TYNSFLIR-GEQTALVDTSHEKFRQLYFDTLTGL----IKPTEIDYLIIS
NostocPCC7120_4_                    TYNSFLIR-GEQIALVDTSHEKFRQLYFDTLTGL----INPTEINYLIIS
TrichodesmiumerythraeumIMS101       TYNSFIIQ-GEKTALVDTSHGKFRQLYLDTLLGL----IKPTEIDYLIIS
SynechocystisPCC6803_1_             TYNSYLIQ-ADKVALVDSSHEKFRQLYLDLLQGL----IDPQRIDYLIVS
Gloeobacterviolaceus                TYNSYLIE-GEQVALVDTSHEKFRSLYLDLLKGH----IDPKRIDYLVIS
NostocPCC7120_1_                    TYNSFLIK-GEKIALVDTSHRKFEKLYLEIVAGL----IDPNTIDYLIVS
Nostocpunctiforme_5_                ------------------------------MGL----IDPTKIDYLIIS
SynechocystisPCC6803_2_             TYNSFLIR-GEKTALIDTSHRKFEAVYLQLLQDL----VDLRSLDYLIVN
Thermosynechococcuselongatus        TYNSFLIK-GERIALVDTSHAKFGDRYLEQLWQL----VNPSDLDYLIVS
SynechococcusWH8102                 TYNAFLVR-GERTALIDTSHAKFRDTWIPLLKEQ----IEPTAIDVLIVS
gi|44454558|gb|EAJ38476.1|          TYNAFLVR-GERTALIDTSHAKFRDTWIPLLKEQ----IDPTAIDVLIVS
gi|44083259|gb|EAH03645.1|          -------R-GERTALIDTSHAKFRDTWIPLLKDQ----IDPSTIDVLIVS
ProchlorococcusmarinusMIT9313       TYNSFLVR-GAKTALIDTNHLKFEDTWLPMLKQQ----IDPKAIDYLIIS
ProchlorococcusmarinusCCMP1375      TYNSFIIQ-GEKTALIDSSHVKFRSTWVDALTKC----IDPKTIDFLIVS
gi|43719610|gb|EAF14811.1|          ----FLIR-GKKTALIDTSHLKFKDIWFEKLRQE----INPTEIDYLIVS
gi|42845529|gb|EAA90143.1|          TYNSFLIR-GKKTALIDTSHLKFKDIWFKKLRQE----INPTEIDYLIVS
gi|44500849|gb|EAJ70075.1|          TYNSFIIK-GKKLAIIDTSHAKFEKLWFEQLLRE----VNPEEIDYLITS
ProchlorococcusmarinusCCMP1378      TYNSFIIK-GQKIAIIDTSHAKFEKLWFEQLLRE----VNPEEIDYLITS
gi|42832038|gb|EAA83473.1|          TYNSFIIK-GQKLAIIDTSHAKFEKLWFEQLLKE----INPKEIDYLITS
gi|44305658|gb|EAI33747.1|          TYNSFIIK-GEKLAIIDTSHAKFEELWFEELLKK----VNPQEVDYLITS
gi|44606330|gb|EAK43227.1|          TYNSFIIK-GEKLAIIDTSHAKFEELWFGELLKK----VNPQEVDYLITS
gi|44126537|gb|EAH26947.1|          TYNSFIIK-GEKLAIIDTSHAKFEELWFEELLKK----VNPQEVDYLITS
gi|44102955|gb|EAH14255.1|          TYNSFIIR-GEKIAIIDTSHAKFEELWFEELLKK----INPQEVDYLISS
Nostocpunctiforme_2_                TANSYLIQ-GEKKALIDPPGESFTEIYLEQLAQY----LDFISLDYIVLS
NostocPCC7120_3_                    TANSYLIQ-ADKKALIDPPGESFTAIYLEQLAQY----LDFTTLDYIILG
SynechocystisPCC6803_3_             TSNSYLIQ-ADHTALIDPPGESFCDLYLAELPKY----LDLAQLDYIVAS
Nostocpunctiforme_4_                TSNCYLIE-ADKTALIDPPPESFTEIYLEALRQT----LDLQSLDYIILG
NostocPCC7120_5_                    TSNSYVIE-GDKTAIIDPPVESFMKIYLEALQQT----VNLKKLDYVILG
Treponema                           SINSYVVK-GEKTALIDIVKDWDGSVDSYRKQLESIG-LSFSSFDYVILN
```

```
                                                                                    250
Methanosarcinamazei                 HAEPDHSSAIRYIMDKAPDSILVA--TERGIKMAGLYHELPE-DRIKVVA
Methanosarcinabarkeri               HAEPDHASAIRYIMDRAPGSVLVT--TERGVKMASLYHDLPD-DRIKVVA
Methanosarcinaacetivorans_C2A       HAEPDHANAIRFILEKAPEALFVT--TKKGVKMAKLYHELPE-ARIKIVA
Methanosarcinabarkeri_3_            ------------------EILLIW--EEK---ICTLLRLPGS-TGLKPCS
P.furiosusDSM3638_1_                HAEPDHAGAIPYIMERNKKALLIT--TEKGKELAKAYYNVPD-ERIIVVK
fprA-1[A.fulgidusDSM4304]           HAEPDHAGAIPFIME-SSDALLVT--TKKGAEMAKFYYDVPE-SRVRVVE
FprA3[M.thermautotrophicus          HAEQDHSGTIPELLEIYPEAEVIG--TPACIELLQELLRING-N-FREVK
Thermoanaerobactertengcongensi      HAEQDHSGSIPAVLEKYKEAKVVC--TPKAKTFLIDLLPIPE-DKFITVE
PorphyromonasgingivalisW83          HMEPDHSGSIGLLRQRYPNMQIVGNKKTHGMLE--GYHHIT--EGLLEVK
BacteroidesthetaiotaomicronVPI      HMEPDHSGSIRLIKQHYPDIIIVGNKQTFGMIE--GFYGVT--GEQYLVK
FusobacteriumATCC25586_1_           HVEPDHSGSIKNMLKIYPELKVVGNAKTIMMLKLLGLDLPD--ERVVIVK
```

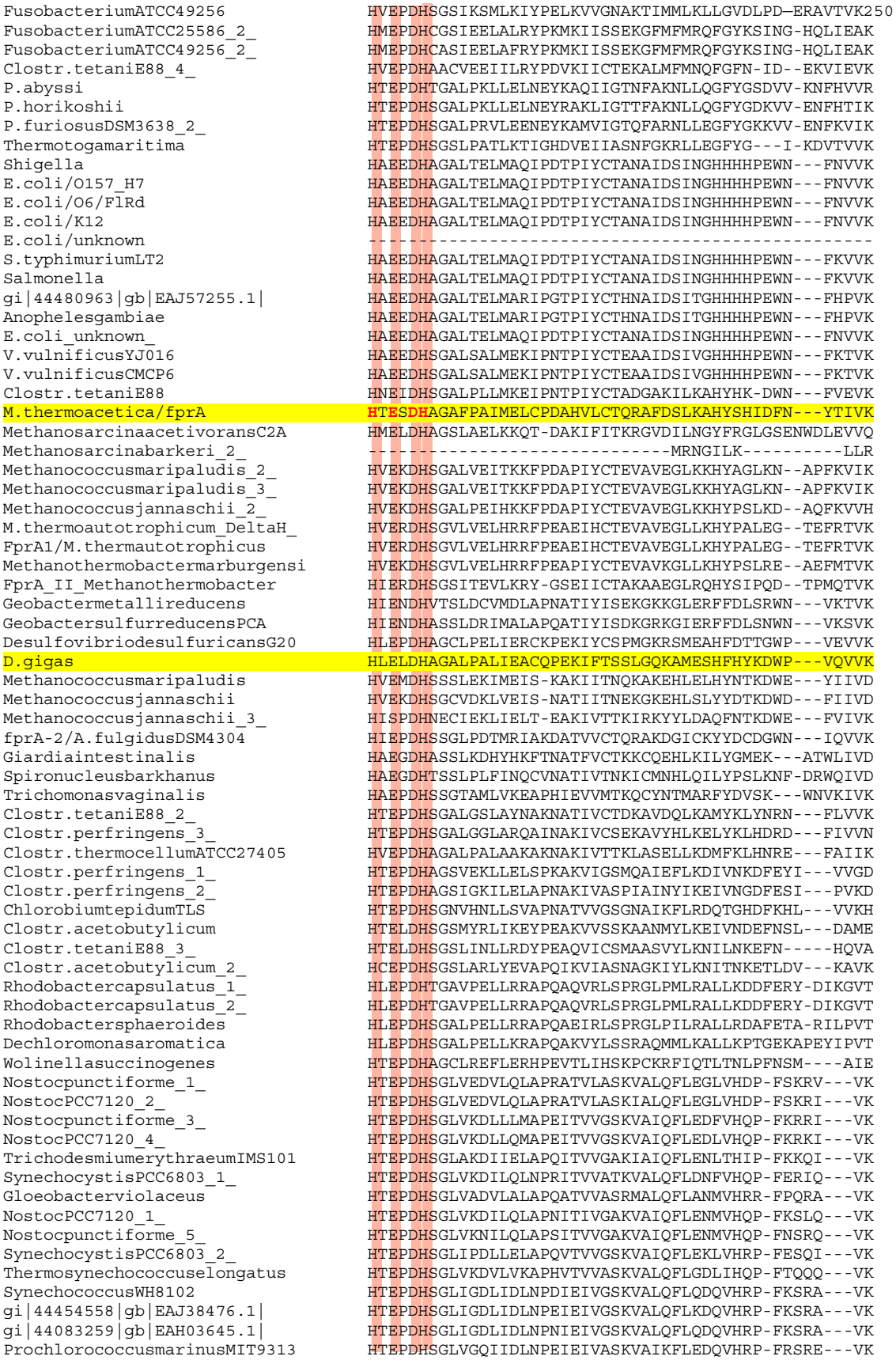
FusobacteriumATCC49256 HVEPDHSGSIKSMLKIYPELKVVGNAKTIMMLKLLGVDLPD—ERAVTVK250
FusobacteriumATCC25586_2_ HMEPDHCGSIEELALRYPKMKIISSEKGFMFMRQFGYKSING-HQLIEAK
FusobacteriumATCC49256_2_ HMEPDHCASIEELAFRYPKMKIISSEKGFMFMRQFGYKSING-HQLIEAK
Clostr.tetaniE88_4_ HVEPDHAACVEEIILRYPDVKIICTEKALMFMNQFGFN-ID--EKVIEVK
P.abyssi HTEPDHTGALPKLLELNEYKAQIIGTNFAKNLLQGFYGSDVV-KNFHVVR
P.horikoshii HTEPDHSGALPKLLELNEYRAKLIGTTFAKNLLQGFYGDKVV-ENFHTIK
P.furiosusDSM3638_2_ HTEPDHSGALPRVLEENEYKAMVIGTQFARNLLEGFYGKKVV-ENFKVIK
Thermotogamaritima HTEPDHSGSLPATLKTIGHDVEIIASNFGKRLLEGFYG---I-KDVTVVK
Shigella HAEEDHAGALTELMAQIPDTPIYCTANAIDSINGHHHHPEWN---FNVVK
E.coli/O157_H7 HAEEDHAGALTELMAQIPDTPIYCTANAIDSINGHHHHPEWN---FNVVK
E.coli/O6/FlRd HAEEDHAGALTELMAQIPDTPIYCTANAIDSINGHHHHPEWN---FNVVK
E.coli/K12 HAEEDHAGALTELMAQIPDTPIYCTANAIDSINGHHHHPEWN---FNVVK
E.coli/unknown ----------
S.typhimuriumLT2 HAEEDHAGALTELMAQIPDTPIYCTANAIDSINGHHHHPEWN---FKVVK
Salmonella HAEEDHAGALTELMAQIPDTPIYCTANAIDSINGHHHHPEWN---FKVVK
gi|44480963|gb|EAJ57255.1| HAEEDHAGALTELMARIPGTPIYCTHNAIDSITGHHHHPEWN---FHPVK
Anophelesgambiae HAEEDHAGALTELMARIPGTPIYCTHNAIDSITGHHHHPEWN---FHPVK
E.coli_unknown_ HAEEDHAGALTELMAQIPDTPIYCTANAIDSINGHHHHPEWN---FNVVK
V.vulnificusYJ016 HAEEDHSGALSALMEKIPNTPIYCTEAAIDSIVGHHHHPEWN---FKTVK
V.vulnificusCMCP6 HAEEDHSGALSALMEKIPNTPIYCTEAAIDSIVGHHHHPEWN---FKTVK
Clostr.tetaniE88 HNEIDHSGALPLLMKEIPNTPIYCTADGAKILKAHYHK-DWN---FVEVK
M.thermoacetica/fprA HTESDHAGAFPAIMELCPDAHVLCTQRAFDSLKAHYSHIDFN---YTIVK
MethanosarcinaacetivoransC2A HMELDHAGSLAELKKQT-DAKIFITKRGVDILNGYFRGLGSENWDLEVVQ
Methanosarcinabarkeri_2_ ----------MRNGILK----------LLR
Methanococcusmaripaludis_2_ HVEKDHSGALVEITKKFPDAPIYCTEVAVEGLKKHYAGLKN--APFKVIK
Methanococcusmaripaludis_3_ HVEKDHSGALVEITKKFPDAPIYCTEVAVEGLKKHYAGLKN--APFKVIK
Methanococcusjannaschii_2_ HVEKDHSGALPEIHKKFPDAPIYCTEVAVEGLKKHYPSLKD--AQFKVVH
M.thermoautotrophicum_DeltaH_ HVERDHSGVLVELHRRFPEAEIHCTEVAVEGLLKHYPALEG--TEFRTVK
FprA1/M.thermautotrophicus HVERDHSGVLVELHRRFPEAEIHCTEVAVEGLLKHYPALEG--TEFRTVK
Methanothermobactermarburgensi HVEKDHSGVLVELHRRFPEAPIYCTEVAVKGLLKHYPSLRE--AEFMTVK
FprA_II_Methanothermobacter HIERDHSGSITEVLKRY-GSEIICTAKAAEGLRQHYSIPQD--TPMQTVK
Geobactermetallireducens HIENDHVTSLDCVMDLAPNATIYISEKGKKGLERFFDLSRWN---VKTVK
GeobactersulfurreducensPCA HIENDHASSLDRIMALAPQATIYISDKGRKGIERFFDLSNWN---VKSVK
DesulfovibriodesulfuricansG20 HLEPDHAGCLPELIERCKPEKIYCSPMGKRSMEAHFDTTGWP---VEVVK
D.gigas HLELDHAGALPALIEACQPEKIFTSSLGQKAMESHFHYKDWP---VQVVK
Methanococcusmaripaludis HVEMDHSSSLEKIMEIS-KAKIITNQKAKEHLELHYNTKDWE---YIIVD
Methanococcusjannaschii HVEKDHSGCVDKLVEIS-NATIITNEKGKEHLSLYYDTKDWD---FIIVD
Methanococcusjannaschii_3_ HISPDHNECIEKLIELT-EAKIVTTKIRKYYLDAQFNTKDWE---FVIVK
fprA-2/A.fulgidusDSM4304 HIEPDHSSGLPDTMRIAKDATVVCTQRAKDGICKYYDCDGWN---IQVVK
Giardiaintestinalis HAEGDHASSLKDHYHKFTNATFVCTKKCQEHLKILYGMEK---ATWLIVD
Spironucleusbarkhanus HAEGDHTSSLPLFINQCVNATIVTNKICMNHLQILYPSLKNF-DRWQIVD
Trichomonasvaginalis HAEPDHSSGTAMLVKEAPHIEVVMTKQCYNTMARFYDVSK---WNVKIVK
Clostr.tetaniE88_2_ HTEPDHSGALGSLAYNAKNATIVCTDKAVDQLKAMYKLYNRN---FLVVK
Clostr.perfringens_3_ HTEPDHSGALGGLARQAINAKIVCSEKAVYHLKELYKLHDRD---FIVVN
Clostr.thermocellumATCC27405 HVEPDHAGALPALAAKAKNAKIVTTKLASELLKDMFKLHNRE---FAIIK
Clostr.perfringens_1_ HTEPDHAGSVEKLLELSPKAKVIGSMQAIEFLKDIVNKDFEYI---VVGD
Clostr.perfringens_2_ HTEPDHAGSIGKILELAPNAKIVASPIAINYIKEIVNGDFESI---PVKD
ChlorobiumtepidumTLS HTEPDHSGNVHNLLSVAPNATVVGSGNAIKFLRDQTGHDFKHL---VVKH
Clostr.acetobutylicum HTELDHSGSMYRLIKEYPEAKVVSSKAANMYLKEIVNDEFNSL---DAME
Clostr.tetaniE88_3_ HTELDHSGSLINLLRDYPEAQVICSMAASVYLKNILNKEFN-----HQVA
Clostr.acetobutylicum_2_ HCEPDHSGSLARLYEVAPQIKVIASNAGKIYLKNITNKETLDV---KAVK
Rhodobactercapsulatus_1_ HLEPDHTGAVPELLRRAPQAQVRLSPRGLPMLRALLKDDFERY-DIKGVT
Rhodobactercapsulatus_2_ HLEPDHTGAVPELLRRAPQAQVRLSPRGLPMLRALLKDDFERY-DIKGVT
Rhodobactersphaeroides HLEPDHSGALPELLRRAPQAEIRLSPRGLPILRALLRDAFETA-RILPVT
Dechloromonasaromatica HLEPDHSGALPELLKRAPQAKVYLSSRAQMMLKALLKPTGEKAPEYIPVT
Wolinellasuccinogenes HTEPDHAGCLREFLERHPEVTLIHSKPCKRFIQTLTNLPFNSM----AIE
Nostocpunctiforme_1_ HTEPDHSGLVEDVLQLAPRATVLASKVALQFLEGLVHDP-FSKRV---VK
NostocPCC7120_2_ HTEPDHSGLVEDVLQLAPRATVLASKIALQFLEGLVHDP-FSKRI---VK
Nostocpunctiforme_3_ HTEPDHSGLVKDLLLMAPEITVVGSKVAIQFLEDFVHQP-FKRRI---VK
NostocPCC7120_4_ HTEPDHSGLVKDLLQMAPEITVVGSKVAIQFLEDLVHQP-FKRKI---VK
TrichodesmiumerythraeumIMS101 HTEPDHSGLAKDIIELAPQITVVGAKIAIQFLENLTHIP-FKKQI---VK
SynechocystisPCC6803_1_ HTEPDHSGLVKDILQLNPRITVVATKVALQFLDNFVHQP-FERIQ---VK
Gloeobacterviolaceus HTEPDHSGLVADVLALAPQATVVASRMALQFLANMVHRR-FPQRA---VK
NostocPCC7120_1_ HTEPDHSGLVKDILQLAPNITIVGAKVAIQFLENMVHQP-FKSLQ---VK
Nostocpunctiforme_5_ HTEPDHSGLVKNILQLAPSITVVGAKVAIQFLENMVHQP-FNSRQ---VK
SynechocystisPCC6803_2_ HTEPDHSGLIPDLLELAPQVTVVGSKVAIQFLEKLVHRP-FESQI---VK
Thermosynechococcuselongatus HTEPDHSGLVKDVLVKAPHVTVVASKVALQFLGDLIHQP-FTQQQ---VK
SynechococcusWH8102 HTEPDHSGLIGDLIDLNPDIEIVGSKVALQFLQDQVHRP-FKSRA---VK
gi|44454558|gb|EAJ38476.1| HTEPDHSGLIGDLIDLNPEIEIVGSKVALQFLKDQVHRP-FKSRA---VK
gi|44083259|gb|EAH03645.1| HTEPDHSGLIGDLIDLNPNIEIVGSKVALQFLQDQVHRP-FKSRA---VK
ProchlorococcusmarinusMIT9313 HTEPDHSGLVGQIIDLNPEIEIVASKVAIKFLEDQVHRP-FRSRE---VK

```
ProchlorococcusmarinusCCMP1375      HTEPDHSGLISDILDLNNDIEIVGSKVAIQFLENQIHRP-FKSTA---IK250
gi|43719610|gb|EAF14811.1|          HTEPDHSGLIKYLIELNPNIEIVASKVAIKFLEDQIHQP-FKSRA---VK
gi|42845529|gb|EAA90143.1|          HTEPDHSGLIKYLIELNPNIEIVASKVAIKFLEDQMHQP-FRSRA---VK
gi|44500849|gb|EAJ70075.1|          HTEPDHSGLIGNLLTLNPQIIVVGSKLALKFIEDQIHIP-FKSLE---VK
ProchlorococcusmarinusCCMP1378      HTEPDHSGLIGKLLTLNPQIIVVGSKLALKFIEDQIHIP-FKSLE---VK
gi|42832038|gb|EAA83473.1|          HTEPDHSGLIGNLLTLNPQIIVVGSKLALKFVEDQIHIP-FKSLE---VK
gi|44305658|gb|EAI33747.1|          HTEPDHSGLIGNLLELNQNITVVGSKLALKFIEDQIHIP-FKRLE---VK
gi|44606330|gb|EAK43227.1|          HTEPDHSGLIGNLLELNQNITVVGSKLALKFIEDQIHIP-FKRLE---VK
gi|44126537|gb|EAH26947.1|          HTEPDHSGLIGNLLELNQNITVVGSKLALKFIEDQIHIP-FKRLE---VK
gi|44102955|gb|EAH14255.1|          HTEPDHSGLIGNLLELNQNITVVGSKLALKFIEDQIHIS-FKRLE---VK
Nostocpunctiforme_2_                HVNPNRRATLQVLLSLVPQATLICSRPAANALKTAFPELESPIQA---VR
NostocPCC7120_3_                    HVNPNRRVTLQELLSKAPQATLICSRPAANALKTAFPEWESRIQA---VR
SynechocystisPCC6803_3_             HVNPNRMVTLEQLLRRATKAKLICSRPAAKVLKATFPHWEERFQT---VR
Nostocpunctiforme_4_                HFSPNRVATLKAILELAPQVTFVCSLPGANNLRAAFLEQDLKVLV---MR
NostocPCC7120_5_                    HFSPNRIPTFKALLELAPQITFVCSLPAAGDLRAAFPDDNLNILP---MR
Treponema                           HLEPDHADLINLVKEENPRAEILASSKGVALIKNFFKINEG----VRAVK
```

```
                                                                                  300
Methanosarcinamazei                 EGDSIDLG-G------KTLRFIEAPWLHWPETMFTYLPEERVLFPCDFFG
Methanosarcinabarkeri               DGDTIDLG-G------KNLHFIEAPWLHWPETMFTYLP------------
Methanosarcinaacetivorans_C2A       EGDSLDLG-G------KTLRFIEAPWLHWPETMFTYLPEDKVLFSCDFFG
Methanosarcinabarkeri_3_            ---------------------------------HTYPEGRVLFPCDFFG
P.furiosusDSM3638_1_                DGDEVDLG-G------KTLRFIEAPWLHWPETMFTYLVEDKVLFPCDFFG
fprA-1[A.fulgidusDSM4304]           DGEEISLG-E------KTLRFIHAPWLHWPETMFTYLVEDGILFPCDFFG
FprA3[M.thermautotrophicus           DGESLSLG-D------RTLRFIVTPWVHWPDTMVTYLEEDGILFTCDFFG
Thermoanaerobactertengcongensi      DGDTLDLG-G------KTLKFIHAPWVHWPETMFTYLVEDKILFTCDFLG
PorphyromonasgingivalisW83          EGDKLSLG-K------NELTFIFAPMVHWPEVMFTYMPTQQVLFSADAFG
BacteroidesthetaiotaomicronVPI      DGDFLALG-K------HMLRFYMTPMVHWPETMMTFDETDGILFSGDGFG
FusobacteriumATCC25586_1_           EKDILDLG-K------HKLTFYLMPMVHWPESMATYDITDKVLFSNDAFG
FusobacteriumATCC49256              EKDILDLG-K------HKLTFYLMPMVHWPESMATYDITDKILFSNDAFG
FusobacteriumATCC25586_2_           EGDKFKFG-K------HEIVFLEAPMVHWPEVLVSFDTTNGALFSADAFG
FusobacteriumATCC49256_2_           EGDKFKFG-K------HEIVFLEAPMVHWPEVLVSLDITNGALFSADAFG
Clostr.tetaniE88_4_                 EGDTMSFG-K------HQVVFVSAPMVHWPEAMVTYDTTEGILFSADAFG
P.abyssi                            DGEEVKIG-D------RTFRFITVPWLHWPDTMITYVIEDKLIFSCDAGG
P.horikoshii                        DGEEVKIG-N------RTFRFITVPWLHWPDTMITYDVEDKLIFSCDAGG
P.furiosusDSM3638_2_                DGEEMKIG-G------KTFRFITVPWLHWPDTMITYLVEDKIIFSCDAGG
Thermotogamaritima                  DGEEREIG-G------KKFKFVMTPWLHWPDTMVTYL--DGILFSCDVGG
Shigella                            TGDTLDIGNG------KQLIFVETPMLHWPDSMMTYLTGDAVLFSNDAFG
E.coli/O157_H7                      TGDTLDIGNG------KQLIFVETPMLHWPDSMMTYLTGDAVLFSNDAFG
E.coli/O6/FlRd                      TGDTLDIGNG------KQLIFVETPMLHWPDSMMTYLTGDAVLFSNDAFG
E.coli/K12                          TGDTLDIGNG------KQLIFVETPMLHWPDSMMTYLTGDAVLFSNDAFG
E.coli/unknown                      ----------------------------------MTYLTGDAVLFSNDAFG
S.typhimuriumLT2                    TGDTLDIGNG------KQLIFVETPMLHWPDSMMTYMTGDAVLFSNDAFG
Salmonella                          TGDTLDIGDG------KQLIFVETPMLHWPDSMMTYMTGDAVLFSNDAFG
gi|44480963|gb|EAJ57255.1|          TGDSLDIGNG------KQLVFIETPMLHWPDSMMTYMTEDAVLFSNDAFG
Anophelesgambiae                    TGDSLDIGNG------KQLVFIETPMLHWPDSMMTYMTEDAVLFSNDAFG
E.coli_unknown_                     TGDTLDIG---------------------------TANSSFLS-----
V.vulnificusYJ016                   TGDSIDIGNG------KQLVFVEAPMLHWPDSMMTYLTGDAVLFSNDAFG
V.vulnificusCMCP6                   TGDSIDIGNG------KQLVFVEAPMLHWPDSMMTYLTGDAVLFSNDAFG
Clostr.tetaniE88                    TGDTLDIGES------K-LTFVEAKMLHWPDSMFTYMSGENILFSNDAFG
M.thermoacetica/fprA                TGTSVSLGK-------RSLTFIEAPMLHWPDSMFTYVPEEALLLPNDAFG
MethanosarcinaacetivoransC2A        TGDELDLG-G------KTLMFLEATMLHWPDSMETFLKEDRILFSNDGFG
Methanosarcinabarkeri_2_            TGDQLDLG-G------KTLIFLEATMLHWPDSMETFLKEDRILFSNDGFG
Methanococcusmaripaludis_2_         SLESVDLG-G------KTLTFLEAPLLHWPDSMFTLYGEAGILFSNDAFG
Methanococcusmaripaludis_3_         SLESVDLG-G------KTLTFLEAPLLHWPDSMFTLYGEAGILFSNDAFG
Methanococcusjannaschii_2_          TGDTVDLG-G------KTLTFLEAPLLHWPDSMFTFYNEGGILFSNDAFG
M.thermoautotrophicum_DeltaH_       TGDSIDLG-G------RTLTFLEAPLLHWPDSMFTFLDT-GILFSNDAFG
FprA1/M.thermautotrophicus          TGDSIDLG-G------RTLTFLEAPLLHWPDSMFTFLDT-GILFSNDAFG
Methanothermobactermarburgensi      TGDVLDLG-G------KTLTFLETPLLHWPDSMFTLLDEDGILFSNDAFG
FprA_II_Methanothermobacter         TGDSTDLG-G------KTLTFLEAPMLHWPDSMFTLLEEEGILFSNDAFG
Geobactermetallireducens            TGDTLTIG-K------RTLEFLETPMLHWPDSMVTYAREDKILFTQDAFG
GeobactersulfurreducensPCA          TGDTLCIG-A------RTLEFLETPMLHWPDSMVTYSRHDRILFTQDAFG
DesulfovibriodesulfuricansG20       TGDSINIG-K------RDIQFVETRMLHWPDSMVSYIPQDKLLICNDAFG
D.gigas                             HGETLSLG-K------RTVTFYETRMLHWPDSMVSWFADEKVLISNDIFG
Methanococcusmaripaludis            SGDSVNIG-K------RNLTFVKTPMLHWPDNMVTYSPEDKILFSNDAFG
Methanococcusjannaschii             TGDEINIG-D------RTLKFIRTPMLHWPDNMLTYCKEEKILFSNDAFG
Methanococcusjannaschii_3_          NGDELNIG-N------RTLKFITDDKCEY---MLTYCVEDKILFSNDLFS
```

```
fprA-2/A.fulgidusDSM4304            GGDTLKIG-K------RTLTFIDMTMLHWPDSMATYINEDKILLSNDAFG300
Giardiaintestinalis                 DKYTLKIG-K------RTLKFIPVPLLHWPDSTFTYCPEDKILFSNDGFG
Spironucleusbarkhanus               AKSTLNIG-K------RTLKFVPVPLLHWPDSMFTYSEFDQTLFSNDGFG
Trichomonasvaginalis                LGEKINLG-D------RVAVMAGVPMAHWPESAVTYLPAQKILFSSDCFG
Clostr.tetaniE88_2_                 NGDTLDIG-G------KTLEFIKTPYLHTEETMVTFTKEDKILFPCDIFS
Clostr.perfringens_3_               DGDTLDIG-G------KTLLFKMTPYLHTEETMITYDVEDKILFPCDIFS
Clostr.thermocellumATCC27405        DGDTLDIG-G------KTLSFFETPYLHTEETMITYVNENKILFPCDIFS
Clostr.perfringens_1_               N-DTISLGN-------KTLQFISAPFLHWPDSMYTYIPEDKALITCDSFG
Clostr.perfringens_2_               G-DSISLGN-------KTLKFMSVPFLHWPDTIYTYVEEDKTLITCDSFG
ChlorobiumtepidumTLS                G-DKLDLGN-------KTIHFIGAPNLHWPDTIYSWLEEDRVLFTCDSFG
Clostr.acetobutylicum               V-KELNLGK-------NTLEFISAPNLHWPDTMFTYNKENNILFTCDVMG
Clostr.tetaniE88_3_                 P-KELSLGN-------TTLNFITAPNLHWPDTMFTYVPEKKALFTCDFLG
Clostr.acetobutylicum_2_            TNDTLDIGNG------KVLKFAIAPFLHWPDSMFTILEEDKIAFTCDFLG
Rhodobactercapsulatus_1_            TGQSVSLGD-------RDLQFFTTPFVHWPDTQCTWLAAERVLFTCDLFG
Rhodobactercapsulatus_2_            TGQSVSLGD-------RICSFFTTPFVHWPDTQCTWLAAERVLFTCDLFG
Rhodobactersphaeroides              TGAEADLGG-------RRLRFLTTPNVHWPDTQCTYLVEEGILFTCDLLG
Dechloromonasaromatica              TDDEVDLGG-------RTLRFLHTPYLHWPDTQCTYLVEDGLLFTGDIFG
Wolinellasuccinogenes               SGDELDLGG-------KTLRFFSTPFLHWPDTMMSYLVEDKILFSCDVMG
Nostocpunctiforme_1_                TGDRIDIGKG------HEMEFVSAPNLHWPDTIFSFDRKTQILYTCDAFG
NostocPCC7120_2_                    SGDRIDIGKG------HEIEFVSAPNLHWPDTIFSYDRKTEVIYTCDAFG
Nostocpunctiforme_3_                NGDRLDLGNG------HEFEFVIAPNLHWPDTIFSFDHKTKTLYTCDAFG
NostocPCC7120_4_                    NGDRLDLGNG------HEFEFVIAPNLHWPDTIFSFDHKTQTLYTCDAFG
TrichodesmiumerythraeumIMS101       NGDQLDLGNG------HVLEFVSAPNLHWPDTIFSYDRKTQTLFTCDAFG
SynechocystisPCC6803_1_             SGDRLDLGQG------HDLEFVSAPNLHWPDTMLTYDPATEILFTCDVFG
Gloeobacterviolaceus                SGDTLDLGGG------HVLEFVSAPNLHWPDTMFTFDRGTGVLYTCDAFG
NostocPCC7120_1_                    SGERLDLGNG------HSLEFVSAPNLHWPDTILTYDHKTGILYTCDVFG
Nostocpunctiforme_5_                SGERLNLGNG------HELEFISAPNLHWPDTIFTYDHKTSTLYTCDVFG
SynechocystisPCC6803_2_             SGHSLDLGQG------HELQFISAPNLHWPDTILTYDSGTQVLYTCDVFG
Thermosynechococcuselongatus        NGDRLDLGKG------HVLEFVMAPNLHWPDTILTFDHGTQTLFTCDVFG
SynechococcusWH8102                 SGEELDLGTNPESGIQHRFEFLSAPNLHWPDTIFSFDHGTGILYTCDAFG
gi|44454558|gb|EAJ38476.1|          SGEELDLGTNPESGIQHRFEFLSAPNLHWPDTIFSFDHGTGILYTCDAFG
gi|44083259|gb|EAH03645.1|          SGEELDLGTNPESGIQHRFEFLSAPNLHWPDTIFSFDHGTGILYTCDAFG
ProchlorococcusmarinusMIT9313       SGEELDLGTNSTSGIAHRFEFLSAPNLHWPDTIFSFDHATGILYTCDAFG
ProchlorococcusmarinusCCMP1375      TGGELDLGINPSNGIHHKLDFISAPNLHWPDTIFSFDHATSILYTCDAFG
gi|43719610|gb|EAF14811.1|          SGEELNLEINSISKIEHRIEFISAPNLHWPDTIFSFDHGTQVLYTCDAFG
gi|42845529|gb|EAA90143.1|          SGEELNLETNSISGIEHKIEFISAPNLHWPDTIFSFDHGTQVLYTCDAFG
gi|44500849|gb|EAJ70075.1|          SGQYLDLGANPTSGVNHNIEFISAPNLHWPDTIFSYDHGTNVLYTCDAFG
ProchlorococcusmarinusCCMP1378      SGQYLDLGANPTSGVNHNIEFISAPNLHWPDTIFSYDHGTNVLYTCDAFG
gi|42832038|gb|EAA83473.1|          SGQYLDLGANPTSGVNHNIEFISAPNLHWPDTIFSYDHGTNVLFTCDAFG
gi|44305658|gb|EAI33747.1|          SGEFLNLGTNPNSGLEHNIEFISAPNLHWPDTIFSYDHSTNVLYTCDAFG
gi|44606330|gb|EAK43227.1|          SGEFLNLGTNPNSGLEHNIEFISAPNLHWPDTIFSYDHSTNVLYTCDAFG
gi|44126537|gb|EAH26947.1|          SGEFLNLGTNPNSGLEHNIEFISAPNLHWPDTIFSYDHSTHVLYTCDAFG
gi|44102955|gb|EAH14255.1|          SGEFLNLGTNPNSGLEHNIEFISAPNLHWPDTIFSYDHSTHVLYTCDAFG
Nostocpunctiforme_2_                SGDTLDLGQG------HHLSFVTVPTPRWADGLCTYDYATKILYTDKLFG
NostocPCC7120_3_                    FEDILDLGQG------HQLTFVTAPTPRWPDGLFTYDSATKILYTDKFFG
SynechocystisPCC6803_3_             SQDMLDLGRG------HKLQLMTLPTPRWPDGLCAYDAGSQILFSDKLFG
Nostocpunctiforme_4_                GKETLDLGKG------HVLKFLPTPSPRWPEGLCTYDRQTQILYTDKLFA
NostocPCC7120_5_                    GKETLDLGKG------HVLKFLPIPSPRWPAGLCTYDVQTQILYTDKIFG
Treponema                           DGEVLDLGGG------KKLVFYETPNIHWPETMMTYDPDDKILFSCDAFG
```

```
                                                                                    350
Methanosarcinamazei                 AHTAQG--VYDDDLEDLIP----LAKR----YYGEIMMPFNKMGAKALEK
Methanosarcinabarkeri               ------------------------------------------------------
Methanosarcinaacetivorans_C2A       AHTAQG--VYDEEIEELVS----LAKR----YYGEIMMPFGKMGARALEK
Methanosarcinabarkeri_3_            AHTAQG--VYDEDLEDLIP----LAKS----YYGEIMMPFGKMGAKALEK
P.furiosusDSM3638_1_                AHTAHG--LYDDEVPSIIE----YAQR----YFGEIMMPFAGMAKRAMEK
fprA-1[A.fulgidusDSM4304]           CHTAYG--FYDDEVPEILY----YAQR----YFGEIMMPFRSMGKKALEK
FprA3[M.thermautotrophicus          SHIATSD-IMETPD-DFLR----EAKR----YYAHIMMPFSQMVASNLRK
Thermoanaerobactertengcongensi      SHLATSE-LYATDECKVYD----SAKR----YYAEIMMPFRNFIEKHLEK
PorphyromonasgingivalisW83          TFGTLDG-HIFDKDMDLS-----FRWEEMYRYYACIVGKYGSFVQKVLTK
BacteroidesthetaiotaomicronVPI      CFGTVDG-GFLDTRINVD-----KYWGEMVRYYSNIVGKYGSPVQKALQK
FusobacteriumATCC25586_1_           SFGALDG-AIFDDEVNTD-----FFTDEMRRYYSNIVGKFGAPVNAILKK
FusobacteriumATCC49256              SFGALDG-AIFDDEINTD-----FFTDEMRRYYSNIVGKFGAPVNAVLKK
FusobacteriumATCC25586_2_           SFKSLDG-RLFNDEVNWDR----DWLDEGRRYLTNIVGKYGPHIQHLLKK
FusobacteriumATCC49256_2_           SFKSLDG-RLFNDEVNWDR----DWLDEGRRYLTNIVGKYGPHIQHLLKK
Clostr.tetaniE88_4_                 SFGSLDG-KLFNDEININR----DWIDEGRRYYTNIVGKYGAHVQSLLKK
```

```
P.abyssi                              GYG-IPR-AIDDSDEEVVK----EYLPYVTKYIVTVIGHYHKYIVQNIKK350
P.horikoshii                          GYG-IPE-AIDDSDEDVVK----KYLPYVTKYIVTVIGHYHKYIVQNIKK
P.furiosusDSM3638_2_                  GYS-IPE-TIDDSSEEVVE----KYLPYVTKYIVTVIGHYHKYIVENIRK
Thermotogamaritima                    GYL-LPE-ILDDSNESVVE----RYLPHVTKYIVTVIGHYKNYILEGAEK
Shigella                              QHYCD---EHLFNDEVDQTE----LFEQCQRYYANILTPFSRLVTPKITE
E.coli/O157_H7                        QHYCD---EHLFNDEVDQTE----LFEQCQRYYANILTPFSRLVTPKITE
E.coli/O6/FlRd                        QHYCD---EHLFNDEVDQTE----LFEQCQRYYANILTPFSRLVTPKITE
E.coli/K12                            QHYCD---EHLFNDEVDQTE----LFEQCQRYYANILTPFSRLVTPKITE
E.coli/unknown                        QHYCD---EHLFNDEVDQTE----LFEQCQRYYANILTPFSRLVTPKITE
S.typhimuriumLT2                      QHYCD---ERLFNDEVDQTE----LFEQCQRYYANILTPFSRLVTPKITE
Salmonella                            QHYCD---EHLFNDEVDQTE----LFEQCQRYYANILTPFSRLVTPKITE
gi|44480963|gb|EAJ57255.1|            QHYCD---EHLFNDEVDQTE----LMEQCQRYYANILTPFSPLVTAKIKE
Anophelesgambiae                      QHYCD---EHLFNDEVDQTE----LMEQCQRYYANILTPFSPLVTAKIKE
E.coli_unknown_                       KHQC----------------------CTGRTA-----------------
V.vulnificusYJ016                     QHYCD---ERLFNDEVDQAE----LMEQCLRYYSNILTPFSALVTAKIQE
V.vulnificusCMCP6                     QHYCD---ERLFNDEVDQAE----LMEQCLRYYSNILTPFSALVTAKIQE
Clostr.tetaniE88                      QHYAS---DLMYNDLVDQAE----LYQESMKYYANILTPFNSFVIKKIEE
M.thermoacetica/fprA                  QHIAT---SVRFDDQVDAGL----IMDEAAKYYANILMPFSNLITKKLDE
MethanosarcinaacetivoransC2A          QHIAT---SKRYDFEVGD------VIPDAAEYYANILMPFHMPLLRFMGV
Methanosarcinabarkeri_2_              QHIAT---SKRYDFEVGN------VLPEAAEYYANILMPFHIALLRYFKL
Methanococcusmaripaludis_2_           QHLCL---TKRFDNEIPENI----LMDANQKFYANLITPLSKLVLKKFNE
Methanococcusmaripaludis_3_           QHLCL---TKRFDNEIPENI----LMDANQKFYANLITPLSKLVLKKFNE
Methanococcusjannaschii_2_            QHLCFPA-HKRFDKDIPEYV----LMDANQKFYANLITPLSKLVLKKFEE
M.thermoautotrophicum_DeltaH_         QHLCY---PQRLDTEIPEYI----LMDAAKKFYANLITPLSKLVLRKFDE
FprA1/M.thermautotrophicus            QHLCY---PQRLDTEIPEYI----LMDAAKKFYANLITPLSKLVLRKFDE
Methanothermobactermarburgensi        QHLCC---PQRLDREIPEYI----LMDAARKFYANLITPLSKLVLKKFDE
FprA_II_Methanothermobacter           QHLCI---SKRFDKDVPEAV----LMDAAMKFYANLLTPLSPLVLRKFSE
Geobactermetallireducens              QHVAS---ANRFDDEYEISNSPVELEDAVVDYYANILMPFGQMIKTKIAE
GeobactersulfurreducensPCA            QHVAS---ASRFDDEFEKSDSAAELEDAVVDYYANILMPFGQMIKTKIAE
DesulfovibriodesulfuricansG20         QNIAC---TERFADEIDRAH----LAHAMKEYYHNIVLPFSPIVIKTLDL
D.gigas                               QNIAA---SERFSDQIPVHT----LERAMREYYANIVNPYAPQTLKAIET
Methanococcusmaripaludis              QHIAS---SERFDFEIDY------TLDSAKEYFANILLPYRTLIPNAVKT
Methanococcusjannaschii               QHIAS---SERFDYEIGEG-----IFEHAKDYFANILMPYKMLIPDAIKA
Methanococcusjannaschii_3_            QHVVY---KEKIDSDIGHK-----IMLDAKEYFANILLPYRKSILKILNI
fprA-2/A.fulgidusDSM4304              QHVAS---EYRFDEEIGVEE----ALKWAKVYYANILMPLGGLIQKKLKE
Giardiaintestinalis                   QHYAT---SRRWADECDVSH----VMHLFKEYTANILGLFSAQMR---KA
Spironucleusbarkhanus                 QHLAS---AERWSDELPQGQ----IERLMDEYTANILGHVPHLIK---KA
Trichomonasvaginalis                  QHIAS---NKRFVDEVDQGL----FLTEIKSYYANILQRLGKPVL---KA
Clostr.tetaniE88_2_                   THISN---YEYFNDKAKED-----ILEDFKTYYSLIMHPHRRYVQNMINK
Clostr.perfringens_3_                 THLTA---KEHFSSKSNED-----ITEDFLTYYKLIMEPHRKYIRPLIDI
Clostr.thermocellumATCC27405          THIAN---YELFNDLAKGE-----YIEDFKVYYRLIMAPHRPYVRDMLEK
Clostr.perfringens_1_                 SHYSCEE---VFNDLVPNE---EEYLDALRYYYDCIFGPYKPYVLKAIDK
Clostr.perfringens_2_                 SHYSCEE---MFDDLIPNE---EEYMEALKYYFDCIMGPFKPYVLKALDK
ChlorobiumtepidumTLS                  CHYCNEA---MYDDLCG------DFDDAFKYYFDAILRPFSKYMLQAIEK
Clostr.acetobutylicum                 CHYCPDG---SIKDEGG-----EDYLPEMRYYFDVIMSPFKKFVNMGLDK
Clostr.tetaniE88_3_                   AHYCPST---NIFDGES-----EDSYEEMVYYFDVIMSPFKKFVLAGLDK
Clostr.acetobutylicum_2_              CHFCEPR---MFDTKITYM---PKYEKSFKEYYDAIFSPFKPYVVKGLDI
Rhodobactercapsulatus_1_              SHYCDGR---LFNDLVG------DFRFSFEYYFDRIMRPFRSFVAQALDL
Rhodobactercapsulatus_2_              SHYCDGR---LFNDLVG------DFRFSFEYYFDRIMRPFRSFVAQVLDL
Rhodobactersphaeroides                SHYCDER---LFDDRVG------DFRFAMDHYFDRLMRPFRSFVTQALDL
Dechloromonasaromatica                CHFCDNR---LFNDTVG------DFRFSFEYYYAHIMRPFREYVLDAIAL
Wolinellasuccinogenes                 SHFTSETNPEIFNSLLDEKDY-LASIEAFKYYYAMIMRPYKEHIIKAFEL
Nostocpunctiforme_1_                  MHFCDDR---TFDEDLE------AIEADFRFYYDCLMGPNARSLLNAMKR
NostocPCC7120_2_                      MHFCDNR---TFDEDLE------AIEADFRFYYDCLMGPNARSLLNAMKR
Nostocpunctiforme_3_                  LHYCSDS---TFDEDLV------AIEEDFHYYYDCLMGPNARSVLSALKR
NostocPCC7120_4_                      MHYCSDI---VFDEDLK------TIEPDFHYYYDCLMGPNARSVLSALKR
TrichodesmiumerythraeumIMS101         MHYCSDK---TYDETLS------DIEADYKFYYECLMAPNARSVLNAMKR
SynechocystisPCC6803_1_               MHYCSDA---VFDIDLG------KIAPDYQFYYDCLMGPNARSVLAAMKR
Gloeobacterviolaceus                  MHYCNER---MFDEDLS------AIEPDYRFYYECLMAPNARSVLTALKR
NostocPCC7120_1_                      MHYCDDQ---TYDENFF------AIEEDFKYYYDCLMGPNARSVLAALKR
Nostocpunctiforme_5_                  MHYCDDH---TYDENIT------LLEEDFQYYYDCLMGPNARSVLAALKR
SynechocystisPCC6803_2_               MHYCDDS---LFDETPE------RLEPDFQYYYNCLMGSNARSVLMALKR
Thermosynechococcuselongatus          AHFCNDD---PFDSEPE------LLAPDFKFYYDCLMGPNARSVLSAFKR
SynechococcusWH8102                   LHYCSDD---VFDSDPG------AIAPDFRFYYDCLMGPNARSVLQALKR
gi|44454558|gb|EAJ38476.1|            LHYCSDD---IFDADPG------AIAPDFRFYYDCLMGPNARSVLQALKR
gi|44083259|gb|EAH03645.1|            LHYCSED---VFDADPG------AIAPDFRFYYDCLMGPNARSVLQALKR
ProchlorococcusmarinusMIT9313         LHYCSEE---LFDQDPS------ALAPDFRFYYDCLMGPNARSVVQALKR
ProchlorococcusmarinusCCMP1375        LHYCTDE---LFDLDPD------AILPDFRYYYDCLMGPNARSVLQALKR
gi|43719610|gb|EAF14811.1|            LHYCSEK---LYDENPS------LLNEDFRFYYDCLMGPNARSVVQALKK
gi|42845529|gb|EAA90143.1|            LHYCSEK---LYDENPS------LLNEDFRFYYDCLMGPNARSVVQALKK
gi|44500849|gb|EAJ70075.1|            LHYCSDE---FFDNDQK------EIYEDFRFYYDCLMGPNARSVLQAIKR
```

```
ProchlorococcusmarinusCCMP1378      LHYCSDE---FFDNDQK------EIYEDFRFYYDCLMGPNARSVLQAIKR350
gi|42832038|gb|EAA83473.1|          LHYCSDE---FFDNDQK------EIYEDFRFYYDCLMGPNARSVLQAIKR
gi|44305658|gb|EAI33747.1|          LHYCSDE---FFDTDQK------EIYDDFRFYYDCLMGPNARSVIQAIKR
gi|44606330|gb|EAK43227.1|          LHYCSEE---FFDTDQK------EIYDDFRFYYDCLMGPNARSVMQAIKR
gi|44126537|gb|EAH26947.1|          LHFCSDE---FFDTDQK------EIYDDFRFYYDCLMGPNARSVIQAIKR
gi|44102955|gb|EAH14255.1|          LHYCSEE---FFDTDQK------EIYDDFRFYYDCLMGPNARSVLQAIKR
Nostocpunctiforme_2_                AHICEDT---LFDEDWK------GLDAERRYYFECLHAPQAKQVEVVLDK
NostocPCC7120_3_                    AHICEDT---LFDEDWK------KLDAERHYYFDCLHAPQAKQVEAALDK
SynechocystisPCC6803_3_             THVCGDA---IFDEDWR------QLGGDRRFYFDCLHAPQTRQVETALDQ
Nostocpunctiforme_4_                THLCGDE---VFDDNWE------ALKEDQRYYFNCLMAPQTPHVQAALEK
NostocPCC7120_5_                    AHICGDD---VFDDNWE------SFKEDQRYYFNCLMAPHAIHVEAALEK
Treponema                           SYGCIG--EKIFDDQHTEDELK-FFENEALRYYANIVASFSSFVNKGIEK
```

```
                                                                                  400
Methanosarcinamazei                 IKDL----EIDIIAPSHGPIYK------NPERILEPYRKWT-AGKTENK
Methanosarcinabarkeri               ----------------------------------------------
Methanosarcinaacetivorans_C2A       IKDL----GIEIIAPSHGPIYK------NPKRILDPYEKWT-QGKTENK
Methanosarcinabarkeri_3_            IKDL----DIAVIAPSHGPIYK------NPQRILEPYAKWT-AGKTENK
P.furiosusDSM3638_1_                LKGL----EIKMIAPSHGPIYR------NPERILKAYESWV-NGETREK
fprA-1[A.fulgidusDSM4304]           IKGL----KINMIAPSHGPIYR------NLEKILSAYEKWT-AGETEEK
FprA3[M.thermautotrophicus          ISEL----EVSMIAPSHGPVIS------EPGLIMDAYDTWT-SGGDG--
Thermoanaerobactertengcongensi      IKDL----DIEIIAPSHGPVYN------NPEFILNAYREWV-LDKPKNI
PorphyromonasgingivalisW83          FKEA--NLPVQYICSTHGPVWTP-----AHFSEAFDLYDRMSRYEA-EEG
BacteroidesthetaiotaomicronVPI      LGG----LPITTICSTHGPVWT------ENISRVIGIYDRLSRYDA-DEG
FusobacteriumATCC25586_1_           LSS----VEISCICPSHGLIWR------KYIKEIIERYQKWANMEPTKEG
FusobacteriumATCC49256              LSS----VEISCICPSHGLVWR------KYIKEIIERYQKWANMEATKEG
FusobacteriumATCC25586_2_           AGPI--VDKIKFICPLHGVVWR------NDFGYLIDKYDKWSRYEPEEKG
FusobacteriumATCC49256_2_           AGPV--VDKIKFICPLHGVVWR------NDFGYIIDKYDKWSRYEPEEKG
Clostr.tetaniE88_4_                 AADL--D--IKIICPLHGPVWR------NNLDYLLDKYDKWSSYEPEEKG
P.abyssi                            LKSLGIIESVRMILPGHGLIWR------RNPVRIFEHYERVGAGIPTKDK
P.horikoshii                        LKELGIIENANMILPGHGLIWR------KSPTRIFEHYERVGAGIPTKDK
P.furiosusDSM3638_2_                LKELGIVKDVKMILPGHGLIWR------RDPIRIFRHYEEVGAGRAEKGK
Thermotogamaritima                  LSSL----KIKALLPGHGLIWK------KDPQRLLNHYVSVAKGDPKKGK
Shigella                            ILGFNLPVD--MIATSHGVVWRDN----PTQ--IVELYLKWAAD-YQEDR
E.coli/O157_H7                      ILGFNLPVD--MIATSHGVVWRDN----PTQ--IVELYLKWAAD-YQEDR
E.coli/O6/FlRd                      ILGFNLPVD--MIATSHGVVWRDN----PTQ--IVELYLKWAAD-YQEDR
E.coli/K12                          ILGFNLPVD--MIATSHGVVWRDN----PTQ--IVELYLKWAAD-YQEDR
E.coli/unknown                      ILGFNLPVD--MIATSHGVVWRDN----PTQ--IVELYLKWAAD-YQEDR
S.typhimuriumLT2                    ILGFNLPVD--MIATSHGVVWRDN----PTQ--IVELYLKWATD-YQEDR
Salmonella                          ILGFNLPVD--MIATSHGVVWRDN----PTQ--IVELYLKWAAD-YQEDR
gi|44480963|gb|EAJ57255.1|          VLGFNLPVS--MVATSHGIVWRED----PTQ--IILKYLEWADH-YQEDR
Anophelesgambiae                    VLGFNLPVS--MVATSHGIVWRED----PTQ--IILKYLEWADH-YQEDR
E.coli_unknown_                     ----------------------------------------------
V.vulnificusYJ016                   VLSFNLPVD--MIATSHGIVWREN----PTQ--IIEQYLAWANN-YQEDR
V.vulnificusCMCP6                   VLSFNLPVD--MIATSHGIVWREN----PTQ--IIEQYLAWAND-YQEDR
Clostr.tetaniE88                    VLALNLPLN--IIATSHGVIWRDN----PAQ--IIEQYIKWANG-YEENQ
M.thermoacetica/fprA                IQKINLAIK--TIAPSHGIIWRKD----PGR--IIEAYARWAEG-QGKAK
MethanosarcinaacetivoransC2A        LDKMGVDP--LQIAPSHGIIWKQD----LKK--ILEAYRAWANG-EVNEK
Methanosarcinabarkeri_2_            IEEMKIEP--LQIAPSHGIIWKQD----LEK--ILAEYKAWANG-EVKEK
Methanococcusmaripaludis_2_         VISLGLLEKITMIAPSHGQIWTDP----MK---VISAYQNFATG-QCKDK
Methanococcusmaripaludis_3_         VISLGLLEKITMIAPSHGQIWTDP----MK---VISAYQNFATG-QCKDK
Methanococcusjannaschii_2_          VIQLGLLEKIKMIAPSHGQIWTDP----MK---VIKAYQDFATGKAAKDK
M.thermoautotrophicum_DeltaH_       VKELGLLDKIGMIAPSHGQIWTEP----MK---IIEAYAAWATG-KVKKK
FprA1/M.thermautotrophicus          VKELGLLDKIGMIAPSHGQIWTEP----MK---IIEAYTAWATG-KVKKK
Methanothermobactermarburgensi      VKELGLLERIQMIAPSHGQIWTDP----MK---IIEAYTGWATG-MVDER
FprA_II_Methanothermobacter         VKELGLLEKIGMIAPSHGQIWTEP----LK---IIAAYTDWATG-KCRDK
Geobactermetallireducens            IQAKGFEIDI--IAPDHGLIWRKD----P--GKVLGMYLDMANG-KARES
GeobactersulfurreducensPCA          IQAKGFDIDI--IAPDHGLIWRAN----P--GKVLSMYMDMANG-KANES
DesulfovibriodesulfuricansG20       LAELKLDIDM--LAPDHGLIFRGE----D-VQYALDSYRSFAQQ-KPRKR
D.gigas                             LVGAGVAPEF--ICPDHGVIFRGA----DQCTFAVQKYVEYAEQ-KPTNK
Methanococcusmaripaludis            VDT--LETDL--ICPSHGIIWKEN----IS--KIKEKYLEFASN-NVINK
Methanococcusjannaschii             VKN--LDIEL--ICPSHGVIWKEY----IN--EIIEKYNEWAMN-KTKNK
Methanococcusjannaschii_3_          LKD--LDLEY--ICPSHGVIWHIM----ID--EILTKYRMWCSD-SYKNT
fprA-2/A.fulgidusDSM4304            IKESGLEIDI--IAPSHGVVWKN-----PG--RIIEAYDRWSRF-EPTNK
Giardiaintestinalis                 LEVASTVE-IKYILSAHGVSWRG-----DAMGLAIAEYDRWSKGQHCQKK
Spironucleusbarkhanus               VEAASTLS-IKNILVAHGASYRG-----DAVGWAVKKYFDFGAQTHFKPK
Trichomonasvaginalis                LATASKLPGLDIVLPAHGVGFRRK----EDLEQAIKLYTQWAT-YKPNPK
```

```
Clostr.tetaniE88_2_                IENLD----IEIIAPSHGFILRED----VKKFINIYDEMS--KNTNIDKK400
Clostr.perfringens_3_              LKDLD----IEVIAPSHGYILDEN----IQSYIDIYDKYS--KETKKGKK
Clostr.thermocellumATCC27405       IKKLN----IEVIAPSHGYILREN----TAKFIQMYDEMSSLAALKQPKK
Clostr.perfringens_1_              IKDLD----IELVCPGHGPILRQD-PWKIIN-TYKEWSTPVKPKINGDKK
Clostr.perfringens_2_              IKGLD----IEIICPGHGPILRSN-PYKVVN-LYKEWSTPAPAKEV--KK
ChlorobiumtepidumTLS               IRPLD----IKVICPGHGPILRSD-WKKYVD-LSERYAKSAIAMPN-EKS
Clostr.acetobutylicum              IKDLK----LDMIAPSHGPVHIND-IEESVK-LYREWAKEKEPKEK---N
Clostr.tetaniE88_3_                IKDLD----FDLVCTSHGTVHTKENIKKYMN-MYREFATGNNEEEK---K
Clostr.acetobutylicum_2_           LDALD----LDFIATSHGPILTREGLLAASKQKYRDLSSEIQSTTK---Y
Rhodobactercapsulatus_1_           IEPLD----FGIIAPAHGPILRSH-PRDYLTHTRRLISSRLAAETGSEKT
Rhodobactercapsulatus_2_           IEPLD----FGIIAPAHGPILRSH-PRDYLTHTRRLISSWLAAETGSEKT
Rhodobactersphaeroides             IEPLD----LTVIAPSHGPVLRTD-PRAYLRQYRRLAGPRSAP--GPDRT
Dechloromonasaromatica             IEPLD----IQLIAPAHGPVLRHK-PRDYVHRYRELATPRLFNEARSEKT
Wolinellasuccinogenes              LEKLD----VQMIAPSHGPILDME-PRFFFDWYRARAKNYLLRLNG--QK
Nostocpunctiforme_1_               MGDLGK---INIIANGHGPLLYHH-----LDVLTGCYENWSQRQAKAETT
NostocPCC7120_2_                   MGDLGK---IKIIANGHGPLLYHH-----LDVLTECYQSWSQRQAKSETT
Nostocpunctiforme_3_               MGELKT---IDMIATGHGPLLSHN-----VEELVGRYRIWSQTQAKPETV
NostocPCC7120_4_                   MGELPS---VKMIATGHGPLLYHN-----VEELTGRYRTWSQNQTKAETS
TrichodesmiumerythraeumIMS101      MKALGD---INTIATGHGPLLRHN-----LVELTNRYQEWSQAKSKAEKT
SynechocystisPCC6803_1_            MDNLGT---ISTVANGHGPLLRHN-----VGELLHRYRHWSESQSKAEKT
Gloeobacterviolaceus               MEPLGE---ITAIATGHGPMLKLH-----LGELVDRYRRWSQEQSEATTS
NostocPCC7120_1_                   IENLA----IKTVATGHGPLLQVH-----ISEWLGRYKNWSLEQAKTETL
Nostocpunctiforme_5_               IEKLE----IGTVATGHGPLLQHY-----IPDWLGRYQNWSLEQAKTETL
SynechocystisPCC6803_2_            IAPLQ----VVLVATGHGPLLQHH-----ISHWLGQYDAWSQNQVKAETF
Thermosynechococcuselongatus       LESLPP---VQLVATGHGPLLRHH-----LDQWLESYRNWSQEQAKAATT
SynechococcusWH8102                MGGLPE---INTIAVGHGPLLRHH-----LSHWVNDYREWSGQRSKGESY
gi|44454558|gb|EAJ38476.1|         MDGLPE---INTIAVGHGPLLRHH-----LSHWISDYREWSGQRSKGESY
gi|44083259|gb|EAH03645.1|         MDGLPE---INTIAVGHGPLLRHH-----LSHWVSDYREWSGQRSKGESY
ProchlorococcusmarinusMIT9313      MDQLPE---ITTIAVGHGPLLRHH-----LKLWVEDYRDWSSQRNQGESY
ProchlorococcusmarinusCCMP1375     IKNLPT---IQTIAVGHGPLLRHN-----LDLWLNNYQEWSGQRSQGEDY
gi|43719610|gb|EAF14811.1|         IDSLPT---IQTIGVGHGPILNFN-----TQLWLNHYREWSKQRSTGENY
gi|42845529|gb|EAA90143.1|         IDALPT---IKTIGVGHGPILNFY-----TQLWLDNYREWSKQK------
gi|44500849|gb|EAJ70075.1|         IDKLPR---IKTIAVGHGPLLHNQ-----VNFWKEKYSEWSSNKSKGNEF
ProchlorococcusmarinusCCMP1378     IDKLPR---LKTIAVGHGPLLHNQ-----VNFWKEKYSEWSSNKSKGNEF
gi|42832038|gb|EAA83473.1|         IDKLPR---LKTIAVGHGPLLHNQ-----VNFWKEKYSEWSSKKSKGNEF
gi|44305658|gb|EAI33747.1|         IDKLPE---LKTIAVGHGPLLHNQ-----VNFWKGKYLEWSSNKSKGNDF
gi|44606330|gb|EAK43227.1|         IDKLPE---LKTIAVGHGPLLHNQ-----VNFWKGKYLEWSSNKSKGNDF
gi|44126537|gb|EAH26947.1|         IDKLPE---LKTLAVGHGPLLHNQ-----VNFWKGKYLEWSSNKSKGNDF
gi|44102955|gb|EAH14255.1|         IDKLPE---LKTIAVGHGPLLHNQ-----VNFWKGKYLEWSSNKSKGNDF
Nostocpunctiforme_2_               LSLLG----ARCYAPAHGPVVRYS-----LSRFTYDYRQWCQGQKSQELS
NostocPCC7120_3_                   VVMLG----ARSYAPGHGPVVRYS-----LSRFTYDYRQWCQGQKSQDLN
SynechocystisPCC6803_3_            FDPLT----LKMIAPGHGPLVRFS-----LSRLYSDYRQWCQQQPSQTLK
Nostocpunctiforme_4_               ISDLQ----VRMYAVGHGPLVRTS-----LIELTKAYGEWSRSHNDREIS
NostocPCC7120_5_                   ISDLQ----VRLYAVGHGPLVRTS-----LIALTQAYADWSKAQKDREIS
Treponema                          LAALEL----KFICPSHGLLWRGN-PSRIVNLYKKFADYNTGTGSGLEKT
```

```
                                                                                    450
Methanosarcinamazei                ALVVYISMWGSTKEMVNAIAETLLKEGVDVRMYDLAAS---DLGDVAREL
Methanosarcinabarkeri              --------------------------------------------------
Methanosarcinaacetivorans_C2A      ALIVYVSMWGSTREMIRTIAETLLKEGVDVRMYDLVAS---DIGDVAREL
Methanosarcinabarkeri_3_           ALIVYVSMWGSTKLMVRTIAETLLKEGVDVRIYDLEVA---NTGDIAREL
P.furiosusDSM3638_1_               VLVAYVSMWGSNREMAKELADLLVAKGIDVKVYDLVSA---DIGELAKDL
fprA-1[A.fulgidusDSM4304]          VLVVYATMWGSTERMVNLLTELLMKEGLKVAVHNLASA---DIGEIAKDL
FprA3[M.thermautotrophicus         VVIAYTTMHGSTRVMVERLTEKLMELDVSVRPVNVAEH---DTGEFLTEL
Thermoanaerobactertengcongensi     VLIPYVTMHGSVKKMVEYLEAALVERGVIVKPFDLSVT---DIGEFAMAL
PorphyromonasgingivalisW83         AVILYGTMYGNTEVLADTIAQGIAAGGIRNVVCHNVAF--SPASNILRDI
BacteroidesthetaiotaomicronVPI     VVIVYGSMYGNTEQMAEAIAAELSAQGIRNIVMHNVTK--SHPSYILADI
FusobacteriumATCC25586_1_          VVIVYGSMYGNTAEMAEILGRELGNRGIKDVIIYDSSK--TDHSYIFSTI
FusobacteriumATCC49256             VVIVYGSMYGHTAEMAEVLGRELGNRGIKDVIIYDSSK--TDHSYIFSTI
FusobacteriumATCC25586_2_          ILIAYASMYGNTENAVEILAAKLAEKGITNIKMFDVSN--THVSYLISNV
FusobacteriumATCC49256_2_          ILIAYASMYGNTENAIEILAKKLAEKGITNIKMFDVSN--THVSYLISNL
Clostr.tetaniE88_4_                VMIVYASMYGNTEAAANDLATRLVEKGMTNVAMYDVSK--THVSYLISET
P.abyssi                           VLVLYDSMYGFVEERMKVVIEELRKYNKKPVIYRFTDKEAPAVSDILGEV
P.horikoshii                       VLVIYDSMYGFVEKRMSVVIEELKRYGKKPVVYRFTDKENPAISDILGEV
P.furiosusDSM3638_2_               VLVVYDSMYGFVEKRMDIVIDELKKHGMKPVIYKYTDKVAPAVSDILGEV
Thermotogamaritima                 VTVIYDSMYGFVENVMKKAIDSLKEKGFTPVVYKFSDEERPAISEILKDI
```

```
Shigella                              ITIFYDTMSNNTRMMADAIAQGIAETDPR-VAVKIFNVARSDKNEILTNV450
E.coli/O157_H7                        ITIFYDTMSNNTRMMADAIAQGIAETDPR-VAV----------------
E.coli/O6/FlRd                        ITIFYDTMSNNTRMMADAIAQGIAETDPR-VAVKIFNVARSDKNEILTNV
E.coli/K12                            ITIFYDTMSNNTRMMADAIAQGIAETDPR-VAVKIFNVARSDKNEILTNV
E.coli/unknown                        ITIFYDTMSNNTRMMADAIAQGIAETDPR-VAVKIFNVARSDKNEILTNV
S.typhimuriumLT2                      ITIFYDTMSNNTRMMADAIAQGINEVDPN-VAVKIFNVARSDKNEILTNV
Salmonella                            ITIFYDTMSNNTRMMADAIAQGINEVDPN-VAVKIFNVARSDKNEILTNV
gi|44480963|gb|EAJ57255.1|            ITLFYDSMSNNTRMMADAIAQGIHEVDPG-VAVKIYNVARHDKNEILTQV
Anophelesgambiae                      ITLFYDSMSNNTRMMADAIAQGIHEVDPG-VAVKIYNVARHDKNEILTQV
E.coli_unknown_                       ------------------------------------------------
V.vulnificusYJ016                     ITIFYDSMSNNTRMMADAIAQGIHDVDPS-VAVKVFNVSKQDKNEILANV
V.vulnificusCMCP6                     ITIFYDSMSNNTRMMADAIAQGIHDVDPS-VAVKVFNVSKQDKNEILANV
Clostr.tetaniE88                      ITVLYDTMWNGTRRMAEGIAEGIKSVNKD-ITVKLFNAAHSDKNDVITEI
M.thermoacetica/fprA                  AVIAYDTMWLSTEKMAHALMDGLVAGG---CEVKLFKLSVSDRNDVIKEI
MethanosarcinaacetivoransC2A          VLVIYDTMWGSTEIMATEIAEAVRAAG---VEVKLLNLRKNTRNHIMKEM
Methanosarcinabarkeri_2_              VLVIYDTMWNSTEIMAKEITEAIWATG---VKVKML--------------
Methanococcusmaripaludis_2_           ATIVYDTMHYSTQKMAHAFAEGLLSEG---IEVVIYNLHSDERSEIVKDI
Methanococcusmaripaludis_3_           ATIVYDTMHYSTQKMAHAFAEGLLSEG---IEVVIYNLHSDERSEIVKDI
Methanococcusjannaschii_2_            AVIVYDTMHYSTQKMAHAFAEGLMSEG---IDVVMYFLHYDERSEIVKDI
M.thermoautotrophicum_DeltaH_         VTVIYDTMHHSTAMMAHAIAEGAMSEG---ADVRVYYLHEDDRSEIVKDI
FprA1/M.thermautotrophicus            VTVIYDTMHHSTAMMAHAIAEGAMSEG---ADVRVYYLHEDDRSEIVKDI
Methanothermobactermarburgensi        VTVIYDTMHGSTRKMAHAIAEGAMSEG---VDVRVYCLHEDDRSEIVKDI
FprA_II_Methanothermobacter           ATIIYDTMHYSTRMLAHAMAEGLMAAD---VDVSMHFLHEDERSEIVKNI
Geobactermetallireducens              VAIIYDTMWQSTEKMAGPIAEGVRAEG---LNCQIIKLRATPTSVAIKEF
GeobactersulfurreducensPCA            VAIIYDTMWQSTEKMAVPIAEGIRAEG---LDCRVVKLRATPMSVAIKEF
DesulfovibriodesulfuricansG20         AVIVFDTMWHSTEKMARAIADGLEAEG---VPARLMWLKANHHSAVMTEL
D.gigas                               VVIFYDSMWHSTEKMARVLAESFRDEG---CTVKLMWCKACHHSQIMSEI
Methanococcusmaripaludis              AVIVYDTMYSSTEKIGLAIAEGLIESG---VEVKVFKISKTPVSKIIAEI
Methanococcusjannaschii               AVIVYDTMYNSTKKMAHAIAEGLMEKG---VEVKIYRVCETSLSRIMTEI
Methanococcusjannaschii_3_            AVIVYATIYSSTEKIAKALGEGLSEEG---VDVIYHRLDTSPLNIIMRDI
fprA-2/A.fulgidusDSM4304              VVIVFDSMWHSTEKLAMAIAEGAGSEG---ADVRVMHIRKDYWTDIVTEI
Giardiaintestinalis                   VTVVLDSMYGTTHRMALALLDGARSTG---CETVLLEMTSSDITKVALHT
Spironucleusbarkhanus                 VSIVYDTMYGTTARAALAIAEGVKSAG---AVPHMLPLSAADITKAALNF
Trichomonasvaginalis                  VSVIYDCNWYGTEKMAEAVASGICKEK---LECIMMNARKTHITRSATEV
Clostr.tetaniE88_2_                   VLILYSTMTNNTKKISELIKEHFERDS---INTELINVNKTSDEEIFKKV
Clostr.perfringens_3_                 ATIVYTTMRNATKKIAEKFKSELENED---IEVYIFNADKSTKEDILASI
Clostr.thermocellumATCC27405          VTIVYSTMTGNTAKIAQKLVQGLESAG---VETSVFNLKNSDLAEVRKKI
Clostr.perfringens_1_                 VTIPYVSAYGYTKELAEEIAKGIQSEHN--VEVKLYDLTYSKQEDVLADI
Clostr.perfringens_2_                 ASIFYVSAYGYTKQLAEKIAEGIKSTGN--LDINLFNIIEHDMTELVGEV
ChlorobiumtepidumTLS                  ILIAYVSAYENTSVLAQKIAEGLRSACD--FNVDVCDIENMSAEKLEEKI
Clostr.acetobutylicum                 VQIFYITAYGNTGIMAKHLCEDINKKG---VKAEVHEITDMKMEDIVELI
Clostr.tetaniE88_3_                   IEIFYISAYNQTKAVADYFYKQLNNMG---IKADIHEITESGIDKCAELI
Clostr.acetobutylicum_2_              IPIFYCSAYGNTEILANEIASGIKSVLND-ANIEMLDIINYDYSDLKEKI
Rhodobactercapsulatus_1_              LLIFYVSAYGATAQLAQAIHDGAAESPD--VRVSLFDLEGGEITPFLDLI
Rhodobactercapsulatus_2_              LLIFYVSAYRATAQLAQAIHDGAAESPD--VRVSLFDLEGGEITPFLDLI
Rhodobactersphaeroides                LAILYISAHGATARLAQAIRDGAAGEPG--VRVSLFDLEGGELHPFLDLI
Dechloromonasaromatica                LVVFYLSAYGNTRRMAEALAAGAESLGG--VRVSLYDLEGGEAEIFTDLV
Wolinellasuccinogenes                 VTIIYASAYGNTAKMMESVKAGLLDAG---VEVAVFDASSSAMAEMIDSI
Nostocpunctiforme_1_                  VGLFFVSDYGYGERLGHAIAEGILKTGVG-VEVLDL-STAES-QEIQELA
NostocPCC7120_2_                      VGLFYVADYGYSNLLVQAIGEGIQKTGVA-VEMIDL-STAEI-QEIQELA
Nostocpunctiforme_3_                  IGIFYVSEYGYSDRLVQAIANGIGKTGVA-VEIVDLGSEVDL-QELRELV
NostocPCC7120_4_                      IGVFYVSEYGYSDRLAQAIINGITKTGVG-VDVVDLGAAVDL-QELRELV
TrichodesmiumerythraeumIMS101         VAVFYISDYGYSDRLSQAIAHGIIKTGVA-VEMMDL-KSADP-QEVRELV
SynechocystisPCC6803_1_               VVVFYVADYGYGDRLSQAIAKGITKTGVG-VDMVDL-SSADP-QEIQELV
Gloeobacterviolaceus                  VAVFYVSDYGYSDRLSQAIAQGITKSHVA-TELVDL-RATPL-AEIQEIV
NostocPCC7120_1_                      VALFYAEDYGYSEHLVHILGHGCTKTGVA-VELIDL-NTAEP-QEVRELV
Nostocpunctiforme_5_                  VALFYVEDYGHSEQLVRTIAHGCAKTGAA-VELFPL-NSSEP-QEVRELV
SynechocystisPCC6803_2_               VALFYVDGYGVSDRLVQTIADGISKTGVA-IELVDL-SVADT-HEVRTLA
Thermosynechococcuselongatus          VAIFYAANYGYSNALAEAIERGTAKTGVV-VEKMDL-LTAEP-QDIRELT
SynechococcusWH8102                   AAVCYLSQYGFSDRISQAIAHGIGKAEAQ-VQLVDL-RATDP-QELTALI
gi|44454558|gb|EAJ38476.1|            AAVCYLSQYGFSDRISQAIAHGIGKADAQ-VQLVDL-RATDP-QELTALV
gi|44083259|gb|EAH03645.1|            AAICYLSQYGFSDRISQAIAHGVGKADAQ-VQLVDL-RATDA-QELTALI
ProchlorococcusmarinusMIT9313         AAICYLSYYGFCDRLSQAIAHGIGKAKGE-VQLVDL-RATDA-QELSALI
ProchlorococcusmarinusCCMP1375        AAVCYISQYGFCDRLSQAIALGINKADAQ-VQLVDI-RASDA-QELSALI
gi|43719610|gb|EAF14811.1|            AVVCYLSQYGFCDRLSQAIAHGIGKANAQ-VQLVDL-IASDT-QELSALI
gi|42845529|gb|EAA90143.1|            ------------------------------------------------
gi|44500849|gb|EAJ70075.1|            VSVCYISDYGFCDRLSQAISHGICKADAQ-VQLIDL-RSSDS-QELTGLI
ProchlorococcusmarinusCCMP1378        VSVCYISDYGYCDRLSQAISHGISKADAQ-VQLIDL-RSSDS-QELTGLI
gi|42832038|gb|EAA83473.1|            VSVCYISDYGYCDRLSQAISHGISKADAQ-VQLIDL-RSSDS-QELTGLI
gi|44305658|gb|EAI33747.1|            VSVCYISDYGYCDRLSQAISHGISKADAQ-VQLIDL-RSSDP-QELTSLI
gi|44606330|gb|EAK43227.1|            VSVCYISDYGYCDRLSQAISHGIS-------------------------
```

```
gi|44126537|gb|EAH26947.1|          VSVCYISDYGYCDRLSQAISHGISKADAQ-VQLIDL-RSSDP--------500
gi|44102955|gb|EAH14255.1|          VSVCYISDYGYCDRLSQAISHGISKA-----------------------
Nostocpunctiforme_2_                VALLYASAYGNTAIMANAIAQGLIQNGVN-VESINC-ELADS-AEINRIV
NostocPCC7120_3_                    VALLYTSAYGNTGILANAIAQGLVQNDVN-VQSVNC-ELADT-AEITRIV
SynechocystisPCC6803_3_             VALIYASAYGNTATMARAIAQGLVKAGVA-VETINC-EIAEP-NEIVEAI
Nostocpunctiforme_4_                VALLYASAYGNTATLAQAIALGLTKGGVA-VKSINC-EFATP-DEIRINL
NostocPCC7120_5_                    VALLYASAYGNTATIARAIALGLTKGGVA-VKSINC-EFATP-EEIQTNL
Treponema                           ICIIWGSMYGYTKAGLDAVIEGIDEEG---VPYSIYRIPDTDATFILGEA
```

```
                                                                                    500
Methanosarcinamazei                 VDSRAIILGTPTVLAGMHPLALYGAYLVKALKPP----AKYGVVLGSFGW
Methanosarcinabarkeri               --------------------------------------------------
Methanosarcinaacetivorans_C2A       VDSRSIVLGAPTVLGGMHPLALYGTYLVKALNPP----AKYGVVLGSFGW
Methanosarcinabarkeri_3_            VDSRAVILGTPTVLAGMHPLALYGTYLVKALKPP----AKYGVILGSFGW
P.furiosusDSM3638_1_                VDSRAIVLAAPTVLGSAHPLAVYAAYLVKALRPP----AKYAVLIGSHGW
fprA-1[A.fulgidusDSM4304]           VDSRAIVLGTPTVLGGMHPLALFAANLVKALRPP----ARYAAVLSSFGW
FprA3[M.thermautotrophicus          VDASVLVVASPTVLTRPHPAIASVLYLVNALRPP----LRHVAVMGSYGW
Thermoanaerobactertengcongensi      VDAATVVMATPTVLVGPHPMAVYAAYLTNALKPK----VKFISVIGSYNW
PorphyromonasgingivalisW83          FKYKAVIIGSPTYSNEIFSPIKNIMEMIRLREVK----DRYLSVFGSFTW
BacteroidesthetaiotaomicronVPI      FRYKGLIVGSPTYSNQIFPEVESLLSKILVRELK----GRYLGYFGSFTW
FusobacteriumATCC25586_1_           WKYKGLMLGSCAHNNDIYPKMEPLLHKLENYGLK----NRYLGIFGNMMW
FusobacteriumATCC49256              WRYKGLMLGSCAHNNDIYPKMEPLLHKLENYGLK----NRYLGIFGNMMW
FusobacteriumATCC25586_2_           FKYSHIVIASPTYNLGIYPVIHNFVMDMKALNLQ----NRTVAIVENGSW
FusobacteriumATCC49256_2_           FKYSHLVIASPTYNLGIYPVIHNFVMDMKALNLQ----NRTVAIVENGSW
Clostr.tetaniE88_4_                 FKYSHVVLASVTYNLNIYPPMFNYIMDMKALNLQ----KRTFALIENGSW
P.abyssi                            PDSEALIIGVSTYEADVHPRIRYTLYEILDKANY----DKPVLIVGAFGW
P.horikoshii                        PDSEALVIGVSTYEADIHPRMRCALYEILDKANY----EKPVLIVGAFGW
P.furiosusDSM3638_2_                PSAEAIVIGVSTYEADIHPRIRYLLYEIIDKANY----EKPVLIVGAFGW
Thermotogamaritima                  PDSEALIFGVSTYEAEIHPLMRFTLLEIIDKANY----EKPVLVFGVHGW
Shigella                            FRSKGVLVGTSTMNNVMMPKIAGLVEEMTGLRFR----NKRASAFGSHGW
E.coli/O157_H7                      --------------------------------------------------
E.coli/O6/FlRd                      FRSKGVLVGTSTMNNVMMPKIAGLVEEMTGLRFR----NKRASAFGSHGW
E.coli/K12                          FRSKGVLVGTSTMNNVMMPKIAGLVEEMTGLRFR----NKRASAFGSHGW
E.coli/unknown                      FRSKGVLVGTSTMNNVMMPKIAGLVEEMTGLRFR----NKRASAFGSHGW
S.typhimuriumLT2                    FRSKGVLVGTSTMNNVMMPKIAGLVEEMTGLRFR----NKRASAFGSHGW
Salmonella                          FRSKGVLVGTSTMNNVMMPKIAGLVEEMTGLRFR----NKRASAFGSHGW
gi|44480963|gb|EAJ57255.1|          FRSKGILVGSSTMNNVMMPKVAGMLEEITGLRFR----NKRASAFGSYGW
Anophelesgambiae                    FRSKGILVGSSTMNNVMMPKVAGMLEEITGLRFR----NKRASAFGSYGW
E.coli_unknown_                     --------------------------------------------------
V.vulnificusYJ016                   FRSKGILVGSSTMNNVMMPKIAGMLEEITGLRFK----AKKAAAFGSYGW
V.vulnificusCMCP6                   FRSKGILVGSSTMNNVMMPKIAGMLEEITGLRFK----AKKAAAFGSYGW
Clostr.tetaniE88                    FKSKVLLVGSATVNKSIMSATAGILDMIRGLGLK----NKKAAAFGAYGW
M.thermoacetica/fprA                LDARAVLVGSPTINNDILPVVSPLLDDLVGLRPK----NKVGLAFGAYGW
MethanosarcinaacetivoransC2A        LDAAAFAVGSPTLNNGLFPTVGDFLVYLKGLRPQ----KKKAVAFGSYGW
Methanosarcinabarkeri_2_            --------------------------------------------------
Methanococcusmaripaludis_2_         LDSKAVLFGIPTINDQPFPSIGDLMYYLRGLRFDRTGFKKLALTFGSMGG
Methanococcusmaripaludis_3_         LDSKAVLFGIPTINDQPFPSIGDLMYYLRGLRFDRTGFKKLALTFGSMGG
Methanococcusjannaschii_2_          LDAKAVLFGIPTIYDEPYPSIGDIIYYLRGLKFNRTGFKRLAVTFGSMGG
M.thermoautotrophicum_DeltaH_       LDSHAIALGAPAIYDEPYPSVGDLLMYLRGLKFNRTGQRR-AMVFGSMGG
FprA1/M.thermautotrophicus          LDSHAIALGAPAIYDEPYPSVGDLLMYLRGLKFNRTGQRR-AMVFGSMGG
Methanothermobactermarburgensi      LESGAIALGAPTIYDEPYPSVGDLLMYLRGLKFNRTLTRK-ALVFGSMGG
FprA_II_Methanothermobacter         LESKAVFIGSPTMFNGPFPSLGDLIYYLKGLTFDRTGFKRLAVVFGSKGW
Geobactermetallireducens            WKCRGALIGSPTLNNILFPSVAEFLTHLRGLRP----KNRIVGAFGSFGW
GeobactersulfurreducensPCA          WKSRGALIGSPTLNNILYPSVAEFLTHLRGLRP----KNRIVGAFGSYGW
DesulfovibriodesulfuricansG20       ADCGAVIVGSPTHNNGIMPNVAKMLTYMKGLRP----QNKVAAAFGSFGW
D.gigas                             SDAGAVIVGSPTHNNGILPYVAGTLQYIKGLRP----QNKIGGAFGSFGW
Methanococcusmaripaludis            LDAKYVLVGSPTLNINLYPEVARFLKYMEGLKP----NKKIAAAFGSYGW
Methanococcusjannaschii             LDAKYVLVGSPTVNRNLYPEVGKFLAYMDCIRP----LDKIGVAFGSYGW
Methanococcusjannaschii_3_          LDAKYVLVGSPTINMNVHPKVGMLLTYIEGLKPS---NKKIGVXFGSYGW
fprA-2/A.fulgidusDSM4304            LDAKAIAVGSPTIHNGLFPTVAGFLTYLKGLKP----QNKKALAFGSYGW
Giardiaintestinalis                 YDSGAVAFASPTLNNTMMPSVAAALNYVRGLTL---IKGKPAFAFGAFGW
Spironucleusbarkhanus               YDSPCVALGSPTLNSTYMPAQAAVINYCGGLKL---LNTRETFLFGAYGW
Trichomonasvaginalis                MDSAAVAFGSSTLHECILPDIAMHLNYLRCLG----IHDKPVGLFGTFGW
Clostr.tetaniE88_2_                 KESDAVLVGTSTKYGDMIGRLEDILKSLKDMDLE----NKIAAAFGSYGW
Clostr.perfringens_3_               KESDSILFGTSTKYGDLIGSIEDILKELPKLDLS----NKLLGAFGSFGW
Clostr.thermocellumATCC27405        TESDGILVGSSTRYADMVGNVEELLKLLEGEEVK----NKFAAAFGSYGW
Clostr.perfringens_1_               GESDGILFGSPTIVGELLPPIRILLANLNPIIHG----GKYAAAFGSFGW
```

```
Clostr.perfringens_2_            GSSDAILFGSPTIVNELVEPVRDLMAKLNPVVHG----GKIAGAFGSYGW500
ChlorobiumtepidumTLS             AHSMGIIIGSPTINQNIVHQIYGIFAVLNPLRDR----GKLAAAFGSYGW
Clostr.acetobutylicum            ADANGVLVGSPTINQDAVRPVWDVLSSVCPIVNR----GKAAAAFGSYGW
Clostr.tetaniE88_3_              EKSKGFLIGSPTINQDAVKPVWDVLSLVSPIVNR----GKPAGAFGSFGW
Clostr.acetobutylicum_2_         NICDAFMLGTPTINKDALFPIWELIGGIDAVNCK----NKPASAFGSFGW
Rhodobactercapsulatus_1_         EEADGIALGTPTINGDAVRTIWEMLAALVDIETR----GKLGAAFGSYGW
Rhodobactercapsulatus_2_         EEADGIALGTPTINGDAVRTIWEMLAALVDIETR----GKLGAAFGSYGW
Rhodobactersphaeroides           EEVDGIALGTPTINGDAVRAIWELLAMLVDIETR----GKLGAVFGSYGW
Dechloromonasaromatica           EEADGLAFGSPTINADAVKPIWDLLSSLTTVNIK----GKLGAAFGSYGW
Wolinellasuccinogenes            ELSTGILLGTSTINAKAPEPILHLIANLVVLSMN----GRKAGVFGSFGW
Nostocpunctiforme_1_             GRAAGIIIGMPPSTA---AAAQASISSVLAVAKN----KQFVGLFECYGG
NostocPCC7120_2_                 GRAAGLIIGMPPTTS---VAAQAGISSLLSVVKD----KQAVGLFECFGG
Nostocpunctiforme_3_             SRCAGLIVGLPPASG--AASIQSALSTVLGSAKE----KQAIGVFETGGG
NostocPCC7120_4_                 GRCTGLVIGMSPAAS--AASIQGALSTILGSVNE----KQAVGIFETGGG
TrichodesmiumerythraeumIMS101    EMAKGIVIGAPPSTGPIATTAEIGISTILAAANK----KQTFGLFESGGG
SynechocystisPCC6803_1_          GHASGVVLGMPPLQAN--ADLSTNFGAVLAAMQP----KQVFGLYESYGG
Gloeobacterviolaceus             RQSAGVVIGTPPTAGPAAQATQAALGVILANVKE----KQAFGIYEACGG
NostocPCC7120_1_                 TQASGLVIAMPSQY---SLTAQAALNTILAAVHH----KQAIGLLESGGG
Nostocpunctiforme_5_             AQSSGLVIAMPPQS---SVIAQASLSTILAAVHK----KQSIGLLESGGG
SynechocystisPCC6803_2_          QCAAGLVVGMPPQSST-STTLDPLLGTILAAVHP----KQVIGLFESGGG
Thermosynechococcuselongatus     EIAAGIIIGTPPTT----AVAKTALSTIRAAAHA----KQAIGVFESGVA
SynechococcusWH8102              GDAKAVVVPTWPAEPD--GELQASIGTLLAALHP----KQLVGVFDAFGG
gi|44454558|gb|EAJ38476.1|       GDAKAVVVPTWPAEPE--PDLQASIGTLLAALHP----KQLVGVYDAFGG
gi|44083259|gb|EAH03645.1|       GDAKAVVAPTWPLEPD--AELQASI-------------------------
ProchlorococcusmarinusMIT9313    GEAKAVVVPTWPSQPD--AELQSSIGTLLAALNQ----KQWVAVYDAYGG
ProchlorococcusmarinusCCMP1375   GDAKAVVVPTWPNKPD--AELQSSIGTLLAALKP----KQWVAVYEGYGK
gi|43719610|gb|EAF14811.1|       SEASAVV-------------------------------------------
gi|42845529|gb|EAA90143.1|       --------------------------------------------------
gi|44500849|gb|EAJ70075.1|       SESKAVVIPTWPVKSD--NELKESLGTLFAALKP----KQFTAVYDAFGG
ProchlorococcusmarinusCCMP1378   SESKAVVIPTWPVTSD--NELKESLGTLFAALKP----KQFTAVYDAFGG
gi|42832038|gb|EAA83473.1|       SESKAVVIPTWPVKSD--NELKESLGTLFAALKP----KQFTAVT-----
gi|44305658|gb|EAI33747.1|       SESKAVVIPTWPVDSD--NELKESLGTLFAALKP----KQFTAVYDAFGG
gi|44606330|gb|EAK43227.1|       --------------------------------------------------
gi|44126537|gb|EAH26947.1|       --------------------------------------------------
gi|44102955|gb|EAH14255.1|       --------------------------------------------------
Nostocpunctiforme_2_             ETCDGLIIGSPTLGGHAPTQIQTALGIVLSVAAK----TKLAGVFGSYGW
NostocPCC7120_3_                 EACDGIIIGSPTLGGHAPTQIQTALGIVLSTAAK----TKLAGVFGSYGW
SynechocystisPCC6803_3_          QACDGFIVGSPTLGSHAPVQIQTALGIVLSSATK----TKLAGVFGSYGW
Nostocpunctiforme_4_             AQSEGFIIGSPTIGGHAPTPIHTALGIVISSGDN----SKLAGVFGSYGW
NostocPCC7120_5_                 EQVDGFLIGSPTIGGHAPTPINTALGIVLKVGDN----NKLAGVFGSYGW
Treponema                        YRSAGLLLAMPTYEYKMFPPMAHILDLFERKHFVN----KKVFRIGSWGW
```

```
                                                                                 550
Methanosarcinamazei              GGGALRQAGDILTPSSMEVVGTHQ-------------VKGRAKEEDLKKI
Methanosarcinabarkeri            --------------------------------------------------
Methanosarcinaacetivorans_C2A    GGGALKQAGELLAPSKIEIVGTLQ-------------VQGRASREKLKKV
Methanosarcinabarkeri_3_         GGGALKQAGEILVPSKMEIVGTLQ-------------VKGKPREEDLNKI
P.furiosusDSM3638_1_             HGRSIDAILEILKGANFEVLGTVD-------------AHARPKEEDYKAL
fprA-1[A.fulgidusDSM4304]        GGGAVKQIEEIVSSLNLEVLGVVE-------------VRAKPSDSDLEKV
FprA3[M.thermautotrophicus       GSLIESEVRKLLSNLNVEYLESVL-------------VKGLPVEEDLQRV
Thermoanaerobactertengcongensi   GSKAVDQITQMFGNLKVEFIPSVY-------------IKGYPKEEDFKAL
PorphyromonasgingivalisW83       AG-QAVKKIVPFAEEM-GWEMVGEPLE----------QKMSTTDELYEKG
BacteroidesthetaiotaomicronVPI   AG-AAVKRMAEFAEKS-KFELVGDPVE----------MKQAMQDITYTQC
FusobacteriumATCC25586_1_        SG-GGVKRIKEFANTLTGLEQVGEPIE----------IKGHVTSAERDRL
FusobacteriumATCC49256           SG-GGVKRIKEFADTLTGLEQIGEPIE----------IKGHITPDERDRL
FusobacteriumATCC25586_2_        ARKSGDLLQEFFETQIKDITVLNERVG----------LTSSANNVNLDEM
FusobacteriumATCC49256_2_        ARKSGDLLQEFFETQIKDITVLNERVG----------LTSSANNVNLDEM
Clostr.tetaniE88_4_              APQSGQLMYKLLD-EMKEMTILDNEIS----------LNSTIKKDDMDSI
P.abyssi                         GGVAGKKIETLISRSKFELVEVVE-------------TKGRPTEEDKEKL
P.horikoshii                     GGVAGKKVETLISRSKFELVDVVE-------------TKGRMTSEDEERL
P.furiosusDSM3638_2_             GGGAGKKIESMITRSKFDHVMTVE-------------SKGAPSAEDEEKI
Thermotogamaritima               APSAERTAGELLKETKFRILSFTE-------------IKG--SNMDERKI
Shigella                         SGGAMDRLSTRLQDAGFEMSLS---LK----------AKWRPDQDALELC
E.coli/O157_H7                   -----DRLSTRLQDAGFEMSLS---LK----------AKWRPDQDALELC
E.coli/O6/FlRd                   SGGAVDRLSTRLQDAGFEMSLS---LK----------AKWRPDQDALELC
E.coli/K12                       SGGAVDRLSTRLQDAGFEMSLS---LK----------AKWRPDQDALKLC
E.coli/unknown                   SGGAVDRLSTRLQDAGFEMSLS---LK----------AKWRPDQDALKLC
```

```
S.typhimuriumLT2                    SGGAVDRLSTRLQDAGFEMSLS---LK----------AKWRPDLDALELC550
Salmonella                          SGGAVDRLSTRLQDAGFEMSLS---LK----------AKWRPDLDALELC
gi|44480963|gb|EAJ57255.1|          TGGAVDRIQTRLMDAGFDISIS---LK----------AKWRPDGSALAEC
Anophelesgambiae                    TGGAVDRIQTRLMDAGFDISIS---LK----------AKWRPDGSALAEC
E.coli_unknown_                     --------------------------------------------------
V.vulnificusYJ016                   NGGAVDRIHARLTDAGFETAIS---LK----------TKWRPDGKAMREC
V.vulnificusCMCP6                   NGGAVDRIHARLTDAGFETAIS---LK----------TKWRPDGKAMREC
Clostr.tetaniE88                    SGEAVKILEEKLKNGKFEILESG--IK----------ELWNPDKDAMNRC
M.thermoacetica/fprA                GGGAQKILEERLKAAKIELIAEP-GPT----------VQWVPRGEDLQRC
MethanosarcinaacetivoransC2A        GGGAVKTVEKELKDTGIEVLEP--GLQ----------IRYRPYEKELERC
Methanosarcinabarkeri_2_            --------------------------------------------------
Methanococcusmaripaludis_2_         NGGATKLIGNDLKECGFEVLDD--SYE----------VLYVPEEDELEKC
Methanococcusmaripaludis_3_         RGGAIEKIANELGSSGFDVVN---EYE----------LYYIPNEDELEKC
Methanococcusjannaschii_2_          EGGAVAKIAEDLAKCGFEVIN---QYE----------LYYVPTEDELTNC
M.thermoautotrophicum_DeltaH_       RGGATGTMQKLLADAGFDVME---ADE----------IYYVPNNEELDAC
FprA1/M.thermautotrophicus          RGGATGTMQKLLADAGFDVME---ADE----------IYYVPNNEELDAC
Methanothermobactermarburgensi      NGGATGTMKELLAEAGFDVAC---EEE----------VYYVPTGDELDAC
FprA_II_Methanothermobacter         GGGAVRTLQEELSGAGFEVAE---TFE----------VNYVPTSGDLDEC
Geobactermetallireducens            GGGAVKESYEVFKQMGLQTVEPG--IQ----------LAYRPSLADEEAC
GeobactersulfurreducensPCA          GGGAVRDAYEEFKKMGLQAVEPG--FQ----------IPYRPSRADEEGA
DesulfovibriodesulfuricansG20       SGESVKNITGWLEDMGFEVPAEG--VK----------CKHVPKHETYEEC
D.gigas                             SGESTKVLAEWLTGMGFDMPATP--VK----------VKNVPTHADYEQL
Methanococcusmaripaludis            AENATKHIKNTFDILSFDTVDDE-CLT----------CRFVPNEEHLKKC
Methanococcusjannaschii             MECATEKIKEIFKNLGFKIVDDE-CLT----------VRFAPKEEHLKKC
Methanococcusjannaschii_3_          KECATKKIIEAFKRLGFKIVDDK-ILT----------FRFAPKENDIKKI
fprA-2/A.fulgidusDSM4304            NGNAVKEVQKVLEELKFETLEP---FM----------VKFKPSEEELQKA
Giardiaintestinalis                 SNRAVPDIVAELRDGCKADVYDEKGIT----------FKFNYTEELLEQA
Spironucleusbarkhanus               AEKATKDMKADVEK--VGAVNSIPAVT----------WKYNVDVDVLNKC
Trichomonasvaginalis                QEKIVPNELRNAIVKPCKIPEVAEPVM----------AHWNPKEADLAKC
Clostr.tetaniE88_2_                 SGEGIEVVQDYLNETNMKVLSTSYIIK----------STGMTDVKFPIRI
Clostr.perfringens_3_               SGEPIEIIQDYLNSTNGNVLNTSSIIK----------STGMIDVHFPVRI
Clostr.thermocellumATCC27405        SGEAIMHIENYLDKIGFNVINQKYLIG----------SAGIDIPLFPLRI
Clostr.perfringens_1_               SGEAVPRIEARLKELKMNIFGPGLRIK------------FKPSTTELKEA
Clostr.perfringens_2_               SGEAVPRIESRLKELRMKMPVEGLRIK------------FKPSEEEAQKA
ChlorobiumtepidumTLS                SGEGVKIIESNLANLKLKVFDQNVMVK------------FQPHEPEFEQC
Clostr.acetobutylicum               SGEGVPMMMDRLKSLKFKTPDNGLKFK------------FVPASKEFSEA
Clostr.tetaniE88_3_                 SGEGVPMMTERLKSLKLKVVEEGFKFK------------FVPSSEDYKNA
Clostr.acetobutylicum_2_            SGEAIPFVISRLKELKLKVFQDGFTCL------------FVPSEDDIKKA
Rhodobactercapsulatus_1_            SGEAVRLVETRLQGLKMRLPEPGLRVK------------LHPSAAELKEG
Rhodobactercapsulatus_2_            SGEAVRLVETRLQGLKMRLPEPGLRVK------------LHPSAAELEEG
Rhodobactersphaeroides              SGEAVRQVEARLQGLKMRLPEPGLKVK------------LEPTDEDLQEA
Dechloromonasaromatica              SGEAVRLIEDRLRGLKLRVPVDGLRIK------------LVPDASELEQC
Wolinellasuccinogenes               SGEGIAMTERICEVMKMKIVQEPYKVQ------------MAPSSAQLEEG
Nostocpunctiforme_1_                DDEPIDTLRRKFIDSGIKEAFPAIRIR------------EAPTASTFQLC
NostocPCC7120_2_                    DDEPVDTIRRKFIDLGVKEAFPAIRIK------------DVPGASAYQLC
Nostocpunctiforme_3_                DDEPIDPLLSKFRNLGLTTVFPAIRIK------------QTPTENTYKLC
NostocPCC7120_4_                    DDEPIDPLLSKFRNLGLTTAFPAIRIK------------QTPTENTYKLC
TrichodesmiumerythraeumIMS101       DDLSIYPLAIQFKGLGLKQAFPNITIK------------ETPSELTYKLC
SynechocystisPCC6803_1_             DDEPIDPLRTKFLDLGLREAFKVIKVK------------DTPSESTYQLC
Gloeobacterviolaceus                FDEPAFPLSSRFADLGLVRAFAPIRIPGREGALAEAEATGTPTPALYKLC
NostocPCC7120_1_                    EDEPVFPLRNKFQELGLVEAFPPILIK------------EAPAQTTEQLC
Nostocpunctiforme_5_                EDEPIYPLRNKFQELGLTEAFPPILVK------------EIPTQATEQLC
SynechocystisPCC6803_2_             QDEPIYPLRNRFQELGLQEAFEPILLK------------TEPTAATDQLC
Thermosynechococcuselongatus        DAEPAYPLLNQFRDAGLVPSFPVIRVT------------AAPTDALFQEA
SynechococcusWH8102                 NDEPIDAVADQLRSQGQKQAFAPLRIR------------QLPQGSDYQRC
gi|44454558|gb|EAJ38476.1|          NDEPIDA-----------------------------------------
gi|44083259|gb|EAH03645.1|          --------------------------------------------------
ProchlorococcusmarinusMIT9313       NDEPIDAVAAQLRSLGQKEAFEPLRVR------------QAPDGNVYQRF
ProchlorococcusmarinusCCMP1375      NDEPIDVVANQLRSLGQKEAFSPLRVK------------QSPDANTFQQF
gi|43719610|gb|EAF14811.1|          --------------------------------------------------
gi|42845529|gb|EAA90143.1|          --------------------------------------------------
gi|44500849|gb|EAJ70075.1|          NDEPIDSLANKLRELGQKEAFSPLRVK------------NIPDPIIYQQF
ProchlorococcusmarinusCCMP1378      NDEPIDSLASKLRELGQKEAFSPLRVK------------NIPDPIIYQQF
gi|42832038|gb|EAA83473.1|          --------------------------------------------------
gi|44305658|gb|EAI33747.1|          NDEPIDSLANKLRELGQKEAFSPLRVK------------NIPDPIVYQQF
gi|44606330|gb|EAK43227.1|          --------------------------------------------------
gi|44126537|gb|EAH26947.1|          --------------------------------------------------
gi|44102955|gb|EAH14255.1|          --------------------------------------------------
Nostocpunctiforme_2_                SGEAIDLIESKLKDANYQLGFETIRVR------------FSPTSEILQQC
NostocPCC7120_3_                    SGEAIDLIESKLKDANYRLGFDTIRVR------------FSPTPEILQQC
SynechocystisPCC6803_3_             SGEAIDLIENKLKDGGYRFGFEAIRIQ------------FSPNLDALDVC
```

```
Nostocpunctiforme_4_              SGEAFDLIEGKLRDSGYRFGFDTLKVK------------FKPDDVTLKFC550
NostocPCC7120_5_                  SGEALDMIEGKLRDAGYRFGLDTLKVK------------FKPDDVTLKFC
Treponema                         VGGAKKEYEEKIEKFKWTNIESHEWQG-------------KLSDEDKRIL
```

```
                                                                                    600
Methanosarcinamazei               EEIGRQLAQKMKA-------------------------------------
Methanosarcinabarkeri             ---------------------------------------------------
Methanosarcinaacetivorans_C2A     EEIGRELARKMKT-------------------------------------
Methanosarcinabarkeri_3_          EGIGRELARKMKA-------------------------------------
P.furiosusDSM3638_1_              HSLADLLAKKVRGE-------------------------------------
fprA-1[A.fulgidusDSM4304]         RKLAEKIAGVVKV-------------------------------------
FprA3[M.thermautotrophicus        DELAMKIKGVNEW-------------------------------------
Thermoanaerobactertengcongensi    DALAEEIVKRHKEAGIM----------------------------------
PorphyromonasgingivalisW83        WELGNKIAERLKADRQ-----------------------------------
BacteroidesthetaiotaomicronVPI    ENLARAMADRLKKDR-----------------------------------
FusobacteriumATCC25586_1_         IELANLMADKLIANRK-----------------------------------
FusobacteriumATCC49256            VELA----------------------------------------------
FusobacteriumATCC25586_2_         DTLVDALVESLNK-------------------------------------
FusobacteriumATCC49256_2_         DALVDALVESLNK-------------------------------------
Clostr.tetaniE88_4_               EELAQNIIESMN--------------------------------------
P.abyssi                          REAVRRLIQWIS--------------------------------------
P.horikoshii                      REAVRKLIQWQL--------------------------------------
P.furiosusDSM3638_2_              RDAVRELIQRSLPTGNT----------------------------------
Thermotogamaritima                EEAISLLKKELE--------------------------------------
Shigella                          REHGREIARQWALAP-LPQSTVNTVVKEET--------------SATTTA
E.coli/O157_H7                    REHGREIARQWALAP-LPQSTVNTVVKEET--------------SATTTA
E.coli/O6/FlRd                    REHGREIARQWALAP-LPQSTVNTVVKEET--------------SAATTA
E.coli/K12                        REHGREIARQWALAP-LPQSTVNTVVKEET--------------SATTTA
E.coli/unknown                    REHGREIARQWALAP-LPQSTVNTVVKRRN--------------LCHHDG
S.typhimuriumLT2                  RQHGRDIARQWALAP-LPETTQQIAPVEET--------------ITCTAA
Salmonella                        RQHGRDIARQWALAP-LPETTQKTAPVEET--------------TTCTAA
gi|44480963|gb|EAJ57255.1|        REHGRQLARQWALHP-LDAPRPITTTQTDVTPAPLMPAVEPIAAAATAEW
Anophelesgambiae                  REHGRQLARQWAL-------------------------------------
E.coli_unknown_                   ---------------------------------------------------
V.vulnificusYJ016                 REHGQQIAKLWAVKDKSTLSTPVNAFQSATPIEGIEAQQPLTETTPTADA
V.vulnificusCMCP6                 REHGQQIAKLWAVKDKSTLSTPVNAFQSATPIEGIEAQQPLTETTPTADA
Clostr.tetaniE88                  RQFGKNIVEKL----------------------------------------
M.thermoacetica/fprA              YELGRKIAARIAD-------------------------------------
MethanosarcinaacetivoransC2A      RKLGEQLAAVAKEQ-------------------------------------
Methanosarcinabarkeri_2_          ---------------------------------------------------
Methanococcusmaripaludis_2_       YNAGKRLGMKLK--------------------------------------
Methanococcusmaripaludis_3_       YSLGNELGKNIKSI------------------------------------
Methanococcusjannaschii_2_        YNMGKELAKRIKEMKIE----------------------------------
M.thermoautotrophicum_DeltaH_     FEAGRRLAGDLNE-------------------------------------
FprA1/M.thermautotrophicus        FEAGRRLAGDLNE-------------------------------------
Methanothermobactermarburgensi    FEAGRKLAAEIRR-------------------------------------
FprA_II_Methanothermobacter       YSIGKSVGERIKKM------------------------------------
Geobactermetallireducens          FEFGRTFARQVSEYHKGF---------------------------------
GeobactersulfurreducensPCA        FEFGRNFARQVIEYHKGF---------------------------------
DesulfovibriodesulfuricansG20     YNLGKAVAQALKAKCEA---------------------------------
D.gigas                           KTMAQTIARALKAKLAA----------------------------------
Methanococcusmaripaludis          QEFGKKLAKM----------------------------------------
Methanococcusjannaschii           YEFGKRLADIGF--------------------------------------
Methanococcusjannaschii_3_        KEFGRKLAKINV--------------------------------------
fprA-2/A.fulgidusDSM4304          FELGRELAR-----------------------------------------
Giardiaintestinalis               YNAGVDLGKRAIAYCEKNAPKQ----------------------------
Spironucleusbarkhanus             KEAGFQLGKKALVRCGK---------------------------------
Trichomonasvaginalis              EELGRKLALAAIEKCK----------------------------------
Clostr.tetaniE88_2_               KFSPEENDKEEIKKTTTFIVDLLLNSI-----------------------
Clostr.perfringens_3_             RFSLNEESEKEVVRAADYISSII---------------------------
Clostr.thermocellumATCC27405      KFARQEGLELAEEAGRVFGEQVLTH-------------------------
Clostr.perfringens_1_             FEFGRDFSRTMFGEKELDYAPNNATETKEVLTGNGKTRYWKCLVCGEIFE
Clostr.perfringens_2_             FDFG----------------------------------------------
ChlorobiumtepidumTLS              REFG----------------------------------------------
Clostr.acetobutylicum             DKFV----------------------------------------------
Clostr.tetaniE88_3_               DTFL----------------------------------------------
Clostr.acetobutylicum_2_          FKFG----------------------------------------------
Rhodobactercapsulatus_1_          RAFG----------------------------------------------
```

```
Rhodobactercapsulatus_2_          RAFG-----------------------------------------------600
Rhodobactersphaeroides            RAFG-----------------------------------------------
Dechloromonasaromatica            RLLG-----------------------------------------------
Wolinellasuccinogenes             REWG-----------------------------------------------
Nostocpunctiforme_1_              EEAGKDLGQLLVRDRNIKQIKSLDVN-----MEKALGRISSGLYIVTTKK
NostocPCC7120_2_                  TEAGTDLGQLLTRERNIKQIKSLDVN-----MEKALGRISNGLYIVTTKK
Nostocpunctiforme_3_              EEAGTDLAQWVTRDRSIKAMKSLGAD-----LDKALGRLSGGLYIITAKK
NostocPCC7120_4_                  EEAGTDLGQWVTRDRSIKAMKSLGAD-----LDKALGRLSGGLYIITAKK
TrichodesmiumerythraeumIMS101     EEAGTDAGQLLSIKENIKQMKSLDSG-----LDKALGRLSGGLYIITASK
SynechocystisPCC6803_1_           DESGTDLGQNLIQAAKIKQLKSLDSD-----LEKAIGRISGGLYIITAQK
Gloeobacterviolaceus              EESGTDLAQWLTRDRTVQQMKAVAVG-----LDKAMGRLSGGLYVLTAAK
NostocPCC7120_1_                  EEAGTDIGQWLTRDRTIKQIKSINTD-----LEKALGRISTGLYIITTKK
Nostocpunctiforme_5_              DEAGTDLGQWLNRDRTIKQIKSINTE-----LEKALGRLSTGLYIITAKK
SynechocystisPCC6803_2_           REAGTDLGQYLTQKQSQQANTDLDPE-----LNQAIGRLSTGLYILTAQK
Thermosynechococcuselongatus      EEAGTDMGQWLLRDRTVKQMKALDTD-----LDKALGRLSGGLYIITAQK
SynechococcusWH8102               EESGTDLGQLLTKEKAIAAMKSLDGD-----LDKALGRISGGLYVVTASQ
gi|44454558|gb|EAJ38476.1|        -----------------------------------------------
gi|44083259|gb|EAH03645.1|        -----------------------------------------------
ProchlorococcusmarinusMIT9313     EEAGTDLGQLLNQKQNIAAMKSLDTE-----LDKAMGTLSGGLYVVTASQ
ProchlorococcusmarinusCCMP1375    DEAGTDLGQLLNRKKNIATIKSFDGD-----LMKAMGRISGGLYVVTASQ
gi|43719610|gb|EAF14811.1|        -----------------------------------------------
gi|42845529|gb|EAA90143.1|        -----------------------------------------------
gi|44500849|gb|EAJ70075.1|        EEAGTDLGQLINKKKNIASMKSLDSN-----LDKALGRLSGGLYVVTASQ
ProchlorococcusmarinusCCMP1378    EEAGTDLGQLINKKKNIASMKSLDSN-----LDKALGRLSGGLYVVTASQ
gi|42832038|gb|EAA83473.1|        -----------------------------------------------
gi|44305658|gb|EAI33747.1|        EEAGTDLGQLINKKKNIASMKSLDSN-----LDKALGRLSGGLYVVTASQ
gi|44606330|gb|EAK43227.1|        -----------------------------------------------
gi|44126537|gb|EAH26947.1|        -----------------------------------------------
gi|44102955|gb|EAH14255.1|        -----------------------------------------------
Nostocpunctiforme_2_              QEAGAFFAQNLKKTKKLRSSRQIVTETHVDRTEQAVGRIIGSLCVVTTRD
NostocPCC7120_3_                  QAAGATFAQTLKKNKKLRTPRQVIPEAKIDRTEQAVGRIIGSLCVVTTRD
SynechocystisPCC6803_3_           TTSGANFARQLRTHKRQRIARQATTETQADRTQQAVGRIIGSIGVVTTQT
Nostocpunctiforme_4_              EELGTDFAQALKKAKKVRVPQQAATP-----VEQAVGRIVGSVCVVTAKQ
NostocPCC7120_5_                  EEVGTDFAQTLKKAKKVRVPQQAATP-----VEQAVGRIVGSVCVITAKQ
Treponema                         KERGRELARAVKNG--------------------------------------
```

```
                                                                                    650
Methanosarcinamazei               -----------------------------------------------
Methanosarcinabarkeri             -----------------------------------------------
Methanosarcinaacetivorans_C2A     -----------------------------------------------
Methanosarcinabarkeri_3_          -----------------------------------------------
P.furiosusDSM3638_1_              -----------------------------------------------
fprA-1[A.fulgidusDSM4304]         -----------------------------------------------
FprA3[M.thermautotrophicus        -----------------------------------------------
Thermoanaerobactertengcongensi    -----------------------------------------------
PorphyromonasgingivalisW83        -----------------------------------------------
BacteroidesthetaiotaomicronVPI    -----------------------------------------------
FusobacteriumATCC25586_1_         -----------------------------------------------
FusobacteriumATCC49256            -----------------------------------------------
FusobacteriumATCC25586_2_         -----------------------------------------------
FusobacteriumATCC49256_2_         -----------------------------------------------
Clostr.tetaniE88_4_               -----------------------------------------------
P.abyssi                          -----------------------------------------------
P.horikoshii                      -----------------------------------------------
P.furiosusDSM3638_2_              -----------------------------------------------
Thermotogamaritima                -----------------------------------------------
Shigella                          DL---GPRMQCSVCQWIYDPAKGEPMQDVAPGTPWSEVPDNFLCPECSLG
E.coli/O157_H7                    DL---GPRMQCSVCQWIYDPAKGEPMQDVAPGTPWSEVPDNFLCPECSLG
E.coli/O6/FlRd                    DL---GPRMQCSVCQWIYDPAKGEPMQDVAPGTPWSEVPDNFLCPECSLG
E.coli/K12                        DL---GPRMQCSVCQWIYDPAKGEPMQDVAPGTPWSEVPDNFLCPECSLG
E.coli/unknown                    -----------------------------------------------
S.typhimuriumLT2                  DL---GPKMQCSVCQWIYDPALGEPLQDVAPGTPWNDVPDNFLCPECSLG
Salmonella                        DL---GPKMQCSVCQWIYDPALGEPLQDVAPGTPWSDVPDNFLCPECSLG
gi|44480963|gb|EAJ57255.1|        DD---DQTMLCTVCQWVYDPAQGEPDQLVAPGTPWAQVPDSFLCPGCGIG
Anophelesgambiae                  -----------------------------------------------
E.coli_unknown_                   -----------------------------------------------
V.vulnificusYJ016                 AHSADCQCMVCTVCNWVYDPAKGEPNQGIEVGTTWADVPDYFLCPECHLG
V.vulnificusCMCP6                 AHSADCQCMVCTVCNWVYDPAKGEPNQGIEVGTTWADVPDYFLCPECHLG
```

```
Clostr.tetaniE88                    --------------------------------------------------650
M.thermoacetica/fprA                --------------------------------------------------
MethanosarcinaacetivoransC2A        --------------------------------------------------
Methanosarcinabarkeri_2_            --------------------------------------------------
Methanococcusmaripaludis_2_         --------------------------------------------------
Methanococcusmaripaludis_3_         --------------------------------------------------
Methanococcusjannaschii_2_          --------------------------------------------------
M.thermoautotrophicum_DeltaH_       --------------------------------------------------
FprA1/M.thermautotrophicus          --------------------------------------------------
Methanothermobactermarburgensi      --------------------------------------------------
FprA_II_Methanothermobacter         --------------------------------------------------
Geobactermetallireducens            --------------------------------------------------
GeobactersulfurreducensPCA          --------------------------------------------------
DesulfovibriodesulfuricansG20       --------------------------------------------------
D.gigas                             --------------------------------------------------
Methanococcusmaripaludis            --------------------------------------------------
Methanococcusjannaschii             --------------------------------------------------
Methanococcusjannaschii_3_          --------------------------------------------------
fprA-2/A.fulgidusDSM4304            --------------------------------------------------
Giardiaintestinalis                 --------------------------------------------------
Spironucleusbarkhanus               --------------------------------------------------
Trichomonasvaginalis                --------------------------------------------------
Clostr.tetaniE88_2_                 --------------------------------------------------
Clostr.perfringens_3_               --------------------------------------------------
Clostr.thermocellumATCC27405        --------------------------------------------------
Clostr.perfringens_1_               SPVCPEVCPVCGAGKEQFIEVEMDTFEKNDTNDNFVIIGNGAAGFYAAKT
Clostr.perfringens_2_               ------------------------------------VEIGN------ALK-
ChlorobiumtepidumTLS                ----------------------------------------------KAFAEKM
Clostr.acetobutylicum               -------------------------------------------------DDF
Clostr.tetaniE88_3_                 -------------------------------------------------EDF
Clostr.acetobutylicum_2_            -------------------------------------------------EDF
Rhodobactercapsulatus_1_            -------------------------------------------------RRL
Rhodobactercapsulatus_2_            -------------------------------------------------RRL
Rhodobactersphaeroides              -------------------------------------------------RRL
Dechloromonasaromatica              -------------------------------------------------ENL
Wolinellasuccinogenes               -------------------------------------------------YNF
Nostocpunctiforme_1_                DN----ASSAMLASWVTQASLQPLGLTIAVAKDRAIDSLMQVGDRFVLNV
NostocPCC7120_2_                    GD----VSSAMLASWVSQASLQPLGFTIAVAKDRAIDSLMQVGDRFVLNV
Nostocpunctiforme_3_                GD----VSSAMLASWVAQASFKPLGFSIAVAKDRAIESLMQVGDRFVLNI
NostocPCC7120_4_                    GD----VSSAMLASWVNQASFKPLGFSIAVAKDRAIESLMQVGDRFVLNV
TrichodesmiumerythraeumIMS101       GE----VSSAMLASWVVQASFKPLGVSIAVAKDRAIEALMQVGDRFVLNV
SynechocystisPCC6803_1_             GE----VKGAMLASWVSQASFNPPGFTVAVAKDRAIESLMQVGDRFVLNI
Gloeobacterviolaceus                GE----LKGAMLASWVNQASFAPLGVTIAVAKDRAIEALMQVGDLFALNV
NostocPCC7120_1_                    GE----IQGAMFASWVTQASLNPLGVAIAVSKERAIESLMQVGDHFVLNV
Nostocpunctiforme_5_                GE----IQSAMLASWVTQASLEPLGVAIAVSKDRAIESLMHVGDRFVLNV
SynechocystisPCC6803_2_             GD----VRSAMLASWVIQGSFEPLGIVIAVAKDRAIESLLHPGDTFVLNV
Thermosynechococcuselongatus        GA----INSAMLASWVAQASTEPLGVSIAVAKDRAIESFLHVGDTFVLNV
SynechococcusWH8102                 GEGESQRRSAMVASWVSQASFSPPGLTVAVAKDRAIEALMQVEDRFVLNV
gi|44454558|gb|EAJ38476.1|          --------------------------------------------------
gi|44083259|gb|EAH03645.1|          --------------------------------------------------
ProchlorococcusmarinusMIT9313       DEESSQRRGAMIASWVSQASFTPPGLTVAVAKDRAIETLMQVGDRFVINV
ProchlorococcusmarinusCCMP1375      GDDSNKRRGAMVASWVSQASFNPPGLTVAVAKDRAIEALMQVGDRFVLNV
gi|43719610|gb|EAF14811.1|          --------------------------------------------------
gi|42845529|gb|EAA90143.1|          --------------------------------------------------
gi|44500849|gb|EAJ70075.1|          GEGSTFRQSAMVASWVSQASFSPPGITVAVAKDRAIESYMQVGEGFVVNI
ProchlorococcusmarinusCCMP1378      GEGSTFRQSAMVASWVSQASFSPPGITVAVAKDRAIESYMQVGEGFVVNI
gi|42832038|gb|EAA83473.1|          --------------------------------------------------
gi|44305658|gb|EAI33747.1|          GEGSTFRQSAMVASWVSQASFSPPGITVAVAKDRAIESYMQVGKGFVVNI
gi|44606330|gb|EAK43227.1|          --------------------------------------------------
gi|44126537|gb|EAH26947.1|          --------------------------------------------------
gi|44102955|gb|EAH14255.1|          --------------------------------------------------
Nostocpunctiforme_2_                EE----THKGVLTSWVSQATFNPPGIMIAIANEQNADLMHHPGDKFVLNI
NostocPCC7120_3_                    QE----SHKGILTSWVSQATFNPPGIMMAIAQEQNADLMSHTGDQFVLNI
SynechocystisPCC6803_3_             TG----RHQGILTSWVSQASFTPPGIMLAIPGEFDAYGLAGQNKAFVLNL
Nostocpunctiforme_4_                GE----VSTAMLGAWVSQATFNPPGITVAIAKERAIESLMYPGGKFALNI
NostocPCC7120_5_                    GD----VSTGMLGSWVSQATFNPPGLTVAIAKERAIESLMYPGGKFALNI
Treponema                           --------------------------------------------------
```

```
                                                                      700
Methanosarcinamazei             --------------------------------------------------
Methanosarcinabarkeri           --------------------------------------------------
Methanosarcinaacetivorans_C2A   --------------------------------------------------
Methanosarcinabarkeri_3_        --------------------------------------------------
P.furiosusDSM3638_1_            --------------------------------------------------
fprA-1[A.fulgidusDSM4304]       --------------------------------------------------
FprA3[M.thermautotrophicus      --------------------------------------------------
Thermoanaerobactertengcongensi  --------------------------------------------------
PorphyromonasgingivalisW83      --------------------------------------------------
BacteroidesthetaiotaomicronVPI  --------------------------------------------------
FusobacteriumATCC25586_1_       --------------------------------------------------
FusobacteriumATCC49256          --------------------------------------------------
FusobacteriumATCC25586_2_       --------------------------------------------------
FusobacteriumATCC49256_2_       --------------------------------------------------
Clostr.tetaniE88_4_             --------------------------------------------------
P.abyssi                        --------------------------------------------------
P.horikoshii                    --------------------------------------------------
P.furiosusDSM3638_2_            --------------------------------------------------
Thermotogamaritima              --------------------------------------------------
Shigella                        KDVFDELASEAK--------------------------------------
E.coli/O157_H7                  KDVFDELASEAK--------------------------------------
E.coli/O6/FlRd                  KDVFDELASEAK--------------------------------------
E.coli/K12                      KDVFEELASEAK--------------------------------------
E.coli/unknown                  --------------------------------------------------
S.typhimuriumLT2                KDVFDVLATEAK--------------------------------------
Salmonella                      KDVFDVLATEAK--------------------------------------
gi|44480963|gb|EAJ57255.1|      KEVFEPCAVEACV-------------------------------------
Anophelesgambiae                --------------------------------------------------
E.coli_unknown_                 --------------------------------------------------
V.vulnificusYJ016               KDVFVEYQG-----------------------------------------
V.vulnificusCMCP6               KDVFVEYQG-----------------------------------------
Clostr.tetaniE88                --------------------------------------------------
M.thermoacetica/fprA            --------------------------------------------------
MethanosarcinaacetivoransC2A    --------------------------------------------------
Methanosarcinabarkeri_2_        --------------------------------------------------
Methanococcusmaripaludis_2_     --------------------------------------------------
Methanococcusmaripaludis_3_     --------------------------------------------------
Methanococcusjannaschii_2_      --------------------------------------------------
M.thermoautotrophicum_DeltaH_   --------------------------------------------------
FprA1/M.thermautotrophicus      --------------------------------------------------
Methanothermobactermarburgensi  --------------------------------------------------
FprA_II_Methanothermobacter     --------------------------------------------------
Geobactermetallireducens        --------------------------------------------------
GeobactersulfurreducensPCA      --------------------------------------------------
DesulfovibriodesulfuricansG20   --------------------------------------------------
D.gigas                         --------------------------------------------------
Methanococcusmaripaludis        --------------------------------------------------
Methanococcusjannaschii         --------------------------------------------------
Methanococcusjannaschii_3_      --------------------------------------------------
fprA-2/A.fulgidusDSM4304        --------------------------------------------------
Giardiaintestinalis             --------------------------------------------------
Spironucleusbarkhanus           --------------------------------------------------
Trichomonasvaginalis            --------------------------------------------------
Clostr.tetaniE88_2_             --------------------------------------------------
Clostr.perfringens_3_           --------------------------------------------------
Clostr.thermocellumATCC27405    --------------------------------------------------
Clostr.perfringens_1_           IREINSTASVKLLSSEEVSSYSRPNLSDLLNEEMNLDTFYLAKSSWYKEN
Clostr.perfringens_2_           --------------------------------------------------
ChlorobiumtepidumTLS            IEMYNLTCNIK---------------------------------------
Clostr.acetobutylicum           IGLL----------------------------------------------
Clostr.tetaniE88_3_             KNLL----------------------------------------------
Clostr.acetobutylicum_2_        AKSI----------------------------------------------
Rhodobactercapsulatus_1_        ADHLTGRAAPREVDFAEIAAR-----------------------------
Rhodobactercapsulatus_2_        ADHLTGRARPREVDFAEIAAR-----------------------------
Rhodobactersphaeroides          AAHLTGRAPPREVDLADLASR-----------------------------
Dechloromonasaromatica          ARHLTGRIEHREIDMAALA-------------------------------
Wolinellasuccinogenes           GLKIIE--------------------------------------------
Nostocpunctiforme_1_            LEEGNYQELKKHFLKR--LHPGADRFAGVKTQT-AKNGSPILTDALAYME
NostocPCC7120_2_                LEEGNYQELKKQFLKR--LHPGADRFAGVRTQT-AKNGSPILTDALAYME
Nostocpunctiforme_3_            LEEGNFQPLMKHFLKR--FAPGADRFEGVRTQP-AENGAPILNDALAYME
```

```
NostocPCC7120_4_                LEEGNYQPLMRHFLKR--FAPGADRFEGVKTQP-AENGAPILGDALAYME750
TrichodesmiumerythraeumIMS101   LREDNYQYLMRHFLKR--FKPGADRFAGVNTQT-ANNGSPILSDALAYLE
SynechocystisPCC6803_1_         LEEGNYQILMKHFLKR--FPPGADRFAGVKTQT-ASNGSPILTDALAYLE
Gloeobacterviolaceus            LEEGKYAPLMRHFLKR--FAPGEDRFVGVETLT-GTGGTPILADALAYME
NostocPCC7120_1_                LEEDNYQGLMKHFLKR--FAPGADRFAGIKTYP-ATDGSPILAESLAYTE
Nostocpunctiforme_5_            LEEGKYQGLMKHFLKR--FAPGVDRFAGVKTYP-AKNESPVLAEALAYME
SynechocystisPCC6803_2_         LEEDNYQSLMRHFLLR--FPPGADRFAGVNTYP-AQNGSPILLETLAYLE
Thermosynechococcuselongatus    LEAENYQPLMRHFLKR--FPPGADRFAHVKTYP-ASNGSPILADALAYME
SynechococcusWH8102             LREDNHQPLLRHFLKR--FPPGADRFAGVNVLEGVADGGPVLTDALAYLS
gi|44454558|gb|EAJ38476.1|      --------------------------------------------------
gi|44083259|gb|EAH03645.1|      --------------------------------------------------
ProchlorococcusmarinusMIT9313   LREDNYQPLLRQFLKR--FPPGADRFEGVNVLNNVAKGGPVLVDALAFLD
ProchlorococcusmarinusCCMP1375  LEENNYQHLFRQFLKR--FPPGANRFEGITVMEDVAKGGPVLGDALAYLD
gi|43719610|gb|EAF14811.1|      --------------------------------------------------
gi|42845529|gb|EAA90143.1|      --------------------------------------------------
gi|44500849|gb|EAJ70075.1|      LREDNYQ----------------------------------------------
ProchlorococcusmarinusCCMP1378  LREDNYQKMFRHFLKR--FAPGADRFADVDVVNNIANGGPVLSDSLAFLD
gi|42832038|gb|EAA83473.1|      --------------------------------------------------
gi|44305658|gb|EAI33747.1|      LREDNYQKMFRHFLKR--FAPGADRFADVDVISNIAEGGPVLSDSLAFLD
gi|44606330|gb|EAK43227.1|      --------------------------------------------------
gi|44126537|gb|EAH26947.1|      --------------------------------------------------
gi|44102955|gb|EAH14255.1|      --------------------------------------------------
Nostocpunctiforme_2_            LKEG--RNVRRYFSRH--STLGDNPFANLATKT-ALNGCLILNEALAYLE
NostocPCC7120_3_                LKEG--RNVRRYFSRQ--STLGDNPFANLKTKT-ADNGCLILTEALAYLE
SynechocystisPCC6803_3_         LQEG--RSVRRHFDHQPLPKDGDNPFSRLEHYS-TQNGCLILAEALAYLE
Nostocpunctiforme_4_            LPEGNHQDYMKHFRKS--FAPGEDRFANFSTAV-ADNGCTVLTDALAYLE
NostocPCC7120_5_                LSEGNHLEYMKHFRKN--FAPGEDRFANFTTTE-ADNGCTVLADALAYVE
Treponema                       --------------------------------------------------
```

```
                                                                                750
Methanosarcinamazei             ------------------------------------------------
Methanosarcinabarkeri           ------------------------------------------------
Methanosarcinaacetivorans_C2A   ------------------------------------------------
Methanosarcinabarkeri_3_        ------------------------------------------------
P.furiosusDSM3638_1_            ------------------------------------------------
fprA-1[A.fulgidusDSM4304]       ------------------------------------------------
FprA3[M.thermautotrophicus      ------------------------------------------------
Thermoanaerobactertengcongensi  ------------------------------------------------
PorphyromonasgingivalisW83      ------------------------------------------------
BacteroidesthetaiotaomicronVPI  ------------------------------------------------
FusobacteriumATCC25586_1_        ------------------------------------------------
FusobacteriumATCC49256          ------------------------------------------------
FusobacteriumATCC25586_2_        ------------------------------------------------
FusobacteriumATCC49256_2_        ------------------------------------------------
Clostr.tetaniE88_4_             ------------------------------------------------
P.abyssi                        ------------------------------------------------
P.horikoshii                    ------------------------------------------------
P.furiosusDSM3638_2_            ------------------------------------------------
Thermotogamaritima              ------------------------------------------------
Shigella                        ------------------------------------------------
E.coli/O157_H7                  ------------------------------------------------
E.coli/O6/FlRd                  ------------------------------------------------
E.coli/K12                      ------------------------------------------------
E.coli/unknown                  ------------------------------------------------
S.typhimuriumLT2                ------------------------------------------------
Salmonella                      ------------------------------------------------
gi|44480963|gb|EAJ57255.1|      ------------------------------------------------
Anophelesgambiae                ------------------------------------------------
E.coli_unknown_                 ------------------------------------------------
V.vulnificusYJ016               ------------------------------------------------
V.vulnificusCMCP6               ------------------------------------------------
Clostr.tetaniE88                ------------------------------------------------
M.thermoacetica/fprA            ------------------------------------------------
MethanosarcinaacetivoransC2A    ------------------------------------------------
Methanosarcinabarkeri_2_        ------------------------------------------------
Methanococcusmaripaludis_2_     ------------------------------------------------
Methanococcusmaripaludis_3_     ------------------------------------------------
Methanococcusjannaschii_2_      ------------------------------------------------
```

```
M.thermoautotrophicum_DeltaH_       --------------------------------------------------750
FprA1/M.thermautotrophicus          --------------------------------------------------
Methanothermobactermarburgensi      --------------------------------------------------
FprA_II_Methanothermobacter         --------------------------------------------------
Geobactermetallireducens            --------------------------------------------------
GeobactersulfurreducensPCA          --------------------------------------------------
DesulfovibriodesulfuricansG20       --------------------------------------------------
D.gigas                             --------------------------------------------------
Methanococcusmaripaludis            --------------------------------------------------
Methanococcusjannaschii             --------------------------------------------------
Methanococcusjannaschii_3_          --------------------------------------------------
fprA-2/A.fulgidusDSM4304            --------------------------------------------------
Giardiaintestinalis                 --------------------------------------------------
Spironucleusbarkhanus               --------------------------------------------------
Trichomonasvaginalis                --------------------------------------------------
Clostr.tetaniE88_2_                 --------------------------------------------------
Clostr.perfringens_3_               --------------------------------------------------
Clostr.thermocellumATCC27405        --------------------------------------------------
Clostr.perfringens_1_               NIEELLGVTVTSIDKDAKKVILKDGTEIPYTKLILANGSHNFIPPFRIKN
Clostr.perfringens_2_               --------------------------------------------------
ChlorobiumtepidumTLS                --------------------------------------------------
Clostr.acetobutylicum               --------------------------------------------------
Clostr.tetaniE88_3_                 --------------------------------------------------
Clostr.acetobutylicum_2_            --------------------------------------------------
Rhodobactercapsulatus_1_            --------------------------------------------------
Rhodobactercapsulatus_2_            --------------------------------------------------
Rhodobactersphaeroides              --------------------------------------------------
Dechloromonasaromatica              --------------------------------------------------
Wolinellasuccinogenes               --------------------------------------------------
Nostocpunctiforme_1_                CEIQSSMECSDHWILYCTVQEGRVSKNDGLTAVRHRKVGNYY--------
NostocPCC7120_2_                    CEIQSSLECSDHYILYCTVEDGRVSKPDGLTAVRHRKVGNYY--------
Nostocpunctiforme_3_                CEVVSRMDCGDHWAVYSNVYAGRVSKPDALTAVHHRKVGNHY--------
NostocPCC7120_4_                    CEVVSRMDCGDHWAVYSTVYAGRVSKSEALTAVHHRKVGNHY--------
TrichodesmiumerythraeumIMS101       CEVATRMEASDHWIIYATVDNGRVSDSDVLPAVHHRKVGNHY--------
SynechocystisPCC6803_1_             CEVASRMECSDHWIVYSQVTNGRVAKAEGLTAVHHRKVGNYY--------
Gloeobacterviolaceus                CRVASRMECSDHWLVYGVVEDGRVSNLEGLTAVHHRKVGNHY--------
NostocPCC7120_1_                    CEITSRMDCGDHWIIYSTVHVGRVANVHAMTAVHHRKVGNHY--------
Nostocpunctiforme_5_                CEITSRMDCGDHWVIYSTVQTGRVAKLDALTAAHHRKIGNHY--------
SynechocystisPCC6803_2_             CEVTSRLDGNDHWLVYSTIQTGRVAKLNALTATHHRKLGNHY--------
Thermosynechococcuselongatus        CTVVSRLDAHDHWIVYSTVDSGRVSKPDGMTAVHHRKVGNHY--------
SynechococcusWH8102                 CRVEQRMEGPDHWIIYAVVEQGNVADAEASTAVHHRKVGNHY--------
gi|44454558|gb|EAJ38476.1|          --------------------------------------------------
gi|44083259|gb|EAH03645.1|          --------------------------------------------------
ProchlorococcusmarinusMIT9313       CLVKQRLETPDHWIIYALVEQGNVADAEAKTAVHHRKVGNHY--------
ProchlorococcusmarinusCCMP1375      CFVKQRLETTDHWIIYALVEHGNISNTETKTAVHHRKVGTSY--------
gi|43719610|gb|EAF14811.1|          --------------------------------------------------
gi|42845529|gb|EAA90143.1|          --------------------------------------------------
gi|44500849|gb|EAJ70075.1|          --------------------------------------------------
ProchlorococcusmarinusCCMP1378      CKVSSRLETPDHWIIYGIVQNGSVSDLSCKTAVHHRKVANHY--------
gi|42832038|gb|EAA83473.1|          --------------------------------------------------
gi|44305658|gb|EAI33747.1|          CKVSSRLETPDHWIIYGIVENGNVSDLSCKTAVHHRKVANHY--------
gi|44606330|gb|EAK43227.1|          --------------------------------------------------
gi|44126537|gb|EAH26947.1|          --------------------------------------------------
gi|44102955|gb|EAH14255.1|          --------------------------------------------------
Nostocpunctiforme_2_                CTVQNQLECGDRWLIYAVIDRGEVLENDGITALEHRKSGSYY--------
NostocPCC7120_3_                    CTVTNQLECGDRLLIYAVVDKGEVLANDGVTAVEHRKSGSH---------
SynechocystisPCC6803_3_             CLVQSWSNIGDHVLVYATVQAGQVLQPNGITAIRHRKSGGQY--------
Nostocpunctiforme_4_                CSVNQRLECGDHWVVYATVDEGKLLKPDAVTAINHRKTGTHY--------
NostocPCC7120_5_                    CSVDQRLECGDHWVVYATVDNGKLLKPDDVTAINHRKTGNHY--------
Treponema                           --------------------------------------------------
```

```
                                                                                    800
Methanosarcinamazei                 --------------------------------------------------
Methanosarcinabarkeri               --------------------------------------------------
Methanosarcinaacetivorans_C2A       --------------------------------------------------
Methanosarcinabarkeri_3_            --------------------------------------------------
P.furiosusDSM3638_1_                --------------------------------------------------
fprA-1[A.fulgidusDSM4304]           --------------------------------------------------
```

```
FprA3[M.thermautotrophicus          ----------------------------------------------------800
Thermoanaerobactertengcongensi      ----------------------------------------------------
PorphyromonasgingivalisW83          ----------------------------------------------------
BacteroidesthetaiotaomicronVPI      ----------------------------------------------------
FusobacteriumATCC25586_1_           ----------------------------------------------------
FusobacteriumATCC49256              ----------------------------------------------------
FusobacteriumATCC25586_2_           ----------------------------------------------------
FusobacteriumATCC49256_2_           ----------------------------------------------------
Clostr.tetaniE88_4_                 ----------------------------------------------------
P.abyssi                            ----------------------------------------------------
P.horikoshii                        ----------------------------------------------------
P.furiosusDSM3638_2_                ----------------------------------------------------
Thermotogamaritima                  ----------------------------------------------------
Shigella                            ----------------------------------------------------
E.coli/O157_H7                      ----------------------------------------------------
E.coli/O6/FlRd                      ----------------------------------------------------
E.coli/K12                          ----------------------------------------------------
E.coli/unknown                      ----------------------------------------------------
S.typhimuriumLT2                    ----------------------------------------------------
Salmonella                          ----------------------------------------------------
gi|44480963|gb|EAJ57255.1|          ----------------------------------------------------
Anophelesgambiae                    ----------------------------------------------------
E.coli_unknown_                     ----------------------------------------------------
V.vulnificusYJ016                   ----------------------------------------------------
V.vulnificusCMCP6                   ----------------------------------------------------
Clostr.tetaniE88                    ----------------------------------------------------
M.thermoacetica/fprA                ----------------------------------------------------
MethanosarcinaacetivoransC2A        ----------------------------------------------------
Methanosarcinabarkeri_2_            ----------------------------------------------------
Methanococcusmaripaludis_2_         ----------------------------------------------------
Methanococcusmaripaludis_3_         ----------------------------------------------------
Methanococcusjannaschii_2_          ----------------------------------------------------
M.thermoautotrophicum_DeltaH_       ----------------------------------------------------
FprA1/M.thermautotrophicus          ----------------------------------------------------
Methanothermobactermarburgensi      ----------------------------------------------------
FprA_II_Methanothermobacter         ----------------------------------------------------
Geobactermetallireducens            ----------------------------------------------------
GeobactersulfurreducensPCA          ----------------------------------------------------
DesulfovibriodesulfuricansG20       ----------------------------------------------------
D.gigas                             ----------------------------------------------------
Methanococcusmaripaludis            ----------------------------------------------------
Methanococcusjannaschii             ----------------------------------------------------
Methanococcusjannaschii_3_          ----------------------------------------------------
fprA-2/A.fulgidusDSM4304            ----------------------------------------------------
Giardiaintestinalis                 ----------------------------------------------------
Spironucleusbarkhanus               ----------------------------------------------------
Trichomonasvaginalis                ----------------------------------------------------
Clostr.tetaniE88_2_                 ----------------------------------------------------
Clostr.perfringens_3_               ----------------------------------------------------
Clostr.thermocellumATCC27405        ----------------------------------------------------
Clostr.perfringens_1_               NDEEVTLNCENIHEFKGIYSIKDLKDTFDVKEEMKEAKKAVVIGAGPLGL
Clostr.perfringens_2_               ----------------------------------------------------
ChlorobiumtepidumTLS                ----------------------------------------------------
Clostr.acetobutylicum               ----------------------------------------------------
Clostr.tetaniE88_3_                 ----------------------------------------------------
Clostr.acetobutylicum_2_            ----------------------------------------------------
Rhodobactercapsulatus_1_            ----------------------------------------------------
Rhodobactercapsulatus_2_            ----------------------------------------------------
Rhodobactersphaeroides              ----------------------------------------------------
Dechloromonasaromatica              ----------------------------------------------------
Wolinellasuccinogenes               ----------------------------------------------------
Nostocpunctiforme_1_                ----------------------------------------------------
NostocPCC7120_2_                    ----------------------------------------------------
Nostocpunctiforme_3_                ----------------------------------------------------
NostocPCC7120_4_                    ----------------------------------------------------
TrichodesmiumerythraeumIMS101       ----------------------------------------------------
SynechocystisPCC6803_1_             ----------------------------------------------------
Gloeobacterviolaceus                ----------------------------------------------------
NostocPCC7120_1_                    ----------------------------------------------------
Nostocpunctiforme_5_                ----------------------------------------------------
SynechocystisPCC6803_2_             ----------------------------------------------------
```

```
Thermosynechococcuselongatus       ----------------------------------------------------800
SynechococcusWH8102                ----------------------------------------------------
gi|44454558|gb|EAJ38476.1|         ----------------------------------------------------
gi|44083259|gb|EAH03645.1|         ----------------------------------------------------
ProchlorococcusmarinusMIT9313      ----------------------------------------------------
ProchlorococcusmarinusCCMP1375     ----------------------------------------------------
gi|43719610|gb|EAF14811.1|         ----------------------------------------------------
gi|42845529|gb|EAA90143.1|         ----------------------------------------------------
gi|44500849|gb|EAJ70075.1|         ----------------------------------------------------
ProchlorococcusmarinusCCMP1378     ----------------------------------------------------
gi|42832038|gb|EAA83473.1|         ----------------------------------------------------
gi|44305658|gb|EAI33747.1|         ----------------------------------------------------
gi|44606330|gb|EAK43227.1|         ----------------------------------------------------
gi|44126537|gb|EAH26947.1|         ----------------------------------------------------
gi|44102955|gb|EAH14255.1|         ----------------------------------------------------
Nostocpunctiforme_2_               ----------------------------------------------------
NostocPCC7120_3_                   ----------------------------------------------------
SynechocystisPCC6803_3_            ----------------------------------------------------
Nostocpunctiforme_4_               ----------------------------------------------------
NostocPCC7120_5_                   ----------------------------------------------------
Treponema                          ----------------------------------------------------
                                   ====================================================

                                                                                     850
Methanosarcinamazei                ----------------------------------------------------
Methanosarcinabarkeri              ----------------------------------------------------
Methanosarcinaacetivorans_C2A      ----------------------------------------------------
Methanosarcinabarkeri_3_           ----------------------------------------------------
P.furiosusDSM3638_1_               ----------------------------------------------------
fprA-1[A.fulgidusDSM4304]          ----------------------------------------------------
FprA3[M.thermautotrophicus         ----------------------------------------------------
Thermoanaerobactertengcongensi     ----------------------------------------------------
PorphyromonasgingivalisW83         ----------------------------------------------------
BacteroidesthetaiotaomicronVPI     ----------------------------------------------------
FusobacteriumATCC25586_1_          ----------------------------------------------------
FusobacteriumATCC49256             ----------------------------------------------------
FusobacteriumATCC25586_2_          ----------------------------------------------------
FusobacteriumATCC49256_2_          ----------------------------------------------------
Clostr.tetaniE88_4_                ----------------------------------------------------
P.abyssi                           ----------------------------------------------------
P.horikoshii                       ----------------------------------------------------
P.furiosusDSM3638_2_               ----------------------------------------------------
Thermotogamaritima                 ----------------------------------------------------
Shigella                           ----------------------------------------------------
E.coli/O157_H7                     ----------------------------------------------------
E.coli/O6/FlRd                     ----------------------------------------------------
E.coli/K12                         ----------------------------------------------------
E.coli/unknown                     ----------------------------------------------------
S.typhimuriumLT2                   ----------------------------------------------------
Salmonella                         ----------------------------------------------------
gi|44480963|gb|EAJ57255.1|         ----------------------------------------------------
Anophelesgambiae                   ----------------------------------------------------
E.coli_unknown_                    ----------------------------------------------------
V.vulnificusYJ016                  ----------------------------------------------------
V.vulnificusCMCP6                  ----------------------------------------------------
Clostr.tetaniE88                   ----------------------------------------------------
M.thermoacetica/fprA               ----------------------------------------------------
MethanosarcinaacetivoransC2A       ----------------------------------------------------
Methanosarcinabarkeri_2_           ----------------------------------------------------
Methanococcusmaripaludis_2_        ----------------------------------------------------
Methanococcusmaripaludis_3_        ----------------------------------------------------
Methanococcusjannaschii_2_         ----------------------------------------------------
M.thermoautotrophicum_DeltaH_      ----------------------------------------------------
FprA1/M.thermautotrophicus         ----------------------------------------------------
Methanothermobactermarburgensi     ----------------------------------------------------
FprA_II_Methanothermobacter        ----------------------------------------------------
Geobactermetallireducens           ----------------------------------------------------
GeobactersulfurreducensPCA         ----------------------------------------------------
DesulfovibriodesulfuricansG20      ----------------------------------------------------
```

```
D.gigas                          --------------------------------------------------850
Methanococcusmaripaludis         --------------------------------------------------
Methanococcusjannaschii          --------------------------------------------------
Methanococcusjannaschii_3_       --------------------------------------------------
fprA-2/A.fulgidusDSM4304         --------------------------------------------------
Giardiaintestinalis              --------------------------------------------------
Spironucleusbarkhanus            --------------------------------------------------
Trichomonasvaginalis             --------------------------------------------------
Clostr.tetaniE88_2_              --------------------------------------------------
Clostr.perfringens_3_            --------------------------------------------------
Clostr.thermocellumATCC27405     --------------------------------------------------
Clostr.perfringens_1_            EAAWEMKLAGLDVTVVEFLPNLMNNQLDQEGADIFKNQVSDCGITFITSD
Clostr.perfringens_2_            --------------------------------------------------
ChlorobiumtepidumTLS             --------------------------------------------------
Clostr.acetobutylicum            --------------------------------------------------
Clostr.tetaniE88_3_              --------------------------------------------------
Clostr.acetobutylicum_2_         --------------------------------------------------
Rhodobactercapsulatus_1_         --------------------------------------------------
Rhodobactercapsulatus_2_         --------------------------------------------------
Rhodobactersphaeroides           --------------------------------------------------
Dechloromonasaromatica           --------------------------------------------------
Wolinellasuccinogenes            --------------------------------------------------
Nostocpunctiforme_1_             --------------------------------------------------
NostocPCC7120_2_                 --------------------------------------------------
Nostocpunctiforme_3_             --------------------------------------------------
NostocPCC7120_4_                 --------------------------------------------------
TrichodesmiumerythraeumIMS101    --------------------------------------------------
SynechocystisPCC6803_1_          --------------------------------------------------
Gloeobacterviolaceus             --------------------------------------------------
NostocPCC7120_1_                 --------------------------------------------------
Nostocpunctiforme_5_             --------------------------------------------------
SynechocystisPCC6803_2_          --------------------------------------------------
Thermosynechococcuselongatus     --------------------------------------------------
SynechococcusWH8102              --------------------------------------------------
gi|44454558|gb|EAJ38476.1|       --------------------------------------------------
gi|44083259|gb|EAH03645.1|       --------------------------------------------------
ProchlorococcusmarinusMIT9313    --------------------------------------------------
ProchlorococcusmarinusCCMP1375   --------------------------------------------------
gi|43719610|gb|EAF14811.1|       --------------------------------------------------
gi|42845529|gb|EAA90143.1|       --------------------------------------------------
gi|44500849|gb|EAJ70075.1|       --------------------------------------------------
ProchlorococcusmarinusCCMP1378   --------------------------------------------------
gi|42832038|gb|EAA83473.1|       --------------------------------------------------
gi|44305658|gb|EAI33747.1|       --------------------------------------------------
gi|44606330|gb|EAK43227.1|       --------------------------------------------------
gi|44126537|gb|EAH26947.1|       --------------------------------------------------
gi|44102955|gb|EAH14255.1|       --------------------------------------------------
Nostocpunctiforme_2_             --------------------------------------------------
NostocPCC7120_3_                 --------------------------------------------------
SynechocystisPCC6803_3_          --------------------------------------------------
Nostocpunctiforme_4_             --------------------------------------------------
NostocPCC7120_5_                 --------------------------------------------------
Treponema                        --------------------------------------------------
```

```
                                                                                 900
Methanosarcinamazei              --------------------------------------------------
Methanosarcinabarkeri            --------------------------------------------------
Methanosarcinaacetivorans_C2A    --------------------------------------------------
Methanosarcinabarkeri_3_         --------------------------------------------------
P.furiosusDSM3638_1_             --------------------------------------------------
fprA-1[A.fulgidusDSM4304]        --------------------------------------------------
FprA3[M.thermautotrophicus       --------------------------------------------------
Thermoanaerobactertengcongensi   --------------------------------------------------
PorphyromonasgingivalisW83       --------------------------------------------------
BacteroidesthetaiotaomicronVPI   --------------------------------------------------
FusobacteriumATCC25586_1_        --------------------------------------------------
FusobacteriumATCC49256           --------------------------------------------------
FusobacteriumATCC25586_2_        --------------------------------------------------
```

```
FusobacteriumATCC49256_2_          ------------------------------------------------900
Clostr.tetaniE88_4_                ------------------------------------------------
P.abyssi                           ------------------------------------------------
P.horikoshii                       ------------------------------------------------
P.furiosusDSM3638_2_               ------------------------------------------------
Thermotogamaritima                 ------------------------------------------------
Shigella                           ------------------------------------------------
E.coli/O157_H7                     ------------------------------------------------
E.coli/O6/FlRd                     ------------------------------------------------
E.coli/K12                         ------------------------------------------------
E.coli/unknown                     ------------------------------------------------
S.typhimuriumLT2                   ------------------------------------------------
Salmonella                         ------------------------------------------------
gi|44480963|gb|EAJ57255.1|         ------------------------------------------------
Anophelesgambiae                   ------------------------------------------------
E.coli_unknown_                    ------------------------------------------------
V.vulnificusYJ016                  ------------------------------------------------
V.vulnificusCMCP6                  ------------------------------------------------
Clostr.tetaniE88                   ------------------------------------------------
M.thermoacetica/fprA               ------------------------------------------------
MethanosarcinaacetivoransC2A       ------------------------------------------------
Methanosarcinabarkeri_2_           ------------------------------------------------
Methanococcusmaripaludis_2_        ------------------------------------------------
Methanococcusmaripaludis_3_        ------------------------------------------------
Methanococcusjannaschii_2_         ------------------------------------------------
M.thermoautotrophicum_DeltaH_      ------------------------------------------------
FprA1/M.thermautotrophicus         ------------------------------------------------
Methanothermobactermarburgensi     ------------------------------------------------
FprA_II_Methanothermobacter        ------------------------------------------------
Geobactermetallireducens           ------------------------------------------------
GeobactersulfurreducensPCA         ------------------------------------------------
DesulfovibriodesulfuricansG20      ------------------------------------------------
D.gigas                            ------------------------------------------------
Methanococcusmaripaludis           ------------------------------------------------
Methanococcusjannaschii            ------------------------------------------------
Methanococcusjannaschii_3_         ------------------------------------------------
fprA-2/A.fulgidusDSM4304           ------------------------------------------------
Giardiaintestinalis                ------------------------------------------------
Spironucleusbarkhanus              ------------------------------------------------
Trichomonasvaginalis               ------------------------------------------------
Clostr.tetaniE88_2_                ------------------------------------------------
Clostr.perfringens_3_              ------------------------------------------------
Clostr.thermocellumATCC27405       ------------------------------------------------
Clostr.perfringens_1_              ECTEIITKDSKLTSLNLKSGKTLDADILLVSTGIRSNIELAKESGIECNR
Clostr.perfringens_2_              ------------------------------------------------
ChlorobiumtepidumTLS               ------------------------------------------------
Clostr.acetobutylicum              ------------------------------------------------
Clostr.tetaniE88_3_                ------------------------------------------------
Clostr.acetobutylicum_2_           ------------------------------------------------
Rhodobactercapsulatus_1_           ------------------------------------------------
Rhodobactercapsulatus_2_           ------------------------------------------------
Rhodobactersphaeroides             ------------------------------------------------
Dechloromonasaromatica             ------------------------------------------------
Wolinellasuccinogenes              ------------------------------------------------
Nostocpunctiforme_1_               ------------------------------------------------
NostocPCC7120_2_                   ------------------------------------------------
Nostocpunctiforme_3_               ------------------------------------------------
NostocPCC7120_4_                   ------------------------------------------------
TrichodesmiumerythraeumIMS101      ------------------------------------------------
SynechocystisPCC6803_1_            ------------------------------------------------
Gloeobacterviolaceus               ------------------------------------------------
NostocPCC7120_1_                   ------------------------------------------------
Nostocpunctiforme_5_               ------------------------------------------------
SynechocystisPCC6803_2_            ------------------------------------------------
Thermosynechococcuselongatus       ------------------------------------------------
SynechococcusWH8102                ------------------------------------------------
gi|44454558|gb|EAJ38476.1|         ------------------------------------------------
gi|44083259|gb|EAH03645.1|         ------------------------------------------------
ProchlorococcusmarinusMIT9313      ------------------------------------------------
ProchlorococcusmarinusCCMP1375     ------------------------------------------------
gi|43719610|gb|EAF14811.1|         ------------------------------------------------
```

```
gi|42845529|gb|EAA90143.1|          ------------------------------------------------900
gi|44500849|gb|EAJ70075.1|          ------------------------------------------------
ProchlorococcusmarinusCCMP1378      ------------------------------------------------
gi|42832038|gb|EAA83473.1|          ------------------------------------------------
gi|44305658|gb|EAI33747.1|          ------------------------------------------------
gi|44606330|gb|EAK43227.1|          ------------------------------------------------
gi|44126537|gb|EAH26947.1|          ------------------------------------------------
gi|44102955|gb|EAH14255.1|          ------------------------------------------------
Nostocpunctiforme_2_                ------------------------------------------------
NostocPCC7120_3_                    ------------------------------------------------
SynechocystisPCC6803_3_             ------------------------------------------------
Nostocpunctiforme_4_                ------------------------------------------------
NostocPCC7120_5_                    ------------------------------------------------
Treponema                           ------------------------------------------------
                                    ================================================

                                                                                    950
Methanosarcinamazei                 ------------------------------------------------
Methanosarcinabarkeri               ------------------------------------------------
Methanosarcinaacetivorans_C2A       ------------------------------------------------
Methanosarcinabarkeri_3_            ------------------------------------------------
P.furiosusDSM3638_1_                ------------------------------------------------
fprA-1[A.fulgidusDSM4304]           ------------------------------------------------
FprA3[M.thermautotrophicus          ------------------------------------------------
Thermoanaerobactertengcongensi      ------------------------------------------------
PorphyromonasgingivalisW83          ------------------------------------------------
BacteroidesthetaiotaomicronVPI      ------------------------------------------------
FusobacteriumATCC25586_1_           ------------------------------------------------
FusobacteriumATCC49256              ------------------------------------------------
FusobacteriumATCC25586_2_           ------------------------------------------------
FusobacteriumATCC49256_2_           ------------------------------------------------
Clostr.tetaniE88_4_                 ------------------------------------------------
P.abyssi                            ------------------------------------------------
P.horikoshii                        ------------------------------------------------
P.furiosusDSM3638_2_                ------------------------------------------------
Thermotogamaritima                  ------------------------------------------------
Shigella                            ------------------------------------------------
E.coli/O157_H7                      ------------------------------------------------
E.coli/O6/FlRd                      ------------------------------------------------
E.coli/K12                          ------------------------------------------------
E.coli/unknown                      ------------------------------------------------
S.typhimuriumLT2                    ------------------------------------------------
Salmonella                          ------------------------------------------------
gi|44480963|gb|EAJ57255.1|          ------------------------------------------------
Anophelesgambiae                    ------------------------------------------------
E.coli_unknown_                     ------------------------------------------------
V.vulnificusYJ016                   ------------------------------------------------
V.vulnificusCMCP6                   ------------------------------------------------
Clostr.tetaniE88                    ------------------------------------------------
M.thermoacetica/fprA                ------------------------------------------------
MethanosarcinaacetivoransC2A        ------------------------------------------------
Methanosarcinabarkeri_2_            ------------------------------------------------
Methanococcusmaripaludis_2_         ------------------------------------------------
Methanococcusmaripaludis_3_         ------------------------------------------------
Methanococcusjannaschii_2_          ------------------------------------------------
M.thermoautotrophicum_DeltaH_       ------------------------------------------------
FprA1/M.thermautotrophicus          ------------------------------------------------
Methanothermobactermarburgensi      ------------------------------------------------
FprA_II_Methanothermobacter         ------------------------------------------------
Geobactermetallireducens            ------------------------------------------------
GeobactersulfurreducensPCA          ------------------------------------------------
DesulfovibriodesulfuricansG20       ------------------------------------------------
D.gigas                             ------------------------------------------------
Methanococcusmaripaludis            ------------------------------------------------
Methanococcusjannaschii             ------------------------------------------------
Methanococcusjannaschii_3_          ------------------------------------------------
fprA-2/A.fulgidusDSM4304            ------------------------------------------------
Giardiaintestinalis                 ------------------------------------------------
Spironucleusbarkhanus               ------------------------------------------------
```

```
Trichomonasvaginalis                ----------------------------------------------------950
Clostr.tetaniE88_2_                 ----------------------------------------------------
Clostr.perfringens_3_               ----------------------------------------------------
Clostr.thermocellumATCC27405        ----------------------------------------------------
Clostr.perfringens_1_               GVIVNERMETSVKDIYACGDVAEFNGLVYGNWPAAIEMGKTAGANACEAE
Clostr.perfringens_2_               ----------------------------------------------------
ChlorobiumtepidumTLS                ----------------------------------------------------
Clostr.acetobutylicum               ----------------------------------------------------
Clostr.tetaniE88_3_                 ----------------------------------------------------
Clostr.acetobutylicum_2_            ----------------------------------------------------
Rhodobactercapsulatus_1_            ----------------------------------------------------
Rhodobactercapsulatus_2_            ----------------------------------------------------
Rhodobactersphaeroides              ----------------------------------------------------
Dechloromonasaromatica              ----------------------------------------------------
Wolinellasuccinogenes               ----------------------------------------------------
Nostocpunctiforme_1_                ----------------------------------------------------
NostocPCC7120_2_                    ----------------------------------------------------
Nostocpunctiforme_3_                ----------------------------------------------------
NostocPCC7120_4_                    ----------------------------------------------------
TrichodesmiumerythraeumIMS101       ----------------------------------------------------
SynechocystisPCC6803_1_             ----------------------------------------------------
Gloeobacterviolaceus                ----------------------------------------------------
NostocPCC7120_1_                    ----------------------------------------------------
Nostocpunctiforme_5_                ----------------------------------------------------
SynechocystisPCC6803_2_             ----------------------------------------------------
Thermosynechococcuselongatus        ----------------------------------------------------
SynechococcusWH8102                 ----------------------------------------------------
gi|44454558|gb|EAJ38476.1|          ----------------------------------------------------
gi|44083259|gb|EAH03645.1|          ----------------------------------------------------
ProchlorococcusmarinusMIT9313       ----------------------------------------------------
ProchlorococcusmarinusCCMP1375      ----------------------------------------------------
gi|43719610|gb|EAF14811.1|          ----------------------------------------------------
gi|42845529|gb|EAA90143.1|          ----------------------------------------------------
gi|44500849|gb|EAJ70075.1|          ----------------------------------------------------
ProchlorococcusmarinusCCMP1378      ----------------------------------------------------
gi|42832038|gb|EAA83473.1|          ----------------------------------------------------
gi|44305658|gb|EAI33747.1|          ----------------------------------------------------
gi|44606330|gb|EAK43227.1|          ----------------------------------------------------
gi|44126537|gb|EAH26947.1|          ----------------------------------------------------
gi|44102955|gb|EAH14255.1|          ----------------------------------------------------
Nostocpunctiforme_2_                ----------------------------------------------------
NostocPCC7120_3_                    ----------------------------------------------------
SynechocystisPCC6803_3_             ----------------------------------------------------
Nostocpunctiforme_4_                ----------------------------------------------------
NostocPCC7120_5_                    ----------------------------------------------------
Treponema                           ----------------------------------------------------
                                    ====================================================

                                                                                    1000
Methanosarcinamazei                 ----------------------------------------------------
Methanosarcinabarkeri               ----------------------------------------------------
Methanosarcinaacetivorans_C2A       ----------------------------------------------------
Methanosarcinabarkeri_3_            ----------------------------------------------------
P.furiosusDSM3638_1_                ----------------------------------------------------
fprA-1[A.fulgidusDSM4304]           ----------------------------------------------------
FprA3[M.thermautotrophicus          ----------------------------------------------------
Thermoanaerobactertengcongensi      ----------------------------------------------------
PorphyromonasgingivalisW83          ----------------------------------------------------
BacteroidesthetaiotaomicronVPI      ----------------------------------------------------
FusobacteriumATCC25586_1_           ----------------------------------------------------
FusobacteriumATCC49256              ----------------------------------------------------
FusobacteriumATCC25586_2_           ----------------------------------------------------
FusobacteriumATCC49256_2_           ----------------------------------------------------
Clostr.tetaniE88_4_                 ----------------------------------------------------
P.abyssi                            ----------------------------------------------------
P.horikoshii                        ----------------------------------------------------
P.furiosusDSM3638_2_                ----------------------------------------------------
Thermotogamaritima                  ----------------------------------------------------
Shigella                            ----------------------------------------------------
```

```
E.coli/O157_H7                          --------------------------------------------------
E.coli/O6/FlRd                          --------------------------------------------------
E.coli/K12                              --------------------------------------------------
E.coli/unknown                          --------------------------------------------------
S.typhimuriumLT2                        --------------------------------------------------
Salmonella                              --------------------------------------------------
gi|44480963|gb|EAJ57255.1|              --------------------------------------------------
Anophelesgambiae                        --------------------------------------------------
E.coli_unknown_                         --------------------------------------------------
V.vulnificusYJ016                       --------------------------------------------------
V.vulnificusCMCP6                       --------------------------------------------------
Clostr.tetaniE88                        --------------------------------------------------
M.thermoacetica/fprA                    --------------------------------------------------
MethanosarcinaacetivoransC2A            --------------------------------------------------
Methanosarcinabarkeri_2_                --------------------------------------------------
Methanococcusmaripaludis_2_             --------------------------------------------------
Methanococcusmaripaludis_3_             --------------------------------------------------
Methanococcusjannaschii_2_              --------------------------------------------------
M.thermoautotrophicum_DeltaH_           --------------------------------------------------
FprA1/M.thermautotrophicus              --------------------------------------------------
Methanothermobactermarburgensi          --------------------------------------------------
FprA_II_Methanothermobacter             --------------------------------------------------
Geobactermetallireducens                --------------------------------------------------
GeobactersulfurreducensPCA              --------------------------------------------------
DesulfovibriodesulfuricansG20           --------------------------------------------------
D.gigas                                 --------------------------------------------------
Methanococcusmaripaludis                --------------------------------------------------
Methanococcusjannaschii                 --------------------------------------------------
Methanococcusjannaschii_3_              --------------------------------------------------
fprA-2/A.fulgidusDSM4304                --------------------------------------------------
Giardiaintestinalis                     --------------------------------------------------
Spironucleusbarkhanus                   --------------------------------------------------
Trichomonasvaginalis                    --------------------------------------------------
Clostr.tetaniE88_2_                     --------------------------------------------------
Clostr.perfringens_3_                   --------------------------------------------------
Clostr.thermocellumATCC27405            --------------------------------------------------
Clostr.perfringens_1_                   KAFENFTPSIILDALNTHVFSAGLIRFNDSSYEKISSKDESKGQYTKLFF
Clostr.perfringens_2_                   --------------------------------------------------
ChlorobiumtepidumTLS                    --------------------------------------------------
Clostr.acetobutylicum                   --------------------------------------------------
Clostr.tetaniE88_3_                     --------------------------------------------------
Clostr.acetobutylicum_2_                --------------------------------------------------
Rhodobactercapsulatus_1_                --------------------------------------------------
Rhodobactercapsulatus_2_                --------------------------------------------------
Rhodobactersphaeroides                  --------------------------------------------------
Dechloromonasaromatica                  --------------------------------------------------
Wolinellasuccinogenes                   --------------------------------------------------
Nostocpunctiforme_1_                    --------------------------------------------------
NostocPCC7120_2_                        --------------------------------------------------
Nostocpunctiforme_3_                    --------------------------------------------------
NostocPCC7120_4_                        --------------------------------------------------
TrichodesmiumerythraeumIMS101           --------------------------------------------------
SynechocystisPCC6803_1_                 --------------------------------------------------
Gloeobacterviolaceus                    --------------------------------------------------
NostocPCC7120_1_                        --------------------------------------------------
Nostocpunctiforme_5_                    --------------------------------------------------
SynechocystisPCC6803_2_                 --------------------------------------------------
Thermosynechococcuselongatus            --------------------------------------------------
SynechococcusWH8102                     --------------------------------------------------
gi|44454558|gb|EAJ38476.1|              --------------------------------------------------
gi|44083259|gb|EAH03645.1|              --------------------------------------------------
ProchlorococcusmarinusMIT9313           --------------------------------------------------
ProchlorococcusmarinusCCMP1375          --------------------------------------------------
gi|43719610|gb|EAF14811.1|              --------------------------------------------------
gi|42845529|gb|EAA90143.1|              --------------------------------------------------
gi|44500849|gb|EAJ70075.1|              --------------------------------------------------
ProchlorococcusmarinusCCMP1378          --------------------------------------------------
gi|42832038|gb|EAA83473.1|              --------------------------------------------------
gi|44305658|gb|EAI33747.1|              --------------------------------------------------
gi|44606330|gb|EAK43227.1|              --------------------------------------------------
gi|44126537|gb|EAH26947.1|              --------------------------------------------------
```

```
                                                                                                                1000
gi|44102955|gb|EAH14255.1|          --------------------------------------------------
Nostocpunctiforme_2_                --------------------------------------------------
NostocPCC7120_3_                    --------------------------------------------------
SynechocystisPCC6803_3_             --------------------------------------------------
Nostocpunctiforme_4_                --------------------------------------------------
NostocPCC7120_5_                    --------------------------------------------------
Treponema                           --------------------------------------------------


                                                                                                          1039
Methanosarcinamazei                 ---------------------------------------
Methanosarcinabarkeri               ---------------------------------------
Methanosarcinaacetivorans_C2A       ---------------------------------------
Methanosarcinabarkeri_3_            ---------------------------------------
P.furiosusDSM3638_1_                ---------------------------------------
fprA-1[A.fulgidusDSM4304]           ---------------------------------------
FprA3[M.thermautotrophicus          ---------------------------------------
Thermoanaerobactertengcongensi      ---------------------------------------
PorphyromonasgingivalisW83          ---------------------------------------
BacteroidesthetaiotaomicronVPI      ---------------------------------------
FusobacteriumATCC25586_1_           ---------------------------------------
FusobacteriumATCC49256              ---------------------------------------
FusobacteriumATCC25586_2_           ---------------------------------------
FusobacteriumATCC49256_2_           ---------------------------------------
Clostr.tetaniE88_4_                 ---------------------------------------
P.abyssi                            ---------------------------------------
P.horikoshii                        ---------------------------------------
P.furiosusDSM3638_2_                ---------------------------------------
Thermotogamaritima                  ---------------------------------------
Shigella                            ---------------------------------------
E.coli/O157_H7                      ---------------------------------------
E.coli/O6/FlRd                      ---------------------------------------
E.coli/K12                          ---------------------------------------
E.coli/unknown                      ---------------------------------------
S.typhimuriumLT2                    ---------------------------------------
Salmonella                          ---------------------------------------
gi|44480963|gb|EAJ57255.1|          ---------------------------------------
Anophelesgambiae                    ---------------------------------------
E.coli_unknown_                     ---------------------------------------
V.vulnificusYJ016                   ---------------------------------------
V.vulnificusCMCP6                   ---------------------------------------
Clostr.tetaniE88                    ---------------------------------------
M.thermoacetica/fprA                ---------------------------------------
MethanosarcinaacetivoransC2A        ---------------------------------------
Methanosarcinabarkeri_2_            ---------------------------------------
Methanococcusmaripaludis_2_         ---------------------------------------
Methanococcusmaripaludis_3_         ---------------------------------------
Methanococcusjannaschii_2_          ---------------------------------------
M.thermoautotrophicum_DeltaH_       ---------------------------------------
FprA1/M.thermautotrophicus          ---------------------------------------
Methanothermobactermarburgensi      ---------------------------------------
FprA_II_Methanothermobacter         ---------------------------------------
Geobactermetallireducens            ---------------------------------------
GeobactersulfurreducensPCA          ---------------------------------------
DesulfovibriodesulfuricansG20       ---------------------------------------
D.gigas                             ---------------------------------------
Methanococcusmaripaludis            ---------------------------------------
Methanococcusjannaschii             ---------------------------------------
Methanococcusjannaschii_3_          ---------------------------------------
fprA-2/A.fulgidusDSM4304            ---------------------------------------
Giardiaintestinalis                 ---------------------------------------
Spironucleusbarkhanus               ---------------------------------------
Trichomonasvaginalis                ---------------------------------------
Clostr.tetaniE88_2_                 ---------------------------------------
Clostr.perfringens_3_               ---------------------------------------
Clostr.thermocellumATCC27405        ---------------------------------------
Clostr.perfringens_1_               KDNILVGGIIVGDISKAGQIIIAIDNKLSKAAALSNDLL
Clostr.perfringens_2_               ---------------------------------------
```

```
ChlorobiumtepidumTLS              ---------------------------------------
Clostr.acetobutylicum             ---------------------------------------
Clostr.tetaniE88_3_               ---------------------------------------
Clostr.acetobutylicum_2_          ---------------------------------------
Rhodobactercapsulatus_1_          ---------------------------------------
Rhodobactercapsulatus_2_          ---------------------------------------
Rhodobactersphaeroides            ---------------------------------------
Dechloromonasaromatica            ---------------------------------------
Wolinellasuccinogenes             ---------------------------------------
Nostocpunctiforme_1_              ---------------------------------------
NostocPCC7120_2_                  ---------------------------------------
Nostocpunctiforme_3_              ---------------------------------------
NostocPCC7120_4_                  ---------------------------------------
TrichodesmiumerythraeumIMS101     ---------------------------------------
SynechocystisPCC6803_1_           ---------------------------------------
Gloeobacterviolaceus              ---------------------------------------
NostocPCC7120_1_                  ---------------------------------------
Nostocpunctiforme_5_              ---------------------------------------
SynechocystisPCC6803_2_           ---------------------------------------
Thermosynechococcuselongatus      ---------------------------------------
SynechococcusWH8102               ---------------------------------------
gi|44454558|gb|EAJ38476.1|        ---------------------------------------
gi|44083259|gb|EAH03645.1|        ---------------------------------------
ProchlorococcusmarinusMIT9313     ---------------------------------------
ProchlorococcusmarinusCCMP1375    ---------------------------------------
gi|43719610|gb|EAF14811.1|        ---------------------------------------
gi|42845529|gb|EAA90143.1|        ---------------------------------------
gi|44500849|gb|EAJ70075.1|        ---------------------------------------
ProchlorococcusmarinusCCMP1378    ---------------------------------------
gi|42832038|gb|EAA83473.1|        ---------------------------------------
gi|44305658|gb|EAI33747.1|        ---------------------------------------
gi|44606330|gb|EAK43227.1|        ---------------------------------------
gi|44126537|gb|EAH26947.1|        ---------------------------------------
gi|44102955|gb|EAH14255.1|        ---------------------------------------
Nostocpunctiforme_2_              ---------------------------------------
NostocPCC7120_3_                  ---------------------------------------
SynechocystisPCC6803_3_           ---------------------------------------
Nostocpunctiforme_4_              ---------------------------------------
NostocPCC7120_5_                  ---------------------------------------
Treponema                         ---------------------------------------
                                  =======================================
```

(1) Combet, C.; Blanchet, C.; Geourjon, C.; Deléage, G. *Trends Biochem. Sci.* **2000**, *25*, 147-150.

(2) Frazão, C.; Silva, G.; Gomes, C. M.; Matias, P.; Coelho, R.; Sieker, L.; Macedo, S.; Liu, M. Y.; Oliveira, S.; Teixeira, M.; Xavier, A. V.; Rodrigues-Pousada, C.; Carrondo, M. A.; Le Gall, J. *Nat. Struct. Biol.* **2000**, *7*, 1041-1045.

APPENDIX B

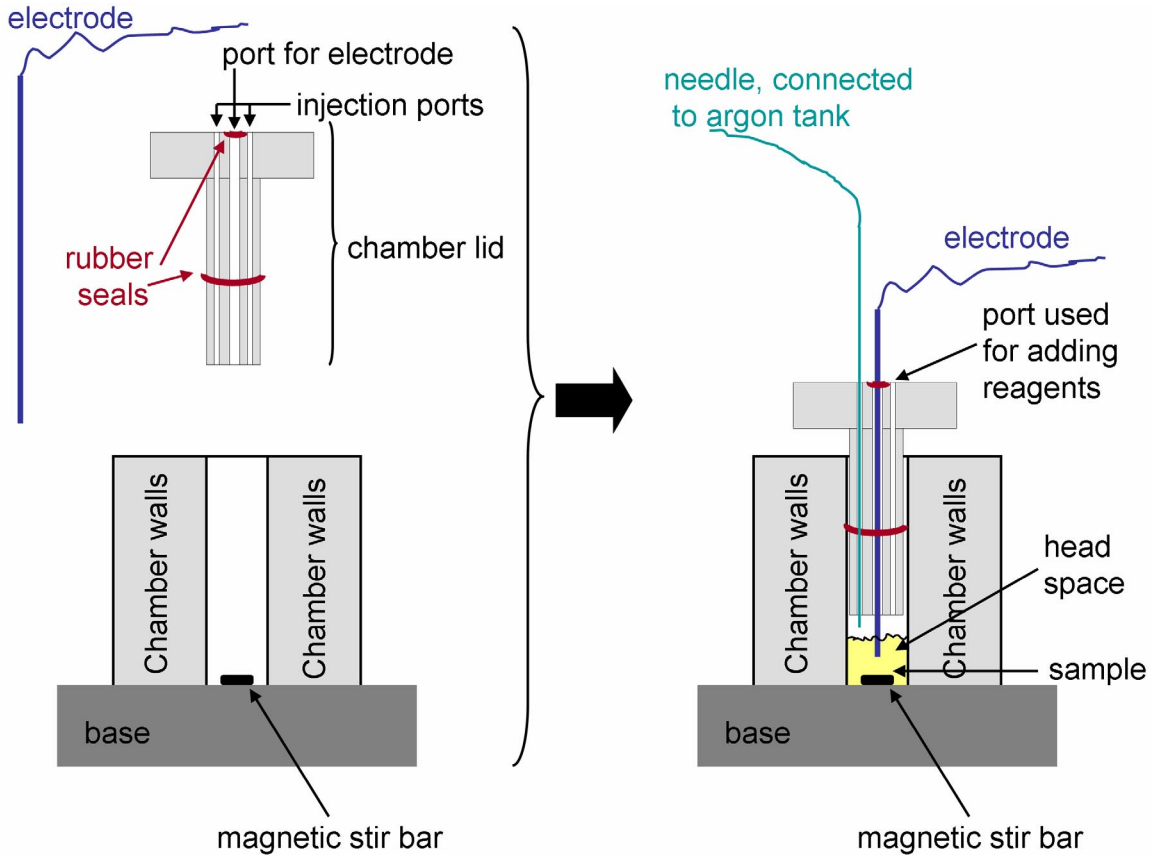

Figure B1. Cross-sectional schematic diagram of the NO chamber and NO electrode (WPI, Inc.) used for nitric oxide measurements. The chamber was assembled as indicated in the diagram, after which anaerobic buffer (in 1 or 2-mL volumes) was added via a gas-tight syringe through the "port used for adding reagents", while the headspace of the chamber was being purged with argon. Argon was further bubbled through the buffer for 5 minutes. At this point, the argon needle was lifted from the sample to the position shown in the diagram (i.e., in the headspace) without interrupting the argon flow, and the other components of the assay mixture (NADH, proteins) were added via gas-tight Hamilton syringes.

Figure B2. Photograph of the NO chamber and NO electrode. Connected at the top (with white wire) is the NO electrode. This photograph also illustrates the ability of the chamber to accommodate more than one electrode. Three extra electrodes are connected through the lateral ports.

APPENDIX C

Based on the *D. gigas* ROO[1] and *M. thermoacetica* FprA crystal structures, the amino acid residues lining the substrate-binding pocket and contributing the diiron ligands occur mainly in four distinct regions of the FprA amino acid sequence. These regions consist of portions of three loops (residues 23-29. 81-86 and 147-149) and one helix (residues 194-200) labeled 1-4, respectively, in Figure C1.

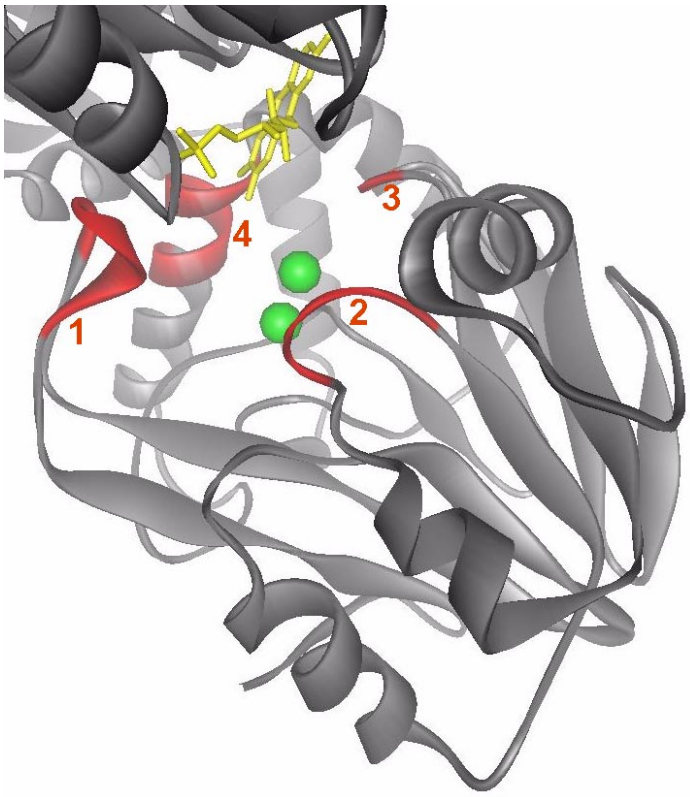

Figure C1. Ribbon drawing of the *M. thermoacetica* FprA monomer showing locations of the four regions contributing amino acid residues for the substrate binding pocket and diiron ligands. Iron atoms are shown as green spheres, FMN is shown as yellow sticks. The four regions are highlighted and numbered in red.

This Appendix analyzes the conservation of residues in these four regions in the ~100 FprA amino acid sequences aligned in Appendix A. Unless otherwise specified, *M. thermoacetica* FprA residue numbering is used in the following discussion.

Region 1: residues 23-29

H25 lines the substrate-binding cavity above the diiron site (cf. Chapter 6, Figure 6.9), and this residue is conserved in approximately half of the known FprA sequences. Most of the other FprAs contain either a glutamate or aspartate at this position. Exceptions are the *M. janaschii* (two homologues, both containing a lysine) and *Treponema denticola* (phenylalanine). As shown in Chapter 6, replacement of *M. thermoacetica* FprA H25 by phenylalanine resulted in significantly decreased NOR activities (dioxygen reductase activities, not shown, were also decreased). *Archaeoglobus fulgidus* contains one FprA homologue (annotated FprA-1) that completely lacks the first ~ 30 residues (including Region 1) of *M. thermoacetica* FprA; on the other hand, the *A. fulgidus* sequence annotated "FprA-2" not only contains Region 1, but also ~80 extra residues at the N-terminus. In almost all FprA sequences, H25 or its homologs are invariably preceded by an aromatic residue, which in most cases is a phenylalanine (F24 in *M. thermoacetica*). The F24 side-chain also lines the substrate-binding cavity. Chapter 6 showed the placements of these residues in *D. gigas* ROO vs. M. *thermoacetica* FprA. H25 sits above the Fe1 ligand E83, whereas F24 sits above the Fe2 ligand, D85, in the M. *thermoacetica* crystal structure. In the crystal structure of the *D. gigas* ROO[1] the homologous residues are slightly dislocated away from the FMN, but still line the substrate binding pocket. The reason for this dislocation appears to be the presence of

Y26 (see below). *T. denticola* FprA is again an exception, in which F24 is replaced by an arginine. This arginine may compensate for the fact that H25 in *T. denticola* is, unlike in all other FprAs, replaced by a non-polar residue (phenylalanine). Thus, in all FprA sequences known to date, residues 24 and 25 together form a module consisting of one aromatic and one polar (possibly proton-donating) residue. Three FprAs (from the archaea *M. maripaludis, M. janaschii*, and *M. thermoautothrophicum*) contain a polar residue 25 *and* a tyrosine rather than phenylalanine at position 24. Immediately following the relatively conserved residues 24 and 25, many FprAs contain a second polar residue, which is either a glutamate or, in cases such as that of *D. gigas* ROO[1], a tyrosine (Y26, lining the substrate-binding cavity cf. Chapter 6, Figure 6.8). On the other hand, in *M. thermoacetica* FprA residue 26 is a glycine and does not appear to have a major role in defining the substrate-binding cavity. The presence of an extra polar residue in Region 1 for some FprAs appears to compensate for differences in Region 4 (see below). Residue 29 in *M. thermoacetica* is a phenylalalanine, which acts as a "roof" over the substrate-binding cavity (cf. Figure Chapter 6). F29 does not appear to be conserved, and in *D. gigas* ROO the "roof" is defined by Y26 alongside smaller residues (e.g., T27).

Region 2: residues 81-86

This region contains four of the six diiron ligand residues, H81, E83, D85, and H86. H81 is conserved in all known FprAs. The E83, D85 pair is conserved in most FprAs, but appears to be replaced by either an N,N or S,N pair in four FprAs from the cyanobacteria, *Nostoc* and *Synechocystis*. Each such substitution of the E83, D85 pair is accompanied by substitution of H86 with an arginine. H86 is otherwise conserved in all

FprAs despite its apparent lack of diiron ligation in *D. gigas* ROO (cf. Chapter 6). In the two *M. janaschii* FprAs E83 is replaced by a serine.

Region 3: residues 147-149

H148 is a ligand to Fe1 in *M. thermoacetica* FprA (as is the corresponding H146 in *D. gigas* ROO). This residue is conserved in almost all known FprAs in an LHW motif. Exceptions are one of the *M janaschii* FprAs, where LHW is replaced by CEY, and *Nostoc* and *Synechocystis* FprAs, where LHW is replaced by PRW. The W149 side-chain is located between H148 and the FMN in both *M. thermoacetica* FprA and *D. gigas* ROO crystal structures, possibly contributing to electron transfer between the two cofactors.

Region 4: residues 194-200

Residue 195 is almost always a tyrosine, with the side-chain pointing towards the substrate-binding cavity in the crystal structures of the *M. thermoacetica* and *D. gigas* FprAs (cf. Chapter 6). Residues 194 and 196 are almost always polar and, in both the *M. thermoacetica* FprA and *D. gigas* ROO crystal structures, their side-chains point away from the active site. Residue 196 is almost always a tyrosine (sometimes replaced by phenylalanine, threonine, or isoleucine). Y195 is replaced by phenylalanine in *M. maripaludis*, *M. janaschii*, and *M. thermoautothrophicus* FprAs. In compensation, these FprAs have an extra tyrosine in Region 1. Residue 199 is placed between Y195 and the FMN, lining the substrate-binding cavity. 199 is always a hydrophobic residue (isoleucine in most cases). Residue 200 is farther away from the diiron site compared to residue 199, but still contributes to defining the active site cavity. Residue 200 is usually

hydrophobic (I, L, F, M), with the notable exception of the cyanobacterial FprAs, where diiron ligands are not conserved, and which feature a histidine at position 200.

Three other residues, H172, D167 and H228, surround the diiron site, without being part of the four "regions". D167 and H228 are ligands to the iron, and are conserved in all FprAs with the exception of *Nostoc* and *Synechocystis* FprAs, where D167 is replaced by arginine. Residue 172 is a histidine in *M. thermoacetica* and most other FprAs. In the *M. thermoacetica* crystal structure, H172 lines the substrate-binding cavity (cf. Figure 6.9). H172 is replaced by asparagine in *D. gigas* ROO and *D desulfuricans* FprA; the crystal structure of *D. gigas* ROO[1] shows this asparagine (N170 in Figure 6.9, Chapter 6) to line the substrate-binding cavity. Residue 172 is a phenylalanine in four FprA homologues and a tyrosine in three *Pyrococcus* homologs.